Bioleaching as a unit operation for the recovery of copper and other metals of value from WEEE

Dumisani Musa Maluleke

Thesis presented for the degree of Doctor of Philosophy

Faculty of Engineering & Built Environment

Department of Chemical Engineering

University of Cape Town

Supervisor: Prof. Susan T.L Harrison

Co-supervisors: Dr Athanasios Kotsiopoulos
Dr Elaine Govender-Opitz

20 July 2024

Plagiarism Declaration

1. I know that plagiarism is wrong. Plagiarism is to use another's work and to pretend that it is ones own.

2. I have used the Harvard system for citation and referencing. Each significant contribution to, and quotation in, this report from the work, or works, of other people has been attributed, and has been cited and referenced.

3. This report is my own unaided work, except for assistance received from the teaching staff.

4. I have not allowed, and will not allow, anyone to copy my work with the intention of passing it off as his or her own work.

Signed by candidate

Date: 20 July 2024

Declaration of inclusion of publication

I confirm that I have been granted permission by the University of Cape Town's Doctoral Degrees Board to include the following publication(s) in my PhD thesis, and where co-authorships are involved, my co-authors have agreed that I may include the publication(s):

List of published peer-reviewed journals:

Maluleke, M. D.; Kotsiopoulos, A.; Govender-Opitz, E.; Harrison, S. T. L. (2024a). Microbial immobilisation and adaptation to Cu^{2+} enhances microbial Fe^{2+} oxidation for bioleaching of printed circuit boards in the presence of mixed metal ions. Research in microbiology 175 (1-2), 104148. DOI: 10.1016/j.resmic.2023.104148.

Maluleke, M. D.; Kotsiopoulos, A.; Govender-Opitz, E.; Harrison, S. T.L. (2024b). Exploring microbial adaptation of immobilised acidophilic cultures to improve microbial oxidation rates and copper tolerance in e-waste bioleaching. Minerals Engineering 207 (3), 108560. DOI: 10.1016/j.mineng.2023.108560.

Maluleke, M. D.; Kotsiopoulos, A.; Govender-Opitz, E.; Harrison, S. T.L. (2024c). Bioleaching of printed circuit boards in a two-stage reactor system with enhanced ferric iron regeneration in a re-circulating packed-bed reactor from PCB leaching. Manuscript under review by Minerals Engineering.

Signature: Signed by candidate Date: 20 July 2024

Abstract

The biohydrometallurgical approach (bioleaching) continues to emerge as the promising option in comparison to pyrometallurgy and hydrometallurgy, in terms of both economic and environmental advantages as well as recovery efficiency, for the extraction of base metals from printed circuit boards (PCBs). The biohydrometallurgical route typically presents less corrosive reagents and lower energy demands as operating temperatures are typically low, thus lower investment is required, distributed systems have potential and the technology may be profitable even for the treatment of low-grade PCBs. Of much benefit to bioleaching is the continuous in-situ regeneration of the ferric (Fe^{3+}) ion reagent by the iron oxidising microorganisms within the system, further lowering operating costs and minimising the disposal of toxic effluent to the environment. Bioleaching of PCBs has thus been explored since the early 2000s, with emphasis on the operating factors affecting the rate and extent of metal extraction, such as choice of microbial consortia, Fe^{3+} and/or Fe^{2+} concentrations and ratios, pH of the system, temperature, particle size of the PCBs, and solid loadings. High metal extractions are reported, especially for Cu (i.e. >90% Cu). Despite such progress, one of the major challenges in further development and commercialisation of bioleaching is the limited rate of microbial regeneration of the Fe^{3+} oxidant relative to the Fe^{3+} reduction rate as a function of metal dissolution, resulting in low leaching rate and extent of metal leached. The low Fe^{3+} regeneration rate is further exacerbated by the inhibition of microbial culture by accumulating metal ions and/or other non-metallic components of PCBs within the system, thus limiting the benefits of microorganisms in the system.

This study thus evaluated chemical leaching (Fe^{3+} reduction) and microbial Fe^{2+} oxidation (Fe^{3+} regeneration) kinetics during the extraction of base metals from PCBs and used such fundamental understanding to inform reactor set-up for the bioleaching of PCBs. Hence, the project was apportioned into three parts: (1) developing chemical leaching kinetics, (2) enhancing microbial Fe^{2+} oxidation kinetic rates through minimising inhibition and maximising volumetric oxidation rates through maximising the volumetric oxidation rate through biomass retention, and (3) bioleaching of PCBs in a bioreactor in which the balance on rates of ferric leaching of base metals from PCBs with microbial ferric regeneration is sought.

The chemical leaching kinetics were evaluated through the leaching of four typical predominant base metals of interest in PCBs, i.e., Cu, Zn, Ni, and Sn, as elementary metal powder. To best evaluate relative metal leaching behavior and associated kinetics, the four metals were leached as individual metals and as mixed metals. The kinetic data obtained for ferric and acid leaching were compared to that of leaching of complex PCBs. Leaching of elementary metals prior to complex PCBs provided useful fundamental leaching kinetics, which remains scarce in the literature. Such data is critical in informing the modeling and design of process flowsheets for the leaching of PCBs. For example, understanding relative metal leaching rates can help in determining residence time and number of leaching tanks required. As metal leaching is also through the attack by proton (H^+), all leaching experiments were also carried out with H^+ oxidant only by using acidified water, in addition to Fe^{3+} leaching. Across all leaching experiments, the Fe^{3+} oxidant exhibited faster leaching rates than H^+, suggesting that Fe^{3+} was a dominant oxidant. Amongst individual elementary metal leaching,

the relative Fe^{3+} leaching rates were in the order of Zn > Sn > Cu > Ni and were the same as that of Fe^{3+} leaching of mixed metals. For acid leaching systems, the relative leaching for both individual and mixed metals was in the order of Zn > Cu > Ni > Sn. This suggested that the difference in the relative leaching rates between Fe^{3+} and H^+ leaching systems was on Sn. This was attributed to the low solubility of Sn in the sulfuric acid (H_2SO_4) medium. Similar order in relative leaching rates between individual and mixed metals was critical as it meant that the kinetic leaching data for individual metals can be useful in understanding mixed metal leaching systems. The Fe^{3+} leaching of individual Cu and Sn was 2^{nd} order with respect to Fe^{3+} concentration and approximately 5^{th} and 1^{st} order for Zn and Ni, respectively. Our estimated leaching kinetics showed no dependence on Fe^{2+} concentration across all four metals. Leaching kinetics for mixed metals were assumed to be dominantly controlled by Cu leaching and the leaching order remained 2^{nd} order with respect to Fe^{3+}. The apparent activation energy for the Fe^{3+} leaching of Cu, Zn, Ni, and Sn was, respectively, 32.7, 24.3, 84.5, and 18.6 $kJ.mol^{-1}$, suggesting that the mechanism for leaching of Cu and Zn was mixed-controlled, Ni was chemically controlled, and Sn was diffusion-controlled. The apparent activation energy for the leaching of mixed metal was 16.3 $kJ.mol^{-1}$, implying a diffusion-limited mechanism.

More than 75% Cu, 85% Zn, 49% Ni, and 4% Sn were successfully leached over 40 min from PCBs by the Fe^{3+} oxidant, but at a lower leaching rate compared to fully liberated elementary metal powders. The relative metal leaching rate was comparable with that of elementary metals, i.e., Zn > Cu > Ni > Sn. The apparent low leaching rate of Sn may have been due to its precipitation. As with the leaching of the elementary metals, Fe^{3+} leaching of PCBs was 2^{nd} order with respect to Fe^{3+} and showed no dependency on Fe^{2+}. The leaching mechanism was mixed-controlled with an apparent activation energy of 26.8 $kJ.mol^{-1}$. Acid leaching of PCBs was also successfully achieved with 72% Cu, 99% Zn, 73% Ni, 9% Sn solubilised over 1440 min and a leaching order of Zn>Ni>Cu>Sn. This first part of this PhD thesis provided critical fundamental data on the leaching of base metals from PCBs and importantly, demonstrated that the kinetic data for leaching of individual metals can be useful in understanding the leaching of complex multi-metal systems.

In the second part of this PhD thesis, microbial Fe^{2+} oxidation kinetics is investigated, mainly focusing on Fe^{2+} oxidation rates in the presence of potential inhibitory metal ions during the bioleaching of PCBs. Microbial Fe^{2+} oxidation rates were evaluated in the presence of the four metals of interest, Cu, Zn, Ni, and Sn, as individual and in combination, and PCB leachates. Metal concentrations tested, added as metal ions, were informed by the expected concentration of each metal per PCB solid loading (0 – 20% w/v, weight PCB per volume of solution) determined from the characterisation of PCBs carried out and were in the range of 0 – 50 g/L Cu^{2+} and 0 - 10 g/L for Zn^{2+}, Ni^{2+}, and Sn^{2+}. PCB leachates tested were prepared by chemically (Fe^{3+}) leaching the custom-made PCB samples and filtering through a 0.45 µm filter to obtain a metal ion-rich (including liberated non-metallic components) solution. The effect of varying concentrations of PCB leachates, 0 – 50% v/v (volume PCB leachate to volume of medium with inoculum), on microbial Fe^{2+} oxidation rate was then studied. Owing to the Fe^{3+} reduction rate exceeding the microbial Fe^{3+} regeneration rate in bioleaching systems, this study explored both the use of microbial adaptation and microbial immobilisation to improve the Fe^{3+} regeneration rate while minimising inhibition of microbial culture. A mixed mesophilic

culture consisting of *Leptospirillum* (*L.*) *ferriphilum* (38%), *Acidibacillus* (*At.*) *caldus* (45%) and *Acidiplasma* (*Ap.*) *cupricumulans* (15%), with additional other species present at <1% abundance, was adapted to 6 g/L Cu^{2+} and immobilised on polyurethane foam (PUFs) as a biomass support structure. Microbial immobilisation was achieved by repeated sub-culturing of the microbial culture, in the presence of PUFs over a period of at least two months. Adaptation was achieved by incrementally adding Cu^{2+} (in increments of 0.5 g/L Cu^{2+} at every subculturing cycle up to 6 g/L Cu^{2+}). Microbial colonisation on PUFs was successfully confirmed by visual analysis of the surface of the PUFs using scanning electron microscopy (SEM). The immobilised cells were then exposed to increasing concentrations of inhibitory metal ions and their performance was compared to that of immobilised and Cu-adapted cells. Control experiments for both these sets of inocula were that of typically used planktonic cells, such that four sets of inocula were studied: 1) non-adapted planktonic cells (NA-PC), 2) Cu-adapted planktonic cells (A-PC), 3) non-adapted immobilised cells (NA-IC), and 4) Cu-adapted immobilised cells (A-IC). Exploring the four sets of inocula allowed screening of the best performing in terms of tolerance to toxic metal ions and microbial Fe^{2+} oxidation rates, and the best was used in Part 3 (reactor studies) of this thesis.

Across all inhibitory metal ions tested, Cu-adapted planktonic cells exhibited better tolerance than non-adapted planktonic cells. This suggested that adapting to Cu^{2+} not only improved their tolerance to Cu^{2+} but also to other individual metal ions (Zn^{2+}, Ni^{2+}, and Sn^{2+}), mixed metals, and PCB leachates. Further, immobilised cells exhibited better metal tolerance than both NA-PC and A-PC. Of much interest was the high metal tolerance exhibited by Cu-adapted immobilised cells compared to all inocula studied. This was attributed to the synergistic benefits of prior adaptation to Cu^{2+}, biofilm formation, and high cell density achievable in immobilised systems. A-IC not only exhibited better tolerance but also maintained their Fe^{2+} oxidation rates better, even at increasing metal concentration. When the culture was subjected to individual metals, microbial Fe^{2+} oxidation was impeded from 3 g metal ions/L and severity increased with an increase in metal ion concentration. Considering the individual inhibitory metal ions, inhibition was in the order of Sn^{2+}>Ni^{2+}>Cu^{2+}>Zn^{2+}. In comparison, mixed metal ions were more inhibitory, attributed to a synergistic inhibitory effect with respect to individual metal ions. Even at low metal ion concentrations, PCB leachates were more inhibitory than both individual and mixed metal ions, postulated to be due to synergistic action with the dissolved non-metallic component of the PCBs and/or the other dissolved metal ions (Cr, Co.). Nevertheless, complete Fe^{2+} oxidation was achieved over 600 h at up to 40% v/v PCB leachates by Cu-adapted immobilised cells. The improved metal ion tolerance and higher microbial Fe^{2+} oxidation rates observed by A-IC validated the novel approach of exploring the compounded benefits of microbial adaptation and immobilisation. As such, Cu-adapted immobilised cells were used as an inoculum in the bioleaching of PCBs in the bioreactor system (Part 3).

The third and final part of this PhD thesis explored a one- and two-stage bioleaching reactor system for the bioleaching of PCBs. The two-stage reactor system was set up by coupling a stirred tank reactor for the chemical leaching of PCBs to a series of packed-bed column reactors for microbial regeneration of the Fe^{3+} leaching agent. The column bioreactor was packed with PUFs immobilised with Cu-adapted cells. The two-stage reactor system was

operated as a continuously re-circulating closed system such that the Fe^{2+}-rich stream (including leached metal ions) generated on Fe^{3+} leaching of PCBs in the stirred tank reactor was circulated through the packed-bed bioreactor for the microbial regeneration of the Fe^{3+} oxidant. While the focus was on the two-stage reactor system, a one-stage reactor system where both Fe^{3+} leaching and microbial Fe^{2+} oxidation occurred in one pot was run concurrently. In both reactor systems, PCBs solid loading was increased incrementally from 3% to 18% w/v in 3% increments while the rate and extent of metal leaching and the microbial Fe^{3+} regeneration rate were studied. Comparably, high metal bioleaching efficiency was achieved in both reactor systems across PCBs loadings tested, shown by the average efficiency achieved across 3 – 18% w/v PCBs in the two-stage reactor system as follows: 98% Al, 58% Ca, 93% Cr, 96% Cu, >100% Mg, 79% Ni, 80% Pb, >100% Sn, >100% Zn, and low efficiency of 7% Co and 11% Sr. Of particular interest was the ability of the Cu-adapted immobilised cells to maintain their activity at increasing PCB solid loading in both reactor systems, with the two-stage system exhibiting faster volumetric Fe^{2+} oxidation rates. The Fe^{3+} reduction rate as a function of metal dissolution (0.211 g $Fe^{3+}.L^{-1}.hr^{-1}$) was 8.71 times the microbial Fe^{3+} regeneration rate (0.0242 $Fe^{3+}.L^{-1}.hr^{-1}$) in the one-stage reactor system, while in the two-stage system, the Fe^{3+} reduction rate of 0.206 g $Fe^{3+}.L^{-1}.hr^{-1}$ was 3.46 times faster than the Fe^{3+} regeneration rate (0.0594 g $Fe^{3+}.L^{-1}.hr^{-1}$). This suggested an improvement of about 60% in the matching of the Fe^{3+} reduction to Fe^{3+} regeneration rates in the two-stage reactor system.

Overall, this study contributed to the understanding of the bioleaching of PCBs by providing fundamental data for both sub-processes, i.e., the chemical leaching and the microbial Fe^{2+} oxidation, involved in bioleaching. It demonstrated that study of the two sub-processes independently can be insightful to the complex integrated system. This is important as the data can be useful in process modelling to aid both system design and improvement of the overall bioleaching performance of PCBs. This study provided as yet unreported data on the kinetics of ferric and acid leaching of elemental base metals and their mixtures. It successfully demonstrated that the inhibitory effect of accumulated metal ions and other dissolved non-metallic components of the PCBs on the microbial culture can be minimised using microbial adaptation and immobilisation systems. In addition to the mitigated inhibition, the microbial Fe^{2+} oxidation rate can be improved through biomass retention, bridging the discrepancy between the high Fe^{3+} reduction rate and slow microbial Fe^{3+} regeneration rate. These results present a novel and promising approach to maximising metal recovery while maintaining and improving microbial activity in the bioleaching of PCBs. In particular, the improved Fe^{3+} regeneration in the two-stage reactor systems presents a promising result for its application in the commercialisation of PCB bioleaching. Further investigation of the reactor configurations, through their modelling to further balance rates of oxidation and reduction, optimisation of operating parameters such as residence time and the number of packed-bed column bioreactors, and conversion of the system to a continuous open system for ongoing metal recovery, amongst others, are recommended to contribute to the refinement of the bioleaching system for base metal recovery from PCBs, prior to recovery of platinum group metals (PGMs).

Acknowledgments

I dedicate this thesis to my mother (Mhani) Mamayila Manganyi. One of your children or grandchildren will convey this message to you as you can't read but look at how far I have come because of your encouragement in focusing on my school work. I cannot thank you enough for the life lessons, discipline, respect, unconditional love, and prayers. "Mi hinkwaswo eka mina, ndza khensa"

To my principal supervisor, Prof Susan T.L. Harrison, thank you for your guidance, inspiration, motivation, support, and for granting me this opportunity to nurture my growth as a researcher under you. I truly appreciate you.

To my co-supervisors, Dr Athanasios Kotsiopoulos (Dr T) and Dr Elaine Govender-Opitz, the regular Tuesday meetings at the green table and your constructive critiques, which I have sometimes mistaken to be a personal attack, have helped me this far. Thank you for your invaluable contribution to the success of this project and my growth.

Financial support for this research project by the Department of Science and Innovation (DSI) and the National Research Foundation of South Africa (NRF), through the SARChI Chair in Bioprocess Engineering (UID 64778), together with the Council of Scientific and Industrial Research (CSIR), South Africa through the Waste Roadmap grant is greatly appreciated.

I would also like to extend my gratitude to past and present CeBER staff and students. Thanks to Tichaona Samkange and Emmanuel Ngoma for your technical assistance in the lab from the first day I arrived in CeBER. To the administrative CeBER staff, Sue Jobson and Ruegshana Ederies, thank you for keeping your door open and always ready to assist me. Thank you to Sisanda Rini, Didi Makaula, Mhlangabezi Tolbert Golela, Msimelelo Gcayiya, Ishaaq Hajee, Bahman Taherian, Sarah Fernandes, and Matome Malatji, just to mention a few – thank you for your contributions during discussion groups and in the lab.

To my friends, Shaine Raseala, Andani Mphinyane, and Motlokoa Khasu, our good chats at the 6th floor students' lofty and outside campus were more than therapeutic.

Equally, my heartfelt gratitude to Vutomi Simango, "Ximatsatsa xa mina". Thank you for your unwavering support, love, years of sacrifice, and the upbringing of our son. To Vangama Maluleke, thank you sonny for giving me no option to fail.

To my brothers and sisters, I am grateful for your support and forever believing in me.

Table of contents

List of Figures

List of Tables

Acronyms and Abbreviations

A-IC	Adapted immobilised cells
A-PC	Adapted planktonic cells
BFRs	Brominated flame retardants
BMs	Base metals
CeBER	Centre for Bioprocess Engineering Research
CFCs	Chlorofluorocarbon
CRMs	Critical raw materials
EEE	Electrical and electronic equipment
EPS	Extracellular polymeric substance
E-waste	Electronic waste
gDNA	Genomic deoxyribonucleic acid
ICP-MS	Inductively coupled plasma mass spectrometry
ICP-OES	Inductive coupled plasma atomic emission spectroscopy
Mt	Million tonnes
NA-IC	Non-adapted immobilised cells
NA-PC	Non-adapted planktonic cells
PBDDs/Fs	Polybrominated dibenzo-p-dioxins and furans
PBDEs	Polybrominated diphenyl ethers
PCBs	Printed circuit boards
PCDDs/Fs	Polychlorinated dibenzo-p-dioxins and furans
PGMs	Platinum group metals
PMs	Precious metals
PUF	Polyurethane foam
PUF-BSP	Polyurethane foam as biomass support particle
qPCR	Quantitative real-time polymerase chain reaction
REEs	Rare earth elements
SEM	Scanning electron microscopy

USD	United State dollar
WEEE	Waste Electrical and Electronic Equipment
XRD	X-ray Diffraction
XRF	X-ray Fluorescence

CHAPTER 1

1 Introduction

1.1 Rapid generation of Waste Electrical and Electronic Equipment (WEEE)

According to the Solving the E-Waste Problem (Step) white paper, *"Waste Electrical and Electronic Equipment, WEEE, widely known as E-Waste, is a term used to cover items of all types of electrical and electronic equipment (EEE) and its parts that have been discarded by the owner as waste without the intention of reuse"* (Step Initiative, 2014). E-waste includes a vast variety of EEE products, household and/or business, which have a power or battery supply. These include equipment and devices such as refrigerators, air conditioners, televisions, laptops, mobile phones, fluorescent lamps, electric kettles, game consoles, electrical cables, printers, washing machines, microwaves. E-waste constitutes one of the fastest growing solid municipal wastes globally. Global generation of E-waste increased from 44.4 million tonnes, Mt (average of 6.4 kg per capita) in 2014 to 62 Mt (7.8 kg per capita) in 2022, valued at $91 billion USD (Baldé et al. 2024). It is forecast to increase to 74.7 Mt by the year 2030 (Forti et al. 2020) and to as high as 110 Mt in 2050 (Parajuly et al. 2019). Of the 62 Mt E-waste generated in 2022, Asia contributed 48.4% (30 Mt), America, 22.6% (14 Mt), Europe, 21.0% (13 Mt), Africa, 5.7% (3.5 Mt) and the least being Oceania at 1.1% (0.707) (Figure 1-1). Of the greatest concern is the low amount of E-waste formally collected and recycled annually against the annual generated. Depending on the legislation set up in the handling of E-waste, recycling channels (collections) and resources (capital investment) for E-waste treatment, the amount of E-waste recycled differs per continent. In 2022, only 43%, 41%, 30%, 12%, and 0.7% of the annually generated was formally collected and recycled in Europe, Oceania, the Americas, Asia, and Africa, respectively (Baldé et al. 2022). Globally, only 22.3.4% was recycled and the remaining 77.6% (valued at $71 billion USD) was undocumented – most likely ending up dumped in landfills, or informally recycled using non-environmentally compliant practices (Baldé et al. 2024).

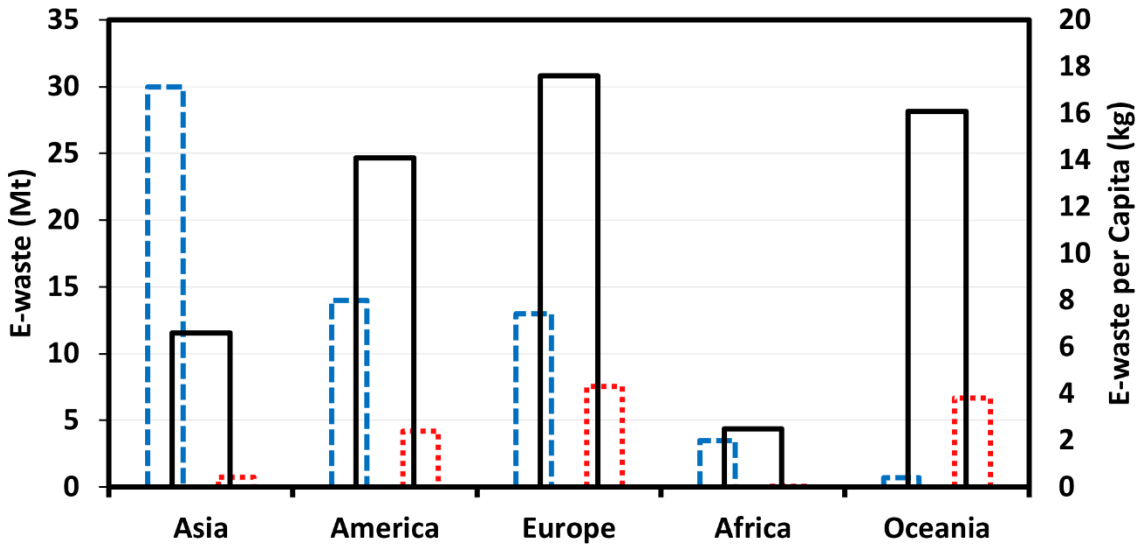

Figure 1-1 Total annual amount of E-waste generated (▭), E-waste generated per capita (▫), and amount of E-waste recycled (▭) at various continents in the year 2022 (Baldé et al. 2024).

The main driving force for this continuous rapid global generation of E-waste is the rapid growth in technological innovations, especially in the information and communication technology sector, and the decrease in the lifespan of electronic products (typically less than 3 years), driving ongoing replacement of electronic products with improved ones, resulting in burgeoning electronic waste (e-waste). Proper recycling of E-waste is complex as E-waste contains a wide range of material compositions (i.e., plastics, nonferrous metals, ferrous metals, wood, glass, as shown in Figure 1-2 (Robinson 2009; Garlapati 2016; Kaya 2019a; Adetunji et al. 2023); and E-waste has traditionally been manufactured with no intent for reuse. As such, E-waste has typically been incinerated or sent to landfills; however, such improper E-waste treatment methods are of serious concern to both the environment and public health (Cao et al. 2020; Abubakar et al. 2022; Ji et al. 2022a). This is owing to the organic and inorganic hazardous substances such as brominated flame retardants (BFRs), polybrominated diphenyl ethers (PBDEs), chlorofluorocarbon (CFCs), polyvinylchloride (PVC), heavy metals (Pb, Hg, Cr^{6+}, Ba, In,), polybrominated dibenzo-*p*-dioxins and furans (PBDDs/Fs), polychlorinated dibenzo-*p*-dioxins and furans (PCDDs/Fs), contained in E-waste (Morf et al. 2007; Robinson 2009; Tsydenova and Bengtsson 2011; Cao et al. 2020). In landfilling, these hazardous substances can leach into and pollute the surrounding soil and water streams. Incineration pollutes the surrounding air as toxic gases and fumes, such as dioxins are emitted. Sepúlveda et al. (2010) reviewed the impact of E-waste on the environment surrounding recycling sites in India and China. Soil, air, water, dust, and sediments around the recycling sites were found to contain high levels of PBDDs/Fs, Pb, PCDDs/Fs, and PBDEs. Concentrations of some of these contaminants were higher than the standard thresholds, posing high risks to the environment and human health (Sepúlveda et al. 2010). Similarly, Oloruntoba et al. (2022) reported high levels of PBDEs in soil (0-45 cm depth) and rainwater ponds around E-waste dumping sites in Lagos, Nigeria. Gases such as CFCs, which are known to be ozone depleting, can escape from air conditioners and refrigerators when these items are dumped on landfills

(Scheutz et al. 2004). This highlights the urgent need for an alternative E-waste handling approaches which are environmentally sound and allow for effective metal recovery and re-use.

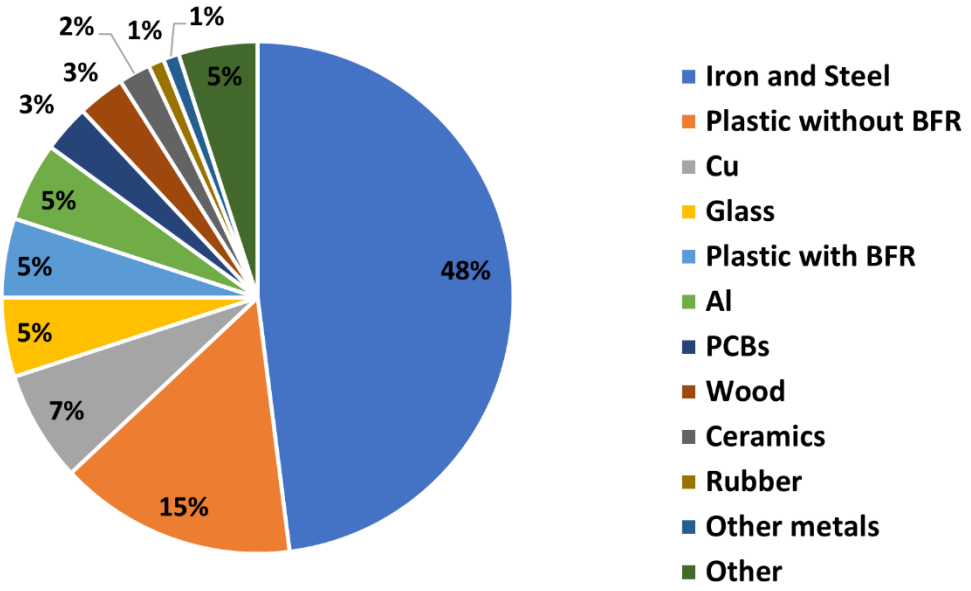

Figure 1-2 Typical composition of various materials (%) in E-waste (adapted from (Kaya 2019a))

1.2 WEEE in circular economy

Despite the human health and environmental concerns associated with E-waste, E-waste hold great potential economic value, derived from their high metal content which can be as high as 50% by weight. E-waste contains up to 69 elements from the periodic table, these vary from rare earth elements, REE (tantalum, indium, and neodymium), critical raw materials, CRMs, and platinum group metals, PMGs (osmium, palladium, platinum, iridium, cobalt, ruthenium, and rhodium), base metals, BMs (copper, iron, zinc, nickel, tin, and aluminium), precious metals, PMs (gold and silver), and other metals (cadmium, chromium, mercury, lead, and silicone) (Tan et al. 2014; Chauhan et al. 2018; Kaya 2019a; Islam et al. 2020). Depending on the type of E-waste, metals such as Cu and Au can be 17 times or more concentrated and purer than found in their respective virgin ores (Davis and Herat 2008; Forti et al. 2020; Kaya 2019a; van Yken et al. 2021; Adetunji et al. 2023). Typical respective copper-bearing virgin ores currently mined contain about 0.3-1% Cu, and that of Au is about 1-10 g/ton, while in E-waste, these metals can be as high as 20% Cu and 250 g/ton Au (Akcil et al. 2015c). This centres E-waste as one of the best secondary sources for metals, mitigating the continuous traditional mining of the already depleting materials and ore grades, in addition to alleviating environmental burden. Furthermore, their high, and mixed, metal content necessitates development of appropriate E-waste recycling methods and environmentally friendly technologies to recover such metals selectively. Such practices can avail critical materials to re-enter the manufacturing process and aid in bridging the increasing deficit between the supply of materials from virgin ores and the high demand for metals to support rapid

advancement in technology, especially for the low carbon economy. This will encourage a circular economy and contribute toward sustainable goals.

Printed circuit boards (PCBs) are the core component of almost all EEE products. Although they constitute about 3-6% by mass of E-waste (Bizzo et al. 2014), they represent the most economical value owing to their high metal content. PCBs are heterogeneous in composition and are typically about 30% metallic and 70% non-metallic. The non-metallic composition includes plastics, glass fiber reinforced epoxy resins, and ceramics, while the metal fraction includes base metals and precious metals. The composition varies across manufacturers and depends on the intended purpose of the EEE. The metal fraction of PCBs is mostly dominated by base metals, with Cu being the predominant metal by mass (Yamane et al. 2011; Bizzo et al. 2014) while Au, Ag, and the PGMs are of the highest value. PCBs are typically categorised based on their Au content. PCBs with less than 100 g/ton Au are classified as low grade, between 100 – 400 g/ton are medium grade, while with more than 400 g/L Au are high grade (Oguchi et al. 2011). The presence of copper typically interferes with the recovery of the high value metals, especially Au, necessitating recovery of base metals prior to the recovery of PMs and PGMs (Pham and Ting 2009; Işıldar et al. 2016). PCBs are by far the most studied secondary source of metals from E-waste (Brandl et al. 2001; Tuncuk et al. 2012a; Ghosh et al. 2015; van Yken et al. 2021; Adetunji et al. 2023). Although metal recovery from PCBs can be challenging due to their complex heterogeneous composition, various methods, including pyrometallurgical (Khaliq et al. 2014; Cayumil et al. 2016), hydrometallurgy (Behnamfard et al. 2013; Akcil et al. 2015c), and biohydrometallurgy (Awasthi et al. 2016; Ji et al. 2022a) have been explored and well documented through review articles.

1.3 Current recycling practices

Pyrometallurgy, where metal extraction is carried out by smelting, is currently the preferred route for the extraction of metals from PCBs by industry and is economically profitable. In state-of-the-art smelters, metal extraction, and refining are rapidly achieved with minimal environmental impact as they are fitted with off-gas treatment units and analysers (Khaliq et al. 2014). Copper or lead smelters such as Rönnskår and Umicore are typically best for the extraction of PMs, Cu, and Pb from E-waste (including PCBs) (Cui and Zhang 2008; Khaliq et al. 2014). Metal recovery is then carried out through hydrometallurgy (i.e., cementation or precipitation) and/or electrometallurgy (i.e., electrowinning). Umicore (located in Hoboken, Belgium) is the world's largest integrated metal smelter and refinery with an annual capacity of about 250 000 tons of waste (including E-waste) treated for the recovery of PMs (annual production of >3400 tons), PGMs (>50 tons), BMs, and other metals (i.e., selenium, bismuth, tellurium, and antimony) (van Heukelem et al. 2004b; Hagelüken 2006). Although pyrometallurgical methods are rapid with high metal recovery efficiency and high economical returns, installation and running a smelter requires high investment as smelters are highly energy intensive and special off-gas treatment is required. Toxic gases such as dioxins emitted during the incineration can escape and result in secondary pollution (Cui and Zhang 2008; Cayumil et al. 2016). Moreover, high grade PCBs are typically required for the process to be economically profitable.

An alternative to pyrometallurgy is hydrometallurgy, where metal extraction is carried out through strong oxidant lixiviants such as hydrogen peroxides (H_2O_2), sulfuric acids (H_2SO_4), aqua-regia, thiosulfates, cyanide, and halides, either as isolated oxidant or in their combinations (Kołodzziej and Adamski 1984; Tuncuk et al. 2012a; Behnamfard et al. 2013; Akcil et al. 2015c; Işıldar et al. 2016). Contrary to pyrometallurgy, metal extraction through hydrometallurgical approaches is selective depending on the choice of lixiviant used. Precious metals are generally targeted by using lixiviants such as cyanides, thiourea, and aqua-regia (Park and Fray 2009; Rocchetti et al. 2013), while base metals are targeted by using oxidants such as H_2O_2, ferric ion (Fe^{3+}) solutions, and H_2SO_4 (Quinet et al. 2005; Yazici and Deveci 2014). Relatively low investment is required as the operating temperatures are low and the process can be profitable even with the low-grade PCBs as a feedstock. As such, hydrometallurgical processes are suitable for small-scale operations. Factors influencing metal extractions and recovery, such as temperature and solution pH, are well established. High extraction of PMs (>95% Au and 100% Ag) can be achieved from PCBs using thiosulfate lixiviant (Oh et al. 2003; Ha et al. 2010). Industrially, metal-rich bullions from the Umicore smelters are refined through hydrometallurgy for the recovery of PMs and BMs (Hagelüken 2006). Despite the wide industrial application of hydrometallurgical routes for the treatment of mineral ores, their industrial and pilot-scale application for the treatment of PCBs remains minimal. Amongst other reasons, this is due to (i) highly intensive mechanical pre-treatment (i.e., physical separation and size reduction) required, which is associated with up to 20% loss of PMs (Cui and Zhang 2008; Khaliq et al. 2014); and (ii) the use of strong corrosive acids, and some highly flammable reagents, which can result in the degradation of equipment and release of toxic effluents (Tuncuk et al. 2012a; Kiddee et al. 2013; Akcil et al. 2015c). The need to treat the effluent before discharging to minimise environmental impact, continuous feed of lixiviant, and special equipment (such as stainless steel) required to minimise degradation increase the operation cost.

Of late, biohydrometallurgical processes (bioleaching in particular) have been promoted over the convectional pyrometallurgical and hydrometallurgical processes as providing improved environmental performance (Tuncuk et al. 2012; Priya and Hait 2017). This technology is based on the use of ferrous iron and/or reduced sulfur oxidising bacteria such as *Leptospirillum (L.) ferrooxidans*, *Acidithiobacillus (At.) ferrooxidans*, *At. caldus and L. ferriphilum*, and archaea such as *Metallosphaera (M.) hakonensis* (Rawlings and Johnson 2007; Watling 2006; Tupikina et al. 2013) to generate the ferric iron and acid lixiviants, respectively. Elemental metal dissolution occurs through the oxidation of metal embedded on PCBs by dissolved ferric iron as a primary oxidising agent, in the presence of oxygen under acidic conditions, producing the soluble metal ion and ferrous iron. The ferrous iron undergoes microbial oxidation back to ferric iron and the microorganisms use the resulting electron released as an energy source. As the primary oxidant is continuously regenerated i*n-situ*, reagent costs are minimized with considerably lower effluent disposal, thereby reducing the environmental burden incurred. This also allows the treatment of low-grade PCBs with potential profits. Similar to hydrometallurgy, bioleaching also requires low investment as the operating temperature can be as low as the ambient temperature and can be suitable for small-scale operations. However, in contrast to hydrometallurgy, operational conditions are less hazardous as the

reagents used are less corrosive and toxic. Moreover, the provision of acid to maintain the required acidic condition (pH <2) can be added chemically (adding H_2SO_4) or can be generated *in-situ* when S^0 or sulfide source (i.e., pyrite) is supplemented in the presence of sulfur-oxidising microorganisms (Ilyas et al. 2013). Similarly, the ferric iron lixiviant is regenerated through microbial metabolism from ferrous iron formed on leaching.

Bioleaching has successfully been demonstrated for the leaching of base and precious metals from E-waste since the early 2000s (Brandl et al. 2001; Tuncuk et al. 2012a; Adetunji et al. 2023). Bioleaching of base metals must precede the leaching of precious metals as they adversely interfere with the leaching efficiency of precious metals (Birloaga et al. 2013; Işıldar et al. 2016). As such, the application of bioleaching has mainly been on the extraction of base metals, with a focus on Cu as the abundant metal. More than 90% Cu (and other base metals) have been extracted from various types of E-wastes (including PCBs) and factors affecting bioleaching rates and efficiency, such as solution pH, type of microbial consortia, PCB solid loading, particle size of PCBs, and initial concentration of Fe (either as Fe^{2+} or Fe^{3+}) continue to be studied. These studies continue to contribute to the fundamental understanding of bioleaching of PCBs. However, to date, there are no commercial nor pilot-scale processes of bioleaching of PCBs despite wide successful commercialised bioleaching processes for the leaching of metals from mineral sulfides. Inhibition of microbial culture by metal ions and/or non-metallic components remains one of the major challenges in bioleaching of E-waste. During the bioleaching process, metal ions and non-metallic components (which may be solubilised) accumulate within the system and adversely impede microbial regeneration of the primary Fe^{3+} oxidants. Microbial Fe^{2+} oxidation is the rate-determining step in bioleaching and enhancing tolerance of the microbial culture to the toxic environment is thus key to improving bioleaching efficiency. While the focus may be on the rate-determining step, the Fe^{3+} reduction rate as a function of metal leaching is as critical in improving overall bioleaching efficiency, owing to the two sub-processes being interdependent. Chemical leaching of PCBs by Fe^{3+} and H^+, and associated leaching kinetics is reported (Yazici and Deveci 2014; Becci et al. 2019); however, there is limited data on the leaching rates of the individual metals or their mixtures, limiting integrated process design and optimisation. This gap in fundamental knowledge of individual metal leaching kinetics is key in modeling of bioleaching and in informing the metal recovery flowsheet (number of recovery tanks and residence time). Moreover, on understanding relative metal leaching rates, metal accumulation and associated concentrations can be modeled, which can aid in minimising metal ion exposure and subsequent inhibition of microbial culture.

1.4 Scope and overall objectives

This study focuses on evaluating ferric iron and acid leaching kinetics of base metals found in PCBs and microbial ferrous iron oxidation kinetics for regeneration of the ferric lixiviant during metal extraction from PCBs. It seeks to use the chemical and microbial oxidation kinetics determined to inform the appropriate staged reactor configurations to enable matched ferric iron-mediated chemical leaching rates with microbial Fe^{3+} regeneration. To this effect, this project can be divided into 3 parts: (1) evaluation of ferric iron-mediated chemical leaching kinetics of both individual metals in elemental form and metal mixtures, (2) microbial Fe^{2+}

oxidation kinetics for Fe^{3+} regeneration with a view to minimising inhibitory impact of the metals in solution and maximising volumetric Fe^{2+} oxidation rates, and (3) integrated reactor studies.

Chemical leaching kinetics were evaluated through the leaching of elementary metals, as individual metals and in their combinations, and lastly, through the leaching of PCBs. Four base metals of interest (i.e., Cu, Zn, Ni, and Sn) were considered as they are typically the most dominant metals across various PCBs. Leaching of individual elementary metals allowed evaluation of metal leaching kinetics, mixed metals (combination of individual metals) allowed evaluating the effect of other metals on relative leaching kinetics, such as potential cementation, while PCB leaching allowed the impact of other metals (other than the four metal of interest) and components liberated from the PCBs on the relative leaching behaviour and kinetics to be studied. All leaching studies were carried out through two oxidants: acidic-ferric iron (H^+-Fe^{3+}) and acid-only (H^+), to evaluate the relative rate of metal oxidation. Each leaching experiment was carried out at five temperatures (i.e., 25, 37, 45, 65, and 75 °C) to evaluate kinetic parameters as a function of temperature as well as activation energy. The rate law governing metal leaching was proposed based on Fe^{3+} reduction rate and experimental data fitted through non-linear regression to estimate the reaction order, n, and rate constant, k. The leaching mechanism governing the leaching, i.e., diffusion- or surface-controlled mechanism, was inferred from the value of the estimated activation energy.

In order to enhance microbial Fe^{2+} oxidation rates to match the high Fe^{3+} reduction rates, high volumetric ferrous iron oxidation rates are required. These can be achieved by both maintaining a high specific ferrous iron oxidation rate and enhancing the active microbial concentration of iron oxidisers. The former is achieved by minimising metal inhibition through microbial adaptation to high metal ion concentrations. The latter is achieved through biomass retention in the reactor through microbial immobilisation and microbial protection through biofilm formation. Microbial Fe^{2+} oxidation rates of adapted and immobilised cells were evaluated in the presence of an increasing concentration of the four metals of interest (Cu, Zn, Ni, and Sn), as individual metal ions and in their combination, and PCB leachates. This enabled the study of the relative inhibitory effect of (1) each metal ion (when exposed to individual metal ions), (2) mixed metal ions (mimicking metal proportions in PCBs leachates), and (3) other metals and liberated substances in PCBs leachates, on microbial Fe^{2+} oxidation rates. Culture performance, in terms of metal tolerance and microbial Fe^{2+} oxidation rates, was compared to that of non-adapted immobilised and planktonic cells. The best performing inoculum was used in the reactor studies. Two reactor set-ups were studied: a one-stage reactor system where both microbial Fe^{2+} oxidation and PCBs occurred in one-pot, and two-stage reactor systems consisting of a stirred tank reactor for Fe^{3+} leaching of PCBs connected to a packed-bed column reactor for microbial Fe^{2+} oxidation. PCB solid loading (% w/v) was increased incrementally in both reactor systems and extent of metal leaching and microbial Fe^{3+} regeneration studied.

1.5 Thesis layout

In **Chapter 2**, the relevant literature pertaining to the overarching scope of the thesis is critically reviewed. The increasing deficit in metals from virgin ore as a result of high demand

to support the advancement in technology is addressed, with a focus on base metals such as Cu and centering PCBs as a secondary resource of such metals. An overview of current studies and industrial approaches, such as pyrometallurgy, hydrometallurgy, and biohydrometallurgy, for metal extraction and recovery from PCBs is provided with an emphasis on bioleaching as a preferred option. The factors influencing the bioleaching of PCBs such as pH, microbial consortia, and challenges in bioleaching are presented, with a focus on the role of the microbial culture in enhancing overall bioleaching efficiency. Recent studies on bioleaching of PCBs at a reactor level are reviewed to assess the current state of development of this process towards pilot and commercialisation scale. This chapter closes by setting out research gaps and opportunities in bioleaching of PCBs and the specific aims and objectives of the project, hypotheses, and key research questions. This is followed by **Chapter 3**, detailing research approach, materials, and methodologies, including experimental plans, used in this study.

Chapter 4 addresses the research findings related to chemical leaching kinetics as Part 1 of the PhD thesis. These include the leaching rates of elemental metals typical in PCBs, how the leaching behaviour and associated kinetics of individual metals compare to those of mixed metals and finally to that of PCBs. It is preceded by a brief background and rationale for this part of the study to narrow down the specific aims whilst contextualising it to the entire PhD thesis. This is presented as a typical thesis chapter rather than a publication.

Chapter 5 and **6** provide Part 2 of the thesis, addressing microbial oxidation kinetics. These are presented as two published journal papers. Each of these chapters is preceded by a preamble to contextualise the research findings with regard to the overarching aims and objectives of the PhD project. **Chapter 5** provides experimental results confirming the establishment of the immobilised cell system (microbial colonisation on polyurethane foams, PUFs) and then compares the oxidation kinetics of immobilised cells to that of planktonic cells in the presence of increasing Cu^{2+} concentrations, as an individual metal. **Chapter 6** further expands the evaluation of the microbial oxidation kinetics of immobilised cells to other individual metals (Zn, Sn, and Ni), mixed metals, and PCBs leachates.

Chapter 7 provides and discusses the reactor studies, forming Part 3 of the PhD thesis. It too is presented as a journal paper (manuscript under review). With insight into the chemical leaching (**Chapter 4**) and microbial oxidation kinetics (**Chapter 5-6**), this chapter explores one- and two-stage bioleaching reactor systems for the leaching of base metals from PCBs.

Chapter 8 provides overall conclusions with respect to the overarching aims and objectives of the PhD project. It presents a brief integrated discussion of research findings from **Chapters 4-7**, highlighting the main results, to bind together the PhD thesis. It closes by providing recommendations for key aspects of focus in future research.

It must be noted that as this thesis is structured as a series of separate journal papers, duplication of information in sections such as introductions and methodologies was unavoidable.

1.6 References

Abubakar, A.; Zangina, A. S.; Maigari, A. I.; Badamasi, M. M.; Ishak, M. Y.; Abdullahi, A. S.; Haruna, J. A. (2022). Pollution of heavy metal threat posed by e-waste burning and its assessment of human health risk. Environmental Science and Pollution Research 29 (40), 61065–61079. DOI: 10.1007/s11356-022-19974-6.

Adetunji, A. I.; Oberholster, P. J.; Erasmus, M. (2023). Bioleaching of metals from E-Waste using microorganisms. A Review. Minerals 13 (6), 828. DOI: 10.3390/min13060828.

Akcil, A.; Erust, C.; Gahan, C. S.; Ozgun, M.; Sahin, M.; Tuncuk, A. (2015). Precious metal recovery from waste printed circuit boards using cyanide and non-cyanide lixiviants--A review. Waste Management 45, 258–271. DOI: 10.1016/j.wasman.2015.01.017.

Awasthi, A. K.; Zeng, X.; Li, J. (2016). Integrated bioleaching of copper metal from waste printed circuit board-a comprehensive review of approaches and challenges. Environmental Science and Pollution Research International 23 (21), 21141–21156. DOI: 10.1007/s11356-016-7529-9.

Balde, C.; Kuehr, R.; Yamamoto, T.; McDonald, R.; D'Angelo, E.; Althaf. et al. (2024). The Global E-waste Monitor 2022. International Telecommunication Union and United Nations Institute for Training and Research. Bonn/Geneva.

Becci, A.; Amato, A.; Rodríguez Maroto, J. M.; Beolchini, F. (2019). Prediction model for Cu chemical leaching from printed circuit boards. Industrial & Engineering Chemistry Research 58 (45), 20585–20591. DOI: 10.1021/acs.iecr.9b04187.

Behnamfard, A.; Salarirad, M. M.; Veglio, F. (2013). Process development for recovery of copper and precious metals from waste printed circuit boards with emphasize on palladium and gold leaching and precipitation. Waste Management 33 (11), 2354–2363. DOI: 10.1016/j.wasman.2013.07.017.

Birloaga, I.; Michelis, I. de; Ferella, F.; Buzatu, M.; Vegliò, F. (2013). Study on the influence of various factors in the hydrometallurgical processing of waste printed circuit boards for copper and gold recovery. Waste Management 33 (4), 935–941. DOI: 10.1016/j.wasman.2013.01.003.

Brandl, H.; Bosshard, R.; Wegmann, M. (2001). Computer-munching microbes: Metal leaching from electronic scrap by bacteria and fungi. Hydrometallurgy 59 (2-3), 319–326. DOI: 10.1016/S0304-386X(00)00188-2.

Cao, P.; Fujimori, T.; Juhasz, A.; Takaoka, M.; Oshita, K. (2020). Bioaccessibility and human health risk assessment of metal(loid)s in soil from an e-waste open burning site in Agbogbloshie, Accra, Ghana. Chemosphere 240, 124909. DOI: 10.1016/j.chemosphere.2019.124909.

Cayumil, R.; Khanna, R.; Rajarao, R.; Mukherjee, P. S.; Sahajwalla, V. (2016). Concentration of precious metals during their recovery from electronic waste. Waste Management 57, 121–130. DOI: 10.1016/j.wasman.2015.12.004.

Chauhan, G.; Jadhao, P. R.; Pant, K. K.; Nigam, K.D.P. (2018). Novel technologies and conventional processes for recovery of metals from waste electrical and electronic equipment. Challenges & opportunities – A review. Journal of Environmental Chemical Engineering 6 (1), 1288–1304. DOI: 10.1016/j.jece.2018.01.032.

Cui, J.; Zhang, L. (2008). Metallurgical recovery of metals from electronic waste. A review. Journal of Hazardous Materials 158 (2-3), 228–256. DOI: 10.1016/j.jhazmat.2008.02.001.

Davis, G.; Herat, S. (2008). Electronic waste. The local government perspective in Queensland, Australia. Resources, Conservation and Recycling 52 (8-9), 1031–1039. DOI: 10.1016/j.resconrec.2008.04.001.

Forti, V.; Balde, C.; Kuehr, R.; Bel, G. (2020). The Global E-waste Monitor 2020. Quantities, flows and the circular economy potential: United Nations University/United Nations Institute for Training and Research, International Telecommunication Union, and International Solid Waste Association. Bonn/Geneva/Rotterdam.

Garlapati, V. K. (2016). E-waste in India and developed countries: Management, recycling, business and biotechnological initiatives. Renewable and Sustainable Energy Reviews 54 (1), 874–881. DOI: 10.1016/j.rser.2015.10.106.

Ghosh, B.; Ghosh, M. K.; Parhi, P.; Mukherjee, P. S.; Mishra, B. K. (2015). Waste printed circuit boards recycling. An extensive assessment of current status. Journal of Cleaner Production 94, 5–19. DOI: 10.1016/j.jclepro.2015.02.024.

Ha, V. H.; Lee, J.-c.; Jeong, J.; Hai, H. T.; Jha, M. K. (2010). Thiosulfate leaching of gold from waste mobile phones. Journal of Hazardous Materials 178 (1-3), 1115–1119. DOI: 10.1016/j.jhazmat.2010.01.099.

Hagelüken, C. (2006). Recycling of electronic scrap at Umicore precious metals refining. Acta Metallurgica Slovaca 12, 111–120.

Ilyas, S.; Lee, J.-c.; Chi, R.-a. (2013). Bioleaching of metals from electronic scrap and its potential for commercial exploitation. Hydrometallurgy 131-132 (11–12), 138–143. DOI: 10.1016/j.hydromet.2012.11.010.

Işıldar, A.; van de Vossenberg, J.; Rene, E. R.; van Hullebusch, E. D.; Lens, P. N. L. (2016). Two-step bioleaching of copper and gold from discarded printed circuit boards (PCB). Waste Management 57, 149–157. DOI: 10.1016/j.wasman.2015.11.033.

Islam, A.; Ahmed, T.; Awual, M. R.; Rahman, A.; Sultana, M.; Aziz, A. A. et al. (2020). Advances in sustainable approaches to recover metals from e-waste-A review. Journal of Cleaner Production 244 (5), 118815. DOI: 10.1016/j.jclepro.2019.118815.

Ji, X.; Yang, M.; Wan, A.; Yu, S.; Yao, Z. (2022). Bioleaching of typical electronic waste-printed circuit boards (WPCBs). A Short Review. International Journal of Environmental Research and Public Health 19 (12). DOI: 10.3390/ijerph19127508.

Kaya, M. (2019). Electronic Waste and Printed Circuit Board Recycling Technologies. Cham: Springer International Publishing Kaya, M.

Khaliq, A.; Rhamdhani, M.; Brooks, G.; Masood, S. (2014). Metal extraction processes for electronic waste and existing industrial routes. A Review and Australian Perspective. Resources 3 (1), 152–179. DOI: 10.3390/resources3010152.

Kiddee, P.; Naidu, R.; Wong, M. H. (2013). Electronic waste management approaches. An overview. Waste Management 33 (5), 1237–1250. DOI: 10.1016/j.wasman.2013.01.006.

Kołodzziej, B.; Adamski, Z. (1984). A ferric chloride hydrometallurgical process for recovery of silver from electronic scrap materials. Hydrometallurgy 12 (1), 117–127. DOI: 10.1016/0304-386X(84)90052-5.

Morf, L. S.; Tremp, J.; Gloor, R.; Schuppisser, F.; Stengele, M.; Taverna, R. (2007). Metals, non-metals and PCB in electrical and electronic waste--actual levels in Switzerland. Waste Management 27 (10), 1306–1316. DOI: 10.1016/j.wasman.2006.06.014.

Oguchi, M.; Murakami, S.; Sakanakura, H.; Kida, A.; Kameya, T. (2011). A preliminary categorization of end-of-life electrical and electronic equipment as secondary metal resources. Waste Management 31 (9-10), 2150–2160. DOI: 10.1016/j.wasman.2011.05.009.

Oh, C. J.; Lee, S. O.; Yang, H. S.; Ha, T. J.; Kim, M. J. (2003). Selective leaching of valuable metals from waste printed circuit boards. Journal of the Air & Waste Management Association (1995) 53 (7), 897–902. DOI: 10.1080/10473289.2003.10466230.

Oloruntoba, K.; Sindiku, O.; Osibanjo, O.; Weber, R. (2022). Polybrominated diphenyl ethers (PBDEs) concentrations in soil, sediment and water samples around electronic wastes dumpsites in Lagos, Nigeria. Emerging Contaminants 8 (8), 206–215. DOI: 10.1016/j.emcon.2022.03.003.

Parajuly, K.; Kuehr, R.; Awasthi, A.; Fitzpatrick, C.; Lepawsky, J.; Smith, E. et al. (2019). Future E-waste Scenarios: StEP Initiative, UNU ViE-SCYCLE, UNEP IETC.

Park, Y. J.; Fray, D. J. (2009). Recovery of high purity precious metals from printed circuit boards. Journal of Hazardous Materials 164 (2-3), 1152–1158. DOI: 10.1016/j.jhazmat.2008.09.043.

Pham, V. A.; Ting, Y. P. (2009). Gold bioleaching of electronic waste by cyanogenic bacteria and its enhancement with bio-oxidation. Advanced Materials Research 71-73, 661–664. DOI: 10.4028/www.scientific.net/AMR.71-73.661.

Quinet, P.; Proost, J.; van Lierde, A. (2005). Recovery of precious metals from electronic scrap by hydrometallurgical processing routes. Mining, Metallurgy & Exploration 22 (1), 17–22. DOI: 10.1007/BF03403191.

Robinson, B. H. (2009). E-waste: An assessment of global production and environmental impacts. Science of The Total Environment 408 (2), 183–191. DOI: 10.1016/j.scitotenv.2009.09.044.

Rocchetti, L.; Vegliò, F.; Kopacek, B.; Beolchini, F. (2013). Environmental impact assessment of hydrometallurgical processes for metal recovery from WEEE residues using a portable

prototype plant. Environmental Science & Technology 47 (3), 1581–1588. DOI: 10.1021/es302192t.

Scheutz, C.; Mosbaek, H.; Kjeldsen, P. (2004). Attenuation of methane and volatile organic compounds in landfill soil covers. Journal of Environmental Quality 33 (1), 61–71. DOI: 10.2134/jeq2004.6100.

Sepúlveda, A.; Schluep, M.; Renaud, F. G.; Streicher, M.; Kuehr, R.; Hagelüken, C.; Gerecke, A. C. (2010). A review of the environmental fate and effects of hazardous substances released from electrical and electronic equipments during recycling: Examples from China and India. Environmental Impact Assessment Review 30 (1), 28–41. DOI: 10.1016/j.eiar.2009.04.001.

Step Initiative, 2014. Available online at chrome-extension://efaidnbmnnnibpcajpcglclefindmkaj/https://www.step-initiative.org/files/_documents/whitepapers/StEP_WP_One%20Global%20Definition%20of%20E-waste_20140603_amended.pdf.

Tan, Q.; Li, J.; Zeng, X. (2014). Rare earth elements recovery from waste fluorescent lamps. A Review. Critical Reviews in Environmental Science and Technology 45 (7), 749–776. DOI: 10.1080/10643389.2014.900240.

Tsydenova, O.; Bengtsson, M. (2011). Chemical hazards associated with treatment of waste electrical and electronic equipment. Waste Management 31 (1), 45–58. DOI: 10.1016/j.wasman.2010.08.014.

Tuncuk, A.; Stazi, V.; Akcil, A.; Yazici, E. Y.; Deveci, H. (2012). Aqueous metal recovery techniques from e-scrap. Hydrometallurgy in recycling. Minerals Engineering 25 (1), 28–37. DOI: 10.1016/j.mineng.2011.09.019.

van Heukelem, A. M. H.; Reuter, M. A.; Huisman, J.; Hagelüken, C.; Brusselaers, J.; Refining, U. P. M. (2004). Eco efficient optimization of pre-processing and metal smelting. Electronic Goes Green, 657–661.

van Yken, J.; Boxall, N. J.; Cheng, K. Y.; Nikoloski, A. N.; Moheimani, N. R.; Kaksonen, A. H. (2021). E-Waste Recycling and Resource Recovery: A Review on Technologies, Barriers and Enablers with a Focus on Oceania. Metals 11 (8), 1313. DOI: 10.3390/met11081313.

Yazici, E. Y.; Deveci, H. (2014). Ferric sulphate leaching of metals from waste printed circuit boards. International Journal of Mineral Processing 133 (4), 39–45. DOI: 10.1016/j.minpro.2014.09.015.

CHAPTER 2

2 Literature review

2.1 Metal composition of PCBs

As mentioned earlier, printed circuit boards (PCBs) represent the most economically valuable component of E-waste owing to their high metal content. Metals in PCBs can be classified as precious metals (PMs), base metals (BMs), platinum group metals (PGMs), and rare earth elements (REEs). PCBs are highly heterogeneous and thus metal composition and concentrations vary depending on the manufacturer, the age of the PCBs, and their intended purpose. A PCB of a mobile phone can contain about 13% wt Cu and 350 g Au/ton, compared to approximately 20% wt Cu and 250 g/ton Au in a PCB of a personal computer (Akcil et al. 2015c). Table 2-1 presents the various metal contents and their relative abundances across different types of PCBs reported in the literature. Cu represents the majority of the metals across various PCB types, followed by Al, Fe, Sn, Ni, and Zn. Although PMs constitute the lowest metal fraction by weight of PCBs relative to BMs, they remain the most valuable and industrially targeted metals for recycling. This is due to the high Au content, which can be more than ten times higher than in the primary virgin ores currently mined (Robinson 2009; Akcil et al. 2015c). Moreover, an astounding amount of 320 tons of Au (constituting about 11% of annual global production) and more than 7.500 tons of Ag are incorporated into electrical and electronic equipment (EEEs) products (in PCBs) annually (Kaya 2019a). To this effect, PCBs are classified as high, medium, and low grade, depending on the content of Au (Hagelüken 2006). However, it must be noted that the content of precious metals, especially Au, has been decreasing since the early 2000s due to the high cost associated with manufacturing of PCBs, particularly high grade PCBs. Before the year 2000, the typical content of Au in PCBs was >1000 ppm (Menetti and Tenório 1995), while in recent years, the Au content is in the range of 100 – 500 ppm (Bizzo et al. 2014). Similarly, Widmer et al. (2005) has reported a decrease in Au in PCBs of personal computers, from 4 g to 1 g. Despite this decrease in Au content, PCBs remained richer in precious metal compared to primary ores. This is due to high precious metal that remains in legacy PCBs (mostly already disposed to landfills), and the continuous depletion in the metal grade in virgin ores (Schipper et al. 2018). Moreover, the content and grade of BMs, particularly that of Cu, remain high (see Table 2-1). Thus, this high content of BMs adds to the economic value of the recycling of metals from PCBs and to contribution to supply of increasing metal demand.

Table 2-1 Metal grades of PCBs as reported by various authors (adapted and modified from Bizzo et al. (2014))

Reference	Metal grade (%wt or ppm)								
	Cu (%)	Zn (%)	Sn (%)	Ni (%)	Fe (%)	Al (%)	Au (ppm)	Ag (ppm)	Pd (ppm)
Menetti and Tenório (1995)	20	0.8	1.1	0.8	3.6	4.1	1000	2000	50
Kim et al. (2004)	15.6	0.16	3.24	0.28	1.4	-	420	1240	-
Creamer et al. (2006)	28.7	-	3.8	-	0.6	1.7	68	79	33
Ogunniyi and Vermaak (2007)	20	-	-	1.0	7.0	5.0	250	100	110
Yoo et al. (2009)	19.2	0.7	2.0	5.4	3.6	7.1	100	70	-
Park and Fray (2009)	16.0	1.0	3.0	1.0	5.0	5.0	250	1000	100
Oliveira et al. (2010)	23.5	1.5	1.5	2.4	1.2	1.3	570	3301	294
Guo et al. (2011)	27.50	2.86	3.43	0.40	1.60	1.32	66	29	-
Birloaga et al. (2013)	30.6	1.9	7.4	1.6	15.2	11.7	240	690	-
Yazici and Deveci (2014)	18.5	-	4.91	0.43	2.05	1.33	94.6	763	106.7
Tapia et al. (2022)	10.63	0.131	0.899	0.400	0.932	>1	99	737	-

Owing to the continuous rapid increase in the demand for base metals such as Cu to support the rapid advancement in technology (i.e., demands for advanced electronics, electric vehicles, and for growth in global constructions), there has been a continuous growth in the mining of base metal-bearing ores (Deetman et al. 2018; The Future of Copper). The demand and global production of Cu was less than 500 thousand tonnes per annum since 1900 and has grown at 3.15% per annum to about 22 million tonnes in 2022 (International Copper Study Group 2024). The current Cu demand is forecast to double by 2035 (to 44 million tonnes) and even further increase by 300% from the current demand by the year 2050 (The Future of Copper). Although running out of Cu from primary sources may be improbable (Copper Alliance 2024; International Copper Study Group 2024; Mudd and Jowitt 2018), there is a continuous degradation in the grade of available ores (Schipper et al. 2018). Cu ore grades were approximately 5 – 10% about 150 years ago, while recently, typical Cu ore grades are less

than 1% (Ruth 1995; Mudd 2010; Crowson 2012; Northey et al. 2014), with grades of 0.2 to 0.5% undergoing heap leaching (Harrison 2016a). Consequently, there is a tremendous increase in mining operation costs and the generation of mine waste, largely as tailings (Norgate and Jahanshahi 2010; Mudd and Jowitt 2018; Hu et al. 2017). The latter is associated with an increase in the release of potentially hazardous chemicals like arsenic and acid rock drainage, the undesirable land use and tailing dam failures due to constrained waste storage, all of these resulting in environmental burden (Azam and Li 2010; Hu et al. 2017). All these necessitate the need for the circular use of copper and other critical metals of value from secondary sources. Further, greener methods for the extraction and recovery of such valuable metals from these secondary sources is desirable. One such secondary source of Cu, Ni, Sn, Zn, Al and Co is PCBs, with Cu being by far the most abundant metal and has fairly remained so across various sources of PCBs and over the years (Table 2-1). Setting up appropriate collections for PCBs, and other WEEEs, and developing effective and greener methods for recovery of valuable metals could contribute to readily availing such metals to re-enter the manufacturing sector. Such practices would not only support a circular economy but also contribute to alleviating the environmental burden associated with both an increase in the mining of primary metal sources and rapid generation of WEEE.

2.2 Recycling of PCBs

2.2.1 General pre-treatment of PCBs

Despite the wide variety of types of PCBs, the fundamental compositional structures and design layouts are typically the same, thus enabling a general mechanical processing approach prior to the preferred route(s) for metal extraction and recovery. Figure 2-1 illustrates such general mechanical processing routes currently followed during the industrial recycling of E-waste, including PCBs (Tuncuk et al. 2012a). Although bioleaching of PCBs is not yet commercialised, this pretreatment processing is also adopted during laboratory studies. Regardless of the preferred route of recycling, various components of E-waste are first dismantled and separated. This includes separating metal-rich components of E-waste such as PCBs and electric cables, from non-metallic fractions such as plastics, paper, wood, batteries, and ceramics. For PCBs, this stage allows the manual removal of all extraneous devices such as capacitors, random-access memory (RAMs), peripheral component interconnect (PCIs), diodes, resistors, sensors, inductors, transistors. In addition to sorting out non-metallic and metallic fractions, this pretreatment stage allows the separation of hazardous components and the sorting of reusable components. While the majority of PCBs undergo size reduction to liberate embedded metals post manual dismantling, some PCB particles can readily be fed into the smelters (Khaliq et al. 2014). Various tools used in both industry and research (laboratory and pilot-scale) to target PCB particle size desired include a grab shredder, ball mill, jaw crusher, cutting mill, pulveriser, hammer mill (Yoo et al. 2009; Birloaga et al. 2013; Dutta et al. 2018; Hubau et al. 2019). Though mechanical PCB size reduction is rapid and effective in liberating metals, they are high cost and energy intensive owing to communition and can also result in the loss of valuable metals (Tuncuk et al. 2012b; Jadhav and Hocheng 2015a; Touze et al. 2020; Yamane et al. 2011). Recently, hydrometallurgical processes have been developed to liberate metals from PCBs with no to

minimal mechanical size reduction required. Adhapure et al. (2014) and Jadhav and Hocheng (2015b) successfully removed the chemical coating on large PCB pieces by chemical treatment with 10% sodium hydroxide to liberate metals. To date, this method remains in the development stage at the laboratory scale, however, the method has potential for industrial application as the use of large PCB pieces is desirable to minimise complications in downstream processing (separating of non-metallic fractions) post leaching of pulverised PCBs.

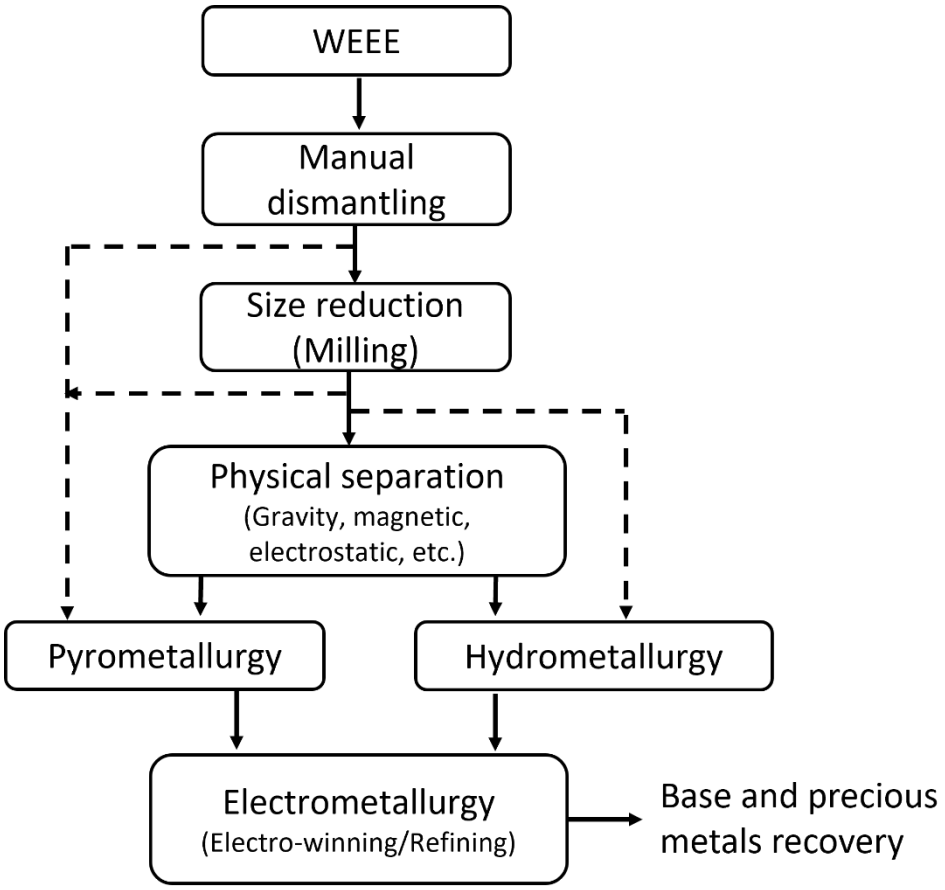

Figure 2-1 Typical flowsheet followed for pretreatment of WEEE (adapted from Tuncuk et al. (2012a))

Nevertheless, fine (typically <2 mm) PCB particles are currently required for hydrometallurgical routes (Zhang and Forssberg 1997; Oliveira et al. 2010), while coarse PCB particles can readily be fed into a smelter (Khaliq et al. 2014; Park et al. 2019). Alternatively, crushed PCB particles are subjected to physical separation (Ruan and Xu 2016; Zhang and Xu 2016) in which physical properties of PCBs such as electric conductivity, specific gravity, and magnetic susceptibility are used to separate non-metallic and metal fractions (Ruan and Xu 2016). Screens such as vibratory, rotating, and trammels screens may be used to sort PCB particles on size into fairly uniform sizes (Kaya 2019a). The physical separation stage can be used to concentrate the metal-rich fractions of the PCBs, increasing the potential economic profit of PCB recycling. In the developing biohydrometallurgical routes, the crushed PCBs are typically screened into uniform sizes and limited studies have reported on the attempt to

separate the non-metallic fractions prior to metal extraction. Ilyas et al. (2007) separated and concentrated their metallic fraction by suspending their finely ground PCBs in saturated sodium chloride solution and stirring the mixture for 10 minutes before allowing it to stand until all heavier particles (metal-rich) settle. Thereafter, the floating particles were decanted while the settled particles were further washed and dried, and used in the bioleaching experiments (Ilyas et al. 2007).

Nonetheless, on the final stage of WEEE recycling, the extracted metals are therefore recovered and refined often through electrometallurgy such as electrowinning (Cui and Zhang 2008; Tuncuk et al. 2012a; Zhang and Xu 2016). Below is the review of pyrometallurgy, hydrometallurgy, and with more focus on the biohydrometallurgy process for the recycling of PCBs.

2.2.2 Pyrometallurgy

Pyrometallurgy is currently the most industrially utilised technique for the recycling of E-waste as nearly any type of E-waste can be processed (Kaya 2019a). In this method, metal extraction is typically through pyrolysis, incineration, combustion, and smelting of the E-waste to produce a copper- and/or lead-metal-rich bullion (Cui and Zhang 2008; Khaliq et al. 2014). High purity Cu is then recovered from the bullions through electrowinning, while PMs are recovered by further electrorefining of the collected slimes (Anindya et al. 2013). There are therefore two types of smelters used globally for the recycling of E-waste, i.e., copper- and lead smelters. Copper smelters are preferred over lead smelters as they produce less hazardous off-gases and fumes, making them suitable to set up and operate near human settlements (Anindya et al. 2013). This has the potential to reduce operational costs associated with the transportation of E-waste and maximise profit during E-waste recycling. The various smelters around Europe currently used for the recycling of E-waste are presented in Table 2-2.

Table 2-2 Current industrial pyrometallurgical processes applied for the recovery of metals from E-waste.

Reference	Company and location	Targeted metals	Feed materials and E-waste annual capacity
Veldhuizen and Sippel (1994); Khaliq et al. (2014)	Noranda process at Noranda, Quebec, Canada	Au, Cu, Pt, Ag, Se, Te, Ni, Pd	Cu concentrates and E-waste (100 kt/year)
L. Theo (1998); Cui and Zhang (2008)	Rönnskår smelter (Boliden Ltd) at Skelleftehamn, Sweden	Pb, Cu, Au, Ni, Ag, Se, Zn	Pb concentrates and E-waste (100 kt/year)
van Heukelem et al. (2004a); Hagelüken (2006)	Umicore integrated metal smelters and refinery at Hoboken, Belgium	Au, Ag, Pt, Se, Te, Sn, Cu, Pb, Ni, As, In, Bi, Ru, Rh, Ir	Waste from non-ferrous industry, PM residues, and PCBs (250 kt/year)
Khaliq et al. (2014); Kaya (2019b)	DOWA group (Kosaka smelter) at Kosaka, Japan	Cu, Au, Ag	E-waste (110 kt/year)
Alvear Flores et al. (2014); Kandalam et al. (2023a)	Aurubis recycling center at Lünen, Germany	Au, Ag, Pd, Pt, Cu, Pb, Zn, Sn	Cu-bearing residues, including E-waste (150 kt/year)
Regel-Rosocka (2018); Recycling towards a circular economy (2022)	Glencore (Horne smelter) at Rouyn-Noranda, Canada	Cu, Ag, Au	Cu- and PMs-bearing materials, including E-waste (118 kt/year)
Wood et al. (2011); Kandalam et al. (2023b)	Global Resources and Materials (GRM Co.) at Danyang, Korea	Cu, Zn, Ni, Au, Ag, Pd, Pt	Cu-bearing residues, and E-waste (110 kt/year)

One of the driving forces for pyrometallurgy as a method of choice for recycling of E-waste is that metal extraction is rapid and recovery efficiency of PMs can be as high as 92 – 98% (Goosey and Kellner 2003). Less mechanical pretreatment is required as some EEEs such as mobile phones can readily be fed into the smelters (Khaliq et al. 2014). In addition, the organic component of E-waste, plastics in particular, can supplement as both an energy source and reducing agent to the traditionally used coke, minimising operation cost. However, pyrometallurgy processes are associated with many limitations, including (Hagelüken 2006; Cui and Zhang 2008; Khaliq et al. 2014):

- The use of plastics as coke limits their recycling practices, post combustion.
- Thermal treatment of materials containing halogenated flame retardants results in the emission of hazardous gases and fumes such as dioxins.
- Only high grade E-waste is suitable as a feedstock for the process to be economically profitable

- Installation and handling of smelters can be challenging and, as such, requires a high level of expertise and large investments.

It must be noted that the latest developed smelters are integrated with off gas systems to isolate emitted hazardous gases and minimise environmental burden. However, such systems add to both installation and running costs.

2.2.3 Hydrometallurgy

Hydrometallurgy is currently an alternative route to pyrometallurgy for metal extraction and recovery from PCBs. Relatively low capital investment is required to set up and operate hydrometallurgy processes compared to pyrometallurgy. As such, the process is suitable even for small scale applications (Cui and Zhang 2008; Dhawan et al. 2009; Kaya 2016b). Moreover, the environmental burden is reduced as there are no emissions of hazardous gases and dust (Khaliq et al. 2014; Zhang and Xu 2016). As metals in PCBs are typically present as alloys, strong oxidants are required for metal extraction (Quinet et al. 2005; Cui and Zhang 2008; Tuncuk et al. 2012a). Contrary to pyrometallurgy, intense mechanical pretreatment is required to liberate metals and improve metal extraction efficiency (Zhang and Forssberg 1997; Khaliq et al. 2014). Nonetheless, another convenience for hydrometallurgical routes is that metals can be targeted selectively based on the choice of leaching lixiviant used. Extraction of precious metals is achieved through the use of strong acids such aqua regia (combination of H_2SO_4, HCl, and HNO_3), cyanide (CN^-/SCN^-), halide ($I^-/Br^-/Cl^-$), thiourea ($CS(NH_2)_2$), ammonium (NH_3–$(NH_4)_2S_2O_8$) or thiosulfate ($CuSO_4$–NH_4OH–$(NH_4)_2S_2O_3$) based lixiviants (Quinet et al. 2005; Cui and Zhang 2008; Sethurajan et al. 2019; Islam et al. 2020; Akcil et al. 2021). On the other hand, base metals can be extracted through acid leaching (i.e., H_2SO_4, HCl, and HNO_3) in combination with strong oxidants such as O_2, H_2O_2, or Fe^{3+} (Kumar et al. 2014; Yazici and Deveci 2014; Cortes and Patiño 2016; Bilczuk et al. 2016; van Yken et al. 2020). Owing to this selectivity in leaching based on the lixiviant used, Birloaga et al. (2013) developed a two-step leaching system to leach both PMs and BMs. The first step involved the leaching of Cu (90% Cu) by H_2SO_4 in the presence of H_2O_2 oxidant as Cu negatively interferes with the leaching of Au. At the second step, Au was then leached (69% Au) through thiourea and Fe^{3+} oxidant in an H_2SO_4 medium (Birloaga et al. 2013). Although metal extraction may not be as rapid as in pyrometallurgy, high metal extraction efficiency can be achieved, i.e., >90% PMs and BMs (Oh et al. 2003; Rabah 2008; Park and Fray 2009; Yazici and Deveci 2014; Sethurajan et al. 2019). Table 2-3 summarises the various PMs and BMs extraction efficiencies achieved through hydrometallurgical leaching of E-wastes using various leaching lixiviants.

Table 2-3 Various reported hydrometallurgical routes for the leaching of valuable metals from different types of E-wastes

Reference	Type of E-waste	Lixiviant used and conditions	Metal targeted and leaching efficiency
Huang et al. (2014)	PCBs	80% (v/v) 1-Butyl-3-methylimidazolium hydrogen sulfate (ionic liquid), 30% H_2O_2, solid/liquid: 1/25, 70 °C, 2 h	Cu (99.92%)
Lambert et al. (2015)	Electric cables	Fe^{3+} in H_2SO_4 medium, 50 °C, 24 h	Cu (90%)
Ficeriová et al. (2011)	PCBs	$CuSO_4.5H_2O$, NH_3, $(NH_4)_2S_2O_3$, 40 °C, 48 h	Au (98%), Ag (93%), Pd (90%)
Oh et al. (2003)	PCBs	NH_4OH, $CuSO_4$, $(NH_4)_2S_2O_3$, 40 °C, 48 h	Au (95%), Ag (100%)
Rabah (2008)	Fluorescent lamps	Aqua regia (HNO_3:H_2SO_4), 125 °C, 5 MPa, 4 h	Y (96%), Eu (93%)
Park and Fray (2009)	PCBs	Aqua regia (HCl: HNO_3), solid liquid: 1/20, 20 °C, 3 h	Au (97%), Ag (98%), Pd (93%)
Yazici and Deveci (2013)	PCBs	H_2SO_4, $CuSO_4$, NaCl, 80 °C, 2 h	Ag (92%), Fe (>90%, Ni (>90%), Pd (58%)
Birloaga et al. (2013)	PCBs	Two-step leaching Step 1: H_2SO_4, H_2O_2 (30%), 30 °C, 3 h. Step 2: $CS(HN_2)_2$, Fe^{3+}, H_2SO_4, 40 °C, 3.5 h	Cu (90%), Au (69%)

Following metal extraction, metal recovery from the pregnant leachates can achieved by cementation, ion exchange, solvent extraction, and/or electrowinning (Vegliò et al. 2003; Veit et al. 2006; Lewis 2010; Yang et al. 2013; Jha et al. 2016). Notwithstanding the advantages of hydrometallurgy over pyrometallurgy, the process is no exception to drawbacks which limit its application at the industrial scale, including (Cui and Zhang 2008; Tuncuk et al. 2012a; Khaliq et al. 2014; Sethurajan et al. 2019):

- Hydrometallurgical processes are typically slow and the long operation times add to the overall capital cost of the process.
- The required intense mechanical pretreatment to liberate embedded metals is reported to result in up to 20% loss of precious metals, lowering the economic value of recycling.

- Leaching lixiviants such as cyanides are highly toxic and pose environmental risks to the surrounding rivers and groundwater if released. Halide-based leaching lixiviants are highly corrosive and result in equipment degradation. Specialised stainless steel or rubber-based equipment is required, which increases capital cost. Moreover, proper handling of the effluent is required.

2.3 Biohydrometallurgy for treatment of PCBs

Biohydrometallurgy (biomining or bioleaching) involves leaching of metals through a hydrometallurgical process catalysed by microorganisms present within the system. This process continues to receive attention as a promising technology over both pyrometallurgy and hydrometallurgy for the recycling of E-waste. Amongst other factors, this is because the process requires less energy as operating temperatures are typically low, reagents used are less corrosive, and lixiviants are continuously regenerated by the microorganisms present, with minimal requirements for continuous addition of lixiviant and effluent (Chauhan et al. 2018; Habibi et al. 2020). Thus, the technology is more environmentally friendly than the traditional routes. Moreover, setting up/installation of bioleaching technology requires less investment and is suitable for small-scale application and recycling of even low-grade PCBs (Priya and Hait 2017). Below is a review of the mechanism of metal leaching, the role of microorganisms, challenges, and opportunities for bioleaching of E-waste.

2.3.1 Mechanism of metal dissolution

Bioleaching is applicable for the leaching of both base and precious metals (Işıldar et al. 2016; Kumar et al. 2018; Srichandan et al. 2019; van Yken et al. 2020). In the leaching of base metals, metal dissolution through bioleaching is generally accepted to occur via the indirect mechanism involving two sub-processes: (i) acidophilic chemolithotrophs, including iron and/or sulfur oxidising bacteria and/or archaea such as *Acidithiobacillus* (*At.*) *ferrooxidans, Leptospirillum* (*L.*) *ferrooxidans*, and *Metallosphaera* (*M.*) *hakonensis* oxidise already solubilised ferrous iron (Fe^{2+}) under acidic conditions to generate ferric iron (Fe^{3+}) as in Eq. 2-1 and/or reduced sulfur compounds such as sulfide or elementary sulfur to generate sulfuric acid as in Eq. 2-2 and Eq. 2-3 (Ilyas et al. 2013; Bryan et al. 2015); (ii) The resultant Fe^{3+} and H^{+} are powerful oxidants which can readily oxidise base metals in PCBs, leading to their dissolution as metal ions as presented in Eq. 2-4 and Eq. 2-5 (Srichandan et al. 2019; Adetunji et al. 2023).

$$2Fe^{2+} + \frac{1}{2}O_2 + 2H^{+} \xrightarrow{microorganims} 2Fe^{3+} + H_2O \qquad \textit{Eq. 2-1}$$

$$4FeS_2 + 15O_2 + 2H_2O \xrightarrow{microorganims} 2Fe_2(SO_4)_3 + 2H_2SO_4 \qquad \textit{Eq. 2-2}$$

$$2S^0 + 3O_2 + 2H_2O \xrightarrow{microorganims} 2H_2SO_4 \qquad \textit{Eq. 2-3}$$

$$2M^0 + 2Fe^{3+} + \frac{1}{2}O_2 + 2H^+ \rightarrow 2M^{2+} + 2Fe^{2+} + H_2O \quad \textit{Eq. 2-4}$$

$$M^0 + \frac{1}{2}O_2 + 2H^+ \rightarrow M^{2+} + H_2O \quad \textit{Eq. 2-5}$$

While the leaching of metals such as Zn by H^+ and O_2 is thermodynamically more spontaneous than Fe^{3+} leaching, their experimental leaching kinetics have been reported to be slower (Lambert et al. 2015). Xiang et al. (2010) reported dissolution of copper by acid (H^+) action during bioleaching of PCB. In their study, the control test was inoculated with microorganisms enriched from natural acid mine drainage, and maintained at pH 2.0, in the absence of ferrous iron. The authors observed that Cu was dissolved into solution, according to Eq. 2-5, but at much slower leaching rates than when in the presence of ferric iron in an acidified solution. Similar results have been reported by Hubau et al. (2020) and van Yken et al. (2020).

On the other hand, leaching of precious metals is achieved by employing organotrophs such as cyanogenic microorganisms (i.e., *Pseudomonas aeruginosa*, *Pseudomonas chlorophis*, *Chromobacterium violaceum*, *Pseudomonas fluorescens*) and fungal species (i.e., *Polysporus* sp. and *Marasmius oreades*) (Natarajan and Ting 2014; Srichandan et al. 2019; Wang et al. 2021). These bioleaching microorganisms solubilise precious metals by producing strong oxidants such as hydrogen cyanide (HCN) through the cyanogenesis process from the organic carbon source (Chi et al. 2011; Wang et al. 2021). The HCN (metabolites) complexes with precious metals from E-wastes to form soluble metal-cyanide complexes, thereby leading to metal extraction Eq. 2-6 (Liang et al. 2014). Cyanogenesis occurs in the presence of glycine as it is the metabolic precursor for the production of HCN. Kumar et al. (2018) reported bioleaching efficiencies of Au (69%) and Ag (34%) from PCBs at optimised conditions of glycine: 5 g/L, temperature: 30 °C, solid loading: 1% w/v, pH: 9.0, and leaching time of 3 h, in the presence of *Pseudomonas balearica* SAE1. Similarly, Işıldar et al. (2016) achieved 44% Au extraction during bioleaching of PCBs by *Pseudomonas putida* at optimum conditions of glycine: 10 g/L, solid loading: 1% w/v, temperature: 30 °C, pH range: 7.3 – 8.6, and leaching time of 2 days. Precious metals are also reported to have been successfully solubilised from different types of E-waste, using various cyanogenic microorganisms (Chi et al. 2011; Motaghed et al. 2014; Li et al. 2020; Golzar-Ahmadi and Mousavi 2021).

$$2Au + 4CN^- + H_2O + \frac{1}{2}O_2 \rightarrow 2Au(CN)_2^- + 2OH^- \quad \textit{Eq. 2-6}$$

It must be noted that the bioleaching of precious metals must be preceded by the bioleaching of base metals as high concentrations of base metals negatively affect the leaching of precious metals by complexing with the metabolites produced (Işıldar et al. 2016). Moreover, bioleaching efficiencies of precious metals are typically low, as low yields of *in-situ* microbial production of cyanide are typically achieved and E-waste can be toxic to the cyanogenic

microorganisms, further impeding cyanide production and subsequent metal leaching (Wang et al. 2021). As such, studies on the application of bioleaching of E-waste have mostly been on the leaching of base metals by acidophilic chemolithotrophs. It is expected that the subsequent chemical leaching of the precious metals may yield improved performance (Wang et al. 2021). As this PhD study also focuses on the bioleaching of base metals, this literature review is mainly limited to the bioleaching of base metals by chemolithotrophic microorganisms.

2.3.2 Role of microorganisms in bioleaching

Acidophilic chemolithotrophs (also known as chemolithoautotrophs), the common microorganisms (bacteria and archaea) implicated in bioleaching of base metals, obtain energy for growth from the oxidation of inorganic elements and compounds such as Fe^{2+} to Fe^{3+} and elemental sulfur or reduced sulfur (i.e., S_8, $S_2O_3^{2-}$, H_2S, and/or polysulfide) to H_2SO_4 (Schippers and Sand 1999; Valdés et al. 2008; Srichandan et al. 2019). In contrast to the traditional bioleaching of mineral sulfides, these microorganisms mainly draw growth energy from the oxidation of Fe^{2+} formed during bioleaching of E-waste in which metals exist in native form or as alloys or both, with no to minimal sulfur elements and compounds present (Tuncuk et al. 2012a). The absolute mechanisms of Fe^{2+} oxidation systems or order of electron transfer in a microbial cell remain a subject of research. Currently, the proposed models are based on three electron carriers as illustrated in Figure 2-2 (Ingledew 1982; Hazra et al. 1992; Giudici-Orticoni et al. 1999; Li et al. 2015). Briefly, electrons are thought to be transferred through the outer-membrane cytochrome into the periplasmic (Yarzábal et al. 2002). The periplasmic is composed of an acid tolerant (outer pH of <2.0) type I blue Cu protein known as rusticyanin (Cobley and Haddock 1975; Blake and Shute 1994). Electrons are further transferred from the rusticyanin via cytochrome a_i by unknown enzymes to molecular oxygen at the cytoplasm and subsequently result in the production of water and maintain the alkaline (pH at approximately 6.5) nature of the inside of the cell (Gai et al. 1992; Sugio et al. 2010).

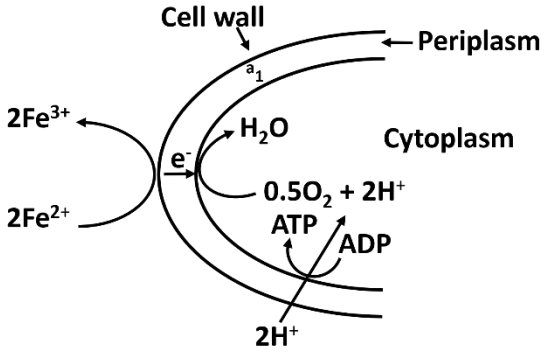

Figure 2-2 Proposed electron pathways during Fe^{2+} oxidation by bacterium, adapted from (Nemati et al. 1998)

Chemolithotrophic bioleaching microorganisms are classified into three categories based on their optimum temperature range for microbial growth. Mesophilic cultures grow at an optimum temperature range of 28 – 37 °C (Rawlings 2005). These are primarily bacteria such

as *L. ferrooxidans*, *At. ferroxidans*, *At. thiooxidans* and some strains of *L. ferriphilum* (Coram and Rawlings 2002). Moderate thermophiles are characterised by a growth temperature range of 40 – 60 °C (Franzmann et al. 2005). These also primarily include bacteria such as *At. caldus*, *Acidimicrobium* sp., *Acidithiomicrobium* sp., and *Sulfobacillus* sp.; but also include archaea such as *Acidiplasma (A.) cupricumulans* (Dew et al. 2011; Brierley 2001). The last category is thermophiles (sometimes referred to as extreme thermophiles) which thrive at a temperature range of 60 – 80 °C. Examples of extreme thermophiles include archaea such as *Metallosphaera (M.) hakonensis*, *Sulfolobus (S.) metallicus*, *Acidianus brierley*, and *S. ambioalous* (Kurosawa et al. 2003; Rawlings and Johnson 2007b). Based on these various optimum temperature ranges for microbial growth and activity, specific microbial cultures can be targeted. In addition to the temperature, other physiochemical parameters such as the composition of the growth medium, solution pH, and redox potential can be exploited in isolating the targeted microbial strains in a bioleaching system. *L. ferriphilum* thrives at pH 1.4 – 1.8 and is tolerant to higher redox potential (>650 mV) compared to *At. ferrooxidans*, with a pH range of 1.7 – 2.5, and thrive at relatively low redox potential (<650 mV) (Pronk and Johnson 1992; Govender et al. 2015). Ngoma et al. (2015) investigated the effect of acid stress (pH) on the microbial community structure of a mesophilic culture initially composed of 90% *L. ferriphilum*, 3% *Ferroplasma* (*F.*) *acidophilum*, 5% *A. cupricumulans* and 1% *At. ferrooxidans*. *L. ferriphilum* was observed to increase in dominance to 97, 98, and 100% when the culture was subjected to 0.34, 0.51, and 0.68 mol.L^{-1} H_2SO_4, respectively, while the other species were below the detection limit at above 0.51 mol.L^{-1} acid (Ngoma et al. 2015).

Mesophiles and moderate thermophiles, particularly *At. ferrooxidans*, *L. ferrooxidans*, *L. ferriphilum*, and *At. thiooxidans* are by far the most exploited cultures in the bioleaching of E-waste. This is mainly due to their low operating temperatures, high metal ion tolerance, and high Fe affinity relative to thermophiles (Awasthi et al. 2016; Baniasadi et al. 2019; Castro et al. 2019; Hubau and Bryan 2023). These microbial cultures have successfully been employed, either as pure or mixed cultures, for the leaching of base metals, especially for Cu, from different types of E-waste as summarised in Table 2-4.

Table 2-4 Summary of reported bioleaching efficiencies achieved during leaching of metals from PCBs.

Characterization of microorganisms	Dominant microorganisms	Conditions	Metal extracted (%)	Reactor type	Reference
Mesophilic bacteria	*At. ferrooxidans*	pH 1.0, 30 °C, particle size 114.02 µm, and 0.85% w/v PCBs.	100% Cu and Ni, in 55 days	Shake flask	Arshadi and Mousavi (2015)
	At. thiooxidans	1.6% w/v PCBs, 30 °C, and 1.6 g/L biochar as catalyst.	98% Cu and 82% Ni, in 72 h	Shake flask	Kadivar et al. (2021)
	At. ferrooxidans	pH 2.0, 20 – 35 °C, and 5% w/v PCBs	96% Cu, 65% Ni, 94% Al, 95% Sn, and 93% Zn in 80 days	Stirred tank	Fu et al. (2021)
	At. ferrooxidans, and *At. caldus*	pH 1.4, 35 °C, and 5% w/v PCB	79% Cu, 73% Ni, 85% Al, and 91% Zn in 50 h	Stirred thank	Van Yken et al. (2023)
	At. ferrivorans and *At. thiooxidans*	pH 1.0 – 1.6, 23 °C, and 1% w/v PCBs	98% Cu in 7 days	Shake flask	Işıldar et al. (2016)
	At. ferrooxidans, ferrooxidans, and *At. thiooxidans*	pH 1.8, 10% w/v PCBs	97% Cu, 56% Al, 79% Ni, and 67% Zn over 8 days	Stirred tank	Erust et al. (2020)
Moderate thermophilic bacteria	*L. ferrooxidans* and *At. ferrooxidans*	pH 1.0, 60 °C, and 1% PCB	99% Cu in 165 days	Stirred tank	Iglesias-González et al. (2024)
	Sulfobacillus thermosulfidooxidans	pH 1.75, 50 °C and 25 g/L PCB	85% Cu in 8 days	Rotating-drum reactor	Rodrigues et al. (2015)
	L. ferriphilum and *At. caldus*	45 °C, pH 2.0, and 8% w/v PCBs.	77% Cu, 85% Zn, 70% Al in 7 days	Stirred tank	Xia et al. (2017)
	L. ferriphilum and *Sulfobacillus thermosulfidooxidans*	pH 0.9, 42 °C and 10% w/v PCBs	93.4% Cu in 9 days	Shake flask	Wu et al. (2018)

2.3.3 Factors affecting bioleaching of PCBs

With the proof of concept of bioleaching successfully adopted from traditional leaching of metals from mineral sulfides to leaching of metals from E-waste since the early 2000s, there has been research interest in factors affecting leaching rates and extent of metal leaching. These factors include solution pH, solid loading, microbial consortium, temperature as reviewed below.

2.3.3.1 Solution pH

Solution pH is one of the crucial parameters in a bioleaching system as it affects: (i) solubility of the primary Fe^{3+} oxidant and formation of jarosite precipitates, (ii) microbial Fe^{2+} oxidation as per Eq. 2-1, (iii) microbial community structure, and (iv) extent of metal extraction as per Eq. 2-5. As such, there have been extensive studies on the effect of solution pH on the bioleaching of PCBs, and the optimum pH range is recommended to be 1.0 to 2.0 (Yang et al. 2009; van Yken et al. 2020). Higher pHs negatively impact maintaining the Fe^{3+} oxidant in solution (Yang et al. 2009; Xiang et al. 2010; Zhu et al. 2011; van Yken et al. 2020), while lower pHs impact the performance of some key microorganisms (Ngoma et al. 2015). Due to the alkaline nature of PCBs (Arshadi et al. 2018), solution pH can increase above 2.0 during metal leaching. At this high pH, precipitation of Fe^{3+}, typically as jarosite, is promoted (Rodrigues et al. 2015; Baniasadi et al. 2019). This adversely affects metal leaching rates as the primary oxidant is reduced in solution. Further, metal leaching can be limited as jarosite can deposit on the surface of the metal-rich PCBs, creating a mass transfer barrier (Niu et al. 2015; Priya and Hait 2018). Solution pH is maintained below 2.0 by continuous addition of H_2SO_4 whenever necessary during metal leaching and also by the addition of combined Fe and S sources such as pyrite (FeS) or elementary sulfur (Xia et al. 2017; Hubau et al. 2020). The latter has been explored as an energy source for microbial culture growth while also compensating for the required H^+ to maintain acidity and provide the Fe^{3+} oxidant, according to Eq. 2-2 and Eq. 2-3 (Ilyas et al. 2013; Bryan et al. 2015).

2.3.3.2 Effect of initial concentration of ferrous iron

Based on the bioleaching reactions presented in Eq. 2-1 and Eq. 2-4, the dissolution of metals from PCBs is dependent, amongst other factors, on the availability of ferrous iron and the rate of regeneration of ferric iron. Yang et al. (2009) investigated the effect of varying the initial concentration of ferrous iron (3 to 9 g/L) on the leaching efficiency of Cu from PCBs using *At. ferrooxidans* at pH 2.0. Copper dissolution was completed at initial ferrous iron concentrations of 3, 5, 7, and 9 g/L, at 96, 60, 48, and 36 h, respectively; indicating that metal leaching efficiency is dependent on initial ferrous iron concentration. Similar results were reported by Bas et al. (2013) in the bioleaching of copper from PCBs, using a mixed culture of mesophilic bacteria dominated by *At. ferrooxidans*, *At. thiooxidans* and *L. ferrooxidans*. Copper extraction was observed to improve with an increase in initial ferrous iron concentration, from 35% at 0 g/L to 89% at 8 g/L ferrous iron. Improvement in metal leaching efficiency with an increase in initial concentration of ferrous iron was attributed to the microbial generation of the Fe^{3+}

product. In the absence of microbial inhibition, a high concentration of the Fe^{3+} oxidant can be availed from a high initial concentration of Fe^{2+}, which promotes faster facilitation of metal leaching. Conversely, similar high metal leaching rates can be achieved by the direct addition of Fe^{3+} rather than Fe^{2+} at the beginning of the bioleaching (Kinnunen and Puhakka 2005; van Yken et al. 2020). In such an approach, microbial growth follows from the resultant Fe^{2+} post-metal leaching. In either approach, the concentration of Fe in the solution is critical as it may result in substrate (Fe^{2+}) and/or product (Fe^{3+}) inhibition (Kinnunen and Puhakka 2005; Ozkaya et al. 2007; Khachatryan et al. 2021). Lastly, the ratio of Fe^{3+}/Fe^{2+} influences the redox potential, which is critical in microbial growth and activity (Smith and Johnson 2018; Erust et al. 2020).

2.3.3.3 Microbial consortia

The type of microbial consortia employed in the bioleaching system affects the leaching efficiency as various microbial communities exhibit different tolerance to accumulated metal ions and have different Fe^{2+} affinity. For example, *Leptospirillum* sp. are reported to have higher Fe^{2+} affinity than *At. ferrooxidans* (Pronk and Johnson 1992; Bryan et al. 2012). Mesophiles exhibit higher metal ions tolerance than thermophiles (Castro et al. 2019). In addition to the type of microbial consortia employed, the use of mixed or pure cultures results in different leaching efficiencies. Liang et al. (2010) investigated bioleaching of PCBs by pure and mixed cultures of *At. thiooxidans* and *At. ferrooxidans*. Bioleaching efficiencies of Cu, Ni, Zn, and Pb were 78, 73, 75, and 71%, respectively by *At. thiooxidans*. These were slightly improved to 80, 73, 76, and 72%, respectively when leached by *At. ferrooxidans*. Further improvements to 94 Cu, 89 Ni, 90 Zn, and 86% Pb for Cu, Ni, and Pb, respectively, were reported when a mixed culture was employed (Liang et al. 2010). Similar results are reported by Mrazikova et al. (2013) – 60% Cu was leached from PCBs by mixed culture of *At. thiooxidans* and *At. ferrooxidans* over 14 days, while only 22% Cu was mobilised by pure cultures over the same leaching period. In both these studies, improvements associated with mixed cultures can be attributed to synergistic effects with respect to individual pure cultures.

Another factor associated with microbial consortia is the effect of initial inoculum concentration. Bas et al. (2013) further studied the effect of microbial population size on the rate and extent of copper extraction from PCBs. By keeping the concentration of PCBs at 1% w/v, adding 1% w/v pyrite, maintaining pH at 1.7, and temperature at 35 °C, they varied the initial microbial concentration from 10% v/v to 50% v/v. The rate and extent of copper extraction was observed to increase with an increase in the microbial population size. At the maximum inoculum size tested (50% v/v), 67% copper was extracted after 37 h compared to 15% copper extracted at 10% v/v over the same duration. The authors attributed the improvement of copper extraction to the rapid conversion of ferrous iron to ferric iron at a higher initial microbial population size.

2.3.3.4 The effect of temperature

As mentioned earlier (Section 2.3.2), the operating temperature can be associated with the choice of the microbial consortia. While the chemical leaching of metals by Fe^{3+} oxidant may

be improved with an increase in temperature, thermophiles may be more susceptible to metal ions inhibition than mesophiles. Therefore, a trade-off between high rates of metal leaching and sustaining microbial activity may be necessary. Nevertheless, several studies have evaluated the effect of temperature on the bioleaching of E-waste (Hong and Valix 2014; Kumar et al. 2018; Fu et al. 2021). Lambert et al. (2015) studied the effect of temperature in the bioleaching of Cu from waste electric cables using *At. ferrooxidans*, across the range of 21 to 50 °C. The copper leaching kinetics were reported to increase with an increase in temperature. The time needed to dissolve 90% copper was found to be 77, 36, and 19 h at temperatures of 21, 35, and 50 °C, respectively. The authors concluded that the rate of Cu leaching in the presence of microorganisms increased with an increase in temperature.

2.3.3.5 Other factors

Other factors affecting the bioleaching of metals from E-waste include (i) the effect of particle size distribution and PCB sample preparation and (ii) solid loading (pulp density). The latter is reviewed in the next section below. The effect of particle size has been highlighted in section 2.2.1. Briefly, fine particle sizes (<2 mm) increase reaction surface area and maximise metal liberation, and high metal extractions can be achieved. High metal leaching efficiencies can also be achieved from coarse to large particles but require prior chemical treatment of the PCB samples to remove the coat and liberate the metal of interest (Adhapure et al. 2014).

2.3.4 Limitation of bioleaching

The research in understanding the factors affecting the bioleaching of PCBs continues to contribute to better understanding and improvement of the process. Although some of these studies, particularly the shake flask experiments, may have limited contribution towards process optimisation as there are limitations in understanding mass transfer, the increased interest in the use of bench-top reactor systems is essential towards pilot-scaling and subsequent commercialisation. In both shake flasks and bench-top reactor systems, one of the major challenges is the discrepancy in rates of Fe^{3+} reduction as a function of metal leaching and the microbial regeneration of Fe^{3+} from the resultant Fe^{2+}. The Fe^{3+} reduction rates has been reported to be 11 times faster than the microbial Fe^{2+} oxidation rates (Wu et al. 2018). As such, microbial Fe^{2+} oxidation is the rate-determining step in bioleaching systems. The slow rates in the microbial Fe^{2+} oxidation result in longer operating duration and to an extent, render no benefits of microbial culture bioleaching systems. In addition to the natural slow growth of microbial culture, the observed slow microbial Fe^{2+} oxidation rate is exacerbated by the inhibition of microbial culture by accumulated metal ions as reviewed below.

2.3.4.1 Microbial inhibition

The toxicity of E-waste to microbial culture remains one of the main challenges in bioleaching systems. As metals leach, they accumulate within the bioleaching system. Metal ions are essential in the metabolism of microorganisms for their growth and activity. Metals such as Cu, Mg, Fe, K, Zn, Mn, Cr, Co, Ca, Mg, and Ni are micronutrients as they serve as co-factors to various enzymes, catalyze some of the biochemical reactions, regulate osmotic pressure, and

act as a stabiliser for protein structures (Nies 1992; Bruins et al. 2000). However, metals such as Au, Ag, Al, Hg, and Pb are nonessential and add no nutritional value (Bruins et al. 2000). Thus, depending on the type of metal ion and its concentration, the accumulated metal ions in the bioleaching system can exert an inhibitory effect on the microbial culture. It is therefore important to evaluate the relative potential inhibitory effect with respect to each metal ion within the bioleaching system. At inhibitory concentrations, these metal ions adversely affect cell functionality by altering enzyme activity, and even damaging deoxyribonucleic acid (DNA) structures (Nies 1992; Bruins et al. 2000; Zhang et al. 2023). Overall microbial activity is therefore impeded and more often results in cell death. Microbial inhibition by metal ions is well documented even on traditional bioleaching of mineral sulfides (De et al. 1997; Sampson and Phillips 2001; Xia et al. 2008; Sajjad et al. 2019). On bioleaching of E-waste, the observed microbial inhibition is thought to be exacerbated by the non-metallic components of E-waste such as organic compounds and plastics which may be liberated during metal leaching (Lambert et al. 2015; Bryan et al. 2015).

In PCB bioleaching systems, potential microbial inhibition is mainly studied by varying PCB solid loading (w/v). The amount of PCBs added per working volume of the reactor system is a critical parameter as it affects concentrations of metal ions in the leachates. While it may be economically desirable to process high solid loading, microbial performance is reduced with an increase in PCB solid loading. Brandl et al. (2001) investigated the effect of varying PCB solid loading (from 0.5 – 10% w/v PCBs) on microbial growth and metal solubilisation by *At. thiooxidans* and *At. ferrooxidans*. Microbial growth was inhibited from 1% loading and above. The inhibition was speculated to be a result of accumulated metal ions such as Al. Zhu et al. (2011) reported a maximum Cu dissolution of 98% at 0.4% w/v PCBs, compared to 93 – 94% Cu at 0.8 – 1.2% w/v PCBs, and 73% Cu at 1.6% PCBs during bioleaching of PCBs by mixed culture of acidophilic bacteria (consisting of genera *Acidithiobacillus*, *Gallionella*, and *Leptospirillum* sp.) isolated from acid mine drainage solution collected from Guangdong, China. The authors attributed reduced metal leaching efficiency with an increase in PCB loading to limited O_2 oxygen mass transfer and elevated metal ions concentrations at high PCB loading and recommended 1.2% w/v PCB as optimum loading (Zhu et al. 2011). Erust et al. (2020) explored higher PCB loading, i.e., 2.5 – 15% w/v PCB, during metal bioleaching by mixed culture of *At. ferrooxidans* DSMZ 583, *L. ferrooxidans* DSM 2705, and *At. thiooxidans* DSMZ 9463. Similarly, the authors observed a decrease in metal leaching with an increase in PCB loading and they recommended an optimum loading of ≤10% w/v PCBs.

Evaluating the potential inhibition of microbial culture at various PCB solid loading provides crucial insight into the optimum PCB loading at which microbial culture performance is maintained with high metal extracted. However, in such systems, there are limitations in understanding the inhibitory effect of each metal ion or in their combination, and that of non-metallic components. Studying potential inhibitory effects by synthetic metal ion solutions, either as individuals or in their combinations, could contribute to the decoupling inhibition by metal ions and that of non-metallic components. As PCBs contain up to 50 metals, priority should be on the dominant metals across different PCBs as those will be in high concentrations in leachates. There are limited studies on the effect of metal ions on microbial activity and subsequent metal leaching in the context of PCB bioleaching systems (Bryan et al. 2015;

Hubau et al. 2020). However, there are several studies on metal ion inhibition in the context of bioleaching of mineral sulfides (Das et al. 1997; De et al. 1997; Sampson and Phillips 2001; Nurmi et al. 2009; Edward et al. 2018). As microbial consortia used in the bioleaching of PCBs and metals of interest (but with different expected metal concentrations in leachates) are generally the same as in the bioleaching of mineral sulfides, knowledge of inhibition by pure metals can be shared to a certain degree. As mentioned earlier, the severity of microbial inhibition is subject to the type of metal ion and its concentration, and the type of microbial consortia used. Sampson and Phillips (2001) investigated and compared the effect of Cu^{2+}, Co^{2+}, and Ni^{2+} on the microbial Fe^{2+} oxidation rates during bioleaching of pyritic-gold concentrate by mixed mesophiles (*At. ferrooxidans* and *L. ferroxidans*) and moderate thermophiles (*S. thermosulphidoxidans* and *S. acidophilus*). At 2.54 and 5.08 g/L Cu^{2+}, the Fe^{2+} oxidation rate was reduced by 30% and 50%, respectively, while the same concentrations of Ni^{2+} and Co^{2+} had no notable inhibitory effect. Microbial Fe^{2+} oxidation rate by moderate thermophiles was reduced between 20 – 30% at the addition of about 0.50 – 5.0 g/L of each metal ion, respectively (Sampson and Phillips 2001). Nurmi et al. (2009) showed that various binary combinations of Fe^{3+}, Zn^{2+}, and Ni^{2+} at 0 – 60 g/L of each metal, had a more severe inhibitory effect on the Fe^{2+} oxidation rate by *L. ferriphilum* dominated culture than individual metal ions.

2.3.5 Strategies to minimise microbial inhibition

Minimising inhibition of the microbial culture so that continued microbial growth and activity is sustained is key to improving bioleaching efficiency. Such can be achieved through the natural tendency of microorganisms to resist metal ion inhibition to a certain degree. Some cells achieve this by self-regulating their physiological functions and/to maintaining their growth and activity in the presence of metal ion stress (Zhang et al. 2023). There are five known mechanisms for microbial resistance to toxic metal ions as reviewed by Bruins et al. (2000) and Dopson et al. (2003). These include, (i) metal exclusion by permeability barrier: prevention of inhibitory metal ions from entering cells by formation of permeable barrier such as extracellular polymeric substances (EPS). (ii) Intra- and extra-cellular sequestration by protein binding: metals that eventually/inevitably permeate into the cell undergo intracellular chelation and are converted to low/non-toxic forms. (iii) Enzymatic detoxification of metal to less toxic forms: certain microorganisms lessen the toxicity of metal ions through enzymatic reactions, a common example is mercury reductase. (iv) Reduction in metal sensitivity of cellular targets: microorganisms adapt to metal stress by mutation, though without altering their basic cell functions, to reduce sensitivity. (v) Active transport of the metal away from the microorganisms: microorganisms can efflux toxic metal ions from their cytoplasm through active transport mechanisms such as plasmid-encoded or chromosomal. These natural metal ions resistance mechanisms can be enhanced by techniques such as adaptation of microbial culture to high metal ions prior to bioleaching and immobilisation of microbial culture on biomass support particles to promote biofilm formation.

2.3.5.1 Microbial adaptation

Microbial adaptation to potential metal ions toxicity is achieved by gradually acclimatising microbial culture to increasing concentrations of target metal ion(s). This method is by far the

most exploited in minimising the inhibition of microbial culture in the bioleaching of both mineral sulfides (Govender et al. 2015; Nkuna et al. 2022; Africa et al. 2013) and PCBs (Arshadi and Mousavi 2015; Fu et al. 2021; Tapia et al. 2022; Lambert et al. 2015). Xia et al. (2008) adapted *At. ferrooxidans* to 5% w/v chalcopyrite and compared their bioleaching performance to that of non-adapted culture. Adapted culture rapidly leached higher Cu^{2+} (48%) from 5% w/v chalcopyrite than non-adapted culture (40% Cu^{2+}). Edward et al. (2018) showed that a pure culture of *L. ferriphilum* adapted to 0.5 $mg.L^{-1}$ thiocyanate (SCN^-) maintained a high specific Fe^{2+} oxidation rate at increasing SCN^- stress (0 – 2 mg/L). While non-adapted culture was compromised from 0.5 mg/L SCN^- and completely inhibited at SCN^- concentration exceeding 1.75 mg/L. Prior adaptation has also been demonstrated to benefit more physiological characteristics of microbial culture beyond metal tolerance (Xia et al. 2008). Africa et al. (2013) observed an improvement in the attachment of *At. ferrooxidans* on pyrite and chalcopyrite concentrate post their prior adaptation to pyrite.

Ilyas et al. (2010) studied the inhibitory effect of mixed metal ions of Ag^+, Al^{3+}, Cu^{2+}, Fe^{3+}, Ni^{2+}, Pb^{2+}, $Sn^{2+,}$ and Zn^{2+} on the growth of adapted and non-adapted mixed culture of *S. thermosulfidooxidans* and *Thermoplasma acidophilum*. Microbial growth of non-adapted culture was completely inhibited at 12 g/L mixed metal and above. Culture adapted to 20 g/L mixed metal ions tolerated up to 16 g/L mixed metals. High bioleaching efficiency of 80% Zn, 64% Al, 86% Cu, and 74% Ni from bioleaching of PCBs in a column bioreactor was further achieved using the adapted culture (Ilyas et al. 2010). As inhibition of microbial culture is also due to non-metallic components of PCBs, Xia et al. (2017) gradually adapted a mixed culture of *L. ferriphilum* and *At. caldus* up to 8% w/v PCBs. Post adaptation, the culture grew at 8% PCBs and 85% Zn, 77% Cu and 70% Al was successfully leached in 7 days. Improvement in metal tolerance post microbial adaptation to either metal ions or PCBs has also been reported elsewhere (Arshadi and Mousavi 2015; Xia et al. 2017; Fu et al. 2021). Despite the observed improvements, other researchers continue to observe inhibition of the adapted culture, especially at increased solid loadings (Lambert et al. 2015; Tapia et al. 2022). Thus, this necessitates the need for continued research in techniques of mitigating inhibition of the microbial culture, in addition to the prior adaptation.

2.3.5.2 Immobilisation of microbial culture

The immobilisation of microbial culture is achieved by growing and maintaining a microbial culture in the presence of biomass support particles (BSPs). Due to the natural tendency of some microorganisms to attach to surfaces, the microbial culture immobilises on BSPs by attachment and/or entrapment. Microbial attachment on BSP is proposed to progress through four steps, i.e., microbial transport, initial adhesion, firm attachment, and finally microbial colonisation as shown in Figure 2-3 (Zobell 1943a; van Loosdrecht et al. 1990). Microbial transport to the vicinity of the BSPs is through various known transport mechanisms such as diffusion, convection, active movement, and chemotaxis (van Loosdrecht et al. 1990). Thereafter, cells adhere onto the BSPs reversible or irreversible. On reversible adhesion, cells deposit onto the surface of the BSPs but can easily be removed back into the bulk solution by either its mobility or even by a mild shear stress. In contrast, irreversible adhesion is characterised by cells with no Brownian motion and thus firmly attached to the BSPs through

the production of EPS (Rohwerder et al. 2003; Sand and Gehrke 2006). The excreted EPS polymer layer is postulated to be highly conducive for microbial proliferation and subsequent microbial colonisation and biofilm formation (van Loosdrecht et al. 1990; Rohwerder et al. 2003; Sand and Gehrke 2006; González et al. 2013). Biofilm may thus be defined as a consortium of sessile microbial communities encapsulated by polymeric/polysaccharide substances (Watnick and Kolter 2000). The rate of microbial colonisation and the nature of biofilm is dependent on the type of microorganisms involved.

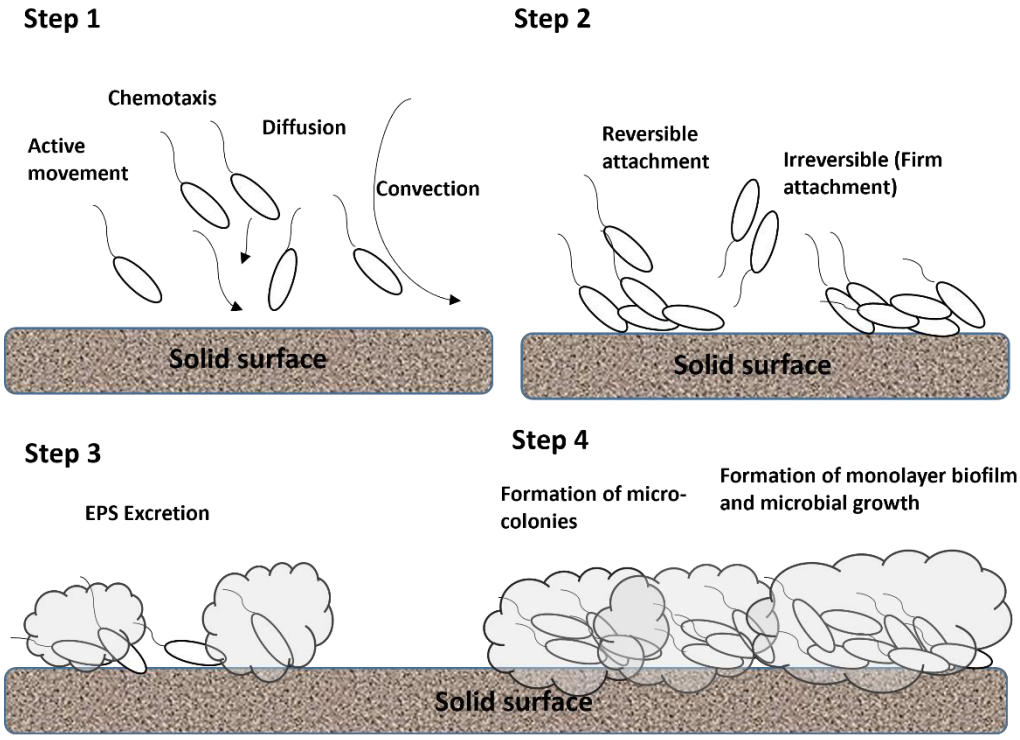

Figure 2-3 Representation of the four steps involved in microbial colonisation on a biomass support particle. **Step 1**: transport of microbes to the surface; **Step 2**: initial adhesion either as reversible or irreversible; **Step 3**: firm attachment facilitated by excretion of extracellular-polymeric substances (EPS); and **Step 4**: final microbial colonisation and formation of biofilm (adapted from van Loosdrecht et al. (1990)).

Amongst other factors, it is the proliferation of the microorganisms within the biofilm and the subsequent high biomass achievable which encourages the application of microbial immobilised systems in improving bioleaching. The high cell density facilitates faster microbial Fe^{2+} oxidation rates (Nemati et al. 1998). Various methods of cell immobilisation have been developed; these include encapsulation, covalent bonding, adsorption, gel entrapment, cross-linking, and adsorption/attachment (Elakkiya et al. 2016). A variety of biomass support particles such as glass beads, activated carbon, ceramic saddles and rings, sand, wood chips, plastic composition support, and polyurethane foam have been explored (Kinnunen and Puhakka 2005; Gómez et al. 2000; Guoqiang et al. 1992; Halfmeier 1993). Halfmeier et al. (1993) reported a volumetric Fe^{2+} oxidation rate of 3.60 $g.L^{-1}.h^{-1}$ by immobilised *At.*

ferrooxidans, which was an improvement of 5-fold compared to free suspended cells. The culture was immobilised on siran rings and packed in a fixed bed bioreactor. Grishin and Tuovinen (1988) compared volumetric Fe^{3+} productivity rates by *At. ferrooxidans* immobolised on activated carbon, glass bead (particle size of 710 – 1180 µm and 425 – 600 µm), and ion-exchange resins. The colonised BSPs were packed in a packed-bed bioreactor. The highest rates were 15.6, 10.0, 3.24, and 1.40 $g.L^{-1}.h^{-1}$ in activated carbon, ion-exchange resins, 425 – 600 µm glass bead, and 710 – 1180 µm glass bead, respectively. Jensen and Webb (1994) reported a Fe^{3+} productivity rate of 4.40 $g.L^{-1}.h^{-1}$ in a trickle-bed bioreactor consisting of polyurethane foam (PUF) immobilised with *At. ferrooxidans*. Similarly, high volumetric Fe^{2+} oxidation of 34.5 $g.L^{-1}.h^{-1}$ was achieved in a packed-bed bioreactor, packed with *At. ferrooxidans* immobilised on PUF . It must be noted that maximum cell retention on a BSP is subject to its total surface area. The higher Fe^{2+} oxidation rates observed on PUF-BSPs may be attributed to its high surface area.

In addition to improved Fe^{2+} oxidation rates, biofilm produced can act as a protective layer against inhibitory metal ions. The typical composition of EPS excreted in bioleaching systems mainly includes a mixture of macromolecules such as lipids, proteins, polysaccharides, nucleic acids, and carbohydrates (Sand and Gehrke 1999; Michel et al. 2009). The latter constitute the majority of EPS alongside with proteins (Xu et al. 2009; Ozturk et al. 2014). The relative composition of these macromolecules is dependent on the type of microbial consortia and physicochemical parameters such as growth medium and pH. Functional groups such as amide, amino, carboxyl, and hydroxyl groups in these macromolecules provide binding sites for chelating (bioadsorb) with metal ions, thereby preventing them from entering the cells. This extracellular metal exclusion is one of the common metal resistance mechanisms as already highlighted (Bruins et al. 2000; Dopson et al. 2003). High heavy metal ions content in EPS composition is also evident of metal adsorption. Li et al. (2022) observed higher Cu^{2+}, Ni^{2+}, Cd^{2+}, and Zn^{2+} adsoption by EPS of *At. ferrooxidans*, *S. themosulfidooxidans*, and *Acidianus* (*A.*) *manzaensis* compared to their planktonic cells (EPS-free). They further observed that *A. manzaensis* exhibited higher adsorption, followed by *S. themosulfidooxidans* and *At. ferrooxidans* being the least.

Despite the compounded benefits of cell immobilisation systems and their wide application in the bioleaching of mineral sulfides, their adoption in bioleaching of E-waste is limited. Hubau et al. (2020) have explored the use of immobilised systems by immobilising mixed culture of *L. ferriphilum* and *S. benefaciens* on activated carbon in a bubble (semi-fluidised) bioreactor. While recently, Van Yken et al. (2023) immobilised a culture dominated by *At. caldus* and *At. ferroxidans* dominated cultures on Mutag BioChip™ in two separate stirred tank reactors for the biogeneration of H^+ and Fe^{3+} lixiviants from waste sulfur pastilles and Fe^{2+}, respectively. The leaching lixiviants generated from these two reactors were used in the bioleaching of PCBs in a stirred tank reactor. Another benefit of immobilised cell systems is that they can be introduced in various reactors, including stirred tanks, fluidised, trickle-bed, and packed-bed bioreactors, subject to minimal shear stress exerted by mixing mechanism, i.e. agitation speed in stirred tanks and flow-rate (dilution rate) in packed-bed bioreactors.

2.3.5.3 Two-step bioleaching

Another technique of minimising inhibition of microbial culture in bioleaching of PCBs is the two-step approach. In this approach, microbial growth and generation of the Fe^{3+} oxidant is first carried in the absence of PCBs but with only Fe^{2+} source to eliminate potential impediments on the microbial Fe^{2+} oxidation. In the second step, PCBs are then added and metal leaching is facilitated by the microbial generated Fe^{3+} oxidant. Wu et al. (2018) studied the volumetric rate of Fe^{2+} oxidation by mixed culture of *S. themosulfidooxidans* and *L. ferriphilum* in the absence and presence of 1.5% w/v PCBs. Complete Fe^{2+} oxidation was achieved within 24 h in the absence of PCB at a rate of 0.583 $g.L^{-1}.h^{-1}$, while at 1.5% PCBs, the rate was decreased to 0.158 $g.L^{-1}.h^{-1}$. The authors mobilised 100% Cu from 1.5% PCBs in 2 h using the microbial generated Fe^{3+} solution (free-cell solution after sterile filtration) and recommended a two-step bioleaching. In a similar approach, Benzal et al. (2020) solubilised 95 – 100% Cu in 48 h from 0.75% PCBs by free-cell Fe^{3+} solution generated by *At. ferrooxidans*. Recently, Tapia et al. (2022) generated Fe^{3+} from Fe^{2+} by *Tissierella*, *Acidiphilium,* and *Leptospirillum* sp. in a stirred tank reactor. PCBs (1% w/v) were thereafter added and 69% Cu and 91% Zn were successfully leached in 18 days.

2.4 Problem statement

Bioleaching of PCBs is best suitable as a pretreatment process for the extraction of base metals prior to the extraction of precious metals, typically through hydrometallurgy. Bioleaching of PCBs has been studied since the early 2000s at the laboratory scale, mostly in batch shake flask experiments (Brandl et al. 2001; Bas et al. 2013; Benzal et al. 2020) with limited reactor studies (Ilyas et al. 2010; Hong and Valix 2014; Hubau et al. 2020). High bioleaching efficiency, with emphasis on extraction of Cu (>90% Cu), has been achieved in the presence of iron oxidising fungal species (Brandl et al. 2001), bacteria (Zhu et al. 2011), and archaea (Işıldar et al. 2016). Factors influencing bioleaching rates and extent of metal leaching, such as solution pH, choice of microbial consortia, operating temperature, PCB solid loading (weight PCB per volume of solution, w/v), initial ferric and ferrous iron concentrations, and particle size of the PCBs, have been widely explored (Yang et al. 2009; Bryan et al. 2015; van Yken et al. 2020). These contribute to the understanding and demonstration of the feasibility of bioleaching of PCBs but are limited in optimisation of the process, especially for studies carried out in shake flasks, as an understanding of mass transfer can be limited. Despite bioleaching emerging as a promising technology, there is currently limited kinetic data available for process design. Further, no pilot-scale nor commercialised processes are reported in the open literature.

In bioleaching of PCBs and other E-waste, Fe^{3+} reduction as a function of metal dissolution is typically much faster than its regeneration, thus, microbial oxidation of Fe^{2+} is the rate determining step (Lambert et al. 2015; Wu et al. 2018). This slow delivery of the Fe^{3+} oxidant can result in longer leaching time, lower leaching efficiency and, to an extent, limit the significance of the presence of microorganisms. One of the major challenges in maintaining or improving the microbial regeneration rate of the Fe^{3+} is microbial inhibition by metals accumulated and other constituents of PCBs within the system (Bryan et al. 2015; Lambert et al. 2015; Hubau et al. 2020). As such, there is a growing interest in the use of a two-step bioleaching approach, where Fe^{3+} is first generated from Fe^{2+} in the presence of

microorganisms, allowing microbial Fe^{2+} oxidation to proceed without any potential inhibitory metal ions and non-metallic component. Thereafter, the Fe^{3+} rich stream is contacted with the PCBs for metal leaching (Wu et al. 2018; Tapia et al. 2022). While Fe^{2+} oxidation rate and metal leaching can be improved compared to the one-step (i.e., onset microbial Fe^{2+} oxidation in the presence of PCBs), microbial activity post metal leaching is usually not reported. Where reported, microbial activity is not reported following leaching of PCBs at concentrations of 2% w/v and above (Bryan et al. 2015; Hubau et al. 2020). This information is a critical aspect of bioleaching as the continuous regeneration of the Fe^{3+} oxidant is key to the sustainability of the process and is one of the major advantages over hydrometallurgy. This also presents an opportunity as sustaining and improving the volumetric rates of microbial regeneration of Fe^{3+}, amongst other aspects, is critical in improving bioleaching efficiency. One of the strategies towards achieving high volumetric microbial activity is through maintaining the specific Fe^{2+} oxidation rate following leaching through minimising microbial inhibition. To date, the most explored method in the mitigation of microbial inhibition is the prior adaptation of the microbial culture to the potential inhibitory metal ions (Lambert et al. 2015; Ilyas et al. 2010; Tapia et al. 2022). This method has been widely adopted in both traditional bioleaching of mineral sulfides ores (Govender et al. 2015; Ngoma et al. 2018) and bioleaching of PCBs (Arshadi and Mousavi 2015; Xia et al. 2017). Another strategy is the enhancement of the amount of the microbial phase present through the use of microbial immobilised systems, where microbial culture is colonised onto a biomass support structure. High cell numbers achievable through microbial colonisation of the biomass support particles (BSPs) can facilitate faster volumetric Fe^{2+} oxidation rates, while retention of biomass within the support particle and the biofilm formed to facilitate immobilisation can minimise microbial inhibition through restricting ease of diffusion and acting as a barrier against the toxic environment (Sand and Gehrke 2006; Luo et al. 2021). Microbial immobilised systems have been proposed in the bioleaching of mineral sulfide ores (Vu et al. 2009; Africa et al. 2010; Nemati et al. 1998); however, their application in the bioleaching of PCBs remains limited. Hubau et al. (2020) immobilised their culture on activated chalk coal and used the immobilised system in a two-stage reactor system in the bioleaching of PCBs. Van Yken et al. (2023) immobilised *At. caldus* and *At. ferrooxidans* dominated cultures on a Mutag Biochip™ to generate H_2SO_4 (H^+ lixiviant) from waste sulfur pastilles and Fe^{3+} lixiviant from Fe^{2+} ($FeSO_4.7H_2O$). The biogenerated lixiviants were used in the bioleaching of PCBs.

Moreover, as metal leaching through bioleaching of PCBs is governed by two sub-processes: microbial Fe^{2+} oxidation to Fe^{3+} and metal oxidation by the Fe^{3+} oxidant, a fundamental understanding of both processes is crucial towards improving the overall bioleaching efficiency. The two sub-processes are interdependent as the Fe^{3+} available for metal leaching is dependent on the microbial Fe^{2+} oxidation rate. Conversely, in a continuous bioleaching process, the availability of the Fe^{2+} needed for microbial growth is dependent on the metal leaching rate. While knowledge of the metal leaching kinetics can be drawn from hydrometallurgical processes, this interdependency should be considered. This said, rigorous kinetic studies of the ferric leaching of metals in elemental form has not been published in the open literature to date. Chemical (Fe^{3+} and H^+) leach kinetics of PCBs continue to receive attention, with emphasis on leaching of Cu. These studies provide useful data in

understanding the leaching behaviour of Cu and its associated kinetics. However, there are limited data on the fundamental understanding of the leaching behaviour and associated kinetics of individual metals embedded in PCBs. Such data is critical to the fundamental understanding of relative metal leaching and modeling of PCBs leaching. Information such as residence time and the number of tanks needed may be modelled from such data. Such data can best be obtained from leaching studies of individual metals prior to study of more complex systems (leaching of PCBs).

2.5 Research scope

Owing to the microbial oxidation of ferrous iron being the rate-determining step in the bioleaching of PCBs, this study seeks to explore a two-stage bioleaching system to minimise inhibition of microbial culture and improve microbial oxidation kinetics. To achieve this, the study aim to evaluate chemical leach kinetics and microbial oxidation kinetics during metal extraction from PCBs. It seeks to use the chemical and microbial oxidation kinetics determined to inform the appropriate staged reactor configurations to enable matched chemical leaching rates with microbial lixiviants regeneration. Chemical leach kinetics are evaluated by studying the leaching behaviour of elementary metals, as individual metals and in combination, and compared to that of complex PCBs. Furthermore, to enhance microbial oxidation rates and minimize microbial inhibition, microbial adaptation to Cu^{2+} and microbial immobilisation on polyurethane foam as biomass support will be exploited.

This study can thus be divided into three major parts:

- The evaluation of chemical leaching kinetics. These include the leaching kinetics of four predominant metals in PCBs (i.e., Cu, Zn, Ni, and Sn), as individual elementary metals and in their combinations before that of actual PCB samples.

- The evaluation of microbial oxidation kinetics. These include the oxidation kinetics of Cu-adapted and immobilised cells compared to the typically used planktonic cells in the presence of increasing concentrations of the four individual metals of interest, in their combinations, and finally PCBs.

- Finally, study of staged reactor configurations through the integration of insights generated from chemical leaching and microbial oxidation kinetics.

2.5.1 Hypothesis and research questions

The chemical leaching studies were directed through research questions rather than being hypothesis-driven. The following research key questions were formulated:

- How does the volumetric leaching rates of base metals by ferric iron compare to that by acid leaching?

- What are the relative metal leaching rates amongst the four metals of interest?

- Are there secondary reactions such as cementation in multi-metal leaching systems?

- How does the relative metal leaching behaviour and associated leaching kinetics compare during individual metal, mixed metals and complex PCB leaching systems?

To direct the investigation of the benefits of the immobilised microbial system and prior adaptation, the following two hypotheses were formulated:

Hypothesis 1

Owing to the ferric leaching rate exceeding the microbial ferrous iron oxidation rate in planktonic culture, immobilisation of the microbial cells to achieve high cell concentrations without loss in rate of specific ferrous iron oxidation rate will contribute to the matching of the volumetric chemical leaching and microbial oxidation rates.

Key question

Will microbial cell immobilisation allow an increased volumetric rate of ferric iron regeneration to match the required regeneration rates to sustain ferric leaching in a continuous flow reactor?

Will immobilisation of the microbial phase reduce the effective metal ion inhibition of the oxidation process and maintain specific ferrous iron oxidation rates?

Hypothesis 2

Microbial immobilisation will reduce the inhibitory effect of metal ions on the microorganisms which may also be further reduced by their prior adaptation to higher metal ion concentrations.

Key question

Will prior adaption of the microbial culture to predominant Cu^{2+} enhance their tolerance to other individual inhibitory metal ions beyond Cu^{2+} and mixed metal ions representing metal content in PCBs*?*

Will microbial cell immobilisation of already adapted microbial cultures further enhance their tolerance to inhibitory metal ions?

Overall, this PhD study was centered on the following overarching hypothesis:

Hypothesis 3

Microbial ferrous iron oxidation, required for the regeneration of ferric iron for the bioleaching of metal-rich printed circuit boards, is inhibited by the accumulation of metal ions released into solution by ferric iron leaching of the PCBs. Microbial inhibition can be partially overcome by the separation of the process into its two sub-processes: chemical leaching and microbial ferrous iron oxidation, through using a two-stage reactor system, i.e. a chemical leaching reactor coupled to a microbial ferrous iron oxidation bioreactor.

Key question

How does the overall leaching performance (metal extraction and overall leaching kinetics) of a two-stage reactor system compare to that of a one-stage reactor system?

2.6 References

Adetunji, A. I.; Oberholster, P. J.; Erasmus, M. (2023). Bioleaching of metals from E-Waste using microorganisms. A Review. Minerals 13 (6), 828. DOI: 10.3390/min13060828.

Adhapure, N. N.; Dhakephalkar, P. K.; Dhakephalkar, A. P.; Tembhurkar, V. R.; Rajgure, A. V.; Deshmukh, A. M. (2014). Use of large pieces of printed circuit boards for bioleaching to avoid 'precipitate contamination problem' and to simplify overall metal recovery. MethodsX 1, 181–186. DOI: 10.1016/j.mex.2014.08.011.

Africa, C. J.; Harrison, S. T.L.; Becker, M.; Hille, R. P.v. (2010). In situ investigation and visualisation of microbial attachment and colonisation in a heap bioleach environment. The novel biofilm reactor. Minerals Engineering 23 (6), 486–491. DOI: 10.1016/j.mineng.2009.12.011.

Africa, C.-J.; van Hille, R. P.; Harrison, S. T. L. (2013). Attachment of *Acidithiobacillus ferrooxidans* and *Leptospirillum ferriphilum* cultured under varying conditions to pyrite, chalcopyrite, low-grade ore and quartz in a packed column reactor. Applied Microbiology and Biotechnology 97 (3), 1317–1324. DOI: 10.1007/s00253-012-3939-x.

Akcil, A.; Erust, C.; Gahan, C. S.; Ozgun, M.; Sahin, M.; Tuncuk, A. (2015). Precious metal recovery from waste printed circuit boards using cyanide and non-cyanide lixiviants-A review. Waste Management 45, 258–271. DOI: 10.1016/j.wasman.2015.01.017.

Akcil, A.; Ibrahim, Y. A.; Meshram, P.; Panda, S. (2021). Hydrometallurgical recycling strategies for recovery of rare earth elements from consumer electronic scraps. A review. Journal of Chemical Technology & Biotechnology 96 (7), 1785–1797. DOI: 10.1002/jctb.6739.

Alvear Flores, G. R. F.; Nikolic, S.; Mackey, P. J. (2014). ISASMELT™ for the recycling of E-Scrap and copper in the U.S. Case study example of a new compact recycling plant. The Journal of The Minerals, Metals & Materials Society 66 (5), 823–832. DOI: 10.1007/s11837-014-0905-3.

Anindya, A.; Swinbourne, D. R.; Reuter, M. A.; Matusewicz, R. W. (2013). Distribution of elements between copper and FeO x –CaO–SiO_2 slags during pyrometallurgical processing of WEEE. Mineral Processing and Extractive Metallurgy 122 (3), 165–173. DOI: 10.1179/1743285513Y.0000000043.

Arshadi, M.; Mousavi, S. M. (2015). Multi-objective optimization of heavy metals bioleaching from discarded mobile phone PCBs. Simultaneous Cu and Ni recovery using *Acidithiobacillus ferrooxidans*. Separation and Purification Technology 147 (1), 210–219. DOI: 10.1016/j.seppur.2015.04.020.

Arshadi, M.; Yaghmaei, S.; Mousavi, S. M. (2018). Content evaluation of different waste PCBs to enhance basic metals recycling. Resources, Conservation and Recycling 139, 298–306. DOI: 10.1016/j.resconrec.2018.08.013.

Awasthi, A. K.; Zeng, X.; Li, J. (2016). Integrated bioleaching of copper metal from waste printed circuit board-a comprehensive review of approaches and challenges. Environmental Science and Pollution Research International 23 (21), 21141–21156. DOI: 10.1007/s11356-016-7529-9.

Azam, S.; Li, Q. (2010). Tailings dam failures. A review of the last one hundred years. Geotechnical News 28 (4), 50–54.

Baniasadi, M.; Vakilchap, F.; Bahaloo-Horeh, N.; Mousavi, S. M.; Farnaud, S. (2019). Advances in bioleaching as a sustainable method for metal recovery from e-waste. A review. Journal of Industrial and Engineering Chemistry 76 (3–4), 75–90. DOI: 10.1016/j.jiec.2019.03.047.

Bas, A. D.; Deveci, H.; Yazici, E. Y. (2013). Bioleaching of copper from low grade scrap TV circuit boards using mesophilic bacteria. Hydrometallurgy 138 (11), 65–70. DOI: 10.1016/j.hydromet.2013.06.015.

Benzal, E.; Solé, M.; Lao, C.; Gamisans, X.; Dorado, A. D. (2020). Elemental copper recovery from e-Wastes mediated with a two-step bioleaching process. Waste Biomass Valoriization 11 (10), 5457–5465. DOI: 10.1007/s12649-020-01040-2.

Bilczuk, D.; Olvera, O. G.; Asselin, E. (2016). Kinetic study of the dissolution of metallic nickel in sulphuric acid solutions in the presence of different oxidants. The Canadian Journal of Chemical Engineering 94 (10), 1872–1879. DOI: 10.1002/cjce.22576.

Birloaga, I.; Michelis, I. de; Ferella, F.; Buzatu, M.; Vegliò, F. (2013). Study on the influence of various factors in the hydrometallurgical processing of waste printed circuit boards for copper and gold recovery. Waste Management 33 (4), 935–941. DOI: 10.1016/j.wasman.2013.01.003.

Bizzo, W. A.; Figueiredo, R. A.; Andrade, V. F. de (2014). Characterization of printed circuit boards for metal and energy recovery after milling and mechanical separation. Materials 7 (6), 4555–4566. DOI: 10.3390/ma7064555.

Blake, R. C.; Shute, E. A. (1994). Respiratory enzymes of *Thiobacillus ferrooxidans*. Kinetic properties of an acid-stable iron. Rusticyanin oxidoreductase. Biochemistry 33 (31), 9220–9228.

Brandl, H.; Bosshard, R.; Wegmann, M. (2001). Computer-munching microbes. Metal leaching from electronic scrap by bacteria and fungi. Hydrometallurgy 59 (2), 319–326. DOI: 10.1016/S0304-386X(00)00188-2.

Brierley, C.L. (2001). Bacterial succession in bioheap leaching. Hydrometallurgy 59 (2-3), 249–255. DOI: 10.1016/S0304-386X(00)00171-7.

Bruins, M. R.; Kapil, S.; Oehme, F. W. (2000). Microbial resistance to metals in the environment. Ecotoxicology and Environmental Safety 45 (3), 198–207. DOI: 10.1006/eesa.1999.1860.

Bryan, C. G.; Davis-Belmar, C. S.; van Wyk, N.; Fraser, M. K.; Dew, D.; Rautenbach, G. F.; Harrison, S. T. L. (2012). The effect of CO_2 availability on the growth, iron oxidation and CO_2-fixation rates of pure cultures of *Leptospirillum ferriphilum* and *Acidithiobacillus ferrooxidans*. Biotechnology and Bioengineering 109 (7), 1693–1703. DOI: 10.1002/bit.24453.

Bryan, C. G.; Watkin, E. L.; McCredden, T. J.; Wong, Z. R.; Harrison, S.T.L.; Kaksonen, A. H. (2015). The use of pyrite as a source of lixiviant in the bioleaching of electronic waste. Hydrometallurgy 152 (2–3), 33–43. DOI: 10.1016/j.hydromet.2014.12.004.

Castro, C.; Urbieta, M. S.; Plaza Cazón, J.; Donati, E. R. (2019). Metal biorecovery and bioremediation. Whether or not thermophilic are better than mesophilic microorganisms. Bioresource Technology 279 (11), 317–326. DOI: 10.1016/j.biortech.2019.02.028.

Chauhan, G.; Jadhao, P. R.; Pant, K. K.; Nigam, K.D.P. (2018). Novel technologies and conventional processes for recovery of metals from waste electrical and electronic equipment. Challenges & opportunities – A review. Journal of Environmental Chemical Engineering 6 (1), 1288–1304. DOI: 10.1016/j.jece.2018.01.032.

Chi, T. D.; Lee, J.-c.; Pandey, B. D.; Yoo, K.; Jeong, J. (2011). Bioleaching of gold and copper from waste mobile phone PCBs by using a cyanogenic bacterium. Minerals Engineering 24 (11), 1219–1222. DOI: 10.1016/j.mineng.2011.05.009.

Cobley, J. G.; Haddock, B. A. (1975). The respiratory chain of *Thiobacillus ferrooxidans*. The reduction of cytochromes by Fe^{2+} and the preliminary characterization of rusticyanin a novel "blue" copper protein. FEBS Letters 60 (1), 29–33.

Copper Alliance (2024). Copper demand and long-term Availability - Copper Alliance. Available online at https://copperalliance.org/sustainable-copper/about-copper/cu-demand-long-term-availability/, updated on 1/23/2024, checked on 1/23/2024.

Coram, N. J.; Rawlings, D. E. (2002). Molecular relationship between two groups of the genus *Leptospirillum* and the finding that *Leptospirillum ferriphilum* sp. nov. dominates South African commercial biooxidation tanks that operate at 40 degrees C. Applied and Environmental Microbiology 68 (2), 838–845. DOI: 10.1128/AEM.68.2.838-845.2002.

Cortes, M. A.; Patiño, M. L. D. (2016). Recycling of electronic waste, using basic and acid leaching. Open Journal of Applied Sciences 06 (03), 169–176. DOI: 10.4236/ojapps.2016.63018.

Creamer, N. J.; Baxter-Plant, V. S.; Henderson, J.; Potter, M.; Macaskie, L. E. (2006). Palladium and gold removal and recovery from precious metal solutions and electronic scrap leachates by *Desulfovibrio desulfuricans*. Biotechnology Letters 28 (18), 1475–1484. DOI: 10.1007/s10529-006-9120-9.

Crowson, P. (2012). Some observations on copper yields and ore grades. Resources Policy 37 (1), 59–72. DOI: 10.1016/j.resourpol.2011.12.004.

Cui, J.; Zhang, L. (2008). Metallurgical recovery of metals from electronic waste. A review. Journal of Hazardous Materials 158 (2-3), 228–256. DOI: 10.1016/j.jhazmat.2008.02.001.

Das, A.; Modak, J. M.; Natarajan, K. A. (1997). Studies on multi-metal ion tolerance of *Thiobacillus ferrooxidans*. Minerals Engineering 10 (7), 743–749. DOI: 10.1016/S0892-6875(97)00052-6.

De, G. C.; Oliver, D. J.; Pesic, B. M. (1997). Effect of heavy metals on the ferrous iron oxidizing ability of *Thiobacillus ferrooxidans*. Hydrometallurgy 44 (1-2), 53–63. DOI: 10.1016/S0304-386X(96)00030-8.

Deetman, S.; Pauliuk, S.; van Vuuren, D. P.; van der Voet, E.; Tukker, A. (2018). Scenarios for demand growth of metals in electricity generation technologies, cars, and electronic appliances. Environmental Science & Technology 52 (8), 4950–4959. DOI: 10.1021/acs.est.7b05549.

Dew, D. W.; Rautenbach, G. F.; van Hille, R. P.; Davis-Belmar, C. S.; Harvey, I. J.; Truelove, J. S. (2011). High temperature heap leaching of chalcopyrite. Method of evaluation and process model validation. Percolation leaching: the status globally and in southern Africa. The Southern African Institute of Mining and Metallurgy, Johannesburg, 201–219.

Dhawan, Nikhil; Wadhwa, M.; Kumar, V.; Kumar, M. (Eds.) (2009). Recovery of metals from electronic scrap by hydrometallurgical route.

Dopson, M.; Baker-Austin, C.; Koppineedi, P. R.; Bond, P. L. (2003). Growth in sulfidic mineral environments. Metal resistance mechanisms in acidophilic micro-organisms. Microbiology 149 (Pt 8), 1959–1970. DOI: 10.1099/mic.0.26296-0.

Dutta, D.; Panda, R.; Kumari, A.; Goel, S.; Jha, M. K. (2018). Sustainable recycling process for metals recovery from used printed circuit boards (PCBs). Sustainable Materials and Technologies 17 (6), e00066. DOI: 10.1016/j.susmat.2018.e00066.

Edward, C. J.; Kotsiopoulos, A.; Harrison, S. T. L. (2018). Low-level thiocyanate concentrations impact on iron oxidation activity and growth of *Leptospirillum ferriphilum* through inhibition and adaptation. Research in Microbiology 169 (10), 576–581. DOI: 10.1016/j.resmic.2018.10.003.

Ngoma, E. I.; Ojumu, T. V.; Harrison, S. T.L. (2015). Investigating the effect of acid stress on selected mesophilic micro-organisms implicated in bioleaching. Minerals Engineering 75 (11), 6–13. DOI: 10.1016/j.mineng.2015.02.007.

Erust, C.; Akcil, A.; Tuncuk, A.; Panda, S. (2020). Intensified acidophilic bioleaching of multi-metals from waste printed circuit boards (WPCBs) of spent mobile phones. Journal of Chemical Technology & Biotechnology 95 (8), 2272–2285. DOI: 10.1002/jctb.6417.

Ficeriová, J.; Baláž, P.; Gock, E. (2011). Leaching of gold, silver and accompanying metals from circuit boards (PCBs) waste. Acta Montanistica Slovaca 16 (2), 128.

Franzmann, P. D.; Haddad, C. M.; Hawkes, R. B.; Robertson, W. J.; Plumb, J. J. (2005). Effects of temperature on the rates of iron and sulfur oxidation by selected bioleaching bacteria and archaea. Application of the Ratkowsky equation. Minerals Engineering 18 (13-14), 1304–1314. DOI: 10.1016/j.mineng.2005.04.006.

Fu, K.; Tian, L.; Hou, P.; Long, M.; Chen, S.; Lin, H. (2021). Stirred-tank leaching of coarse-grained waste, printed circuit boards with *Acidithiobacillus ferrooxidans*. Physicochemical Problems of Mineral Processing 57 (5).

Gai, M.; Yano, T.; Tamegai, H.; Fukumori, Y.; Yamanaka, T. (1992). *Thiobacillus ferrooxidans* cytochrome c oxidase. Purification, and molecular and enzymatic features. The Journal of Biochemistry 112 (6), 816–821.

Giudici-Orticoni, M. T.; Guerlesquin, F.; Bruschi, M.; Nitschke, W. (1999). Interaction-induced redox switch in the electron transfer complex rusticyanin-cytochrome c(4). The Journal of Biological Chemistry 274 (43), 30365–30369. DOI: 10.1074/jbc.274.43.30365.

Golzar-Ahmadi, M.; Mousavi, S. M. (2021). Extraction of valuable metals from discarded AMOLED displays in smartphones using Bacillus foraminis as an alkali-tolerant strain. Waste Management 131, 226–236. DOI: 10.1016/j.wasman.2021.06.006.

González, A.; Bellenberg, S.; Mamani, S.; Ruiz, L.; Echeverría, A.; Soulère, L. et al. (2013). AHL signaling molecules with a large acyl chain enhance biofilm formation on sulfur and metal sulfides by the bioleaching bacterium *Acidithiobacillus ferrooxidans*. Applied Microbiology and Biotechnology 97 (8), 3729–3737. DOI: 10.1007/s00253-012-4229-3.

Goosey, M.; Kellner, R. (2003). Recycling technologies for the treatment of end of life printed circuit boards (PCBs). Circuit World 29 (3), 33–37. DOI: 10.1108/03056120310460801.

Govender, E.; Bryan, C. G.; Harrison, S. T.L. (2015). Effect of physico-chemical and operating conditions on the growth and activity of *Acidithiobacillus ferrooxidans* in a simulated heap bioleaching environment. Minerals Engineering 75, 14–25. DOI: 10.1016/j.mineng.2015.02.006.

Grishin, S. I.; Tuovinen, O. H. (1988). Fast kinetics of Fe oxidation in packed-bed reactors. Applied and Environmental Microbiology 54 (12), 3092–3100. DOI: 10.1128/aem.54.12.3092-3100.1988.

Guo, C.; Wang, H.; Liang, W.; Fu, J.; Yi, X. (2011). Liberation characteristic and physical separation of printed circuit board (PCB). Waste Management 31 (9-10), 2161–2166. DOI: 10.1016/j.wasman.2011.05.011.

Habibi, A.; Shamshiri Kourdestani, S.; Hadadi, M. (2020). Biohydrometallurgy as an environmentally friendly approach in metals recovery from electrical waste. A review. Waste Management & Research 38 (3), 232–244. DOI: 10.1177/0734242X19895321.

Hagelüken, C. (2006). Recycling of electronic scrap at Umicore precious metals refining. Acta Metallurgica Slovaca 12, 111–120.

Halfmeier, H.; Schfer-Treffenfeldt, W.; Reuss, M. (1993). Potential of *Thiobacillus ferrooxidans* for waste gas purification. Part 2. Increase in continuous ferrous iron oxidation kinetics using immobilized cells. Applied Microbiology and Biotechnology 40 (4). DOI: 10.1007/BF00175751.

Harrison, S. T. L. (2016). Biotechnologies that utilize acidophiles. In Acidophiles: life in extremely acidic environments: Quantrini, R and Johnson, D. B (Eds.). WYMONDHAM: Caister Academic Press, 265–284.

Hazra, T. K.; Mukherjea, M.; Mukherjea, R. N. (1992). Role of rusticyanin in the electron transport process in *Thiobacillus ferrooxidans*. Indian Journal of Biochemistry & Biophysics 29 (1), 77–81.

Hong, Y.; Valix, M. (2014). Bioleaching of electronic waste using acidophilic sulfur oxidising bacteria. Journal of Cleaner Production 65, 465–472. DOI: 10.1016/j.jclepro.2013.08.043.

Hu, L.; Wu, H.; Zhang, L.; Zhang, P.; Wen, Q. (2017). Geotechnical properties of mine tailings. Journal of Materials in Civil Engineering 29 (2), 50. DOI: 10.1061/(ASCE)MT.1943-5533.0001736.

Huang, J.; Chen, M.; Chen, H.; Chen, S.; Sun, Q. (2014). Leaching behavior of copper from waste printed circuit boards with Brønsted acidic ionic liquid. Waste Management 34 (2), 483–488. DOI: 10.1016/j.wasman.2013.10.027.

Hubau, A., Bryan, C.G., (2023). Metal recovery from E-wastes. In: Johnson, D.B., Bryan, C. G., Schlomann, M., Roberto, F.F. (Eds.), Biomining Technologies. Springer, Cham.

Hubau, A.; Chagnes, A.; Minier, M.; Touzé, S.; Chapron, S.; Guezennec, A.-G. (2019). Recycling-oriented methodology to sample and characterize the metal composition of waste Printed Circuit Boards. Waste Management 91, 62–71. DOI: 10.1016/j.wasman.2019.04.041.

Hubau, A.; Minier, M.; Chagnes, A.; Joulian, C.; Silvente, C.; Guezennec, A.-G. (2020). Recovery of metals in a double-stage continuous bioreactor for acidic bioleaching of printed circuit boards (PCBs). Separation and Purification Technology 238 (3), 116481. DOI: 10.1016/j.seppur.2019.116481.

Iglesias-González, N.; Dorado, A. D.; Ramírez, P.; Mazuelos, A. (2024). A high productivity bioprocess for obtaining metallic copper from printed circuit boards (PCBs). Minerals Engineering 205 (10), 108459. DOI: 10.1016/j.mineng.2023.108459.

Ilyas, S.; Anwar, M. A.; Niazi, S. B.; Afzal Ghauri, M. (2007). Bioleaching of metals from electronic scrap by moderately thermophilic acidophilic bacteria. Hydrometallurgy 88 (1-4), 180–188. DOI: 10.1016/j.hydromet.2007.04.007.

Ilyas, S.; Lee, J.-c.; Chi, R.-a. (2013). Bioleaching of metals from electronic scrap and its potential for commercial exploitation. Hydrometallurgy 131-132 (11–12), 138–143. DOI: 10.1016/j.hydromet.2012.11.010.

Ilyas, S.; Ruan, C.; Bhatti, H. N.; Ghauri, M. A.; Anwar, M. A. (2010). Column bioleaching of metals from electronic scrap. Hydrometallurgy 101 (3-4), 135–140. DOI: 10.1016/j.hydromet.2009.12.007.

Ingledew, W. J. (1982). *Thiobacillus ferrooxidans*. The bioenergetics of an acidophilic chemolithotroph. Biochimica et Biophysica Acta 683 (2), 89–117. DOI: 10.1016/0304-4173(82)90007-6.

International Copper Study Group (2024). Copper Factbook. Available online at https://icsg.org/copper-factbook/, updated on 1/23/2024, checked on 1/23/2024.

Işıldar, A.; van de Vossenberg, J.; Rene, E. R.; van Hullebusch, E. D.; Lens, P. N. L. (2016). Two-step bioleaching of copper and gold from discarded printed circuit boards (PCB). Waste Management 57, 149–157. DOI: 10.1016/j.wasman.2015.11.033.

Islam, A.; Ahmed, T.; Awual, M. R.; Rahman, A.; Sultana, M.; Aziz, A. A. et al. (2020). Advances in sustainable approaches to recover metals from e-waste-A review. Journal of Cleaner Production 244 (5), 118815. DOI: 10.1016/j.jclepro.2019.118815.

Jadhav, U.; Hocheng, H. (2015). Hydrometallurgical Recovery of metals from large printed circuit board pieces. Scientific Reports 5, 14574. DOI: 10.1038/srep14574.

Jensen, A. B.; Webb, C. (1994). A trickle bed reactor for ferrous sulphate oxidation using *Thiobacillus ferrooxidans*. Biotechnology Techniques 8 (2), 87–92. DOI: 10.1007/BF00152846.

Jha, M. K.; Kumari, A.; Panda, R.; Rajesh Kumar, J.; Yoo, K.; Lee, J. Y. (2016). Review on hydrometallurgical recovery of rare earth metals. Hydrometallurgy 165 (6), 2–26. DOI: 10.1016/j.hydromet.2016.01.035.

Kadivar, S.; Pourhossein, F.; Mousavi, S. M. (2021). Recovery of valuable metals from spent mobile phone printed circuit boards using biochar in indirect bioleaching. Journal of Environmental Management 280, 111642. DOI: 10.1016/j.jenvman.2020.111642.

Kandalam, A.; Reuter, M. A.; Stelter, M.; Reinmöller, M.; Gräbner, M.; Richter, A.; Charitos, A. (2023a). A Review of Top Submerged Lance (TSL) Processing—Part II. Thermodynamics, Slag Chemistry and Plant Flowsheets. Metals 13 (10), 1742. DOI: 10.3390/met13101742.

Kandalam, A.; Reuter, M. A.; Stelter, M.; Reinmöller, M.; Gräbner, M.; Richter, A.; Charitos, A. (2023b). A Review of Top-Submerged Lance (TSL) Processing—Part I. Plant and Reactor Engineering. Metals 13 (10), 1728. DOI: 10.3390/met13101728.

Kaya, M. (2016). Recovery of metals from electronic waste by physical and chemical recycling processes. International Journal of Chemical and Molecular Engineering 10 (2), 259–270.

Kaya, M. (2019a). Electronic Waste and Printed Circuit Board Recycling Technologies. Cham: Springer International Publishing.

Kaya, M. (2019b). Industrial-Scale E-Waste/WPCB Recycling Lines: Springer International Publishing, M. (The Minerals, Metals & Materials Series).

Khachatryan, A.; Vardanyan, N.; Vardanyan, A.; Zhang, R.; Castro, L. (2021). The effect of metal ions on the growth and ferrous iron oxidation by *Leptospirillum ferriphilum CC* isolated from Armenia mine sites. Metals 11 (3), 425. DOI: 10.3390/met11030425.

Khaliq, A.; Rhamdhani, M.; Brooks, G.; Masood, S. (2014). Metal extraction processes for electronic waste and existing industrial routes. A Review and Australian Perspective. Resources 3 (1), 152–179. DOI: 10.3390/resources3010152.

Kim, B.-S.; Lee, J.-c.; Seo, S.-P.; Park, Y.-K.; Sohn, H. Y. (2004). A process for extracting precious metals from spent printed circuit boards and automobile catalysts. JOM 56 (12), 55–58. DOI: 10.1007/s11837-004-0237-9.

Kinnunen, P. H. M.; Puhakka, J. A. (2005). High-rate iron oxidation at below pH 1 and at elevated iron and copper concentrations by a *Leptospirillum ferriphilum* dominated biofilm. Process Biochemistry 40 (11), 3536–3541. DOI: 10.1016/j.procbio.2005.03.050.

Kumar, A.; Saini, H. S.; Kumar, S. (2018). Bioleaching of gold and silver from waste printed circuit boards by *Pseudomonas balearica SAE1* isolated from an e-waste recycling facility. Current Microbiology 75 (2), 194–201. DOI: 10.1007/s00284-017-1365-0.

Kumar, M.; Lee, J.-c.; Kim, M.-S.; Jeong, J.; Yoo, K. (2014). Leaching of metals from waste printed circuit boards (WPCBS) using sulfuric and nitric acids. Environmental Engineering & Management Journal 13 (10).

Kurosawa, N.; Itoh, Y. H.; Itoh, T. (2003). Reclassification of *Sulfolobus hakonensis* Takayanagi et al. 1996 as *Metallosphaera hakonensis* comb. nov. based on phylogenetic evidence and DNA G+C content. International Journal of Systematic and Evolutionary Microbiology 53 (Pt 5), 1607–1608. DOI: 10.1099/ijs.0.02716-0.

Theo, L. (1998). Integrated recycling of non-ferrous metals at Boliden Ltd. In Ronnskar smelter: Proceedings of the International Symposium on Electronics and the Environment (Cat. No.98CH36145): Theo, L (Eds). Oak Brook, IL, USA: Institute of Electrical and Electronics Engineers, 42-47. DOI: 10.1109/ISEE.1998.675028

Lambert, F.; Gaydardzhiev, S.; Léonard, G.; Lewis, G.; Bareel, P.-F.; Bastin, D. (2015). Copper leaching from waste electric cables by biohydrometallurgy. Minerals Engineering 76 (1), 38–46. DOI: 10.1016/j.mineng.2014.12.029.

Lewis, A. E. (2010). Review of metal sulphide precipitation. Hydrometallurgy 104 (2), 222–234. DOI: 10.1016/j.hydromet.2010.06.010.

Li, J.; Wen, J.; Guo, Y.; An, N.; Liang, C.; Ge, Z. (2020). Bioleaching of gold from waste printed circuit boards by alkali-tolerant Pseudomonas fluorescens. Hydrometallurgy 194 (24), 105260. DOI: 10.1016/j.hydromet.2020.105260.

Li, M.; Deng, X.; Sun, W.; Hu, L.; Zhong, H.; He, Z.; Xiong, D. (2022). Extracellular polymeric substances of acidophilic microorganisms play a crucial role in heavy metal ions adsorption. International Journal of Environmental Science and Technology 19 (6), 4857–4868. DOI: 10.1007/s13762-021-03352-9.

Li, T.-F.; Painter, R. G.; Ban, B.; Blake, R. C. (2015). The multicenter aerobic iron respiratory chain of *Acidithiobacillus ferrooxidans* functions as an ensemble with a single macroscopic rate constant. The Journal of Biological Chemistry 290 (30), 18293–18303. DOI: 10.1074/jbc.M115.657551.

Liang, C. J.; Li, J. Y.; Ma, C. J. (2014). Review on cyanogenic bacteria for gold recovery from E-Waste. Advanced Materials Research 878, 355–367. DOI: 10.4028/www.scientific.net/AMR.878.355.

Liang, G.; Mo, Y.; Zhou, Q. (2010). Novel strategies of bioleaching metals from printed circuit boards (PCBs) in mixed cultivation of two acidophiles. Enzyme and Microbial Technology 47 (7), 322–326. DOI: 10.1016/j.enzmictec.2010.08.002.

Luo, A.; Wang, F.; Sun, D.; Liu, X.; Xin, B. (2021). Formation, development, and cross-species interactions in biofilms. Frontiers in Microbiology 12, 757327. DOI: 10.3389/fmicb.2021.757327.

Menetti, R. P.; Tenório, S. A.J. (Eds.) (1995). Recycling of precious metals from electronic scraps.

Michel, C.; Bény, C.; Delorme, F.; Poirier, L.; Spolaore, P.; Morin, D.; d'Hugues, P. (2009). New protocol for the rapid quantification of exopolysaccharides in continuous culture systems of acidophilic bioleaching bacteria. Applied Microbiology and Biotechnology 82 (2), 371–378. DOI: 10.1007/s00253-008-1824-4.

Motaghed, M.; Mousavi, S. M.; Rastegar, S. O.; Shojaosadati, S. A. (2014). Platinum and rhenium extraction from a spent refinery catalyst using Bacillus megaterium as a cyanogenic bacterium. Statistical modeling and process optimization. Bioresource Technology 171, 401–409. DOI: 10.1016/j.biortech.2014.08.032.

Mrazikova, A.; Marcincakova, R.; Kadukova, J.; Velgosova, O. (2013). Influence of bacterial culture to copper bioleaching from printed circuit boards. Inżynieria Mineralna R 14 (2), 59–62.

Mudd, G. M. (2010). The Environmental sustainability of mining in Australia. Key mega-trends and looming constraints. Resources Policy 35 (2), 98–115. DOI: 10.1016/j.resourpol.2009.12.001.

Mudd, G. M.; Jowitt, S. M. (2018). Growing global copper resources, reserves and production. discovery is not the only control on supply. Economic Geology 113 (6), 1235–1267. DOI: 10.5382/econgeo.2018.4590.

Natarajan, G.; Ting, Y.-P. (2014). Pretreatment of e-waste and mutation of alkali-tolerant cyanogenic bacteria promote gold biorecovery. Bioresource Technology 152, 80–85. DOI: 10.1016/j.biortech.2013.10.108.

Nemati, M.; Harrison, S.T.L.; Hansford, G. S.; Webb, C. (1998). Biological oxidation of ferrous sulphate by *Thiobacillus ferrooxidans*. A review on the kinetic aspects. Biochemical Engineering Journal 1 (3), 171–190. DOI: 10.1016/S1369-703X(98)00006-0.

Ngoma, E.; Borja, D.; Smart, M.; Shaik, K.; Kim, H.; Petersen, J.; Harrison, S. T.L. (2018). Bioleaching of arsenopyrite from Janggun mine tailings (South Korea) using an adapted mixed mesophilic culture. Hydrometallurgy 181 (1), 21–28. DOI: 10.1016/j.hydromet.2018.08.010.

Nies, D. H. (1992). Resistance to cadmium, cobalt, zinc, and nickel in microbes. Plasmid 27 (1), 17–28. DOI: 10.1016/0147-619X(92)90003-S.

Niu, Z.; Huang, Q.; Wang, J.; Yang, Y.; Xin, B.; Chen, S. (2015). Metallic ions catalysis for improving bioleaching yield of Zn and Mn from spent Zn-Mn batteries at high pulp density of 10. Journal of Hazardous Materials 298, 170–177. DOI: 10.1016/j.jhazmat.2015.05.038.

Nkuna, R.; Ijoma, G. N.; Matambo, T. S.; Chimwani, N. (2022). Accessing metals from low-grade ores and the environmental impact considerations. A Review of the perspectives of conventional versus bioleaching strategies. Minerals 12 (5), 506. DOI: 10.3390/min12050506.

Norgate, T.; Jahanshahi, S. (2010). Low grade ores – Smelt, leach or concentrate? Minerals Engineering 23 (2), 65–73. DOI: 10.1016/j.mineng.2009.10.002.

Northey, S.; Mohr, S.; Mudd, G. M.; Weng, Z.; Giurco, D. (2014). Modelling future copper ore grade decline based on a detailed assessment of copper resources and mining. Resources, Conservation and Recycling 83 (5), 190–201. DOI: 10.1016/j.resconrec.2013.10.005.

Nurmi, P.; Özkaya, B.; Kaksonen, A. H.; Tuovinen, O. H.; Puhakka, J. A. (2009). Inhibition kinetics of iron oxidation by *Leptospirillum ferriphilum* in the presence of ferric, nickel and zinc ions. Hydrometallurgy 97 (3-4), 137–145. DOI: 10.1016/j.hydromet.2009.02.003.

Ogunniyi, I. O.; Vermaak, M. K.G. (Eds.) (2007). Improving printed circuit board physical processing–an overview.

Oh, C. J.; Lee, S. O.; Yang, H. S.; Ha, T. J.; Kim, M. J. (2003). Selective leaching of valuable metals from waste printed circuit boards. Journal of the Air & Waste Management Association (1995) 53 (7), 897–902. DOI: 10.1080/10473289.2003.10466230.

Oliveira, P. C.; Cabral, M.; Nogueira, C. A.; Margarido, F. (2010). Printed circuit boards recycling. Characterization of granulometric fractions from shredding process. Material Science Forum 636-637, 1434–1439. DOI: 10.4028/www.scientific.net/MSF.636-637.1434.

Ozkaya, B.; Sahinkaya, E.; Nurmi, P.; Kaksonen, A. H.; Puhakka, J. A. (2007). Kinetics of iron oxidation by *Leptospirillum ferriphilum* dominated culture at pH below one. Biotechnology and Bioengineering 97 (5), 1121–1127. DOI: 10.1002/bit.21313.

Ozturk, S.; Aslim, B.; Suludere, Z.; Tan, S. (2014). Metal removal of cyanobacterial exopolysaccharides by uronic acid content and monosaccharide composition. Carbohydrate Polymers 101, 265–271. DOI: 10.1016/j.carbpol.2013.09.040.

Park, H. S.; Han, Y. S.; Park, J. H. (2019). Massive Recycling of Waste Mobile Phones. Pyrolysis, Physical Treatment, and Pyrometallurgical Processing of Insoluble Residue. ACS Sustainable Chemistry & Engineering. 7 (16), 14119–14125. DOI: 10.1021/acssuschemeng.9b02725.

Park, Y. J.; Fray, D. J. (2009). Recovery of high purity precious metals from printed circuit boards. Journal of Hazardous Materials 164 (2-3), 1152–1158. DOI: 10.1016/j.jhazmat.2008.09.043.

Priya, A.; Hait, S. (2017). Comparative assessment of metallurgical recovery of metals from electronic waste with special emphasis on bioleaching. Environmental Science and Pollution Research International 24 (8), 6989–7008. DOI: 10.1007/s11356-016-8313-6.

Priya, A.; Hait, S. (2018). Extraction of metals from high grade waste printed circuit board by conventional and hybrid bioleaching using Acidithiobacillus ferrooxidans. Hydrometallurgy 177, 132–139. DOI: 10.1016/j.hydromet.2018.03.005.

Pronk, J. T.; Johnson, D. B. (1992). Oxidation and reduction of iron by acidophilic bacteria. Geomicrobiology Journal 10 (3-4), 153–171. DOI: 10.1080/01490459209377918.

Quinet, P.; Proost, J.; van Lierde, A. (2005). Recovery of precious metals from electronic scrap by hydrometallurgical processing routes. Mining, Metallurgy & Exploration 22 (1), 17–22. DOI: 10.1007/BF03403191.

Rabah, M. A. (2008). Recyclables recovery of europium and yttrium metals and some salts from spent fluorescent lamps. Waste Management 28 (2), 318–325. DOI: 10.1016/j.wasman.2007.02.006.

Rawlings, D. E. (2005). Characteristics and adaptability of iron- and sulfur-oxidizing microorganisms used for the recovery of metals from minerals and their concentrates. Microbial Cell Factories 4 (1), 13. DOI: 10.1186/1475-2859-4-13.

Rawlings, D. E.; Johnson, D. B. (2007). The microbiology of biomining. Development and optimization of mineral-oxidizing microbial consortia. Microbiology 153 (2), 315–324. DOI: 10.1099/mic.0.2006/001206-0.

Recycling towards a circular economy (2022). Available online at https://www.glencore.com/media-and-insights/insights/2022-10-recycling-towards-a-circular-economy, updated on 2/13/2024, checked on 2/13/2024.

Regel-Rosocka, M. (2018). Electronic wastes. Physical Sciences Reviews 3 (5), 7. DOI: 10.1515/psr-2018-0020.

Robinson, B. H. (2009). E-waste. An assessment of global production and environmental impacts. The Science of the Total Environment 408 (2), 183–191. DOI: 10.1016/j.scitotenv.2009.09.044.

Rodrigues, M. L.M.; Leão, V. A.; Gomes, O.; Lambert, F.; Bastin, D.; Gaydardzhiev, S. (2015). Copper extraction from coarsely ground printed circuit boards using moderate thermophilic bacteria in a rotating-drum reactor. Waste Management 41 (0), 148–158. DOI: 10.1016/j.wasman.2015.04.001.

Rohwerder, T.; Gehrke, T.; Kinzler, K.; Sand, W. (2003). Bioleaching review part A. Progress in bioleaching: fundamentals and mechanisms of bacterial metal sulfide oxidation. Applied Microbiology and Biotechnology 63 (3), 239–248. DOI: 10.1007/s00253-003-1448-7.

Ruan, J.; Xu, Z. (2016). Constructing environment-friendly return road of metals from e-waste. Combination of physical separation technologies. Renewable and Sustainable Energy Reviews 54, 745–760. DOI: 10.1016/j.rser.2015.10.114.

Ruth, M. (1995). Thermodynamic constraints on optimal depletion of copper and aluminum in the United States. A dynamic model of substitution and technical change. Ecological Economics 15 (3), 197–213. DOI: 10.1016/0921-8009(95)00053-4.

Sajjad, W.; Zheng, G.; Din, G.; Ma, X.; Rafiq, M.; Xu, W. (2019). Metals extraction from sulfide ores with microorganisms. The bioleaching technology and recent developments. Transactions of the Indian Institute of Metals 72 (3), 559–579. DOI: 10.1007/s12666-018-1516-4.

Sampson, M. I.; Phillips, C. V. (2001). Influence of base metals on the oxidising ability of acidophilic bacteria during the oxidation of ferrous sulfate and mineral sulfide concentrates, using mesophiles and moderate thermophiles. Minerals Engineering 14 (3), 317–340. DOI: 10.1016/S0892-6875(01)00004-8.

Sand, W.; Gehrke, T. (1999). Analysis and function of the EPS from the strong acidophile *Thiobacillus ferrooxidans*. In Jost Wingender, Thomas R. Neu, Hans-Curt Flemming (Eds.): Microbial Extracellular Polymeric Substances: Characterization, Structure and Function.: Springer Berlin Heidelberg, 127–141.

Sand, W.; Gehrke, T. (2006). Extracellular polymeric substances mediate bioleaching/biocorrosion via interfacial processes involving iron(III) ions and acidophilic bacteria. Research in Microbiology 157 (1), 49–56. DOI: 10.1016/j.resmic.2005.07.012.

Schipper, B. W.; Lin, H.-C.; Meloni, M. A.; Wansleeben, K.; Heijungs, R.; van der Voet, E. (2018). Estimating global copper demand until 2100 with regression and stock dynamics. Resources, Conservation and Recycling 132, 28–36. DOI: 10.1016/j.resconrec.2018.01.004.

Schippers, A.; Sand, W. (1999). Bacterial leaching of metal sulfides proceeds by two indirect mechanisms via thiosulfate or via polysulfides and sulfur. Applied and Environmental Microbiology 65 (1), 319–321. DOI: 10.1128/AEM.65.1.319-321.1999.

Sethurajan, M.; van Hullebusch, E. D.; Fontana, D.; Akcil, A.; Deveci, H.; Batinic, B. et al. (2019). Recent advances on hydrometallurgical recovery of critical and precious elements from end of life electronic wastes - a review. Critical Reviews in Environmental Science and Technology 49 (3), 212–275. DOI: 10.1080/10643389.2018.1540760.

Smith, S. L.; Johnson, D. B. (2018). Growth of *Leptospirillum ferriphilum* in sulfur medium in co-culture with *Acidithiobacillus caldus*. Extremophiles: life under extreme conditions 22 (2), 327–333. DOI: 10.1007/s00792-018-1001-3.

Srichandan, H.; Mohapatra, R. K.; Parhi, P. K.; Mishra, S. (2019). Bioleaching approach for extraction of metal values from secondary solid wastes. A critical review. Hydrometallurgy 189, 105122. DOI: 10.1016/j.hydromet.2019.105122.

Sugio, T.; Ako, A.; Takeuchi, F. (2010). Sulfite oxidation catalyzed by aa 3-type cytochrome c oxidase in *Acidithiobacillus ferrooxidans*. Bioscience, Biotechnology, and Biochemistry 74 (11), 2242–2247.

Tapia, J.; Dueñas, A.; Cheje, N.; Soclle, G.; Patiño, N.; Ancalla, W. et al. (2022). Bioleaching of heavy metals from printed circuit boards with an acidophilic iron-oxidizing Microbial consortium in stirred tank reactors. Bioengineering 9 (2). DOI: 10.3390/bioengineering9020079.

The Future of Copper (2022). The future of copper: Will the looming supply gap short-circuit the energy transition? Available online at chrome-extension://efaidnbmnnnibpcajpcglclefindmkaj/https://cdn.ihsmarkit.com/www/pdf/0722/The-Future-of-Copper_Full-Report-14July2022.pdf, checked on 2/26/2024.

Touze, S.; Guignot, S.; Hubau, A.; Devau, N.; Chapron, S. (2020). Sampling waste printed circuit boards. Achieving the right combination between particle size and sample mass to measure metal content. Waste Management 118, 380–390. DOI: 10.1016/j.wasman.2020.08.054.

Tuncuk, A.; Stazi, V.; Akcil, A.; Yazici, E. Y.; Deveci, H. (2012). Aqueous metal recovery techniques from e-scrap. Hydrometallurgy in Recycling. Minerals Engineering 25 (1), 28–37. DOI: 10.1016/j.mineng.2011.09.019.

Valdés, J.; Pedroso, I.; Quatrini, R.; Dodson, R. J.; Tettelin, H.; Blake, R. et al. (2008). *Acidithiobacillus ferrooxidans* metabolism. From genome sequence to industrial applications. BMC genomics 9, 597. DOI: 10.1186/1471-2164-9-597.

van Heukelem, A. M. H.; Reuter, M. A.; Huisman, J.; Hagelüken, C.; Brusselaers, J.; Refining, U. P. M. (2004). Eco efficient optimization of pre-processing and metal smelting. Electronic Goes Green, 657–661.

van Loosdrecht, M. C.; Lyklema, J.; Norde, W.; Zehnder, A. J. (1990). Influence of interfaces on microbial activity. Microbiological Reviews 54 (1), 75–87. DOI: 10.1128/mr.54.1.75-87.1990.

van Yken, J.; Cheng, K. Y.; Boxall, N. J.; Nikoloski, A. N.; Moheimani, N.; Valix, M. et al. (2020). Potential of metals leaching from printed circuit boards with biological and chemical lixiviants. Hydrometallurgy 196, 105433. DOI: 10.1016/j.hydromet.2020.105433.

van Yken, J.; Cheng, K. Y.; Boxall, N. J.; Nikoloski, A. N.; Moheimani, N.; Valix, M.; Kaksonen, A. H. (2023). An integrated biohydrometallurgical approach for the extraction of base metals from printed circuit boards. Hydrometallurgy 216 (4), 105998. DOI: 10.1016/j.hydromet.2022.105998.

Vegliò, F.; Quaresima, R.; Fornari, P.; Ubaldini, S. (2003). Recovery of valuable metals from electronic and galvanic industrial wastes by leaching and electrowinning. Waste Management 23 (3), 245–252. DOI: 10.1016/S0956-053X(02)00157-5.

Veit, H. M.; Bernardes, A. M.; Ferreira, J. Z.; Tenório, J. A. S.; Fraga Malfatti, C. de (2006). Recovery of copper from printed circuit boards scraps by mechanical processing and electrometallurgy. Journal of Hazardous Materials 137 (3), 1704–1709. DOI: 10.1016/j.jhazmat.2006.05.010.

Veldhuizen, H.; Sippel, B. (1994). Mining discarded electronics. Industrial Environment 17 (3), 7–11.

Vu, B.; Chen, M.; Crawford, R. J.; Ivanova, E. P. (2009). Bacterial extracellular polysaccharides involved in biofilm formation. Molecules 14 (7), 2535–2554. DOI: 10.3390/molecules14072535.

Wang, J.; Faraji, F.; Ramsay, J.; Ghahreman, A. (2021). A review of biocyanidation as a sustainable route for gold recovery from primary and secondary low-grade resources. Journal of Cleaner Production 296 (30), 126457. DOI: 10.1016/j.jclepro.2021.126457.

Watnick, P.; Kolter, R. (2000). Biofilm, city of microbes. Journal of Bacteriology 182 (10), 2675–2679. DOI: 10.1128/jb.182.10.2675-2679.2000.

Widmer, R.; Oswald-Krapf, H.; Sinha-Khetriwal, D.; Schnellmann, M.; Böni, H. (2005). Global perspectives on e-waste. Environmental Impact Assessment Review 25 (5), 436–458. DOI: 10.1016/j.eiar.2005.04.001.

Wood, J.; Creedy, S.; Matusewicz, R.; Reuter, M. (2011). Secondary copper processing using Outotec Ausmelt TSL technology. Proceedings of MetPlant, 460–467.

Wu, W.; Liu, X.; Zhang, X.; Zhu, M.; Tan, W. (2018). Bioleaching of copper from waste printed circuit boards by bacteria-free cultural supernatant of iron–sulfur-oxidizing bacteria. Bioresources and Bioprocessing. 5 (1), 233. DOI: 10.1186/s40643-018-0196-6.

Xia, L.; Liu, X.; Zeng, J.; Yin, C.; Gao, J.; Liu, J.; Qiu, G. (2008). Mechanism of enhanced bioleaching efficiency of *Acidithiobacillus ferrooxidans* after adaptation with chalcopyrite. Hydrometallurgy 92 (3-4), 95–101. DOI: 10.1016/j.hydromet.2008.01.002.

Xia, M.-C.; Wang, Y.-P.; Peng, T.-J.; Shen, L.; Yu, R.-L.; Liu, Y.-D. et al. (2017). Recycling of metals from pretreated waste printed circuit boards effectively in stirred tank reactor by a moderately thermophilic culture. Journal of Bioscience and Bioengineering 123 (6), 714–721. DOI: 10.1016/j.jbiosc.2016.12.017.

Xiang, Y.; Wu, P.; Zhu, N.; Zhang, T.; Liu, W.; Wu, J.; Li, P. (2010). Bioleaching of copper from waste printed circuit boards by bacterial consortium enriched from acid mine drainage. Journal of Hazardous Materials 184 (1-3), 812–818. DOI: 10.1016/j.jhazmat.2010.08.113.

Xu, C.; Santschi, P. H.; Schwehr, K. A.; Hung, C.-C. (2009). Optimized isolation procedure for obtaining strongly actinide binding exopolymeric substances (EPS) from two bacteria (*Sagittula stellata* and *Pseudomonas fluorescens Biovar II*). Bioresource Technology 100 (23), 6010–6021. DOI: 10.1016/j.biortech.2009.06.008.

Yamane, L. H.; Moraes, V. T. de; Espinosa, D. C. R.; Tenório, J. A. S. (2011). Recycling of WEEE. Characterization of spent printed circuit boards from mobile phones and computers. Waste Management 31 (12), 2553–2558. DOI: 10.1016/j.wasman.2011.07.006.

Yang, J.; Retegan, T.; Ekberg, C. (2013). Indium recovery from discarded LCD panel glass by solvent extraction. Hydrometallurgy 137 (8), 68–77. DOI: 10.1016/j.hydromet.2013.05.008.

Yang, T.; Xu, Z.; Wen, J.; Yang, L. (2009). Factors influencing bioleaching copper from waste printed circuit boards by *Acidithiobacillus ferrooxidans*. Hydrometallurgy 97 (1-2), 29–32. DOI: 10.1016/j.hydromet.2008.12.011.

Yarzábal, A.; Brasseur, G.; Ratouchniak, J.; Lund, K.; Lemesle-Meunier, D.; DeMoss, J. A.; Bonnefoy, V. (2002). The high-molecular-weight cytochrome c Cyc2 of *Acidithiobacillus ferrooxidans* is an outer membrane protein. Journal of Bacteriology 184 (1), 313–317. DOI: 10.1128/jb.184.1.313-317.2002.

Yazici, E. Y.; Deveci, H. (2013). Extraction of metals from waste printed circuit boards (WPCBs) in H_2SO_4–$CuSO_4$–NaCl solutions. Hydrometallurgy 139, 30–38. DOI: 10.1016/j.hydromet.2013.06.018.

Yazici, E. Y.; Deveci, H. (2014). Ferric sulphate leaching of metals from waste printed circuit boards. International Journal of Mineral Processing 133 (4), 39–45. DOI: 10.1016/j.minpro.2014.09.015.

Yoo, J.-M.; Jeong, J.; Yoo, K.; Lee, J.-c.; Kim, W. (2009). Enrichment of the metallic components from waste printed circuit boards by a mechanical separation process using a stamp mill. Waste Management 29 (3), 1132–1137. DOI: 10.1016/j.wasman.2008.06.035.

Zhang, L.; Xu, Z. (2016). A review of current progress of recycling technologies for metals from waste electrical and electronic equipment. Journal of Cleaner Production 127, 19–36. DOI: 10.1016/j.jclepro.2016.04.004.

Zhang, S.; Forssberg, E. (1997). Mechanical separation-oriented characterization of electronic scrap. Resources, Conservation and Recycling 21 (4), 247–269. DOI: 10.1016/S0921-3449(97)00039-6.

Zhang, X.; Shi, H.; Tan, N.; Zhu, M.; Tan, W.; Daramola, D.; Gu, T. (2023). Advances in bioleaching of waste lithium batteries under metal ion stress. Bioresource and Bioprocessing. 10 (1), 2193. DOI: 10.1186/s40643-023-00636-5.

Zhu, N.; Xiang, Y.; Zhang, T.; Wu, P.; Dang, Z.; Li, P.; Wu, J. (2011). Bioleaching of metal concentrates of waste printed circuit boards by mixed culture of acidophilic bacteria. Journal of Hazardous Materials 192 (2), 614–619. DOI: 10.1016/j.jhazmat.2011.05.062.

Zobell, C. E. (1943). The effect of solid surfaces upon bacterial activity. Journal of Bacteriology 46 (1), 39–56.

CHAPTER 3

3 Material and methods

This chapter seeks to detail the overview of the general experimental design, procedures, materials, and analytical protocols followed in this study. A description of the source and type of the printed circuit boards (PCBs) used, the comminution techniques used for size reduction and analysis of PCB particle size distribution together with metal content characterisation are provided. The research approaches adopted for collection of data for chemical leaching kinetics, microbial oxidation kinetics, and bioleaching kinetics of PCBs in a novel two-stage reactor system are then presented in detail. These experimental procedures are also included in the respective chapters, i.e., Chapter 4 to 7. In addition, all analytical techniques used in this study are described in detail; these include pH and redox potential measurement protocols, the ferric chloride assay for calorimetric measurements of ferric iron, ferrous iron and total iron, and scanning electron microscopy (SEM) analysis for visual assessment of the immobilised polyurethane form as biomass support particle (PUF-BSPs).

3.1 PCB sample preparation and pre-treatment

3.1.1 Printed circuit boards used

The heterogeneity of PCBs in terms of size, and metallic and non-metallic contents remains a challenge in the handling and treatment of waste PCBs. As such, to ensure experimental reproducibility and confidence in experimental outputs, all printed circuit boards used in this study were custom-made and manufactured by Trax Interconnect (Pty) Ltd, Cape Town, South Africa. The PCBs were representative of each other in terms of design, quality, and material composition. Although the PCBs had no extraneous parts (i.e., random-access memory (RAMs), peripheral component interconnect (PCI), and chip slots) soldered on, these PCBs represent the typical base design that the company's clients most frequently request. The boards were 105 mm in height, 142 mm in length, and thickness of 1.45 mm; and on average, the PCBs weighed approximately 52.94 g. Images of the front and back view of the PCBs are provided in, Figure 3-1.

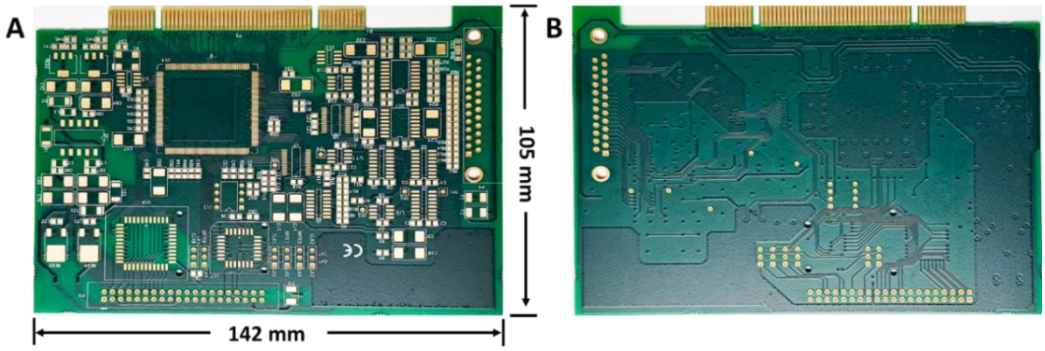

Figure 3-1 Custom-made printed circuit boards used in this study; A – Top side and B – Bottom side.

3.1.2 Size reduction of the PCBs

The size of the custom-made PCBs was first reduced by shredding the whole board using a bench Industrial Grab Shredder (length: 170 mm, width: 140 mm, and 14 circular blades) supplied by Filamaker Gmbh, Germany (Figure 3-2A, B and C) The shredder had a 1.1 kW motor which runs at 50 Hz frequency, operated by Siemen inverter with Sinamatic version 20 software (Figure 3E). A single board was shredded by repeatedly passing it through the shredder six times (6x). The number of passes through the shredder was informed by the study carried out by (Prestele 2020b), which suggested no further size reduction above 6 passes. The shredded boards, referred to as PCB chips, were further reduced into finer particles (≤1180 µm) by pulverisation for one minute using a ring mill pulveriser obtained from the Ferguson industrial equipment group in Johannesburg, South Africa (Figure 3-2C). To obtain a representative sample, the pulverised boards were split into 10 equivalent samples of approximately 5 g each using a Dickie and Stockler rotary splitter (Figure 3-2F).

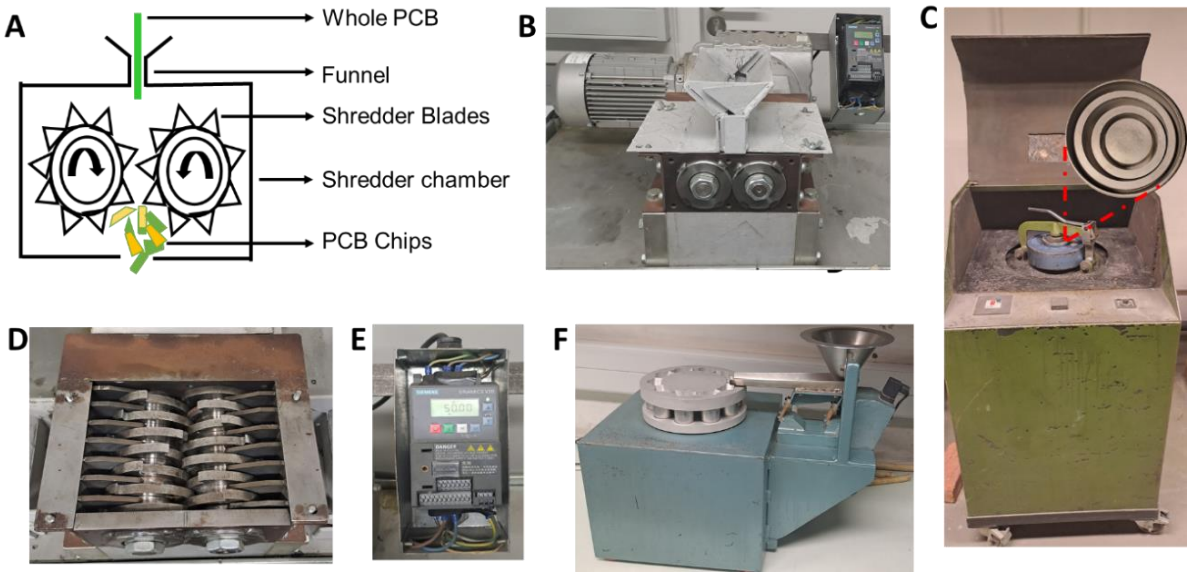

Figure 3-2 Equipments used for size reduction of the whole PCBs. Bench Industrial Grab Shredder used to shred a whole PCB into PCB chips: **A** – Schematic representation of the shredder, **B** – Front (full) view of the shredder. **C** - Ring mill pulveriser, **D** – Top view of shredder without the safety cover (funnel), **E** - Siemen inverter, and **F** - Dickie and Stockler rotary splitter.

Unless stated otherwise, the finer PCB particles (<1180 µm) were used in all PCB chemical leaching experiments. This approach addresses the impact of surface area on the overall leaching kinetics, thereby facilitating a more relevant comparison of the chemical leaching kinetics determined from the leaching of the elementary metals to that from PCB leaching (Chapter 4).

In the experiments for PCBs bioleaching (Chapter 7) however, PCB chips were used rather than the finer particles (<1180 µm). Instead of pulverising the shredded PCBs for one minute,

PCB chips were prepared by pulverising for only 20 seconds. Pulverising for 20 seconds liberated metals by mechanical disruption of the outer layers of the PCBs and allowed further size reduction after shredding but not into finer particles. The particle size distribution (PSD) of these PCB chips was determined by the dry sieve analysis method (Iyasara et al. 2023). The PCB chips were sieved into 5 fractions (<1180 µm, 1180 µm, 1700 µm, 3350 µm, and 4750 µm) using a Filtra FTL0200 sieve shaker (Figure 3-3C), operated for 10 minutes. The cumulative particle size distribution (%) is shown in Figure 3-4.

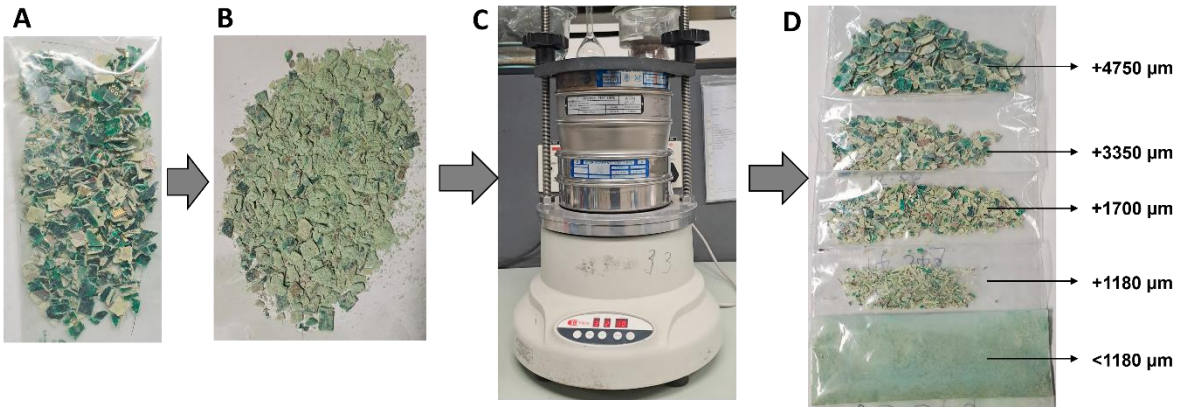

Figure 3-3 Screening of pulverised PCB into different size fraction; **A** – Shredded PCB chips, **B** – 20 sec Pulverised PCBs, **C** – Sieve shaker, and **D** – different size fractions of PCBs.

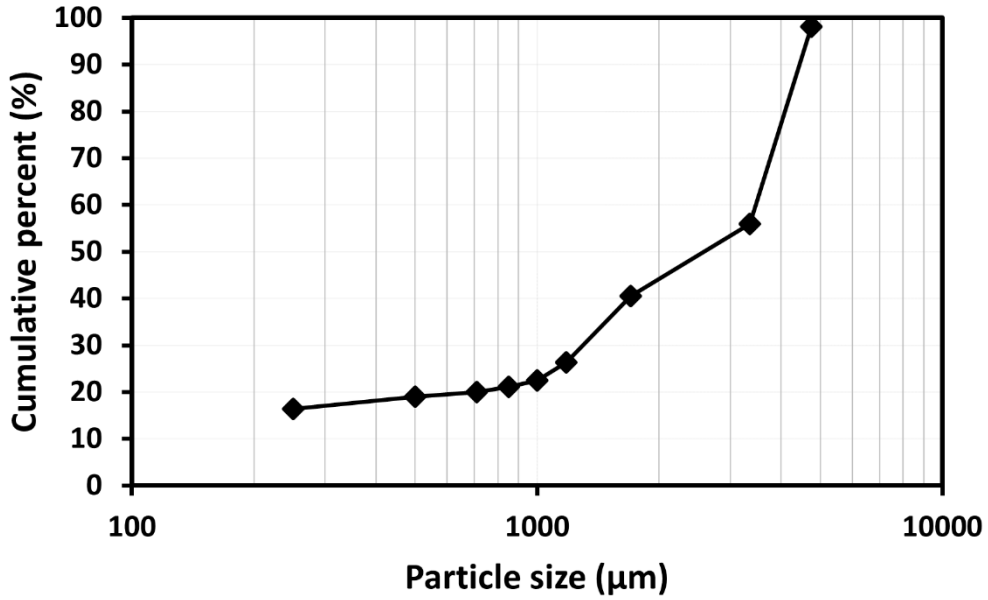

Figure 3-4 Particle size distribution of the PCB pulverised for 20 sec.

3.1.3 Analysis of metals in PCBs

In preparing the PCB templates for metal analysis, a whole PCB was cut into three equivalent sections. Each section was weighed, shredded, pulverised, and split into equal mass using the same procedure as presented in section 3.1.2 above. Metal extraction from these pulverised boards was achieved using the aqua regia approach. Aqua regia was prepared by mixing 6 mL of 15.7 M ultra-pure Nitric acid (HNO_3, Merck with 2 mL of 12.1 M ultra-pure Hydrochloric acid (HCl, Merck), (i.e. 3 parts HNO_3 to 1 part HCl on a volume to volume basis).

A representative PCB sample of 0.1 g from each section was added into the separately prepared shake flasks containing aqua regia solution and digested using MARS microwave digester vessels at 300 °C and 800 psi, for a total of 35 min (Ramp time – 25 min and Hold time – 10 min). The digested liquid sample was then cooled and diluted to a final volume of 50 mL using deionised water. Thereafter, the samples were filtered with a 0.2 µm filter, and the metal concentrations in the filtrates were determined using Inductively Coupled Plasma Mass Spectroscopy (ICP-MS, Agilent 7900). The digestates were air-dried and analysed for metal content using X-ray Fluorescence (XRF). The total metal content in the whole PCB was reported as the sum of the content determined from the 3 sections (Table 3-1).

Table 3-1 Metal composition (in g/100g, % mass) in the custom-made PCBs.

Element	Content (%)	Element	Content (%) ($x10^{-3}$)
Cu	11.0	Sn	1.01
Fe	0.150	Cr	3.81
Zn	0.040	Pb	0.860
Ni	0.180	Mg	7.98
Al	0.090	V	2.71
Co	0.020	Mo	0.180
Ba	0.110	Zr	4.31
Sr	0.040	La	0.670
Ca	0.230	Ce	1.42
Si	0.280	*Au ($x10^{-5}$)	1.41

*Note the concentration of Au is 1.41 x 10^{-5} g/100g and deviates from the column heading.

3.2 Chemical leaching

An evaluation of relative metal leach kinetic rates for Cu, Zn, Ni, and Sn, typically predominant in PCBs was achieved through chemical attack by Fe^{3+} and H^+ as the oxidants. The leaching experiments for each metal, were carried out separately in acidic-ferric (Fe^{3+}) and acid-only (H^+) oxidation environments. Metals were added as elementary metal powder. The four selected elementary metals were leached separately, to evaluate the leaching rate of each individual metal. In addition, a combination of metals mimicking the composition of the leachate as noted during the PCB leaching was also designed. Metal leaching in combination

also allowed for the evaluation of potential secondary reactions such as cementation reactions and subsequent precipitation reactions.

Ferric leaching was carried out in a 500 mL jacketed glass reactor as a batch study, with an initial concentration of 20 g/L Fe^{3+} at pH 1.1. The mass of metal added, in both individual and mixed metal leaching systems, was calculated such that the required stoichiometric molar ratio of 2 mol Fe^{3+}: 1 mol M (metal) was achieved. The acid leaching experiments were carried out using acidified deionised water (adjusted to pH 1.1 by H_2SO_4) and the metal added met a stoichiometric molar ratio of 1 mol H^+: 1 mol M. For the leaching of mixed metals, the proportion (% weight of each metal per total weight of the four metals) of each metal added was informed by the metal content of the PCB sample used in this study.

In both the ferric and acid leaching systems, the temperature was varied across the setpoints 25, 37, 45, 65, and 75 °C to establish the dependence of the metal leaching rates on temperature. Varying the temperature also enabled the evaluation of relative activation energies through the Arrhenius plot to deduce the governing reaction mechanism.

To facilitate appropriate comparison between experiments, PCB leaching in the presence of both acidic-ferric and acid oxidant, were performed at the same leaching conditions, i.e. initial Fe^{3+} concentration of 20 g/L, pH 1.1, and temperature range of 25 – 75 °C, as in the leaching of elementary metal powder. PCB metal characterisation was used to determine the mass of PCB required such that the stoichiometry is met in both acidic-ferric and acid-leaching systems.

Across all leaching systems studied, the progress of metal extraction was monitored by sampling the leachate at various time intervals (every 1 minute for the initial 5 min, 2 min for 20 min, 5 min for 30 min, 10 min for 30 min, 20 min for 1 hour, 30 min for 1 hour, then every hour) over a total of five (5) hours leaching time, unless stated otherwise. A 500 µL solution sample was withdrawn at each sampling interval to ensure that the total volume of liquid sampled by the end of the experiment remained less than 10% of the total working volume. Samples were passed through a 0.45 µm filter and the filtrates were analysed for ferric ion (Fe^{3+}), ferrous ion (Fe^{2+}), total iron (Fe^{tot}) and other specified dissolved metal ion concentrations. Changes in pH and redox potential were continuously monitored by maintaining the pH and redox probes in the leaching solution throughout the leaching period.

3.3 Microbial inhibition studies

The second part of this experimental study focused on understanding microbial inhibition in PCB bioleaching systems as a result of metal ions accumulation and/or other components of the PCBs within the bioleaching system. The aim was to assess and manage the extent of microbial inhibition. Prior to microbial inhibition studies, microbial culture was immobilised onto a PUF-BSPs to increase biomass concentration and minimise inhibition through biofilm protection and diffusion resistance. Metal tolerance was further enhanced by adaptation of the culture to inhibitory Cu^{2+}. In all studies, changes to the microbial ferrous iron oxidation rate as a result of inhibition of the microbial culture by accumulation of metal ions was investigated.

3.3.1 Microbial culture

A mixed mesophilic culture consisting of *Leptospirrilum (L.) ferriphilum*, *Acidithiobacillus (At.) ferrooxidans*, *Acidiplasma (Ap.) cupricumulans* as the dominant species was first grown and colonised onto polyurethane foams used as a biomass support particle (PUF-BSPs). The immobilised microbial system was gradually adapted up to 6 g/L Cu^{2+}. The culture was maintained over two months by replacing the spent medium whenever the substrate was depleted, with fresh Autotrophic basal salts (ABS) medium (Johnson et al. 2008a) containing ferrous iron substrate. Microbial immobilisation on PUF-BSPs was confirmed by scanning electron microscopy (Chapter 5, Section 5.3.1).Four sets of inocula of the same strain, namely non-adapted planktonic cells (NA-PC), immobilised cells (NA-IC), Cu-adapted planktonic cells (A-PC) and Cu-adapted immobilised cells (A-IC), were considered.

3.3.2 Metal ion solutions

Four metals, namely Cu, Zn, Ni, and Sn were considered as potential inhibitory metals as these metals are generally found in significant concentrations in PCB leachates (Yamane et al. 2011; Zhang et al. 2012; Akcil et al. 2015b) These were added as metal ions in the form of their respective metal sulfate salts, i.e., copper sulfate heptahydrate ($CuSO_4.7H_2O$), zinc sulfate heptahydrate ($ZnSO_4.7H_2O$), nickel sulfate heptahydrate ($NiSO_4.7H_2O$), and tin sulfate heptahydrate ($SnSO_4.7H_2O$). In addition, the effect of the leachate from PCB leaching on microbial activity was also investigated.

The inhibitory effect of Cu^{2+} (Chapter 5), Sn^{2+}, Ni^{2+}, and Zn^{2+} ions (Chapter 6) on the microbial ferrous iron oxidation rates of the immobilised and Cu-adapted microbial cultures was then studied. Individual metal ion solutions (Cu^{2+}: 0 – 50 g/L, Zn^{2+}, Ni^{2+}, and Sn^{2+}: 0 – 10 g/L), a mixed metal ion solution (0 – 20% weight/volume, w/v, PCB solid loading mimicked) and the PCB leachates (0 – 50% volume of PCB leachates/total volume of growth medium) was used in this study. The impact of inhibitory metal ion on the performance of the immobilised and Cu-adapted microbial cultures was assessed by monitoring substrate (Fe^{2+} ions) utilisation rates in the presence of increasing concentrations of metal ions of interest. In investigating the effect of the PCB leachates on microbial performance (Chapter 6), the PCBs were first chemically leached using ferric ion, filtered, and the leachates were added in different proportions (0 - 50%v/v).

3.4 Bioleaching of PCBs and reactor studies

Having achieved insight into the chemical leaching rates and microbial oxidation rates in the presence of inhibitory metal ions, bioleaching of PCBs was then performed in two reactor systems (Chapter 7). The first reactor system was a single-stage bioleaching reactor within which chemical leaching of PCBs and *in-situ* microbial regeneration of the ferric iron occurred. In the second, the two-stage bioleaching reactor set-up compromised of a PCB chemical leaching reactor separate from the reactor within which microbial regeneration of ferric iron occurred; with the reactors coupled by a leachate re-circulating system.

The two reactor systems were operated at the same conditions in terms of temperature, Fe^{3+}/Fe^{2+} concentrations, inoculum type, total working volume, and PCB solid loaded (% w/v).

Both reactor systems were inoculated with Cu-adapted immobilised cells as they exhibited higher Fe^{2+} oxidation rates and improved metal ion tolerance against NA-PC, A-PC, and NA-IC.

In the one-stage reactor system, two custom-made stainless steel baskets were fitted into a 1 L stirred tank reactor (STR). One basket housed PUF-BSPs (as A-IC) as an inoculum, while the other was for the added PCB chips. In the two-stage reactor system, one basket was fitted into a stirred tank reactor to house PCB chips, and the PUF-BSPs were packed into six column bioreactors connected in series, such that on Fe^{3+} leaching of PCBs in the STR, the metal-rich stream is recirculated through the packed-bed column bioreactors for microbial generation of Fe^{3+}.

In both reactors, PCBs were added at increments of 3% w/v, up to an accumulative 18% w/v. With the addition of each increment of 3% PCB, the volumetric rate of Fe^{3+} reduction as a function of metal leaching, the rate of microbial oxidation of the resultant Fe^{2+}, and the extent of metal leaching was measured and evaluated.

3.5 Analytical techniques

3.5.1 pH and redox potential

All regular pH measurements were performed using a pH electrode (Model: iConnect 854), connected to a Metrohm 867 meter. The electrode was calibrated at pH 1.0 and 4.0 prior to any measurement using Merck instrumental standard buffer solutions. Redox potential measurements were carried out using a glass electrode with a built-in platinum ring (Ag/AgCl reference, 3 M KCl, Model 6.0451.100), which was connected to pH/Eh 867 Metrohm meter. Precision of all readings was ensured by testing the electrode against the standard solution (650 mV at 25 °C) prior to routine measurements. Both pH and redox potential meters were connected to a desktop computer equipped with Metrohm Tiamo version 2.5 software to control and display any measurement.

3.5.2 Iron analysis

All dissolved iron concentrations (Fe^{2+}, Fe^{3+}, Fe^{total}) were determined spectrophotometrically using the ferric chloride assay (Govender et al. 2012). The assay is based on the formation of a yellow ferric chloride complex formed when 2 M hydrochloric acid is added to a solution containing Fe^{3+} ions. The 2 mL sample (with necessary dilutions) of unknown concentration and 2 M HCl solution (1:1 volumetric ratio) were thoroughly mixed by vortexing at 3200 rpm. Thereafter, the absorbance was measured at 340 nm wavelength using a Genesys 10S UV-Visible spectrophotometer (Thermo Scientific, Visionlite, version 5.2 software). A scoop of potassium persulfate crystals (in excess) was then added into the mixed solution to oxidise all Fe^{2+} ions into Fe^{3+} ions, vortexed and left for 5 minutes. Absorbance was measured again and considered as absorbance for total Fe. Measured absorbances were converted into corresponding Fe concentrations using a standard calibration curve (Appendix A1). The concentration of Fe^{2+} ions is deduced by subtracting the concentration of Fe^{total} ion from Fe^{3+}.

3.5.3 Direct microbial cell counts

The concentration of planktonic microbial cells was determined by direct microscopic cell count on the Thoma counting chamber (Depth of chamber: 0.02 mm and Area: 0.0025 mm^2) using an Olympus BX40 phase contract microscope at 1000x magnification. The counting chamber was provided by HAWSLEY (Helber Bacteria, 1 Cell Thoma, CAT No Z30000, LOT 15632). The sample was diluted using acidified deionised water (pH 1.4) and a 1 µL sample was then pipetted into the centre of the chamber and covered with a glass slide coverslip. Microbial cells were then directly counted using an oil immersion phase contrast. Microbial cell concentration in the sample was determined using Eq. 3-1:

$$Cell\ concentration\ (cell.mL^{-1}) = \frac{C \times \frac{N_T}{N_L}}{D \times A} \times \frac{1}{d} \times 10^3 \qquad Eq.\ 3\text{-}1$$

Where: C = Number of cells counted

N_T = Total number of large squares (16)

N_L = Number of large squares counted (4)

A = Area of the chamber

D = Depth of the chamber (0.02 µm)

d = Dilution factor

3.5.4 Scanning Electron Microscopy (SEM)

The surface of the colonised PUF-BSPs was assessed visually for attached cells and EPS (biofilm) using a scanning electron microscopy (SEM). In this method, the biomass support particles were first cut into smaller pieces with a sterile scissors and fixed in 2.5% (v/v) glutaraldehyde for at least 8 h to 24 h at 4°C. The samples were then gently rinsed three times (3x) with sterile deionised water and dehydrated through a succession of alcohol, 30, 50, 90, 95, and 100% (v/v) analytical grade ethanol (Merck), by keeping the sample in alcohol for 10 minutes at each step. Samples were then dried to critical point using analytical grade hexamethyldisilane (HDMS, Sigma) and mounted on a stub covered with carbon glue. The stub was sputter-coated with carbon and assessed visually at various magnifications using the SEM (FEI NOVA NANOSEM 230 with a field emission gun or Tescan MIRA3 with a Confocal Raman Imaging Extension).

3.6 References

Akcil, A.; Erust, C.; Gahan, C. S.; Ozgun, M.; Sahin, M.; Tuncuk, A. (2015). Precious metal recovery from waste printed circuit boards using cyanide and non-cyanide lixiviants-A review. Waste Management 45, 258–271. DOI: 10.1016/j.wasman.2015.01.017.

Govender, E.; Harrison, S.T.L.; Bryan, C. G. (2012). Modification of the ferric chloride assay for the spectrophotometric determination of ferric and total iron in acidic solutions containing

high concentrations of copper. Minerals Engineering 35, 46–48. DOI: 10.1016/j.mineng.2012.05.006.

Iyasara, A. C.; Nduka, J. A.; Irogbele, G. C. (2023). Design and fabrication of mechanical sieve shaker for particle size analysis of ceramics. Journal of Engineering Research and Reports 24 (8), 12–19. DOI: 10.9734/jerr/2023/v24i8834.

Johnson, D. B.; Joulian, C.; d'Hugues, P.; Hallberg, K. B. (2008). *Sulfobacillus benefaciens* sp. nov., an acidophilic facultative anaerobic Firmicute isolated from mineral bioleaching operations. Extremophiles 12 (6), 789–798. DOI: 10.1007/s00792-008-0184-4.

Prestele, M. P. (2020). Assessment of a Shredding Technology of Waste Printed Circuit Boards in preparation for Ammonia-based Copper leaching. Masters thesis, University of Cape Town.

Yamane, L. H.; Moraes, V. T. de; Espinosa, D. C. R.; Tenório, J. A. S. (2011). Recycling of WEEE. characterization of spent printed circuit boards from mobile phones and computers. Waste Management 31 (12), 2553–2558. DOI: 10.1016/j.wasman.2011.07.006.

Zhang, Y.; Liu, S.; Xie, H.; Zeng, X.; Li, J. (2012). Current status on leaching precious metals from waste printed circuit boards. Procedia Environmental Sciences 16, 560–568. DOI: 10.1016/j.proenv.2012.10.077.

CHAPTER 4

4 Chemical leaching of elementary metals

4.1 Introduction

The leaching of base metals, generally undertaken as the first stage of leaching to liberate precious metals, is selectively undertaken using mineral acid in combination with oxidants (i.e., H_2SO_4/Fe^{3+}, H_2SO_4/O_2, $HClO_4$, HNO_3/H_2O_2, and HCl/O_2). Subsequent extraction of precious metals proceeds using strong acids such as aqua regia (HNO_3/HCl), ammonia-based reagents (NH_3-$(NH_4)_2S_2O_8$) and organic-based oxidative reagents such as thiourea-ferric sulfate, amongst others (Akcil et al. 2015; Wu et al. 2017; Udayakumar et al. 2022). Hydrogen peroxide, H_2O_2, is a strong oxidant and is commonly used in combination with acid suliate solutions, for the extraction of base metals, particularly, copper. Although H_2O_2 is a more effective oxidant compared to O_2 and Fe^{3+}, it is relatively costly to produce, and it is more prone to catalytic decomposition at high temperatures and in the presence of metal ions (Quinet et al. 2005; Tuncuk et al. 2012; Bas et al. 2012; Yazici and Deveci 2014). In comparison, ferric iron can be produced at a relatively low cost and is known to be a strong oxidiser which can oxidise most of the base metals to their respective metal ions (Eq. 4-1). Ferric iron can easily be regenerated *in-situ* using suitable iron-oxidising acidophilic microorganisms (bioleaching systems), or chemically at a slower rate by an oxidant such as O_2.

$$2M^0 + 2Fe^{3+} + \frac{1}{2}O_2 + 2H^+ \rightarrow 2M^{2+} + 2Fe^{2+} + H_2O \qquad \textit{Eq. 4-1}$$

Metal dissolution by Fe^{3+} has been successfully employed in metal leaching from virgin ores at a pilot and industrial level (Du Plessis et al. 2007; Domic 2007; Bryan et al. 2011; Nicolle et al. 2015). While ferric iron leaching of metals from printed circuit boards (PCBs) has been demonstrated on a laboratory scale, this is not yet commercialised. In leaching with the Fe^{3+} oxidant, metal solubility is driven by the difference in the standard hydrogen reduction potential between Fe^{3+} (0.77 V) and metal of interest, i.e., Cu (0.34 V), Zn (-0.76 V). From an electrochemistry point of view, the higher the standard potential difference, the more plausibly and rapidly the metal is leached. A key requirement in Fe^{3+} leaching systems is maintaining pH below 2 to prevent Fe^{3+} precipitation, which can reduce accessible lixiviant and limit mass transfer as its deposits on the surface of the metal or mineral grain, resulting in slower metal leaching rates and low metal extractions. At the required acidic conditions (pH <2), the kinetics of metal leaching depends on the concentration of Fe^{3+} and the operating temperature, amongst other factors. Lambert et al. (2015) reported an improvement in Cu leaching rates from waste electric cables from 19 $mg.L^{-1}.h^{-1}$ to 65 $mg.L^{-1}.h^{-1}$, then 750 $mg.L^{-1}.h^{-1}$ when initial Fe^{3+} concentration was increased from 0 to 2 and 6 g/L, respectively. This resulted in the leaching time reducing from 7 days through 3 days to 1 day (Lambert et al.

2015). A similar dependence of reaction rate on the concentration of Fe^{3+} has been reported elsewhere (Yang et al. 2009; Yazici and Deveci 2014).

As ferric leaching takes place under acidic conditions, proton (H^+) attack contributes to metal leaching, but at a relatively slower leaching rate (Xiang et al. 2010; Lambert et al. 2015). The rate of Fe^{3+} and H^+ leaching is also affected by mass transfer and the type of metal being leached (Casas et al. 2013; Yazici and Deveci 2014; Bilczuk et al. 2016), necessitating the importance of insight into the leaching mechanism and metal relative leaching rate.

The interdependence of the two vital sub-processes involved in bioleaching, that is (i) reduction of Fe^{3+} through metal dissolution, and (ii) microbial regeneration of Fe^{3+} from the resultant Fe^{2+} is recognised. The slower oxidation reaction is the rate-determining step in the overall bioleaching rate. Thus, to optimize this process, it is critical to study the reaction kinetics of both sub-processes. This chapter focuses on the kinetics of the chemical (Fe^{3+}) leaching sub-process. Specifically, it focuses on evaluating chemical leaching kinetics, with the aim of (i) determining relative rates between the Fe^{3+} and H^+ oxidant, (ii) evaluating the relative metal leaching rates, particularly amongst the predominant metals in PCBs (i.e., Cu, Zn, Sn, Ni), and their relative leaching mechanisms, and lastly (iii) developing rate law expressions to describe metal leaching. Notwithstanding the continuous progress in understanding and improving metal recovery from PCBs through Fe^{3+} leaching, the leaching kinetics of individual metals present in PCBs, and other E-waste components, remain limited in the literature. Here, the metal leaching kinetics of individual metals typical in PCBs (Cu, Zn, Ni, Sn) are studied individually and as mixtures prior to exploring a complex PCB leaching system to better understand the expected leaching behaviour of such metals during the leaching of actual PCB samples. Relative kinetic data for metal leaching is critical in the development of a flowsheet for biohydrometallurgical metal extraction and recovery.

4.2 Materials and methods

4.2.1 Leaching procedure

4.2.1.1 Reactor system for leaching study

All chemical leaching experiments were carried out in a jacketed glass reactor (height: 12.51 cm, outer diameter: 10.67 cm, inner diameter: 8.51, with a 500 mL working volume), with warm water recirculated from a water bath to maintain the desired temperature. The reactor was mixed by an 801 Metrohm magnetic stirrer (4.45 cm) at 120 rpm. A Perspex lid (length:13.8 cm, width: 13.2 cm, and height: 0.5 cm) was used to minimise evaporation. The lid had three (3) ports, two to house the pH and redox electrodes and the third for sampling. Measurements from the pH and redox meters (Metrohm 867) were logged continuously and displayed through a desktop computer installed with Tiamo software (Figure 4-1), along with the stirrer speed.

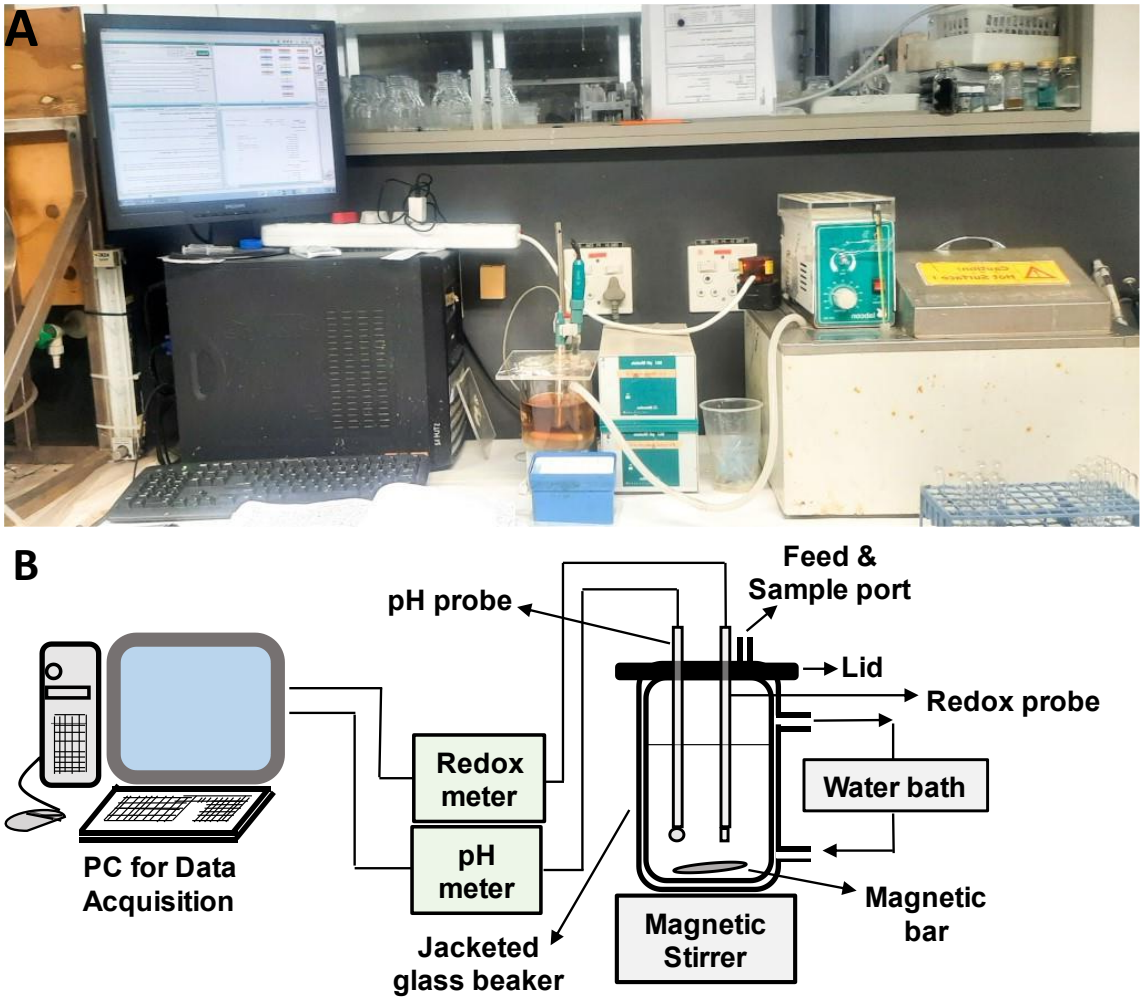

Figure 4-1 A photograph (**A**) and schematic diagram (**B**) of the apparatus and setup used in this study for all chemical leaching (both ferric and acid-only leaching) experiments.

4.2.1.2 Materials leached

The four elementary metals of interest, i.e. Cu powder (purity: ≥99.9%, particle size distribution: <63 µm), Zn powder (≥98.9%, <10 µm), Ni powder (≥99.5%, <10 µm), and Sn powder (≥99.8%, <45 µm), were supplied by Merck South Africa. In all leaching experiments, the elementary metals were used without any pretreatment. The type, source, and pretreatment of the PCBs used in this study, unless stated otherwise, is discussed in Section 3.1.All leaching reagents used, including ferric sulfate hydrate ($Fe_2(SO_4)_3.4.5H_2O$, 97%) and sulfuric acid (H_2SO_4, 96%), were supplied by Merck South Africa.

4.2.1.3 Ferric leaching of elementary metals and PCBs

To explore the leaching rate of selected elementary metal powders via ferric iron leaching, the metal of interest was added into 250 mL of 20 g/L ferric sulfate hydrate solution (prepared from $Fe_2(SO_4)_3.4.5H_2O$). The pH of the Fe^{3+} solution was adjusted to 1.1 using 96% H_2SO_4 and the solution equilibrated to the desired temperature. Thereafter, metal powder was added

into the beaker at time zero. Samples were taken at a predetermined time interval (500 µL every minute for the first 5 minutes, every 2 minutes for the next 20 minutes, every 5 minutes for the next 30 minutes, every 10 minutes for 30 minutes, 30 minutes for 1 hour, and then hourly over a period of the experiment) and analysed for Fe^{3+} and Fe^{tot} concentrations, and dissolved metal ions concentration. The experiments were run in triplicate. This experimental procedure was followed for individual and mixed metal powder studied, i.e., Cu, Zn, Sn, and Ni; and PCBs at five (5) temperatures 25, 37, 45, 65, and 75 °C.

Owing to the slow rate of metal leaching by H^+ relative to Fe^{3+} in the ferric leaching systems (Yazici and Deveci 2014), the ferric reduction rate can be assumed to be dominantly a function of base metal dissolution. The mechanism presented in Eq. 4-1 can thus be reduced into Eq. 4-2 (Lambert et al. 2015; van Yken et al. 2020).

$$M^0 + 2Fe^{3+} \rightarrow M^{2+} + 2Fe^{2+} \qquad Eq.\ 4\text{-}2$$

Thus, the amount of each metal added was calculated to ensure that an appropriate stoichiometric ratio of 2 moles Fe^{3+} ions to 1 mole metal (M^0) ion, or greater, is achieved. A volume of 250 mL of 20.0 g/L Fe^{3+} contains 0.0895 mol Fe^{3+} ion, therefore for each individual metal leached, 2.50 g of Cu (0.0393 mol Cu), 2.50 g Zn (0.0382 mol Zn), 2.50 g Ni (0.0426 mol Ni), and 5.00 g Sn (0.0421 mol Sn) was added.

Proportions of the mixed metals (Cu, Zn, Sn, and Ni) required to achieve the required moles were calculated based on the metal proportions (percent of each metal, as %w/v PCBs) as per characterised PCB samples (Table 3-1). This approach was considered to mimic the expected metal proportions in PCB leachates while maintaining the 2:1 ratio for Fe^{3+}: M^0. Therefore, the mixed metals added contained 2.74 g Cu (0.0432 mol Cu), 9.70×10^{-3} g Zn (1.00×10^{-4} mol Zn), 2.00×10^{-4} g Sn (1.68×10^{-6} mol Sn), and 0.0448 g Ni (8.00×10^{-4} mol Ni), which added up to 0.0441 mol M^0.

For the Fe^{3+} leaching of PCBs, 12.5 g treated PCBs were added, which was equivalent to a total of about 0.0441 moles of M^0 ions, creating a 2:1 ratio with the 0.0895 mol Fe^{3+} ions in the 250 mL of 20.0 g/L Fe^{3+} solution.

4.2.1.4 Acid leaching of elementary metals and PCBs

For acid leaching, an experimental approach similar to that for ferric leaching was adopted. Instead of Fe^{3+} ions as an oxidant, only protons (H^+ ions) were considered. This was achieved by adjusting a pH of 250 mL deionised water to pH 1.1 using 96% H_2SO_4. The acidified water was then equilibrated to the desired temperature and metal powder was thereafter added. Samples were aliquoted from time zero (when metal was added) and over the 24 h leaching period. The aliquoted samples were analysed for the concentration of dissolved metal ions over time. Redox potential and pH were also monitored over the same leaching period. In the absence of Fe oxidant, acid leaching of base metal is through the following mechanism (van Yken et al. 2020):

$$2M^0 + 2H_2SO_4 + O_2 \rightarrow 2M^{2+} + 2SO_4^{2-} + 2H_2O \qquad Eq.\ 4\text{-}3$$

The amount of each metal added was calculated based on the appropriate stoichiometry of 1 mole H^+ to 1 mole metal (Eq. 4-3). The number of moles of H^+ ions in 250 mL acidified water at pH 1.1 was calculated to be 0.0199 mol H^+. To achieve a 1:1 mole ratio, the amount of Cu added was 1.27 g (0.0199 mol Cu), 1.30 g Zn (0.0198 mol Zn), 2.35 g Sn (0.0199 mol Sn), and 1.17 g Ni (0.0198 mol Ni).

To maintain the required 1 mol H^+ ions to 1 mol M^0 ions, mixed metals proportion was made up of 1.22 g Cu (0.0192 mol Cu), 4.30×10^{-3} g Zn (6.56×10^{-5} mol Zn), 1.00×10^{-4} g Sn (9.27×10^{-7} mol Sn), and 0.0199 g Ni (3.00×10^{-4} mol Ni), to make up the total required moles of 0.0196 mol M^0 ions to 0.0199 mol H^+ ions. For PCBs, about 5.00 g of treated PCB was added, to maintain the required stoichiometry.

4.2.2 Kinetic data analysis

In addressing reaction kinetics, the rate law for the extraction of base metal from its elemental solid form by dissolved ferric iron in an acidic aqueous solution was determined across the temperature range of 25 to 75 °C. Insight into the dissolution mechanism and associated reaction kinetics is vital in designing and controlling the reactor configuration and operating conditions to optimise the bioleaching process. Kinetic parameters such as rate constants, reaction order, and activation energy, were determined from Fe^{3+}, Fe^{2+}, and Fe^{tot} concentration as a function of time and dissolved metal concentration against time.

By considering the stoichiometry as per Eq. 4-2, the rate law for calculating a volumetric rate of metal dissolution can be written as:

$$r_M = \frac{1}{2} r_{Fe^{3+}} \qquad \textit{Eq. 4-4}$$

where

$$\frac{d[M^0]}{dt} = -r_M \qquad \textit{Eq. 4-5}$$

$$\frac{d[Fe^{3+}]}{dt} = -r_{Fe^{3+}} = -k[Fe^{3+}]^n[M^0]^m \qquad \textit{Eq. 4-6}$$

where r_M is the rate of metal dissolution, $r_{Fe^{3+}}$ is the reduction rate of Fe^{3+}, k is the rate constant (min^{-1}), and $[M^0]$ and $[Fe^{3+}]$ are metal and Fe^{3+} concentrations, respectively, and are in $mol.L^{-1}$. It must be noted that this proposed rate law related to the concentration of Fe^{3+} in solution, requiring acidic conditions (pH <2). Assuming that at the beginning of the leaching reaction, M^0 is considered to be in excess and the effect of the M^0 concentration can be neglected over the initial reaction period. Therefore, two rate laws, rate law 1, R1 (Eq. 4-7), and rate law 2, R2 (Eq. 4-8) are proposed to evaluate the volumetric rates as a function of Fe^{3+} and Fe^{2+} over time:

$$\frac{d[Fe^{3+}]}{dt} = -k[Fe^{3+}]^n \qquad \textit{Eq. 4-7}$$

$$\frac{d[Fe^{3+}]}{dt} = -k'\frac{[Fe^{3+}]^n}{[Fe^{2+}]^m} \qquad \textit{Eq. 4-8}$$

Here, *n* and *m* are reaction orders with respect to Fe^{3+} and Fe^{2+}, respectively. Both Eq. 4-7 and Eq. 4-8 are differential equations and can be solved using Euler's numerical method to give solutions as Eq. 4-9 and Eq. 4-10. The latter solutions can be used to approximate concentrations of Fe^{3+}, $[Fe^{3+}]_{i+1}$, at any given time, t_{i+1}, given that the initial concentration of Fe^{3+}, $[Fe^{3+}]_i$, and initial time t_i is known.

$$[Fe^{3+}]_{i+1} = -k[Fe^{3+}]^n(t_{i+1} - t_i) + [Fe^{3+}]_i \qquad \textit{Eq. 4-9}$$

$$[Fe^{3+}]_{i+1} = -k'\frac{[Fe^{3+}]_i^n}{[Fe^{2+}]^m}(t_{i+1} - t_i) + [Fe^{3+}]_i \qquad \textit{Eq. 4-10}$$

The kinetic parameters, *k*, *n*, and *m* were estimated by fitting the Fe^{3+} and Fe^{2+} data collected into the proposed models (Eq. 4-9 and Eq. 4-10) using non-linear regression. The estimated rate constants over the temperature range (25 – 75 °C) were then used to estimate the activation energy using the Arrhenius equation (Eq. 4-11). Rearranging the Arrhenius equation gives an equation of a straight line in a form of Eq. 4-10. Plotting 1/T against ln k gives a slope of $\frac{-E_a}{R}$, from which the activation energy can be deduced, and a y-intercept as ln *A*. The rate-controlling mechanism governing the leaching reaction was inferred from the value of the estimated activation energy. Diffusion-controlled reaction is characterised by activation energy less than 21.0 kJ.mol^{-1}. An activation energy greater than 41.81 kJ.mol^{-1} is characteristic of a chemically-controlled reaction mechanism, while a value in between is characteristic of a mixed controlled reaction, i.e. combination of both diffusion through the fluid film and chemical control on the surface of the unreacted particle (Rossi 2001; Abdel-Aal 2000; Luo et al. 2010; Habashi 2017).

$$k = Ae^{\frac{-E_a}{RT}} \qquad \textit{Eq. 4-11}$$

$$ln\, k = \frac{-E_a}{RT} + ln\, A \qquad \textit{Eq. 4-12}$$

where E_a is activation energy, *k* is rate constant, *R* is the universal gas constant (8.314 JK^{-1} mol^{-1}), *A* is the Arrhenius constant, and *T* is the absolute temperature (K).

By considering the stoichiometry, Eq. 4-4 can be solved by Euler's numerical approach to model a concentration of metal in solution at a given time, t:

$$[M^{2+}]_{i+1} = \frac{1}{2}k[Fe^{3+}]^n(t_{i+1} - t_i) + [M^{2+}]_i \quad \textit{Eq. 4-13}$$

$$[M^{2+}]_{i+1} = \frac{1}{2}k\frac{[Fe^{3+}]^n}{[Fe^{2+}]^m}(t_{i+1} - t_i) + [M^{2+}]_i \quad \textit{Eq. 4-14}$$

This study acknowledges that while metal leaching is dominantly through Fe^{3+} attack, metal leaching also occurs through H^+ attack. It is therefore important to determine the relative contribution of H^+ relative to Fe^{3+} leaching in acidic conditions. Thus acid-only leaching and its leaching rates were evaluated by acid leaching of base metals in the absence of ferric iron. The rate law was formulated by assuming that metal dissolution is solely a function of acid (H^+) attack (Eq. 4-3), thus leaching kinetics in acid-only leaching systems were evaluated using the following rate law:

$$r_M = r_{H^+} \quad \textit{Eq. 4-15}$$

$$\frac{d[M^0]}{dt} = -r_M \quad \textit{Eq. 4-16}$$

$$\frac{d[H^+]}{dt} = -r_{H^+} = -k[H^+]^n \quad \textit{Eq. 4-17}$$

$$[M^{2+}]_{i+1} = k[H^+]^n(t_{i+1} - t_i) + [M^{2+}]_i \quad \textit{Eq. 4-18}$$

where the concentration of H^+ (mol.L^{-1}) was calculated from pH measurement. Similar to Fe^{3+} leaching systems, kinetic parameters were determined by fitting the H^+ utilisation data over time using non-linear regression. Activation energy was estimated using the Arrhenius relationship and the reaction mechanism was inferred thereafter.

4.3 Results and discussion

4.3.1 Leaching of individual elemental metals

For each individual metal leached, both 'acid only' leaching and Fe^{3+} leaching under acidic conditions were studied. These are presented in the sections below.

4.3.1.1 Leaching of copper

To understand the acid leaching of Cu, elementary Cu metal powder was leached by acid (H^+) in the absence of Fe^{3+}. The acid lixiviant was prepared by adjusting the pH of deionised water

to pH 1.1 with concentrated H_2SO_4. Changes in solution pH and corresponding H^+ concentrations (calculated from pH values), %Cu mobilised, and redox potentials throughout the progressive acid leaching of Cu are presented in Figure 4-2. The H^+ leaching was slow as characterised by a gentle slope in H^+ consumption with time across the different temperatures. With increasing temperature, the proton consumption plateaued earlier, indicative of higher reaction rates. At 25, 45, 65 and 75 °C, proton consumption plateaued at approximately 800, 420, 200 and 200 min, respectively. Noteworthy was the final pH reached, and the corresponding $[H^+]$ depletion at the end of leaching. The final pH peaked at 4.55, 3.33, 1.91, 1.33, and 1.40 at 25, 37, 45, 65 and 75 °C, respectively. This difference could be attributed to the effect of temperature on the concentration of dissolved O_2 in the leaching solution. Solubility of O_2 in aqueous solution decreases with an increase in temperature (Kaskiala 2002; Tromans 1998; Battino 1981), thus there is limited dissolved O_2 at high temperatures to promote the formation of hydronium ions (water) by-product as per Eq. 4-3, which can neutralise the pH. Kaskiala (2002) reported a decrease in solubility of oxygen in aqueous solution of H_2SO_4 from 1.2 to 0.8 $mmol.L^{-1}$ when the temperature was increased from 25 to 55 °C. Despite the low pH observed and subsequent low calculated H^+ consumptions at higher temperature, the progressive increase in the amount (%) of Cu mobilised over the leaching time (Figure 4-2D) showed that Cu dissolution was successfully achieved across the temperature range studied. The Cu dissolution rate was dependent on temperature, with 59, 73, 79, 86, and 91% of Cu mobilised within 300 min at 25, 37, 45, 65, and 75 °C (Figure 4-2D). Total Cu dissolution was achieved at 1400 min across all temperatures.

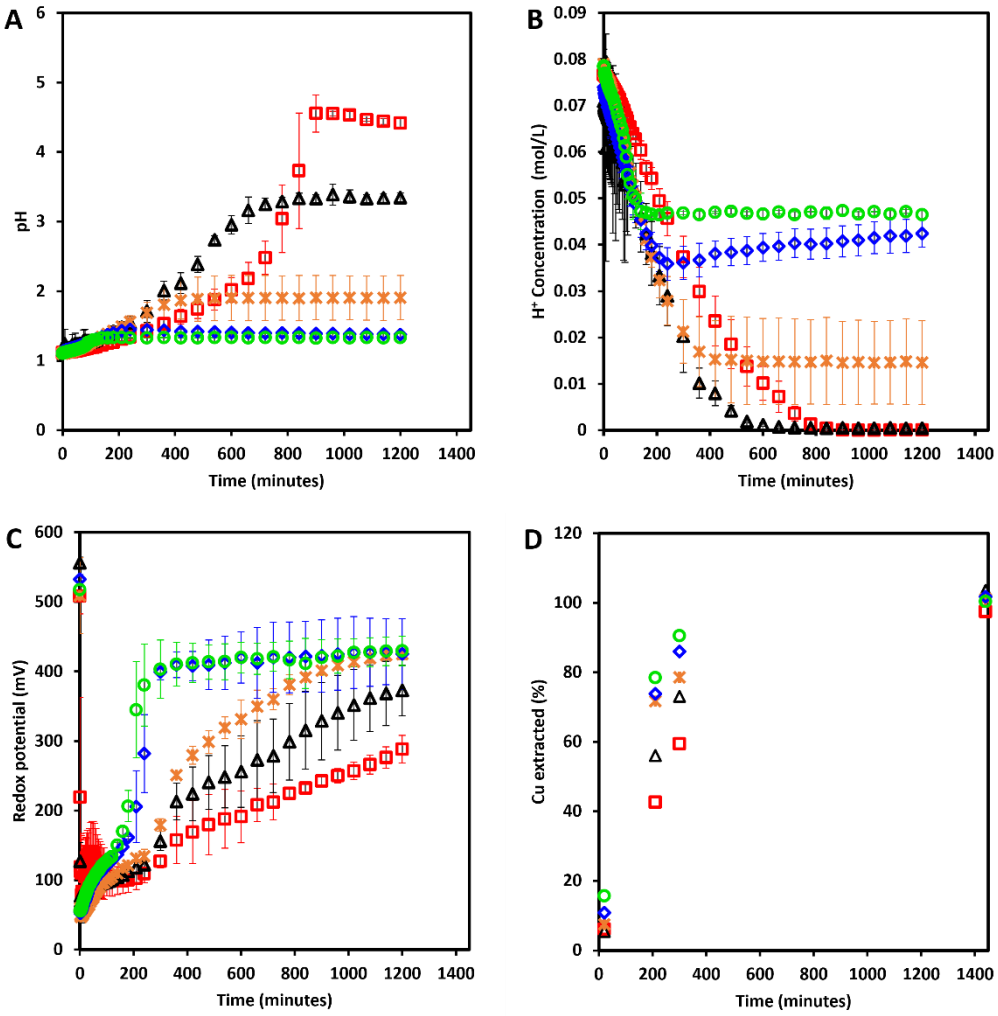

Figure 4-2 Change in pH (**A**), proton concentration (**B**), redox potential (**C**) and extracted Cu (%) (**D**) over time during the acid leaching of elementary Cu metal at molar ratio of 1:1 at 25 °C (□), 37 °C (Δ), 45 °C (✕), 65 °C (◇), and 75°C (○). Error bars represent standard deviation, n = 3.

The redox potential sharply decreased from approximately 500 mV to 100 mV at the addition of Cu metal powder (Figure 4-2C). Thereafter, the redox potential gradually increased as the leaching progresses. The rate of increase in the redox potential and the final redox reached was dependent on temperature. At low temperature range, 25 – 45 °C, the redox increased noticeably between 200 and 300 min, reaching a final redox potential at 1200 min of approximately 288, 373, and 425 mV at 25, 37, and 45 °C, respectively (Figure 4-2C). At high temperatures, 65 and 75 °C, the redox plateaued at approximately 400 mV within 300 min, indicative of the faster leaching rates. In the absence of Fe (Fe^{3+}/Fe^{2+}), we postulate that the redox coupling here was of Cu^{2+}/Cu^{+} coupling as the standard reduction potential of Cu^{2+}/Cu^{+} is 0.153 V (153 mV), which is equivalent to about 356 mV (0.153 + 0.204 V) against Ag/AgCl electrode and was close to the redox observed at the end of the leaching.

To determine the relative rates between the Fe^{3+} and H^+ oxidant, elementary Cu was leached through Fe^{3+} in acidic conditions and the Fe^{3+} leaching rates were compared to the H^+-only leaching. A full data set for ferric leaching of elementary Cu metal powder as a function of temperature (25 – 75 °C) over time is presented in Figure 4-3. The data presented includes changes in Fe^{3+} and Fe^{2+} concentrations, pH, and redox potential over the leaching time. The ferric iron reduction rate was high over the first 5 min as observed by the steep slope (Figure 4-3C). The rate decreased between 10 – 40 min due to the gradual decrease in Fe^{3+} oxidant in solution and Cu metal powder. At the lowest temperature of 25 °C, the average Fe^{3+} reduction rate was 2.66×10^{-2} $mol.L^{-1}.min^{-1}$ during the first 5 min, and it reduced to 3.61×10^{-3} $mol.L^{-1}.min^{-1}$ between 10 – 40 min before its further reduction to 1.43×10^{-5} $mol.L^{-1}.min^{-1}$ at 40 – 120 min. At the highest temperature of 75 °C, the average rate was 2.97×10^{-2} $mol.L^{-1}.min^{-1}$ between 0 – 5 min, reducing to 3.66×10^{-3} $mol.L^{-1}.min^{-1}$, and 2.90×10^{-4} $mol.L^{-1}.min^{-1}$) between 10 – 40 and 40 – 120 min, respectively. Consistent with the rapid reduction of Fe^{3+} into Fe^{2+} as Cu is oxidised into solution, redox potential decreased from 650 mV and plateaued approximately 380 mV (Figure 4-3B).

The change in H^+ concentration in solution was monitored through the change in pH. The effect of temperature on the change in pH was marked (Figure 4-3A); the higher the temperature, the faster the H^+ consumption. Within the temperature range of 25 – 45 °C, the final pH achieved at the end of the Cu dissolution was between 1.52 – 1.56, whereas at high temperatures of 65 and 75 °C, the pH plateaued at 1.81 and 1.92, respectively. High acid consumption as a function of temperature during Fe^{3+} leaching of Cu was also reported by Lambert et al. (2015). The authors studied the effect of temperature on the Fe^{3+} leaching of Cu from waste electric cables while maintaining the pH of the system below 2 by adding H_2SO_4. Consistent with the findings in this study, high acid consumption at high temperatures was observed, i.e. acid consumption increased from 1.81 to 2.76 H_2SO_4/mol Cu^{2+} as the temperature was increased from 21 to 50 °C, respectively (Lambert et al. 2015). The highest final pH of 1.92 at 75 °C observed in this study was important as it is within the required pH <2 limits to avoid Fe^{3+} precipitation as a result of pH.

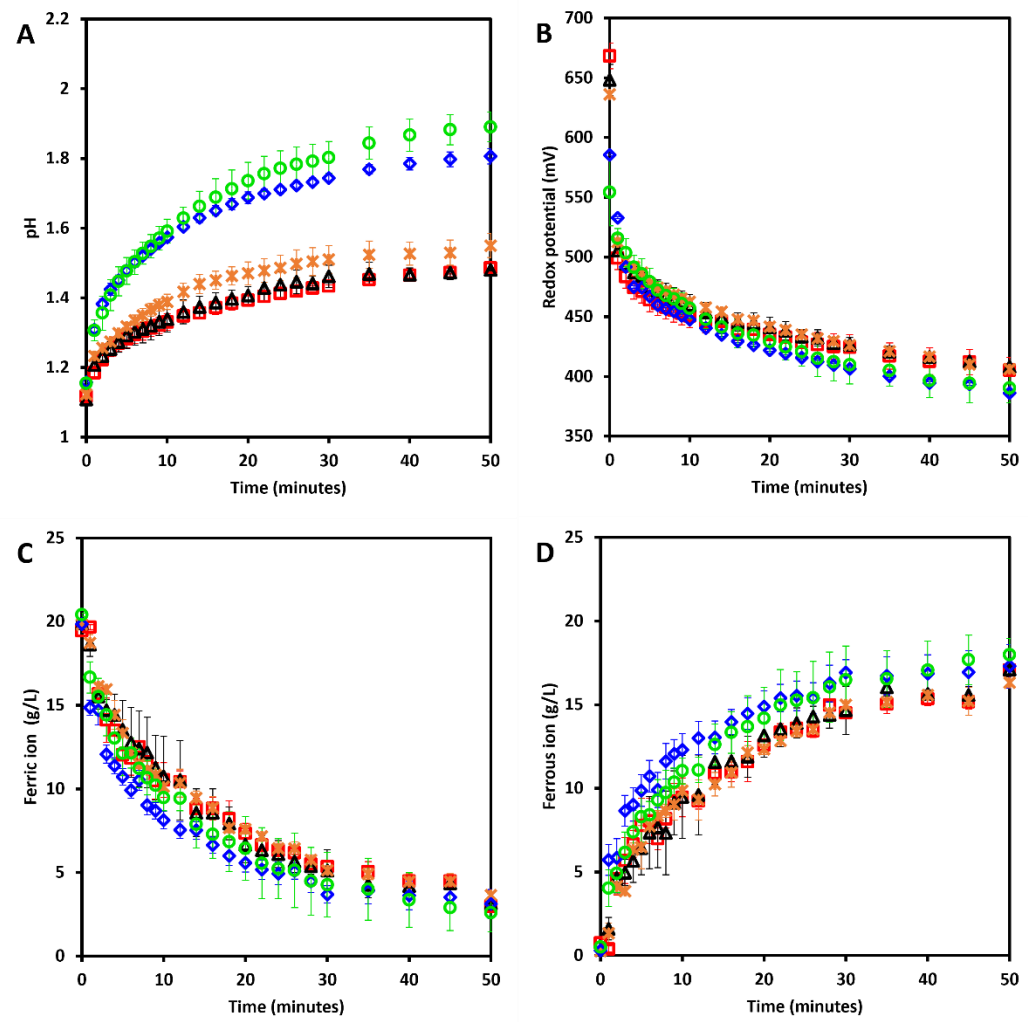

Figure 4-3 Change in pH (**A**), redox potential (**B**), Fe^{3+} (**C**) and Fe^{2+} (**D**) concentration over time during the ferric leaching of elementary Cu metal at 25 °C (□), 37 °C (Δ), 45 °C (✕), 65 °C (◇), and 75°C (○). Error bars represent standard deviation, n = 3.

The rapid Fe^{3+} leaching relative to the gradual leaching rates observed in the H^+-only leaching systems suggested that Fe^{3+} was a dominant leaching oxidant. This is consistent with literature (Yazici and Deveci 2014; Lambert et al. 2015; van Yken et al. 2020). Moreover, it validates the assumption that the H^+ leaching in the ferric leaching system is negligible, such that Fe^{3+} leaching is the dominant leaching mechanism as per Eq. 4-2, however, acidic conditions are required to maintain Fe^{3+} in solution. The stoichiometry in Eq. 4-2 (2 mol Fe^{3+}: 1 mol Cu) was also validated by evaluating and comparing the moles of Fe^{3+} used up at 1:1 and 2:1 Fe^{3+} to metal mole ratio. The leaching was carried out at 37 °C, an initial pH of 1.1 and Fe^{3+} concentration varied from 10 g/L (0.0470 mol) to 20 g/L (0.0903 mol), whereas Cu added was maintained at 2.50 g (0.0393 mol), corresponding to Fe^{3+}:M^0 of 1.2 to 2.3. At 10 g/L Fe^{3+}, a significant amount of Cu powder remained at complete Fe^{3+} depletion compared to complete Cu dissolution at 20 g/L Fe^{3+} (Appendix B1). As such, the proposed rate laws Eq. 4-7 and Eq. 4-8 were used to model Fe^{3+} reduction rate as a function of base metal dissolution throughout this study.

In evaluating Fe^{3+} leaching kinetics, the proposed rate laws, given in Eq. 4-4 and Eq. 4-6, were re-arranged into rate law equations Eq. 4-9 and Eq. 4-10, and fitted to the experimental data of Fe^{3+} and Fe^{2+}. The kinetic parameters *n*, *m*, and *k* were estimated by the least squares methods through non-linear regression analysis and are summarised in Table 4-1. These results suggested that the order of reaction with respect to Fe^{3+} was approximately 2, while it was approximately 0.2 with respect to Fe^{2+}, suggesting that the dissolution rate of Cu was not strongly dependent on Fe^{2+}. Attempts to determine the rate dependence on proton concentrations during the ferric leaching of Cu were made by including the $[H^+]$ term in the formulated rate laws, either on the numerator or denominator. However, the change in proton concentration could not be modelled. We postulate that this could have been due to the reaction of H^+ and dissolved oxygen in the system (Eq. 4-3) which is unaccounted for in this study as dissolved O_2 was not measured. This needs to be investigated further by either measuring dissolved O_2 throughout the leaching experiment or running the leaching in the absence of O_2 by continuous purging with nitrogen (N_2). In the absence of H^+ dependence, a plot of the experimental Fe^{3+} concentrations against the modelled concentrations yielded a correlation coefficient (R^2) of ≥0.978 (Table 4-1) across the temperature range tested (25 – 75 °C), indicating that the Fe^{3+} reduction rate could be modelled well with the proposed rate laws (Eq. 4-7 and Eq. 4-8).

Table 4-1 Estimated kinetic parameters for the Fe^{3+} leaching of elementary Cu metal obtained by fitting Fe^{3+} reduction data (Figure 4-3) into the proposed rate law R1 and R2.

Rate law	Kinetic parameters	25 °C	37 °C	45 °C	65 °C	75 °C
R1	*n* (Ave)			2.04		
	k (min^{-1})	0.097	0.175	0.290	0.505	0.659
	R^2	0.978	0.992	0.992	0.986	0.983
R2	*n* (Ave)			1.91		
	m (Ave)			0.19		
	k (min^{-1})	0.063	0.080	0.159	0.276	0.354
	R^2	0.986	0.995	0.992	0.986	0.983

Progressive Cu dissolution at a Fe^{3+}:M ratio of 2.0 or greater is presented in Figure 4-4A. Within the first 5 min of leaching, 44, 45, 49, 58, and 63% Cu had been mobilised at 25, 37, 45, 65, and 75 °C, indicative of the rapid Fe^{3+} leaching of Cu, with the dissolution rate increasing with an increase in temperature. At 40 min leaching time, more than 90% Cu was mobilised across all temperatures studied. Similar rapid Fe^{3+} leaching of Cu from various electronic waste is reported elsewhere (Casas et al. 2013; Yazici and Deveci 2014; Lambert et al. 2015). To further validate the proposed rate laws, the rate of Cu dissolution was related to the Fe^{3+} reduction rate by considering the mass balance and appropriate stoichiometry in Eq. 4-2. With the leaching rate showing no dependency on Fe^{2+} concentration, the concentration of dissolved Cu at any given time, $[Cu^{2+}]_{i+1}$, was then modelled by a solution of the differential equation Eq. 4-7 only, obtained through the Euler's numerical approach. Experimental Cu^{2+} concentrations were fitted into Eq. 4-13 and plotted against the modelled Cu^{2+} concentrations (Figure 4-4B). A regression coefficient of R^2 ≥0.992 across the considered temperature range

was obtained, suggesting that the proposed rate law modelled the Cu dissolution rate well. Thus, the volumetric rate law for Cu dissolution as a function of Fe^{3+} reduction during Fe^{3+} leaching of elementary Cu metal powder can be expressed, within the experimental errors, as:

$$\frac{d[Cu^0]}{dt} = -\frac{1}{2}k[Fe^{3+}]^2 \qquad \textit{Eq. 4-19}$$

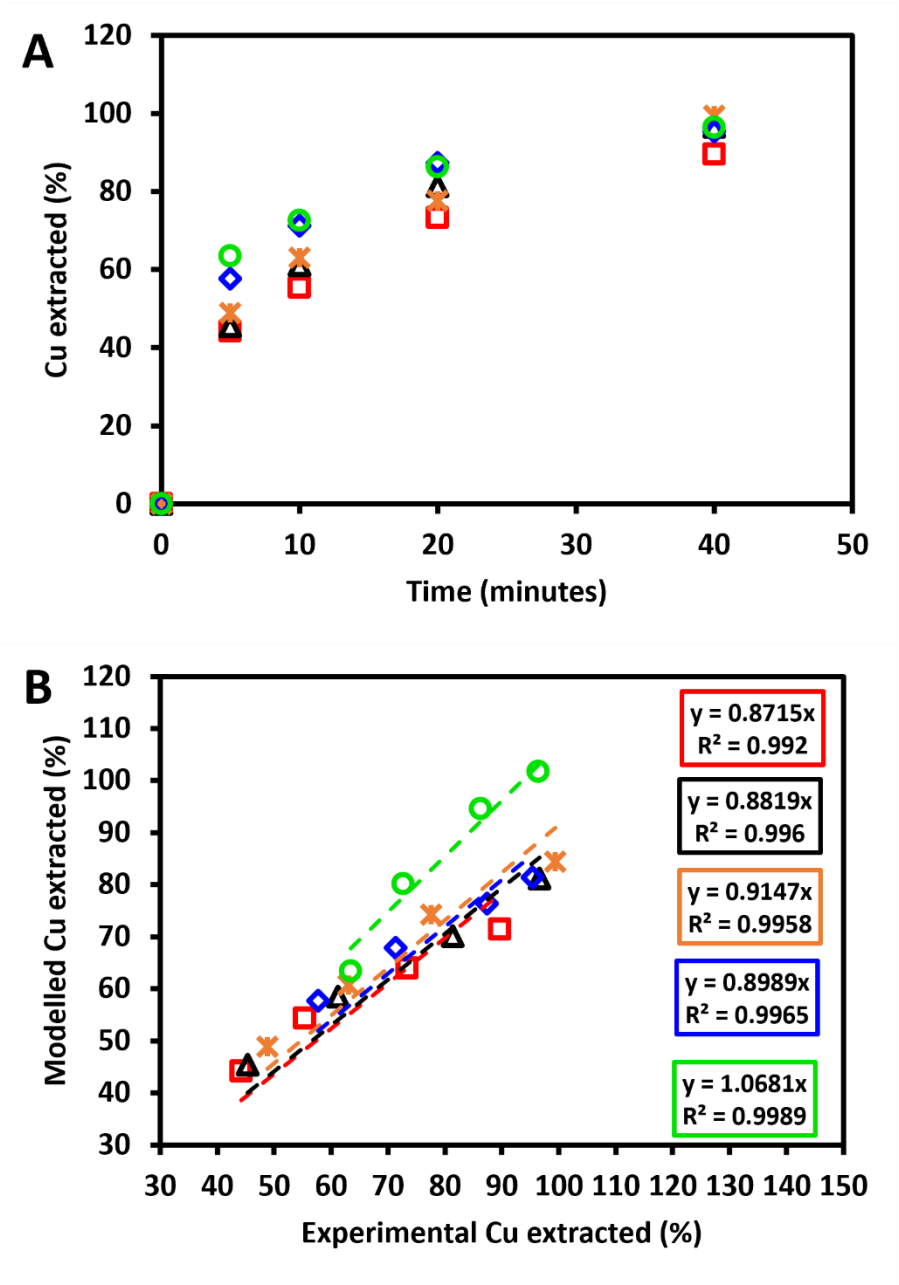

Figure 4-4 Extracted Cu(%) over time (**A**) and parity plot (**B**) for the ferric leaching of elementary Cu metal at 25 °C ( ), 37 °C ( ), 45 °C ( ), 65 °C ( ), and 75 °C ( ).

The estimated rate constants, *k*, increased from 0.0974 to 0.659 min^{-1} as temperature increased from 25 °C to 75 °C (Table 4-1), indicating the expected increase of rate of reaction with an increase in temperature. An Arrhenius plot of the estimated rate constants against 1/T for the estimation of the activation energy, E_a, is presented in Figure 4-5. An apparent activation energy of 32.7 $kJ.mol^{-1}$ was calculated, with an R^2 value of 0.982 for rate law 1 (Eq. 4-7). The value of the apparent activation energy obtained in this study suggested that Fe^{3+} leaching of Cu was through the mixed-controlled mechanism. Limited studies are reported on the leaching kinetics of elementary Cu metal. To our best knowledge, only Casas et al. (2013) have investigated the Fe^{3+} leaching of metallic Cu. Most of the Cu leaching kinetic data in literature are from Fe^{3+} leaching of copper minerals such as chalcopyrite and mixed metal containing PCBs. Casas et al. (2013) reported that the Fe^{3+} leaching of metallic Cu sheet (3 x 4 x 0.05 cm) under acidic conditions was governed by the chemical reaction mechanism, characterised by an activation energy of 175 $kJ.mol^{-1}$, at the temperature range of 25 – 65 °C. The difference in the activation energy to our study could be attributed to the difference in the reaction surface area. Arslan et al. (2004) reported an activation energy of 36.7 $kJ.mol^{-1}$ for Fe^{3+} leaching of Cu from copper sulfide ore in the temperature range of 50 – 94 °C. Lambert et al. (2015) estimated an activation energy of 20.4 $kJ.mol^{-1}$ from Fe^{3+} leaching of Cu from waste electric cables in the temperature range of 21 – 50 °C. The activation energy estimated in the present study is within the range reported in the literature. However, these estimated activation energies should be compared cautiously as the Cu sources are different, as are the temperature range studied.

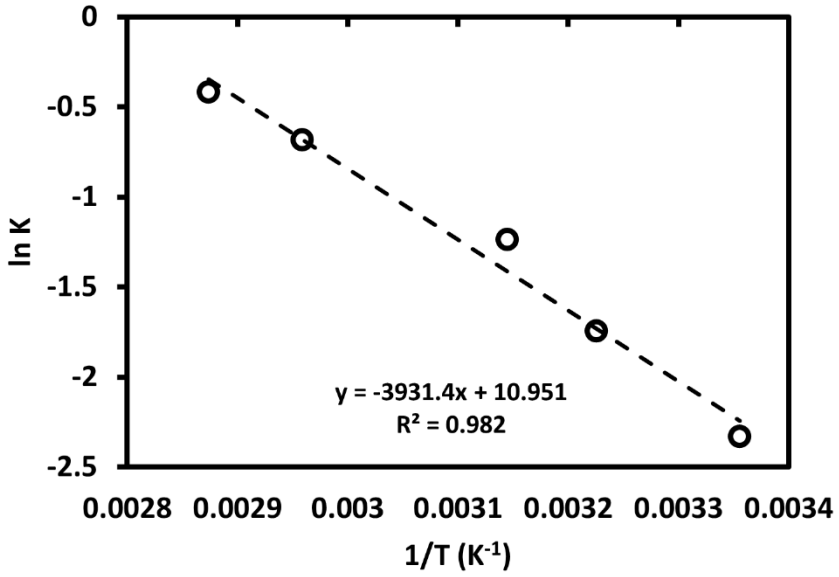

Figure 4-5 Arrhenius plot for the ferric leaching of elementary Cu metal across the temperature range of 25 - 75 °C.

To evaluate the acid leaching kinetics of Cu in acid-only leaching system, rate law 3 (Eq. 4-13) was proposed by assuming that Cu dissolution was through the H^+ attack. Kinetic parameters, *n*, and *k* were estimated by fitting the experimental H^+ concentrations (Figure 4-5B) into Eq.

4-14 by non-linear regression. Due to no data on the concentration of dissolved O_2 throughout the leaching, the kinetic parameters were poorly estimated, especially at high temperatures (45 – 75 °C) as the solubility of O_2 is mostly affected and pH remained low irrespective of the H^+ consumption as Cu is oxidised. As such, the kinetics of acid leaching were not included in all acid leaching systems, instead, the acid leaching behaviour was discussed. Alternatively, with rigorous data sets of the dissolved Cu concentration over time, [Cu^{2+}] could be used to model acid leaching kinetics as opposite to H^+ concentration.

4.3.1.2 Leaching of zinc

The leaching kinetics of elementary Zn metal powder was studied in the same leaching conditions as the Cu metal powder. The change in the solution pH, redox potential, Fe^{3+}, and Fe^{2+} concentrations over time during the Fe^{3+} leaching of Zn is presented in Figure 4-6. Ferric leaching of Zn was rapid, and much faster than the Fe^{3+} leaching of Cu, as observed by the steep slope in the Fe^{3+} reduction within the initial 5 min. The initial Fe^{3+} reduction rate was 2.94×10^{-2} mol.L^{-1}.min^{-1} within the first 5 min at 25 °C. It reduced to 9.65×10^{-3} mol.L^{-1}.min^{-1} between 5 – 10 min, and to 6.15×10^{-4} mol.L^{-1}.min^{-1} between 20 – 40 min as both Fe^{3+} and added Zn metal depletes in solution. At 75 °C, the Fe^{3+} reduction rate was 3.56×10^{-2}, 4.28×10^{-3}, and 2.09×10^{-4} mol.L^{-1}.min^{-1} between 0 – 5, 5 – 10, and 20 – 40 min, respectively. This was indicative of the rapid Fe^{3+} reduction, with the rate increasing with an increase in temperature. The rapid Fe^{3+} reduction rate was consistent with the rapid zinc dissolution (Figure 4-7). More than 69% Zn (69% at 25 °C and 85% at 75 °C) was mobilised within the initial leaching period of 5 min across all temperatures studied. Within the leaching period of 30 min, more than 93% of Zn was mobilised even at the lowest temperature of 25 °C. The rapid Fe^{3+} leaching of Zn relative to Cu was in accordance with electrochemistry based on the difference in the standard reduction potential between Fe^{3+} (+0.77 V) and Zn (-0.76 V).

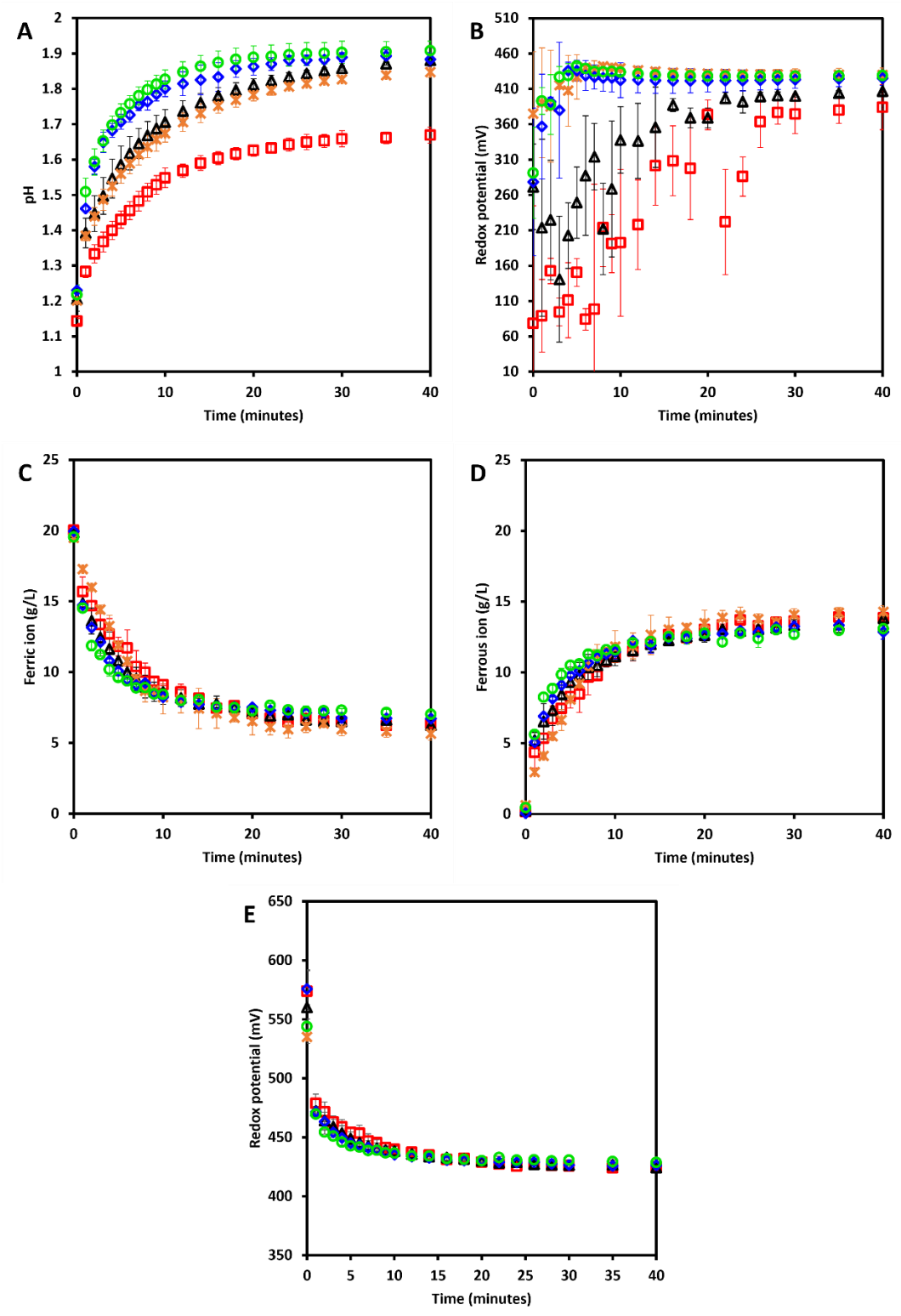

Figure 4-6 Change in pH (**A**), redox potential (**B**), Fe^{3+} (**C**) and Fe^{2+} (**D**) concentration, and calculated redox potential (**E**) over time during the ferric leaching of elementary Zn metal at 25 °C (□), 37 °C (Δ), 45 °C (✕), 65 °C (◇), and 75°C (○). Error bars represent standard deviation, n = 3.

The measured redox potential had shifted from typical Fe^{3+}/Fe^{2+} coupling during the dissolution of Zn (Figure 4-6B). Thus, the redox potentials were corrected by calculating the expected redox from Fe^{3+} and Fe^{2+} concentrations using the Nernst equation. These calculated redox potentials are presented in Figure 4-6E. Nevertheless, at 25 and 37 °C, the measured redox potential sharply decreased to below 200 mV at the addition of Zn metal. Thereafter, the redox potential gradually increased and plateaued at approximately 400 mV from 40 min. At 45 – 75 °C, the measured redox sharply decreased to approximately 300 mV and rapidly increased and plateaued to approximately 400 mV, within 10 min. At the end of the leaching, the measured redox potential coincided with the calculated values across all temperatures. This confirmed that the measured redox potentials were not of Fe^{3+}/Fe^{2+} coupling. The rapid increase in the measured redox potential at 45 – 75 °C, and the relative gradual increase observed at 25 – 37 °C, suggested that the redox coupling could have been that of Zn/Zn^{2+} coupling and the difference with respect to the temperature was indicative of the effect of temperature on the leaching rates. At 45 – 75 °C, the redox rapidly increased as the Zn dissolution is faster with limited time for Zn/Zn^{2+} coupling to be observed, relative to the gradual depletion of Zn at 25 – 37 °C, allowing time to observe the Zn/Zn^{2+} coupling. The higher measured redox potential relative to the expected reduction potential of Zn/Zn^{2+} (-556 mV against Ag/AgCl electrode) could be due to the high leaching rates of Zn with limited time to measure lower redox values. At the complete depletion of Zn and with only Zn^{2+} in solution, the redox potential was the same as the calculated Fe^{3+}/Fe^{2+} coupling.

The solution pH increased rapidly on the addition of Zn, with the rate, the final pH reached on Zn leaching and the corresponding H^+ consumed, all showing dependence on the temperature. The final pH reached at a low temperature of 25 °C was 1.71, while at 75 °C, the final pH was 1.89.

The kinetic parameters, *n*, *m*, and *k*, for the ferric leaching of Zn were estimated as discussed in Section 4.3.1.1 and are summarised in Table 4-2. The high correlation coefficient, R^2 >0.926 across all temperatures except at 45 °C where R^2 >0.875, showed that the proposed rate laws modelled the Fe^{3+} reduction rate acceptably well. These R^2 values were lower than those for Fe^{3+} leaching of Cu. It was hypothesised that this could result from the higher contribution of H^+ leaching as observed by higher final pH and $[Fe^{3+}]$ residual. The estimated *n* of approximately 4.61 (R1) and 4.57 (R2) suggested that the oxidation of Zn had a high degree of dependence on Fe^{3+} concentration and had no dependence on Fe^{2+} as signified by *m* of approximately 0.0. Estimated rate constants increased from 5.85 min^{-1} to 26.9 min^{-1} at 25 to 75 °C, respectively. The large values of the rate constants obtained signify the fast-leaching rates of Zn, while the increase in *k* with temperature is consistent with the expected effect of temperature on a reaction rate.

Table 4-2 Estimated kinetic parameters for the Fe^{3+} leaching of elementary Zn metal obtained by fitting Fe^{3+} reduction data (Figure 4-6) into the proposed rate law R1 and R2.

Rate law	Kinetic parameters	25 °C	37 °C	45 °C	65 °C	75 °C
R1	*n* (Ave)			4.61		
	k (min^{-1})	5.85	11.5	15.5	20.9	26.9
	R^2	0.958	0.951	0.876	0.938	0.926
R2	*n* (Ave)			4.57		
	m (Ave)			0		
	k (min^{-1})	5.79	9.99	13.4	18.1	25.0
	R^2	0.958	0.953	0.892	0.943	0.934

Thus, the rate law for Fe^{3+} reduction as a function of Zn metal dissolution can be expressed as:

$$\frac{d[Zn^0]}{dt} = -\frac{1}{2}k[Fe^{3+}]^{4.61} \qquad \textit{Eq. 4-20}$$

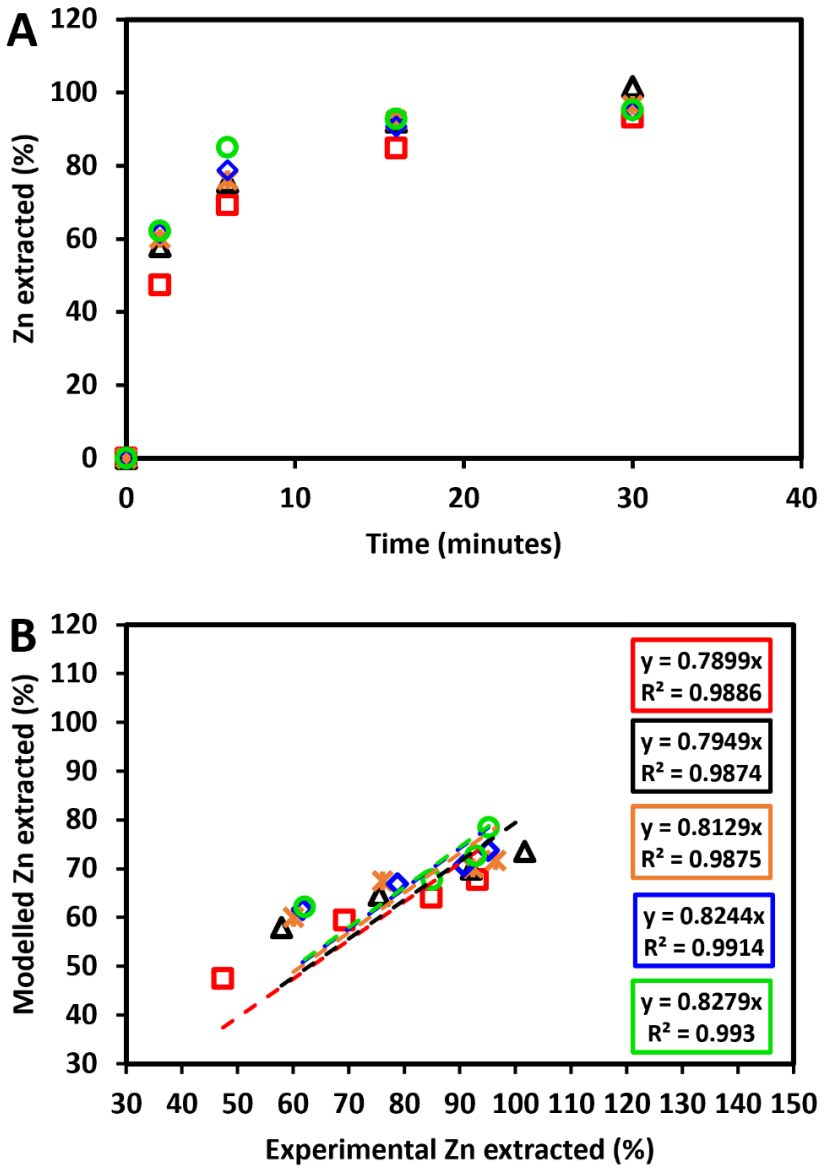

Figure 4-7 Extracted Zn (%) over time (**A**) and parity plot (**B**) for the ferric leaching of elementary Zn metal at a molar ratio of 1:1 and at 25 °C (□), 37 °C (△), 45 °C (✕), 65 °C (◇), and 75 °C (○).

The Arrhenius plot for the estimation of activation energy is presented in Figure 4-8. The apparent activation energy for the Fe^{3+} leaching of Zn metal powder was estimated to be 24.3 $kJ.mol^{-1}$, suggesting that the Fe^{3+} leaching of Zn was also limited by mixed-controlled mechanism on the solid-liquid phase. There are no reported activation energies for the Fe^{3+} leaching of elementary Zn metal in the open literature. Verbaan and Crundwell (1986) reported an activation energy of 79.4 $kJ.mol^{-1}$ at 25 to 85 °C for ferric leaching of a sphalerite concentrate. Markus et al. (2004) obtained an activation energy of 47.4 $kJ.mol^{-1}$ across the temperature range 75 to 95 °C for the ferric leaching of sphalerite. These reported activation energies are not comparable to the low activation energy obtained in the present study. This

may be attributed to the difference in the degree of Zn liberation in the Zn mineral, affecting the leaching rate, relative to the fully liberated elemental Zn in the present study.

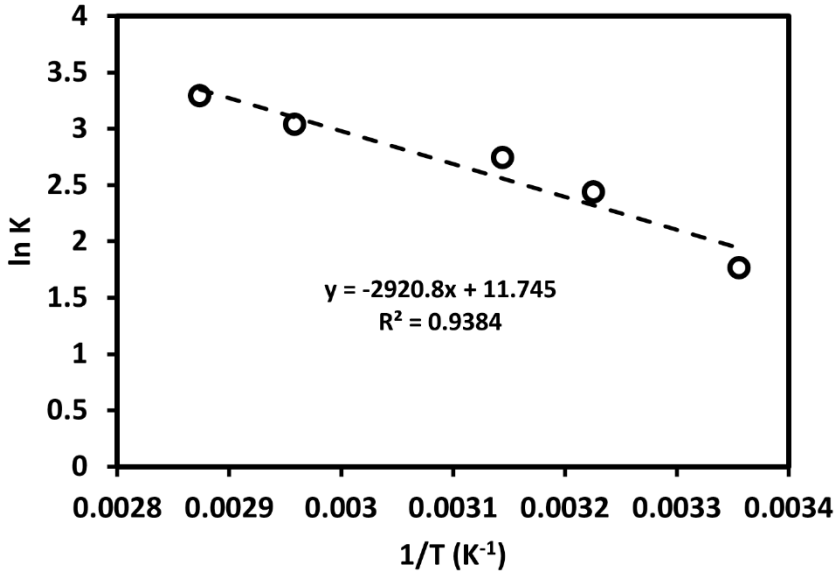

Figure 4-8 Arrhenius plot for the ferric leaching of elementary Zn metal across the temperature range of 25 to 75 °C.

The leaching behaviour of Zn metal powder through the proton attack was studied using acidified water, at pH 1.1, and these results are presented in Figure 4-9. The final pH achieved and the corresponding H^+ used for complete Zn leaching was dependent on the temperature studied. Contrary to the acidic Fe^{3+} leaching of Zn powder, a higher final pH was reached at the lowest temperature studied. At 25, 37, and 45 °C, the final pH reached was 2.16, 1.84, and 1.46, respectively. At high temperatures, 65 and 75 °C, the final pH remained at approximately 1.34. This difference in the final pH reached as a function of temperature is attributed to the limited dissolved oxygen at high temperatures as discussed in the H^+ leaching of Cu in Section 4.3.1.1. At 25 °C, the pH plateaued by 780 min, while at 75 °C, it plateaued as early as from 210 min. This was supported by the metal leaching rate profiles illustrated in Figure 4-9D in which Zn dissolution is complete at 75 °C by 210 min. Despite the pH remaining low at 65 and 75 °C, 57 and 71% Zn was mobilised over the first 20 min, compared to about 40% Zn mobilised at 25 to 45 °C at the same leaching time. More than 92% Zn was mobilised at 37 to 75 °C, and 73% Zn mobilised at 25 °C at 210 min. In comparison to acid leaching of Cu, about 43 and 78% Cu was mobilised over the same leaching time of 210 min at 25 and 75 °C, respectively, indicating that the acid leaching of Zn was faster than that of Cu. Although complete Zn dissolution was achieved in 210 min at 75 °C, complete leaching was achieved in 30 min with acidic Fe^{3+}, indicating that Fe^{3+} leaching exhibited faster leaching rates.

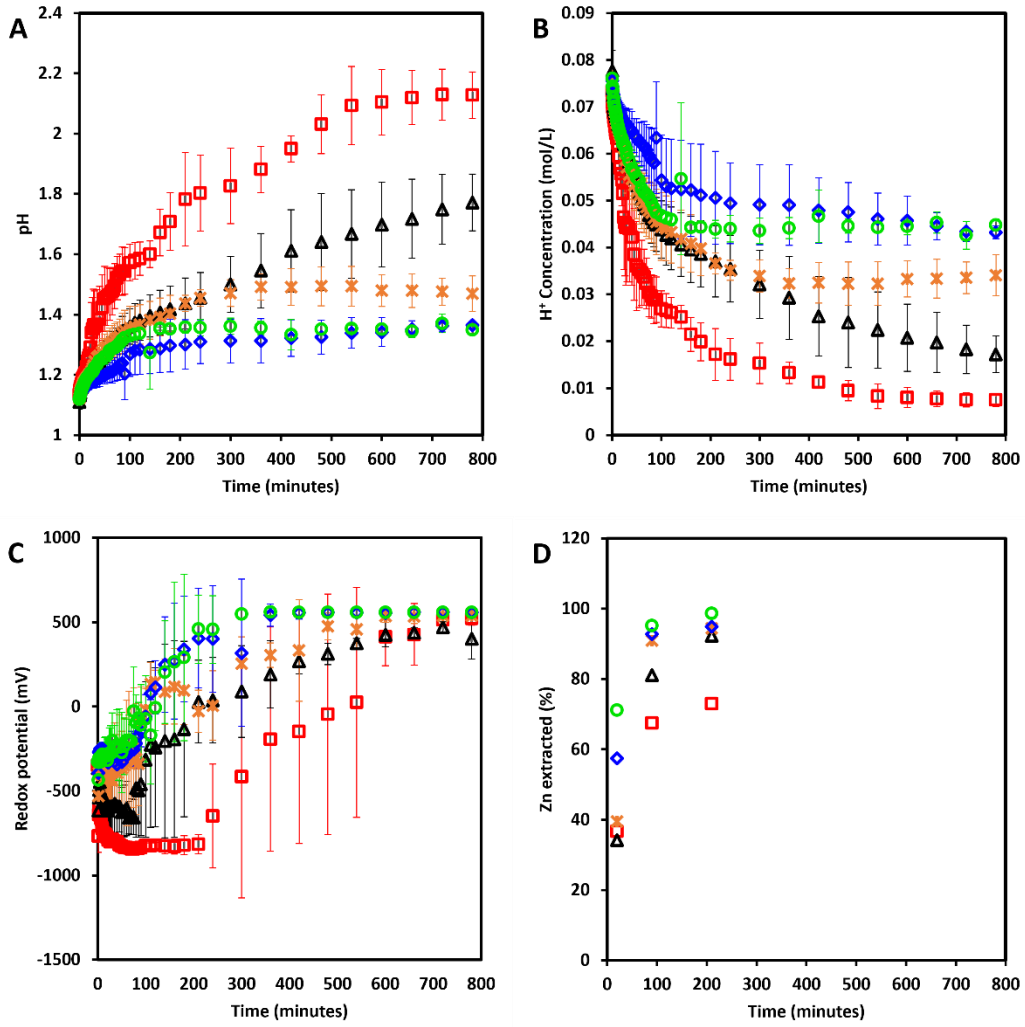

Figure 4-9 Change in pH (**A**), proton concentration (**B**), redox potential (**C**), and extracted Zn (%) (**D**) over time during the acid leaching of elementary Zn metal at molar ratio of 1:1 at 25 °C (□), 37 °C (Δ), 45 °C (✕), 65 °C (◇), and 75°C (○). Error bars represent standard deviation, n = 3.

4.3.1.3 Leaching of nickel

The pH, redox potential, Fe^{3+}, and Fe^{2+} concentration profiles for the Fe^{3+} leaching of elementary nickel powder with time at temperatures from 37 to 75 °C are presented in Figure 4-10. Based on the Fe^{3+} reduction, the initial dissolution of Ni was slower than that of Cu and Zn. Moreover, the Fe^{3+} leaching behaviour of Ni was strongly dependent on temperature. Fe^{3+} reduction and associated Ni dissolution remained minimal over a leaching period of 30 h at 25 °C with some 20% Fe^{3+} reduced and a minimal change in pH from 1.10 to 1.18 and redox potential from 687 to 497 mV (Appendices B3), suggesting a slow rate of Ni dissolution at 25 °C. Hence, Ni leaching at 25 °C was not considered in the evaluation of leaching kinetics. At 37 and 45 °C, Ni leaching was low as characterised by minimal changes in Fe^{3+} concentration and low Fe^{3+} reduction rate of 7.82×10^{-4} and 8.69×10^{-4} $mol.L^{-1}min^{-1}$ at 37 and 45 °C, respectively, over the initial 50 min. Thereafter, the Fe^{3+} reduction gradually progressed with progressive

Ni leaching, at 37 °C. Over 110 min, 40% Ni was mobilised at 45 °C, whereas only 35% Ni was mobilised over 420 min at 37 °C. At the end of the leaching, Ni mobilised peaked at 68% at 37 °C after 1200 min and at 91% at 45 °C after 400 min. At 37 °C, the redox potential gradually decreased from approximately 670 mV to plateau at approximately 400 mV at 1440 min. At 45 °C, the redox potential plateaued at approximately 420 mV from as early as 360 min. The pH increased to plateau at a similar time to the Fe^{3+} reduction and redox potential and peaked at pH 1.48 at 37 °C and at pH 1.46 at 45 °C.

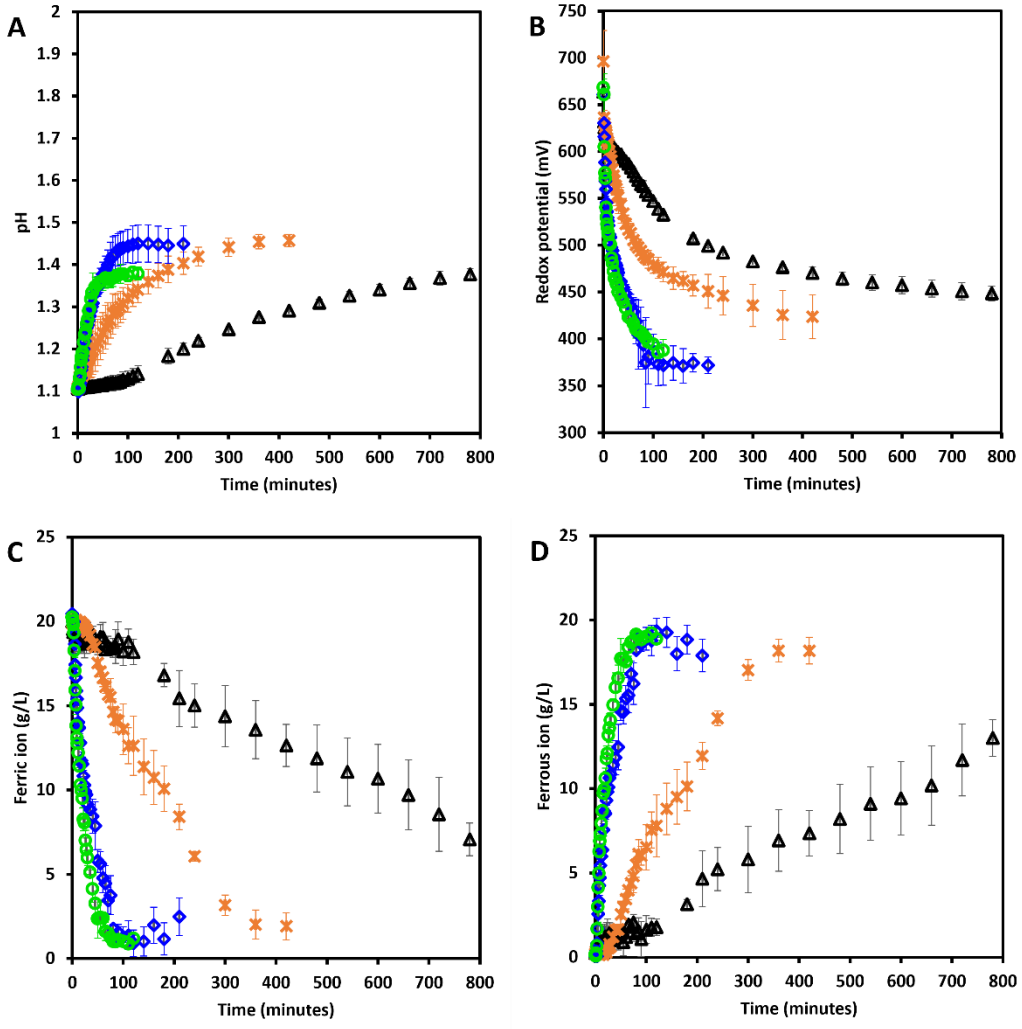

Figure 4-10 Change in pH (**A**), redox potential (**B**), Fe^{3+} (**C**) and Fe^{2+} (**D**) concentration over time during the ferric leaching of elementary Ni metal at 37 °C (Δ), 45 °C (✕), 65 °C (◇), and 75°C (○). Error bars represent standard deviation, n = 3

While low relative leaching rates were observed at 37 and 45 °C, improved leaching rates were observed at 65 and 75 °C. The Fe^{3+} reduction rate was 8.35×10^{-3} and 1.34×10^{-2} $mol.L^{-1}min^{-1}$ over the initial 10 min, and 4.89×10^{-3} and 5.15×10^{-3} $mol.L^{-1}min^{-1}$ between 10 – 40 min at 65 and 75 °C, respectively. Within the initial 5 min, 11 and 20% Ni were, respectively, mobilised at 65 and 75 °C. Over the 50 min leaching time, more than 76% Ni was mobilised in both temperatures and complete Ni dissolution was achieved within 200 min. In accordance with

the rapid leaching, changes in both redox potential and solution pH were rapid and plateaued from approximately 100 min in both temperatures. The pH plateaued below pH 1.50 and the redox potential above 385 mV. The lower redox potential observed at 65 and 75 °C, relative to lower temperatures (37 and 45 °C) was consistent with the extent of Ni (%) mobilised and thereby Fe^{3+} reduced. The similarity in final pH across all temperatures suggested that H^+ used is not affected by temperature. The observed difference in the Ni leaching rate and extent as a function of temperature at 25 – 45 °C, compared to 65 – 75 °C, was postulated to be due to the formation of a NiO and/or $NiFe_2O_4$ film on the surface of Ni powder at low temperatures (<45 °C). This nano-sized passive layer(s) may have limited the mass transfer at the liquid-solid phase, thereby lowering the leaching rates. These potential passivation layers have been reported to form in Ni leaching systems similar to that in the present study (Delichere et al. 1986; Bilczuk et al. 2016). Bilczuk et al. (2016) observed slow Fe^{3+} leaching rate of elementary Ni powder at <45 °C and attributed the limitation to the potential passivation layers on the surface of the Ni powder. Thermodynamically, the dominant species at the conditions used (pH and redox potential range) are Ni^{2+} and $NiSO_4$ (Bilczuk et al. 2016). Surface reaction studies were not conducted in the present study to confirm the presence of these passivation layers; however, other observed physical properties such as high magnetism of the Ni powder at low temperatures (Ni powder sticks to the magnetic stirrer bar) compared to none observed at high temperatures suggested potential for the presence of these layers, particularly $NiFe_2O_4$ as shown in Eq. 4-21. Synthesis and properties (including its magnetism) of $NiFe_2O_4$ nano-particles are well studied and reported in catalysis (Alarifi et al. 2009; Li et al. 2010). Thus, here we postulate that the formation of $NiFe_2O_4$ at low temperatures was most likely responsible for the observed low leaching rates rather than NiO. Moreover, the leaching behaviour of Ni in acid-only leaching (discussed below) supported the presence of $NiFe_2O_4$.

$$Ni^{2+} + 2Fe^{3+}\ 4H_2O \rightarrow NiFe_2O_4 + 8H^+ \qquad \textit{Eq. 4-21}$$

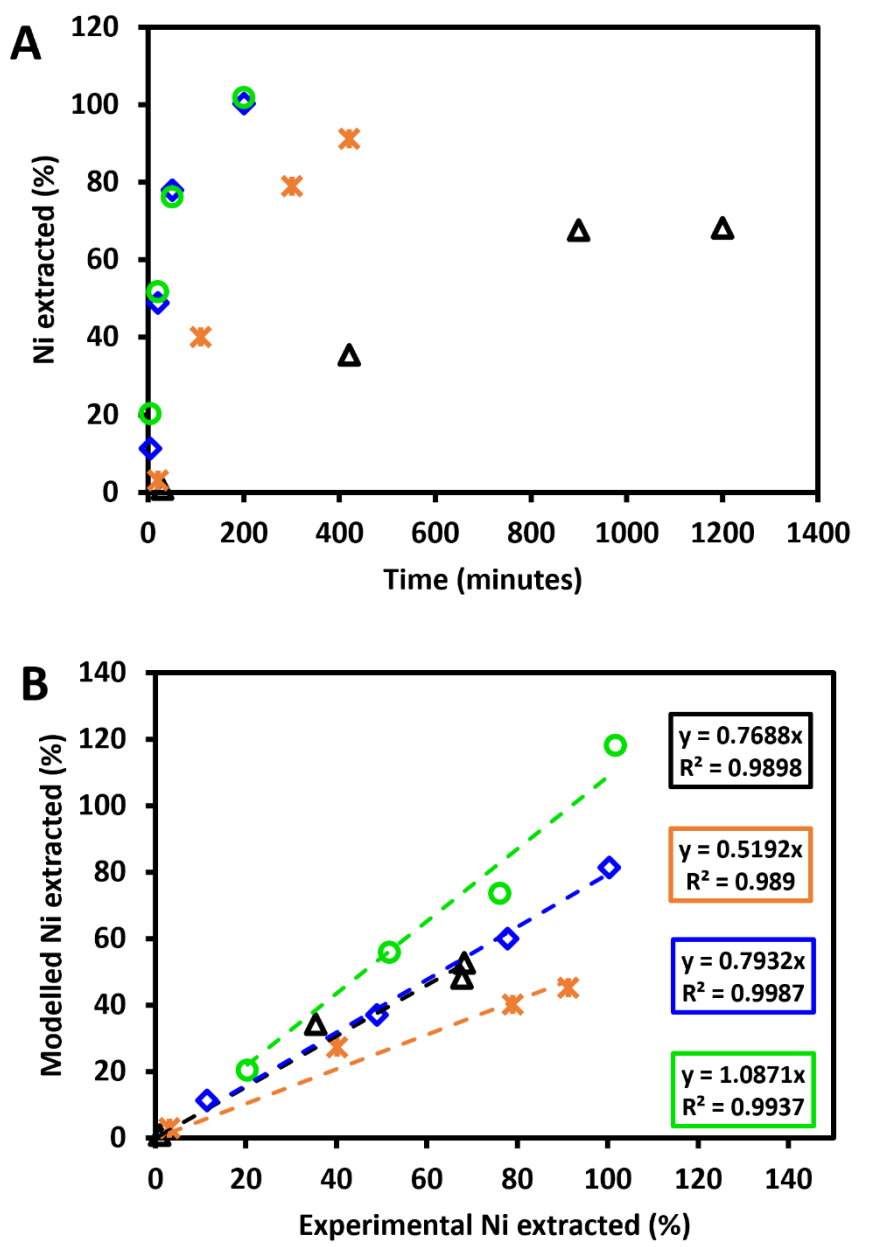

Figure 4-11 Ni (%) extracted over time (**A**) and parity plot (**B**) for the modelled Ni extraction at a Fe^{3+}:Ni molar ratio of 2:1, based on modelling ferric leaching of elementary Ni metal at 37 °C (Δ), 45 °C (✖), 65 °C (◇), and 75 °C (○), compared to experimental measurement.

Kinetic parameters estimated for Fe^{3+} leaching of Ni are presented in Table 4-3. These indicate the reaction order, *n*, of 1.0 for the Fe^{3+} leaching of Ni with respect to Fe^{3+} concentration and 0.0 with respect to Fe^{2+} concentration, indicating no dependence on Fe^{2+} concentration. The estimated rate constants, *k*, increased from 0.00138 min^{-1} to 0.0474 min^{-1}, as temperature increased from 37 to 75 °C. The high regression coefficients (R^2 ≥0.980) obtained showed that the proposed rate law modelled the Fe^{3+} reduction rate well. Fitting the experimental leached Ni concentration to the proposed rate law gave R^2 ≥0.989 across all temperatures studied,

further validating the proposed rate law. Thus, the rate law for Ni dissolution as a function of Fe^{3+} concentration is given as:

$$\frac{d[Ni^0]}{dt} = -\frac{1}{2}k[Fe^{3+}]^1 \qquad \textit{Eq. 4-22}$$

Table 4-3 Estimated kinetic parameters for the Fe^{3+} leaching of elementary Ni metal obtained by fitting Fe^{3+} reduction data (Figure 4-10) into the proposed rate law R1 and R2.

Rate law	Kinetic parameters	25 °C	37 °C	45 °C	65 °C	75 °C
R1	*n* (Ave)			1.00		
	k (min^{-1})	-	1.38×10^{-3}	3.85×10^{-3}	0.0279	0.0474
	R^2	-	0.974	0.938	0.996	0.995
R2	*n* (Ave)			1.00		
	m (Ave)			0.0		
	k (min^{-1})	-	1.18×10^{-3}	3.90×10^{-3}	0.0279	0.0474
	R^2	-	0.970	0.983	0.996	0.995

The apparent activation energy, estimated from the Arrhenius plot (Figure 4-12), for the Fe^{3+} leaching of elementary Ni metal powder was 84.5 $kJ.mol^{-1}$. This suggested that the Fe^{3+} leaching mechanism of Ni at 37 – 75 °C was governed by chemical reaction at the solid-liquid interface. The activation energy obtained here was comparable to the value reported by Bilczuk et al. (2016) (82.3 $kJ.mol^{-1}$) for Fe^{3+} leaching of metallic Ni at 45 - 75 °C. Other reported values of activation energy for Fe^{3+} leaching of Ni are mostly that of leaching of Ni mineral such as nickelferrous pyrrhotite tailings (62.1 $kJ.mol^{-1}$ at 30 – 55 °C, (Samadifard et al. 2015)) and pentlandite concentrate (60.7 $kJ.mol^{-1}$ at 30 – 80 °C (Corrans and Scholtz 1976)).

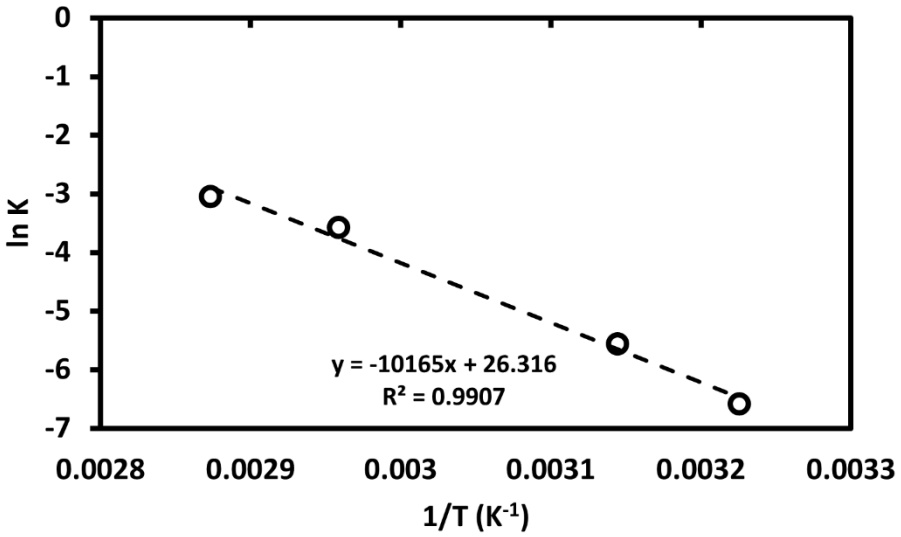

Figure 4-12 Arrhenius plot for the ferric leaching of elementary Ni metal across the temperature range of 37 to 75 °C.

The data set for acid-only leaching of elementary Ni metal powder is presented in Figure 4-13. The rate of Ni leaching through the proton attack was slow compared to the Fe^{3+} leaching. In contrast to the Fe^{3+} leaching, the discrepancy in the initial leaching rates as a function of temperature comparing low temperatures (37 – 45 °C) to high temperatures (65 – 75 °C) was not as large. Similar to the acid leaching of Cu and Zn, the final pH achieved at the end of the leaching was dependent on temperature. At temperatures of 37, 45, 60 and 75 °C, the final pH plateaued at pH 1.91, pH 1.60, pH 1.40 and 1.34, respectively. The time at which the pH reached plateaued stage was indicative of the leaching rate as a function of temperature and was consistent with the Ni (%) mobilised over time. Within the initial 20 min, 5, 9, 16, and 24% Ni was mobilised at 37, 45, 65, and 75 °C, respectively. Over 210 min, 69 and 97% Ni was mobilised at 65 and 75 °C, while 42 and 46% Ni was mobilised at 37 and 45 °C (Figure 4-13D). The total dissolution of Ni was successfully achieved across all temperatures over a leaching period of 1440 min. The effect of temperature on the redox potential is presented in Figure 4-13C. At 37 °C, the redox potential gradually decreased to approximately -40 mV over 20 min following the addition of Ni, while at 45 °C, it decreases to as low as -200 mV. In both these temperatures, the redox recovered and remained relatively constant (between 0 – 10 mV) from the initial 50 min to approximately 200 min. At 65 and 75 °C, the redox potential jumped to approximately -200 mV at the addition of Ni and remained constant for about 100 min before it increased to the initial redox potential values. Based on these observations, it appeared the redox remained constant throughout the dissolution of Ni as both Ni/Ni^{2+} species co-exist and increased once most of the Ni is in solution. A similar anomalous leaching behaviour was observed by Bilczuk et al. (2016).

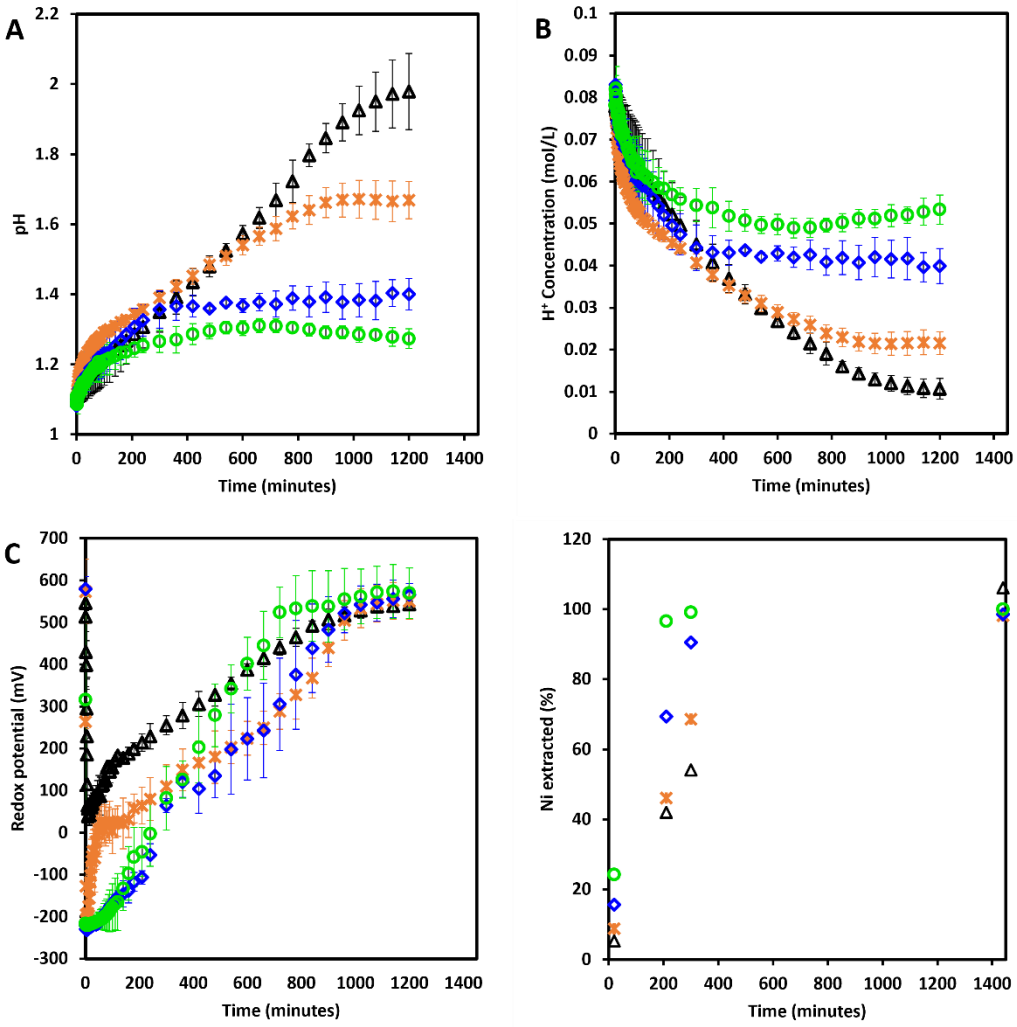

Figure 4-13 Change in pH (**A**), proton concentration (**B**), redox potential (**C**), and extracted Ni (%) (**D**) over time during the acid leaching of elementary Ni metal at molar ratio of 1:1 at 37 °C (Δ), 45 °C (✕), 65 °C (◇), and 75°C (○). Error bars represent standard deviation, n = 3.

4.3.1.4 Leaching of tin

Figure 4-14 shows the change in pH, redox potential, Fe^{3+} and Fe^{2+} concentration over time during the Fe^{3+} leaching of elementary Sn metal powder across a temperature range of 25 to 75 °C. Similarly to the Fe^{3+} leaching of Cu and Zn, the leaching of Sn was mainly completed within the initial 40 min as observed by the plateau in Fe^{3+} reduction within this leaching time across all temperatures. The leaching rates of Sn improved with increasing temperature. At 25 °C, the Fe^{3+} reduction rate was 1.76×10^{-2} mol.$L^{-1}h^{-1}$ at the initial 5 min, and at 75 °C, the Fe^{3+} reduction increased to 3.14×10^{-2} mol.$L^{-1}h^{-1}$. Thereafter, the Fe^{3+} reduction rate reduced across all temperatures as the added Sn powder and Fe^{3+} in solution depleted. In accordance with the rapid Fe^{3+} reduction into Fe^{2+}, the redox potential rapidly decreased across all temperatures. At 25 – 45 °C, the redox potential plateaued at approximately 384 – 365 mV. At 65 and 75 °C, it plateaued at 320 and 266 mV, suggesting an effect of temperature on the

extent of Sn dissolution based on the extent of Fe^{3+} reduction. The final pH reached and the corresponding H^+ used by the end of the reaction was slightly higher at low temperatures (25 – 45 °C, pH 1.29 – 1.22) than at high temperatures (65 – 75 °C, pH 1.12 – 1.06). This was indicative of the effect of temperature on the co-occurring acid leaching.

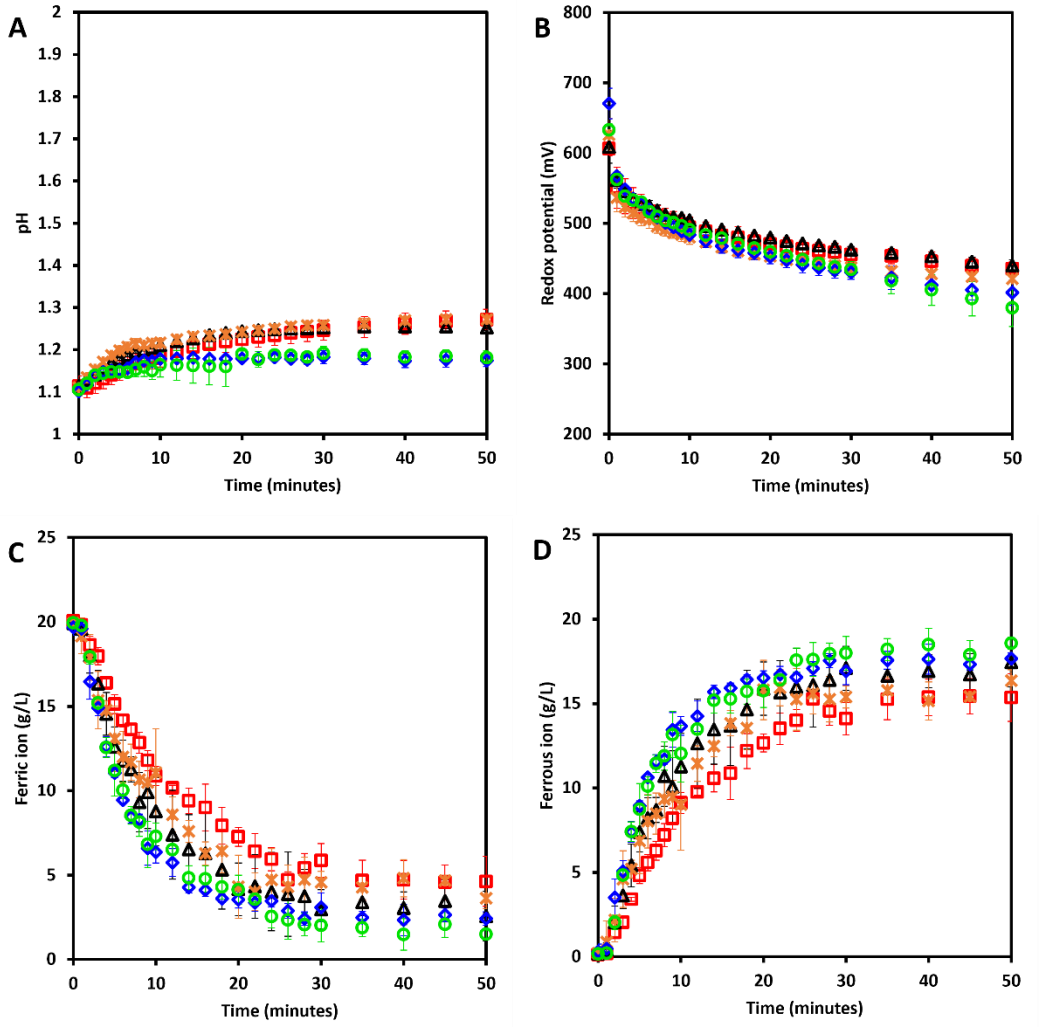

Figure 4-14 Change in pH (**A**), redox potential (**B**), Fe^{3+} (**C**) and Fe^{2+} (**D**) concentration over time during the ferric leaching of elementary Sn metal at 37 °C (▲), 45 °C (✖), 65 °C (◆), and 75°C (●). Error bars represent standard deviation, n = 3.

Despite the observed rapid Fe^{3+} reduction, decrease in the corresponding redox potential, and the increase in pH, analysis of Sn^{2+} in the leachates was inconsistent and remained below 1% Sn^{2+}. The low Sn concentration in solution was expected as a whitish-yellowish precipitate was observed even within the initial 60 min across all temperatures. The X-ray diffraction (XRD) analysis of the sample indicated that the precipitate was SnO_2 (Figure 4-15). The mass balance on Fe (Fe^{3+}, Fe^{2+}, and Fe^{tot} concentrations) in this present study confirmed that the observed precipitate contained no Fe.

The Fe^{3+} reduction observed suggested that the Sn dissolution was rapid as was precipitation as insoluble SnO_2. Jeon et al. (2015) reported rapid leaching kinetics and detected no Sn in the

leachates post the leaching of Sn from Pb-free solders at 30 to 90 °C. Similar Sn precipitates are typically reported during the leaching of PCBs and other Sn concentrates, such as cassiterite (Scott et al. 1997; Barakat 1998; Zhang et al. 2015; Yang et al. 2017). To this effect, Sn is typically recovered by filtering the SnO_2 (Scott et al. 1997; Yang et al. 2017) and recovery efficiency can be improved by increasing the pH of the leachates (Barakat 1998). From a thermodynamic view, the dominant species in Sn leaching systems is the quadrivalent Sn ion, Sn^{4+} which only remains in solution at highly acidic environments, pH <-1, (Palazhchenko 2012). This is widely achieved by leaching of the Sn concentrate through HCl and HNO_3 (Castro and Martins 2009; Havlik et al. 2011; Zhang et al. 2015; Moosakazemi et al. 2019).

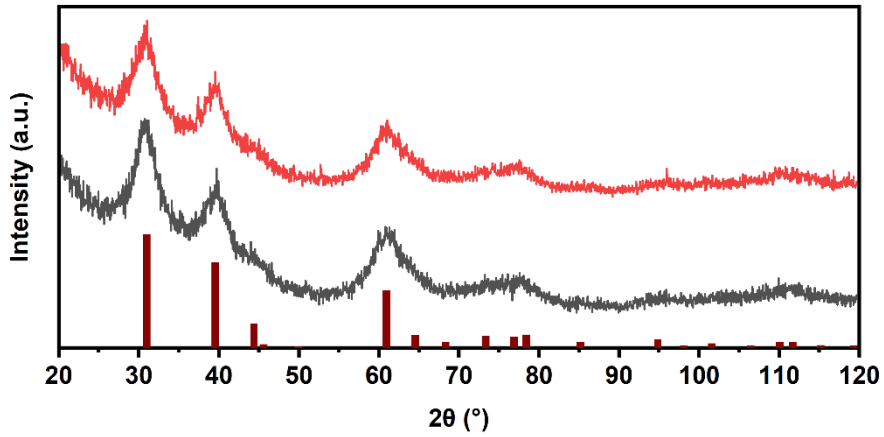

Figure 4-15 XRD spectrum of observed precipitates during ferric leaching ( ) and acid leaching ( ) of elementary Sn metal powder against reference SnO_2 ( ).

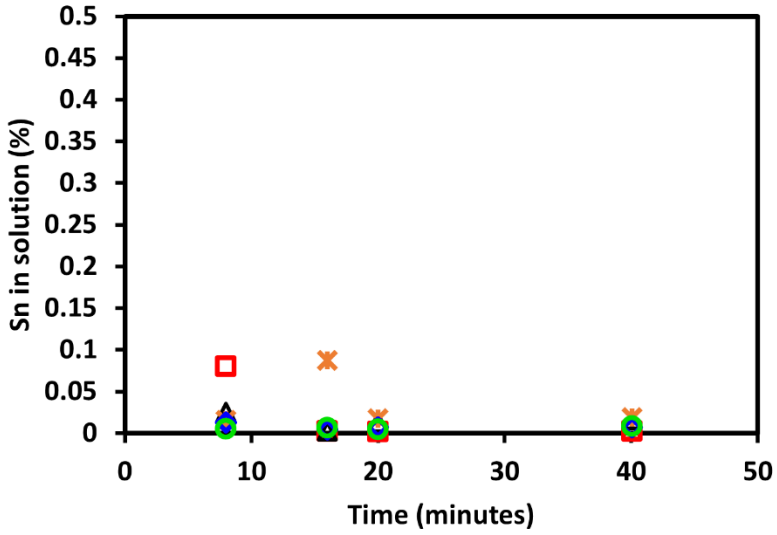

Figure 4-16 Sn (%) extracted into solution over time during the ferric leaching of elementary Sn metal at 25 °C ( ), 37 °C ( ), 45 °C ( ), 65 °C ( ), and 75 °C ( ).

The instantaneous leaching kinetics of Sn were evaluated from the Fe^{3+} reduction profiles; the estimated kinetic parameters are presented in Table 4-4. The reaction order, *n*, was approximately 2nd order with respect to Fe^{3+} concentration and had no dependence on Fe^{2+} concentration, *m* = 0. High correlation coefficients, R^2 ≥0.956, obtained across all temperatures suggested that the proposed rate law modelled the Fe^{3+} reduction rate well. The concentration of Sn^{2+} in the solution could not be modelled due to the SnO_2 precipitation. Therefore, based on the Fe^{3+} reduction rate as a function of Sn dissolution, the rate law for Fe^{3+} leaching of Sn can be given as:

$$\frac{d[Sn^0]}{dt} = -\frac{1}{2}k[Fe^{3+}]^2 \qquad \textit{Eq. 4-23}$$

Table 4-4 Estimated kinetic parameters for the Fe^{3+} leaching of elementary Sn metal obtained by fitting Fe^{3+} reduction data (Figure 4-14) into the proposed rate law R1 and R2.

Rate law	Kinetic parameters	25 °C	37 °C	45 °C	65 °C	75 °C
R1	*n* (Ave)			2.10		
	k (min^{-1})	0.226	0.323	0.417	0.542	0.705
	R^2	0.975	0.960	0.956	0.970	0.965
R2	*n* (Ave)			2.08		
	m (Ave)			0.0		
	k (min^{-1})	0.224	0.324	0.423	0.541	0.701
	R^2	0.974	0.959	0.955	0.971	0.961

The rate constant, *k*, increased from 0.226 to 0.705 min^{-1}, as the leaching rate increased with an increase in temperature from 25 to 75 °C. From the Arrhenius plot (Figure 4-17), the apparent activation energy was estimated to be 18.6 $kJ.mol^{-1}$, suggesting that the Fe^{3+} leaching of Sn was diffusion controlled. To the best of our knowledge, the current study is the first to report the activation energy of Fe^{3+} leaching of elementary Sn metal. The reported activation energies in literature are that of acid leaching of Sn. Hao et al. (2022) reported an activation energy of 20.3 $kJ.mol^{-1}$ for the acid (HCl) leaching of Sn from PCBs at 45 to 75 °C and concluded that the leaching mechanism was a mixed controlled reaction. Jha et al. (2012) estimated an activation energy of 117.7 $kJ.mol^{-1}$ for acid (HCl) leaching of Sn from PCBs at 60 to 90 °C.

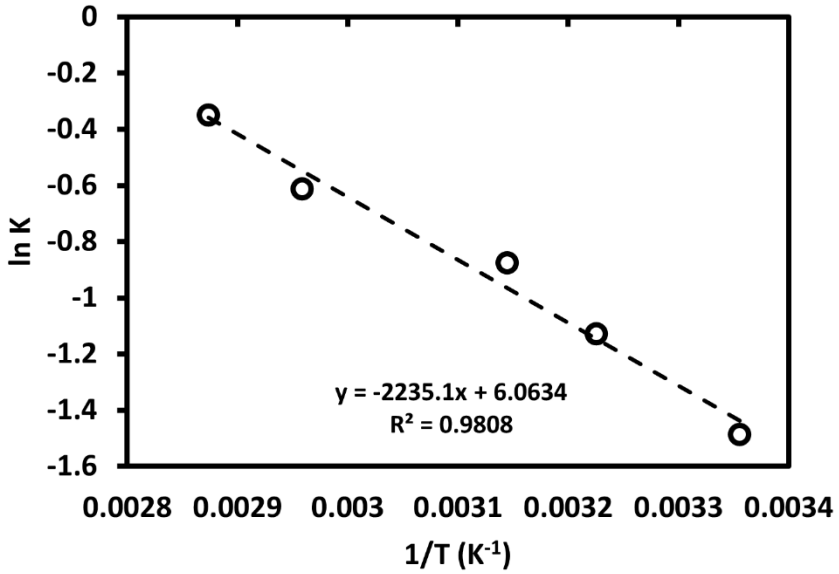

Figure 4-17 Arrhenius plot for the ferric leaching of elementary Sn metal at the temperature range of 25 - 75 °C.

Owing to the low solubility of Sn in H_2SO_4 media (Li et al. 2011; Jha et al. 2012), the acid leaching of Sn was poor as observed by minimal changes in the pH throughout the leaching (Figure 4-18). However, slightly improved leaching was observed with an increase in temperature. At 65 and 75 °C, the highest pH reached over the 1200 min leaching was 1.17 and 1.22, respectively, indicating some proton used in oxidising Sn into solution. The solution changed slightly in colour from clear to milky with some precipitate forming which was visually similar to the precipitates observed in the Fe^{3+} leaching system. The XRD showed that these precipitates were also SnO_2 (Figure 4-15). At 25 to 45 °C, the pH remained low (pH ≤1.40) over 24 h leaching, suggesting poor leaching. At the same low temperatures (25 – 45 °C), the redox potential sharply decreased to approximately 200 mV on the addition of Sn. Thereafter, it increased to the starting redox potential values over the initial 50 min and remained constant. At high temperatures, 65 and 75 °C, the redox also sharply decreased to approximately 100 mV at the addition of Sn and further decreased to approximately -100 mV and remained low, as Sn gradually leached. This suggested that although Sn leaching was limited, there was improved leaching with an increase in temperature. Across all temperatures, the dissolution of the elementary Sn metal was not complete. Although such low Sn in solution was expected as the most efficient acidic media for Sn is HCl, study of the Sn leaching here was necessary to understand the Sn leaching behaviour in H_2SO_4 media. Jha et al. (2012) also reported negligible Sn (%) in solution during extraction through the HNO_3 and H_2SO_4 leaching from Pb-Sn solders, whereas 96% Sn was extracted with 5.5 M HCl at 60 to 90 °C. Tin remained below 8% during the acid (H_2SO_4, 0.5 – 2 M) leaching of Indium tin oxide (ITO) at 50 to 95 °C.

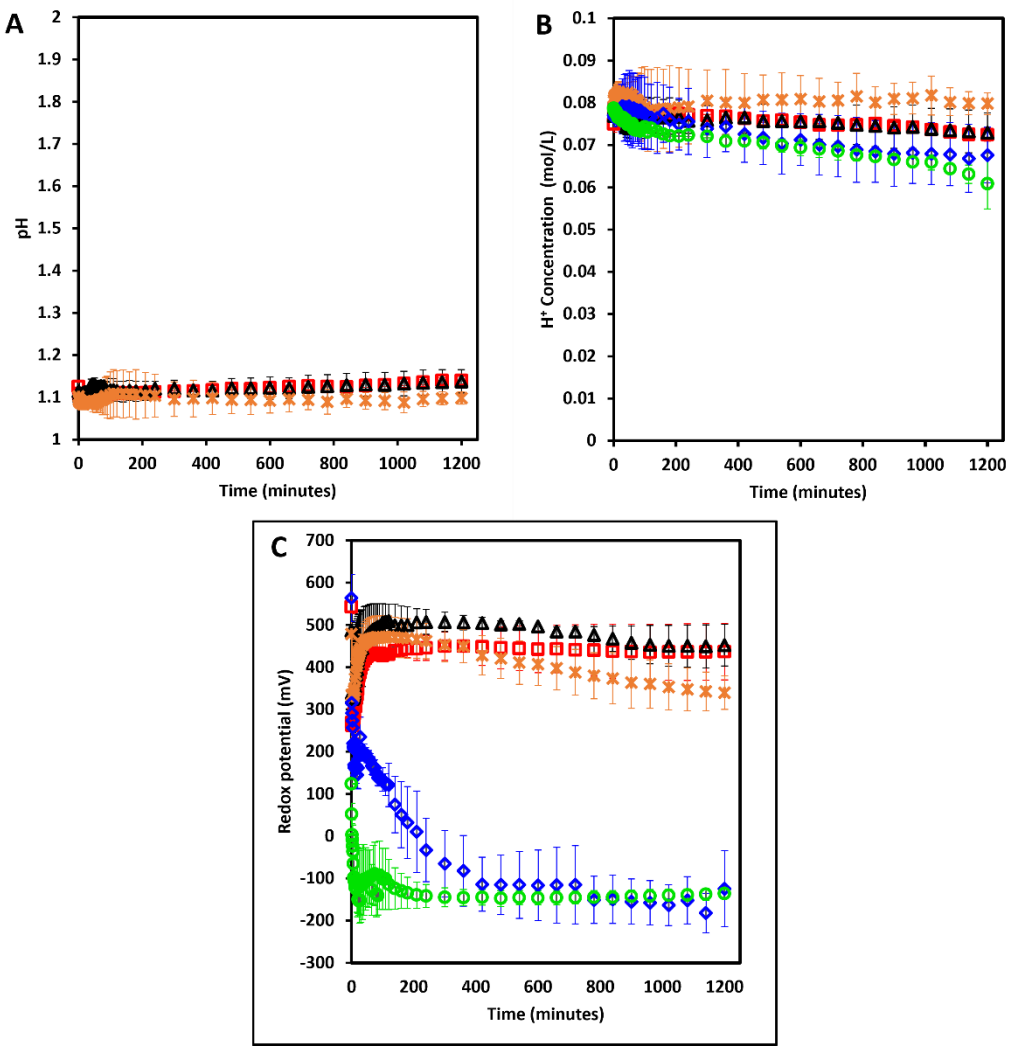

Figure 4-18 Change in pH (**A**), proton concentration (**B**), redox potential (**C**) and extracted Sn (%) (**D**) over time during the acid leaching of elementary Sn metal at at molar ratio of 1:1 25 °C (□), 37 °C (△), 45 °C (✕), 65 °C (◇), and 75°C (○). Error bars represent standard deviation, n = 3.

4.3.2 Leaching of mixed elemental metals

4.3.2.1 Ferric leaching of mixed elemental metals

To study the interactive effect of mixed metals on their relative metal leaching behaviour and its associated kinetics, and potential cementation reactions, the four metals of interest (Cu, Zn, Sn, and Ni) were leached in combination. To mimic PCB leaching, metals were added in proportion to the metal content of the PCB template (Section 3.1.3, Table 3-1) used throughout this PhD study. Results for ferric leaching of mixed metals are shown in Figure 4-19. Owing to the high competition for Fe^{3+} oxidant in the presence of multiple metals, the rate of Fe^{3+} reduction as a function of metal dissolution was more rapid than observed in the Fe^{3+} leaching of individual metals, with most of the Fe^{3+} reduction occurring within the initial 5 min across all temperatures studied. At 25 °C, the Fe^{3+} reduction rate was 5.30×10^{-2} mol.L^{-1}.min^{-1} within the initial 5 min and increased with temperature to 6.11×10^{-2} mol.L^{-1}.min^{-1} at

75 °C. Thereafter, the Fe^{3+} reduction rate decreased as Fe^{3+} in solution depleted, and the Fe^{3+} concentration plateaued from 10 min across all temperatures, suggesting complete metal leaching. In accordance with Fe^{3+} reduction, the redox potential decreased at the addition of mixed metals and plateaued after 10 min. The proton consumption was also as rapid, observed by the rapid increase in pH at the addition of the mixed metals. At 25 °C, the pH increased to 1.28 from 1.11 within the initial 1 min, while at 75 °C, it increased to 1.43, indicating improved leaching with an increase in temperature.

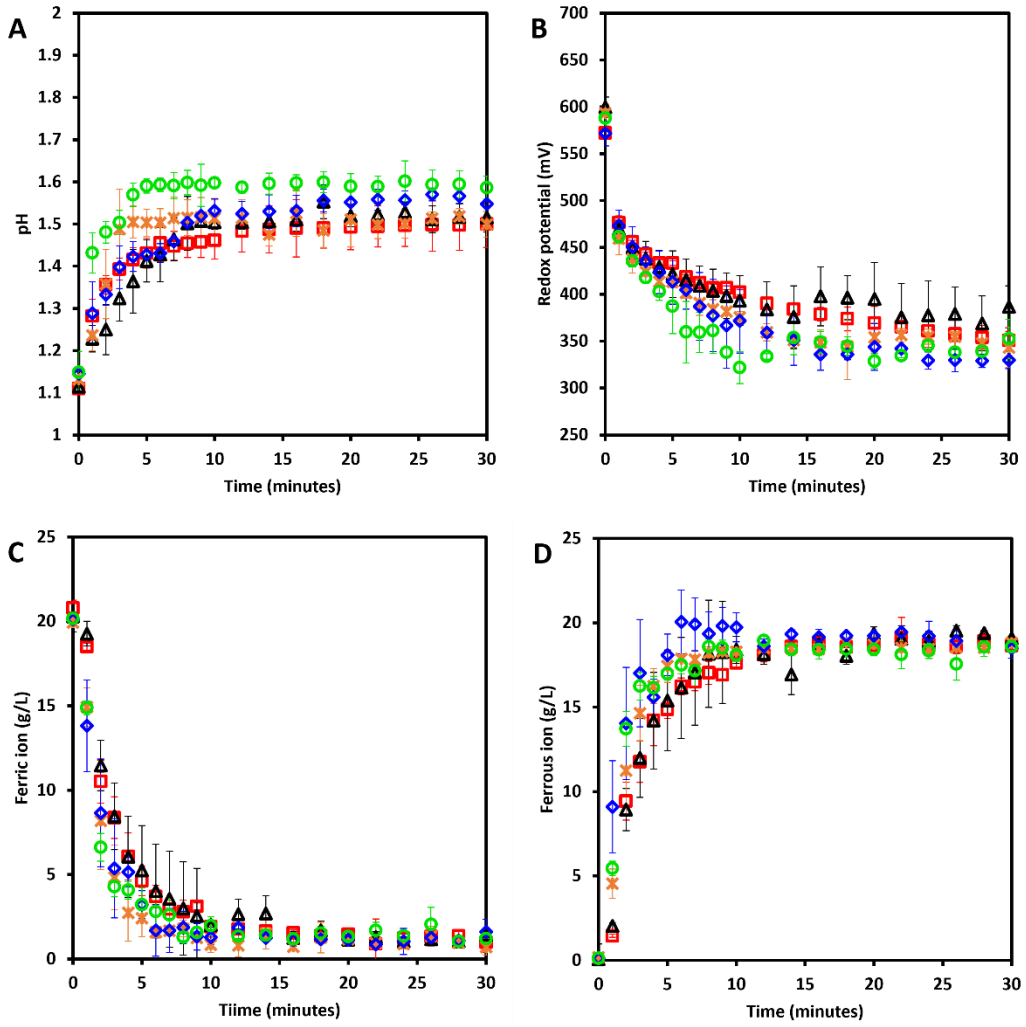

Figure 4-19 Change in pH (**A**), redox potential (**B**), Fe^{3+} (**C**) and Fe^{2+} (**D**) concentration over time during the ferric leaching of elementary mixed metals (Cu, Zn, Sn and Ni) at 37 °C (Δ), 45 °C (✕), 65 °C (◇), and 75°C (○). Error bars represent standard deviation, n = 3.

The rates of metal dissolution were rapid, with leaching rates increasing with temperature (Figure 4-20). At 25 °C, 69% Cu, 90% Zn, 45% Sn, and 5% Ni, were mobilised within the initial 2 min, while at 75 °C, 96% Cu, 104% Zn, 86% Sn, and 9% Ni was mobilised within the same leaching time. Across all temperatures, metal leaching was completed within the initial 10 min. Comparing the relative metal leaching rates, Zn leached the fastest, followed by Sn, Cu,

and Ni being the least. These observed relative metal leaching rates were comparable to these observed in the ferric leaching of individual metals. Moreover, they were in accordance with what is expected from an electrochemistry perspective based on the relative standard reduction potential with respect to that of Fe^{3+} as an oxidant, except for Ni, which was expected to be the 2nd fastest after Zn. This could be attributed to the postulated potential passive nano-Ni film forming on the surface of the unreacted Ni particles as discussed in Section 4.3.1.3. To this effect, dissolved Ni (%) in solution remained low as its leaching rate was relatively slow. Sn remained in the solution as observed by a high %Sn, compared to low Sn concentrations measured in the leaching of individual Sn metal (Section 4.3.1.4). This could be attributed to the relatively lower total Sn^{2+} concentration (6.74×10^{-6} mol.L^{-1}) expected as a low amount of Sn metal was added (0.0448 g), which could have been within the saturation level of Sn^{2+} in the solution.

As the leaching system was composed of mixed metal matrix, secondary reaction such as cementation could be expected, however, no precipitates were observed within 3 h across all temperatures. Cementation of metals such as Cu by Zn could be expected as such reaction is thermodynamically plausible and has been successfully applied in industrial level for Cu recovery since the 10th century (Veit and Bernardes 2015). Similarly, cementation of Ni and Sn by Zn could be expected (Boyanov et al. 2004; Luo et al. 2019). The absence of precipitates in the Fe^{3+} leaching system could be attributed to relatively low amount of other metals (Zn, Sn and Ni) added with respect to Cu, to effect a noticeable cementation reactions as well as the shorter leaching period.

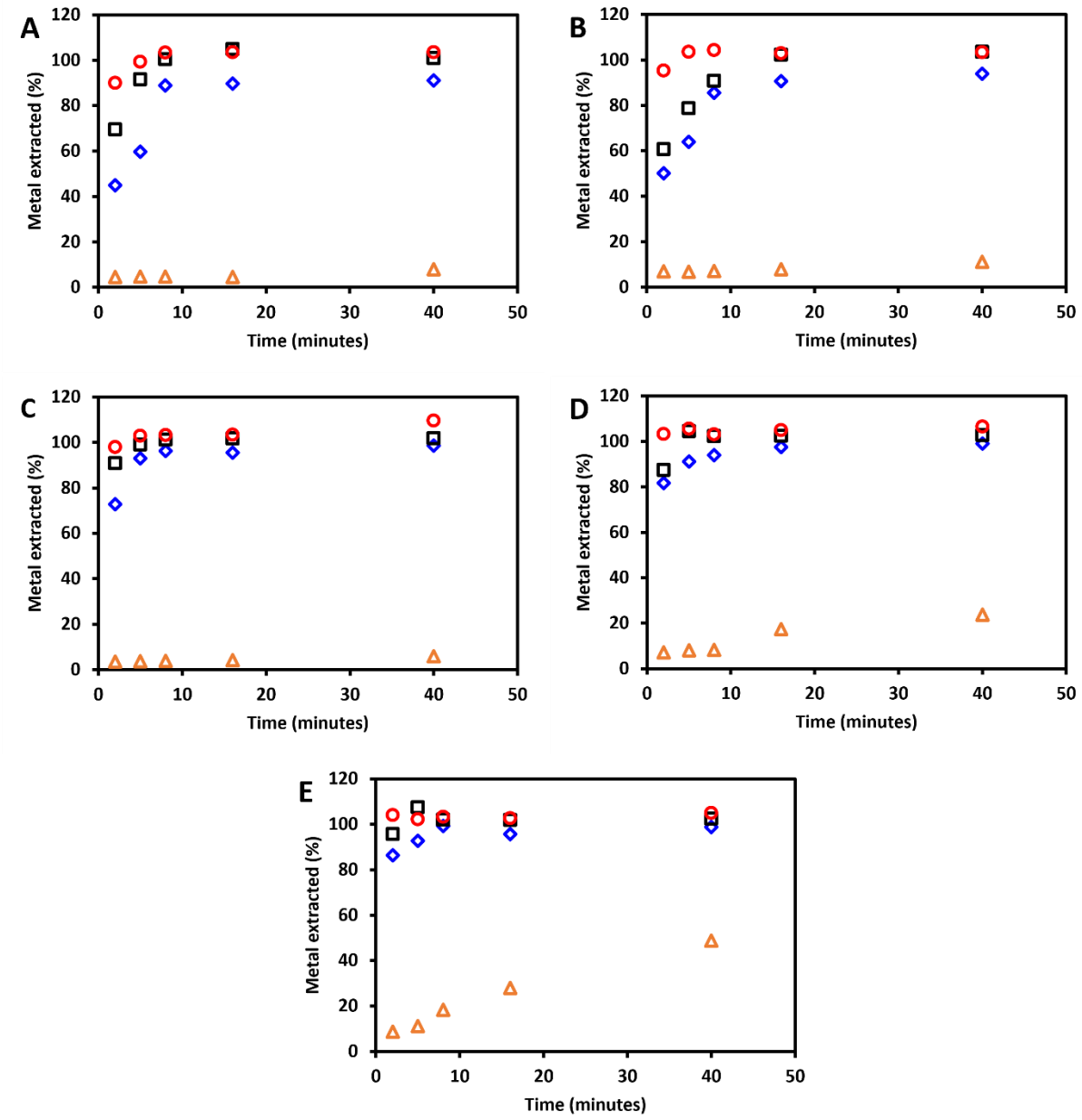

Figure 4-20 Amount (%) of Cu(□), Zn(○), Sn(◇), and Ni(△) extracted over time during the ferric leaching of mixed elementary metals at 25 °C (**A**), 37 °C (**B**), 45 °C (**C**), 65 °C (**D**), and 75°C (**E**).

Table 4-5 summarises the leaching kinetic parameters, *n*, *m*, and *k*, estimated from the Fe^{3+} reduction data. The Ni dissolution rate was approximately 2nd order with respect to Fe^{3+} concentration, and had no dependence on Fe^{2+} concentration, such that *m* is approximately 0. There was a good agreement between the modelled concentrations of Fe^{3+} and experimental concentrations, with R^2 ranging from 0.882 to 0.948 across the temperature range studied. Owing to the low amount of other metals (Zn, Sn, and Ni) added, relative to Cu, the Fe^{3+} reduction rates and its associated instantaneous kinetics were assumed to be mainly a function of Cu dissolution. This was validated by relatively high correlation coefficients, R^2 of >0.992 for fitting of experimental Cu concentration to the modelled values (Figure 4-21).

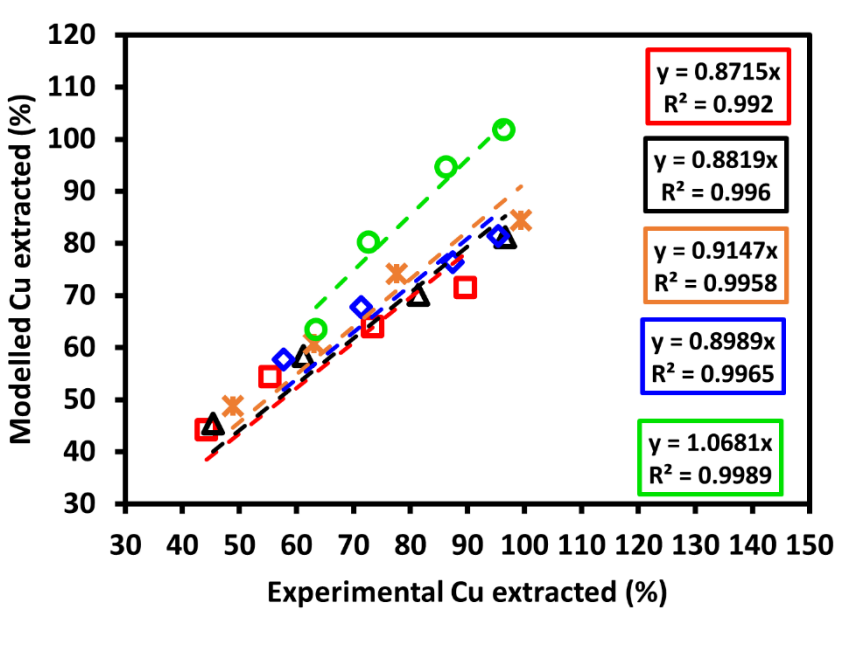

Figure 4-21 Parity plot for Cu for ferric leaching of mixed metals at 25 °C (□), 37 °C (△), 45 °C (✕), 65 °C (◇), and 75 °C (○).

Conversely, there was poor to no agreement between modelled and experimental concentrations of other metals (Zn, Ni, and Sn). The slightly low regression coefficients obtained here for Cu, relative to the ones obtained for individual leaching could be attributed to some Fe^{3+} reduction being due to the leaching of the other metals. The poor fitting at 75 °C, for both Fe^{3+} reduction and Cu concentration could be attributed to experimental error or the higher instantaneous leaching rate, making it challenging to collect sufficient data points within the initial leaching period to populate the model. The rate law for the Fe^{3+} leaching of mixed metals, dominated by Cu, can be expressed as:

$$\frac{d[Cu^0]}{dt} = -\frac{1}{2}k[Fe^{3+}]^2 \qquad \textit{Eq. 4-24}$$

Table 4-5 Estimated kinetic parameters for the Fe^{3+} leaching of mixed elementary metal obtained by fitting Fe^{3+} reduction data (Figure 4-19) into the proposed rate law R1 and R2.

Rate law	Kinetic parameters	25 °C	37 °C	45 °C	65 °C	75 °C
R1	*n* (Ave)			1.99		
	k (min^{-1})	0.776	0.818	1.09	1.61	1.85
	R^2	0.948	0.945	0.905	0.911	0.882
R2	*n* (Ave)			1.92		
	m (Ave)			0.0		
	k (min^{-1})	0.540	0.760	1.10	1.52	1.73
	R^2	0.953	0.948	0.908	0.917	0.889

The estimated rate constants, *k*, typically increased from 0.776 to 1.85 min^{-1}, with an increase in temperature from 25 to 75 °C. From the Arrhenius plot (Figure 4-22), the apparent activation energy was estimated to be 16.3 $kJ.mol^{-1}$, indicating a diffusion-controlled mechanism. There are no reported activation energy values for Fe^{3+} leaching of mixed elementary metals. Compared to activation energy obtained for Fe^{3+} leaching of individual metals, especially that of Cu as the leaching of mixed metal herein was assumed to be governed by dominant Cu metal, the estimated values were not comparable. This could be attributed to the fact that some Fe^{3+} reduction was a result of leaching of other added metals (Zn, Sn, and Ni) and not limited to Cu as assumed.

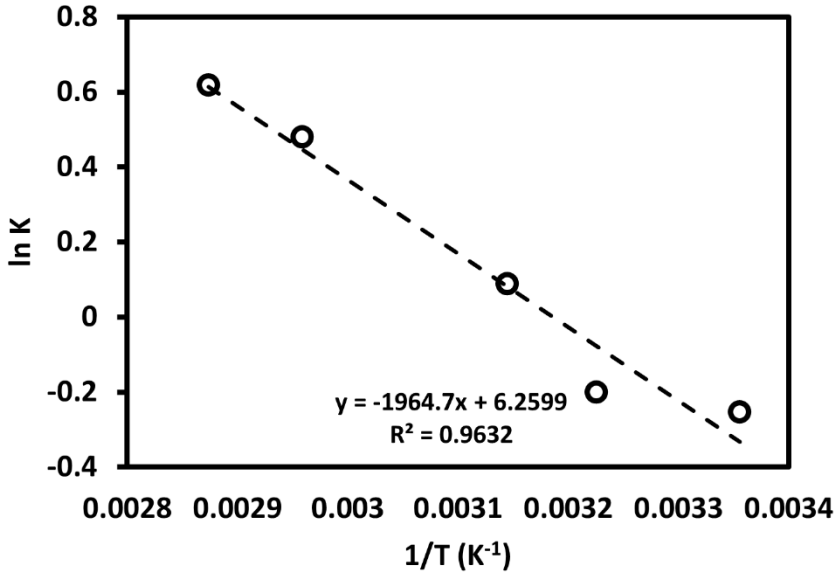

Figure 4-22 Arrhenius plot for the ferric leaching of mixed elementary metals across the temperature range of 25 to 75 °C.

4.3.2.2 Acid leaching of mixed elemental metals

Figure 4-23 shows the change in pH and its corresponding proton concentration, and redox potential for the acid leaching of mixed elementary metals. Compared to Fe^{3+} leaching systems, acid leaching was slow as characterised by gently slope(s) in the increase of pH as proton was consumed as a function of metal leaching. Metal leaching was improved with an increase in temperature. At 25 °C, the pH plateaued from 800 min, as an indication of complete metal leaching, while at 75 °C the pH plateaued from as early as approximately 200 min. Similar to the observations in the acid leaching of individual metals, higher final pH was observed at the lower temperature, i.e. pH 2.80 and 2.45 at 25 and 37 °C, respectively. At 65 and 75 °C, the pH remained at approximately pH 1.40. As discussed in Section 4.3.1.1, the low O_2 solubility with increasing temperature was postulated to be the cause of the effect of temperature on final pH reached. At the addition of the mixed metals, the redox sharply dropped to below 100 mV across all temperatures and increased as the metal leaching proceeded (Figure 4-23C). The rate at which the redox potential increased was dependent on temperature. At 75 °C, the redox potential increased rapidly to the initial redox potential from

approximately 200 min, while at 25 °C, the redox potential increased to plateau at approximately 350 mV from 800 min. This was an indication of improved leaching rates at increased temperature.

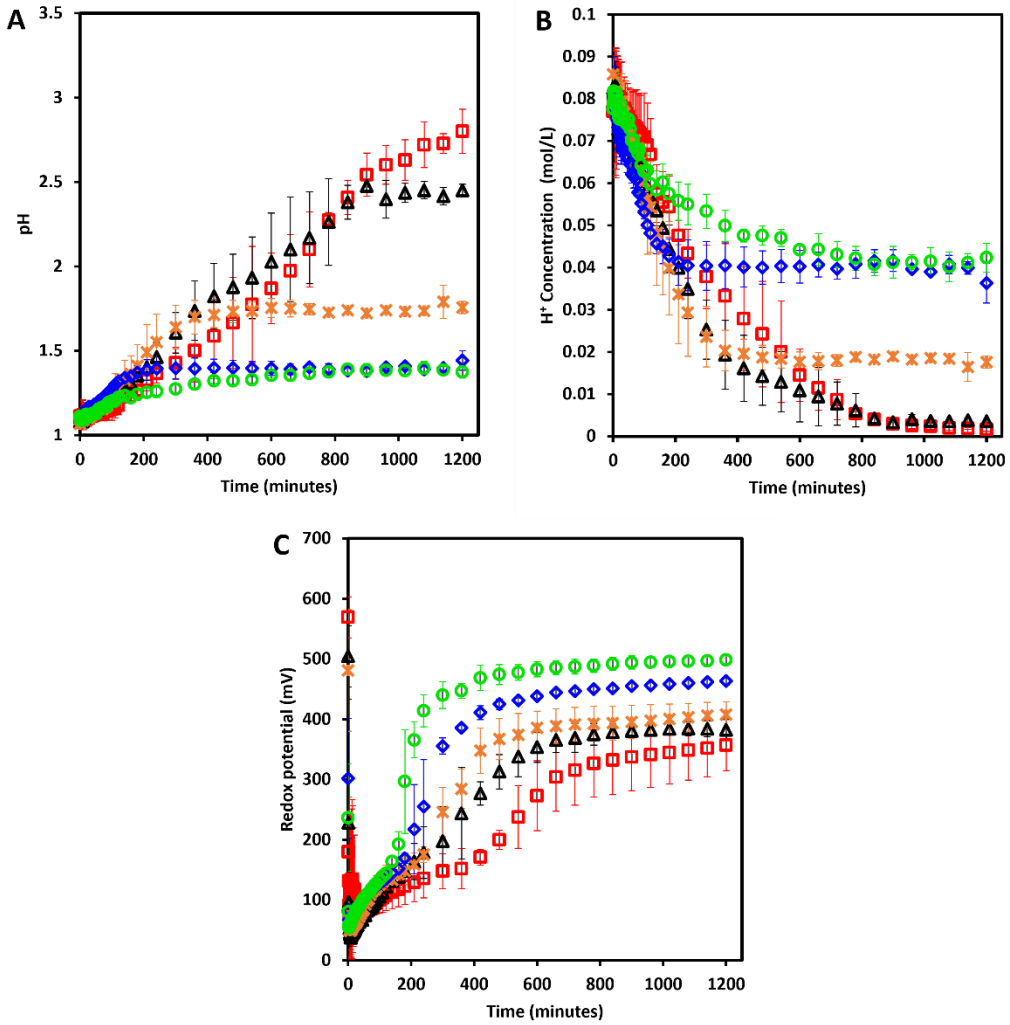

Figure 4-23 Change in pH (**A**), proton concentration (**B**), and redox potential (**C**) over time during the acid leaching of mixed elementary metals at 25 °C (□), 37 °C (Δ), 45 °C (✕), 65 °C (◇), and 75°C (○). Error bars represent standard deviation, n = 3.

Amount (in %) of leached metals in solution progressively increased over the leaching time (Figure 4-24). The metal leaching rate increased with increasing temperature. At, 25 °C, 86% Zn, 1% Ni, 39% Sn, and 7% Cu were mobilised within the initial 20 min. The extracted metal progressively increased to 102% Zn, 29% Ni, 24% Sn, and 89% C over 300 min. At 75 °C, 99% Zn, 20% Ni, 31% Sn, and 8% Cu was already mobilised within the initial 20 min and increased to 100% Zn, 95% Ni, 39% Sn, and 95% Cu at 300 min leaching time. After 24 h, complete leaching of Zn, Ni, and Cu was successfully achieved across all temperatures, except 63% Ni mobilised at 25 °C. This could be attributed to the slow leaching rate of Ni, especially at lower temperatures. Due to the low solubility of Sn in aqueous H_2SO_4 solution (Li et al. 2011), Sn remained below 40% across all temperatures.

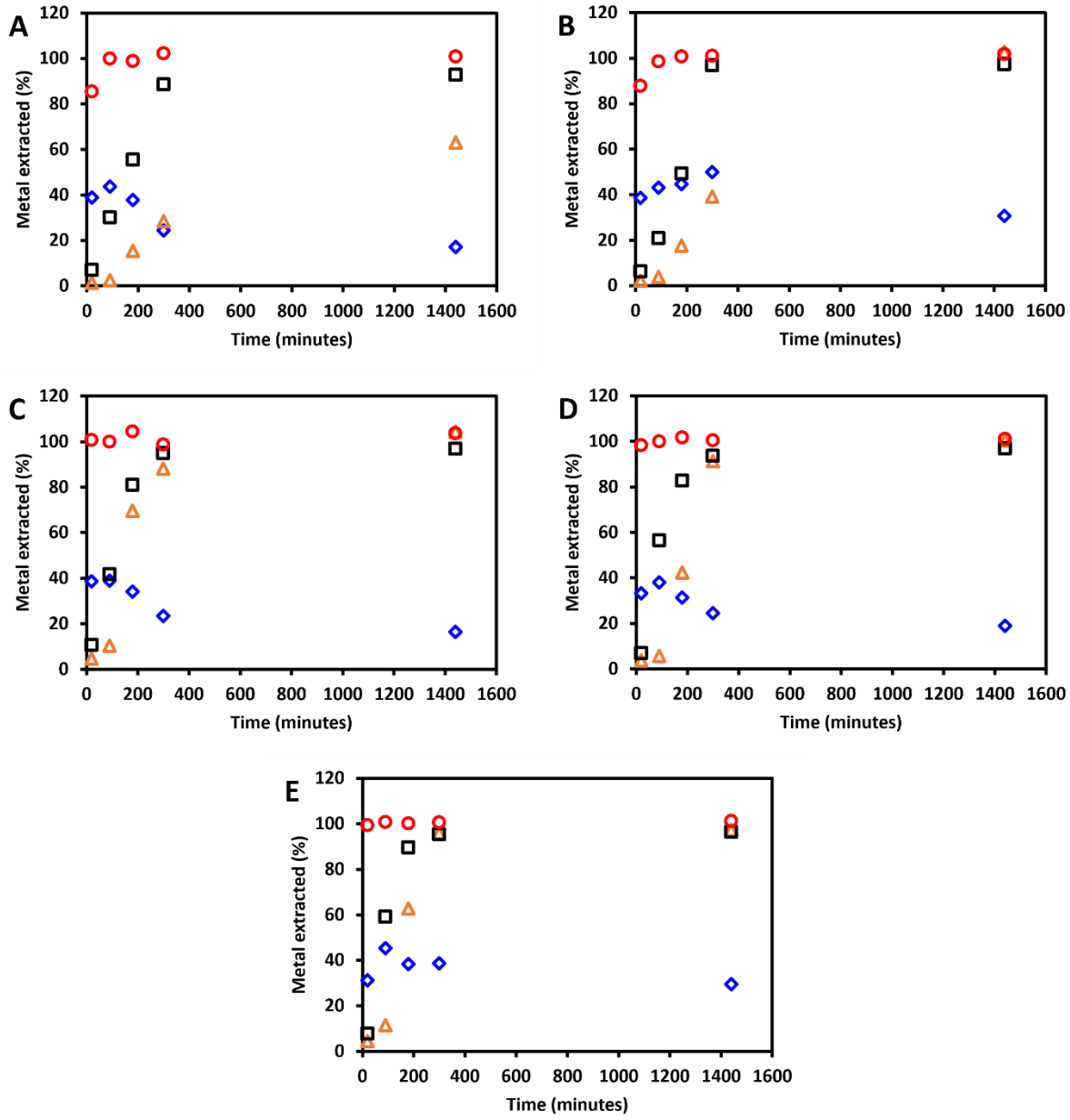

Figure 4-24 Amount (%) of Cu(□), Zn(○), Sn(◇), and Ni(△) extracted over time during the acid leaching of mixed elementary metals at 25 °C (**A**), 37 °C (**B**), 45 °C (**C**), 65 °C (**D**), and 75°C (**E**).

4.3.3 Leaching of PCBs

4.3.3.1 Ferric leaching of PCBs

Finally, to understand the leaching behaviour of PCBs with respect to the leaching of individual and mixed elementary metals, PCBs were leached in the same conditions as the elementary metals. Prior to the leaching, PCBs were shredded and pulverised into fine particle size to increase liberation and surface area for reaction (see Section 3.1.2), comparably to that of elementary metals. While focusing on the chemical leaching of the fine PCBs particles, leaching of two more particle sizes was explored. Different particle sizes were achieved by

varying the pulverising time. The fully powdered PCBs samples (≤1180 µm) were prepared by pulverising for 1 minute post shredding, while the second particle size PCB samples (1180 – 4750 µm) was prepared by pulverising for only 20 seconds. The third particle size of PCB samples were prepared by manually cutting the PCB boards using a bolt cutter into 0.5 cm^2 PCB chips, without shredding. Size reduction of PCBs prior to leaching is vital as it directly affects the metal liberation, the resultant leaching rates and the downstream processing, which in turn affects the economic value of PCB recycling. Though powdered (fine fractions) PCB samples results in high leaching rates, comminution processes are energy intensive and are associated with loss of valuable metals during size reduction (Kaya 2016). Fine particle size can also encourage precipitation during the leaching, complicating the separation of the non-metallic fraction post leaching (Chen et al. 2021). Large PCB pieces can easily be separated and recycled post leaching and feasibility for the use of such large PCB pieces has been demonstrated by Adhapure et al. (2014) and Jadhav and Hocheng (2015), amongst other researchers. However, a balance between high leaching rates and extent of metal leaching, and the particle size of the PCB samples is needed. To this effect, the three particle sizes explored here add to the knowledge of finding such balance.

Results for the ferric leaching of 1-minute, and 20-seconds pulverised PCBs, and PCB chips (0.5 cm^2) at 37 °C, against that of mixed elementary metals are presented in Figure 4-25. With an increased surface area for the leaching reaction, the ferric leaching of 1-minute pulverised samples was comparable to that of mixed elementary metals. Based on the observed slopes in the progressive increase in pH, the proton consumption rate in the leaching of 1-minute pulverised PCBs was relatively close to that of mixed metals within the initial 10 min. However, the pH for the PCB leaching plateaued from 35 min compared to 10 min for mixed metals, indicating faster leaching rates on mixed metals. The final pH reached in PCB leaching was pH 1.80 compared to pH 1.50 for mixed metals. This was attributed to the more metals in the PCBs and the natural alkalinity of PCBs (Arshadi et al. 2018). Despite the high Fe^{3+} reduction rate of 4.37×10^{-2} $mol.L^{-1}.min^{-1}$ in the initial 5 min for the Fe^{3+} leaching of mixed metals, compared to 2.41×10^{-2} $mol.L^{-1}.min^{-1}$ for the leaching of 1-minute pulverised PCBs, complete leaching was reached within the initial 30 min in both systems. This was indicative of the comparable high leaching rates in both these systems. Reduced Fe^{3+} reduction rates were observed with an increase in particle size of the PCBs samples. The rate was reduced to 6.01×10^{-3} and 2.60×10^{-3} $mol.L^{-1}.min^{-1}$ within the initial 5 min for the leaching of 20-seconds pulverised PCBs and PCB chips, respectively. The reduced leaching rate was due to the reduced reaction surface area with limitation in metal liberation, especially in PCB chips, further reduced the mass transfer. Over 300 min leaching time, only 42% Fe^{3+} was reduced as a function of metal leaching in the leaching of PCB chips, while 69% Fe^{3+} was reduced in the leaching of 20-seconds pulverised PCBs, further indicating limitations in leaching rates. Similarly, the proton consumption was limited as observed by low pH of approximately pH 1.30 over 300 min in both these leaching systems.

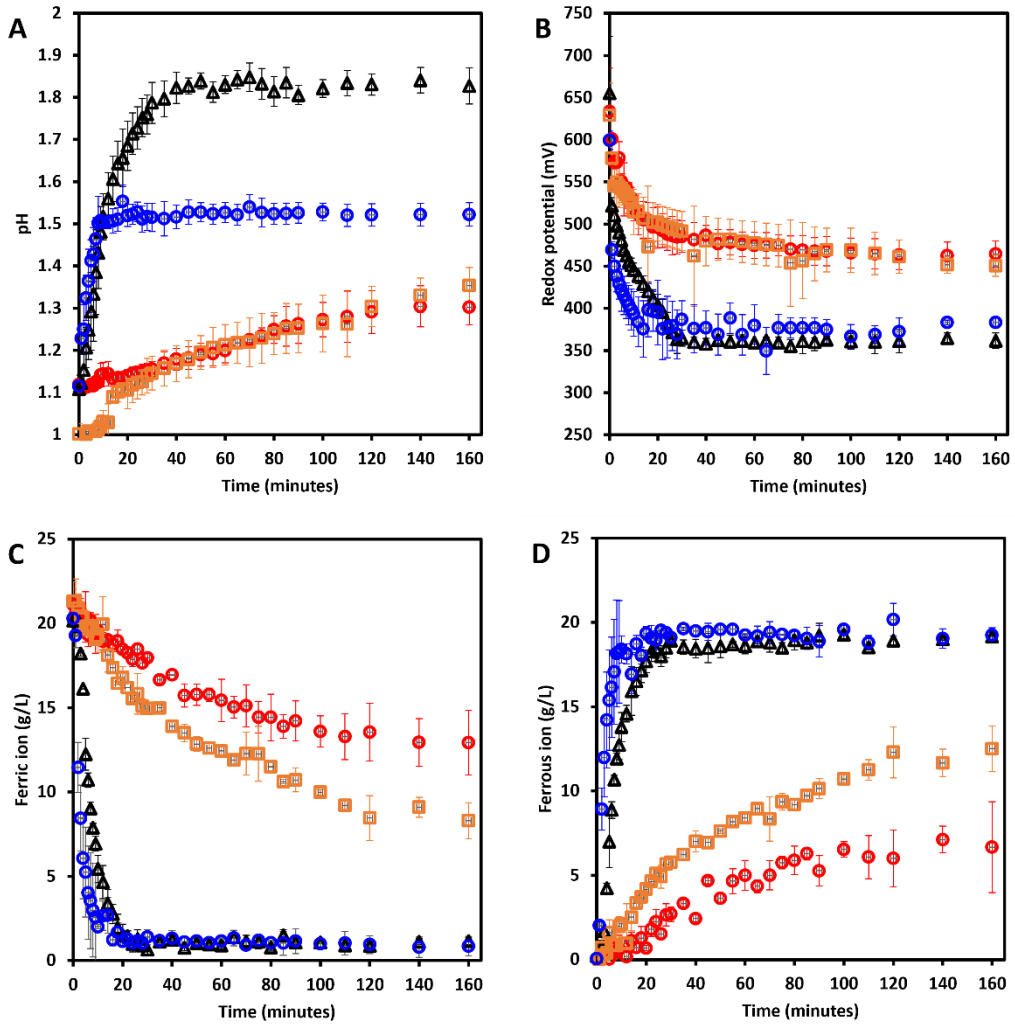

Figure 4-25 Change in pH (**A**), redox potential (**B**), Fe^{3+} (**C**) and Fe^{2+} (**D**) concentration over time during the ferric leaching of various particle sizes of PCBs and mixed metals at 37 °C; mixed elementraty metals (○), 1-minute pulverised PCBs (△), 20-seconds pulverised PCBs (□), and 0.5 cm^2 PCB chips (○). Error bars represent standard deviation, n = 3.

Figure 4-26 shows the extent of metals leached (in %) over 24 h for the leaching of the three particle size PCB fractions studied. Metal leaching efficiency was 59% Cu, 64% Zn, 35% Ni, with Sn in solution below detection limits in the leaching of PCB chips. It improved to 85% Cu, 91% Zn, 64% Ni, and 0.078% Sn in solution on the leaching of 20-second pulverised PCBs. Metals leaching further improved to 96% Cu, 103% Zn, 94% Zn, and 0.062% Sn in solution on the leaching of the 1-minuted pulverised PCBs. The high leaching efficiency achieved even with PCB chips was promising in terms of the use of such fractions to avoid the milling of PCBs. The leaching efficiency of such fractions is reported to be improved by pre-treating with sodium hydroxide (NaOH) or diluted HCl to remove the chemical coat on the PCB surface to further liberate metals (Adhapure et al. 2014; Jadhav and Hocheng 2015).

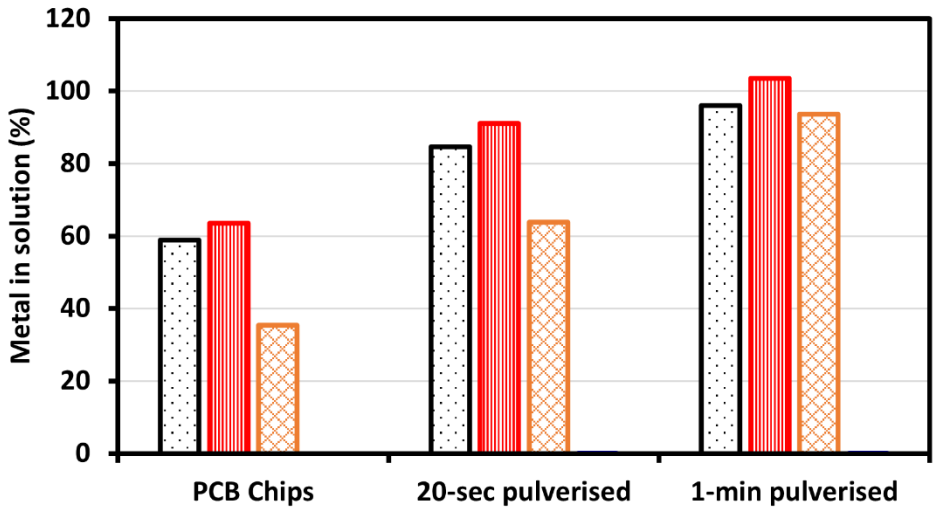

Figure 4-26 Amount (%) of Cu(■), Zn(■), Ni(■), and Sn(■) extracted over 24 h during the ferric leaching of various particle sizes of PCBs, 0.5 cm^2 PCB chips, 20-second, and 1-minute pulverised PCBs at 37 °C. Note that no leaching of Sn was observed, hence the absence of these bars.

With the relatively comparable leaching behaviour of 1-minute pulverised PCBs samples to the elementary metals, leaching kinetics of PCBs were evaluated by Fe^{3+} leaching of 1-minute pulverised PCBs at the temperature range of 25 to 75 °C. These results are presented in Figure 4-27. Similar to the observations in the Fe^{3+} leaching of elementary metals, acid consumption increased slightly with increasing temperature as observed by higher final pH reached at high temperatures (pH at approximately 2.30 at 65 and 75 °C) compared to low temperatures (pH at approximately 1.80 at 25 and 37 °C). The Fe^{3+} reduction rate increased from 8.94×10^{-3} $mol.L^{-1}.min^{-1}$ within the initial 5 min at 25 °C, to 5.45×10^{-2} $mol.L^{-1}.min^{-1}$ at 75 °C. Across the temperature range, complete metal leaching was achieved within the initial 40 min.

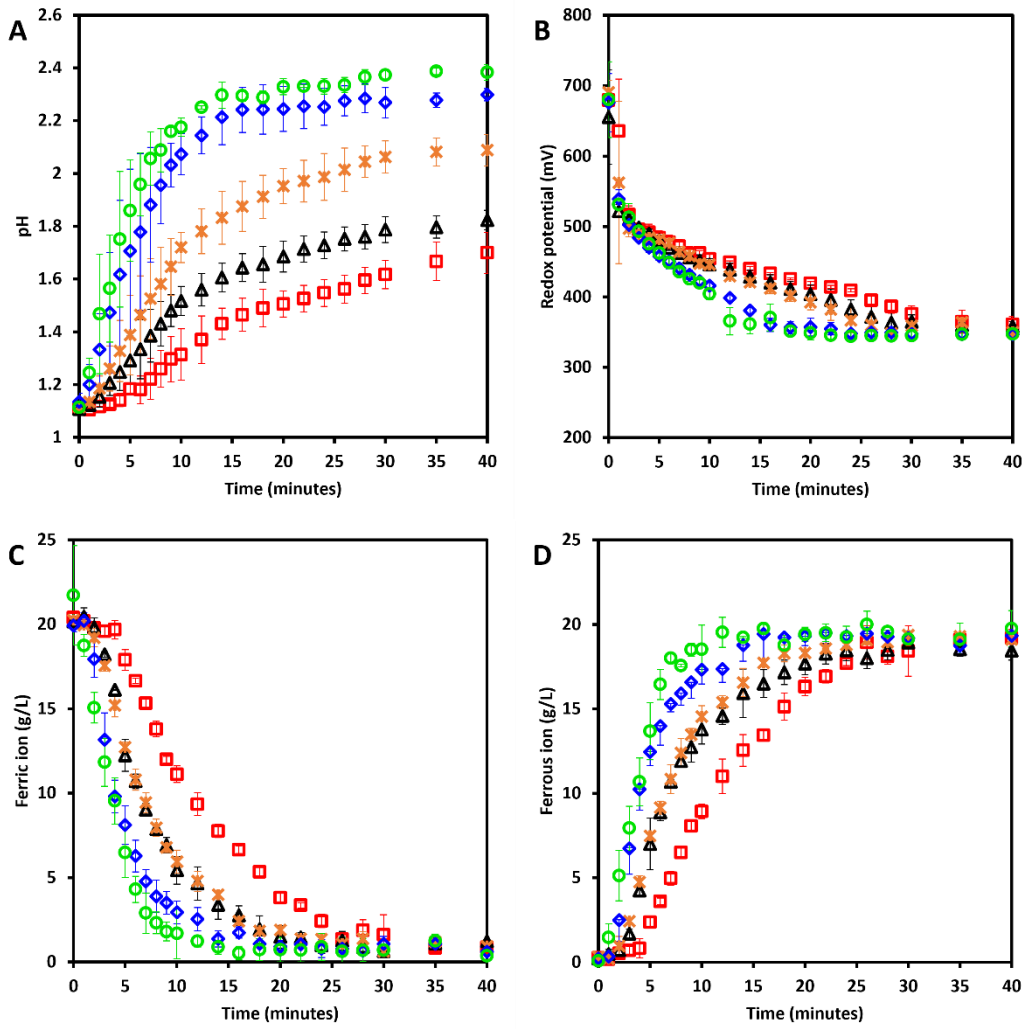

Figure 4-27 Change in pH (**A**), redox potential (**B**), Fe^{3+} (**C**) and Fe^{2+} (**D**) concentration over time during the ferric leaching of 1-minute pulverised PCBs at 25 °C (□), 37 °C (△), 45 °C (✕), 65 °C (◇), and 75°C (○). Error bars represent standard deviation, n = 3.

Consistent with the rapid Fe^{3+} reduction rates, metal extraction rates were as rapid (Figure 4-28). At 25 °C, 13% Cu, 26% Zn, and 5% Ni was mobilised within the initial 5 min and increased to 75% Cu, 85% Zn, and 77% Ni over 40 min leaching time. At 75 °C, 45% Cu, 77% Zn, and 44% Ni was mobilised within the initial 5 min. Across all temperatures, both Zn and Cu had completely leached by 40 min, while Ni was at 86%. The concentration of Sn in the leachates was inconsistent across the temperature range. This could be attributed to the low concentration of Sn in the PCB sample used and its proneness to precipitate out of solution. High leaching rates and efficiency achieved in this study from the Fe^{3+} leaching of PCBs is common elsewhere in literature (Yang et al. 2009; Yazici and Deveci 2014; van Yken et al. 2020). Yazici and Deveci (2014) reported high leaching yields of 99% Cu, 88% Ni, 21% Ag, and 69% Pd over a short period of 120 min during the Fe^{3+} leaching of PCBs. However, caution should be practiced in comparing the leaching efficiency to other reported studies, as PCBs are highly heterogeneous (different types of PCBs, with notable variations in metal content), while different leaching conditions (working temperature, pH, and Fe^{3+} concentrations), as

well as the different in particle sizes, can affect the leaching efficiency (Yang et al. 2009; Zhu et al. 2011; Bas et al. 2012; Gu et al. 2019; van Yken et al. 2020). Similar to the Fe^{3+} leaching of elementary metals, both individual and mixed metals, the instantaneous leaching of Zn was faster. The faster leaching of Zn was as expected from its high electronegativity and can readily leach into acidic medium (Speight et al. 2005); followed by Cu, and Ni being the least.

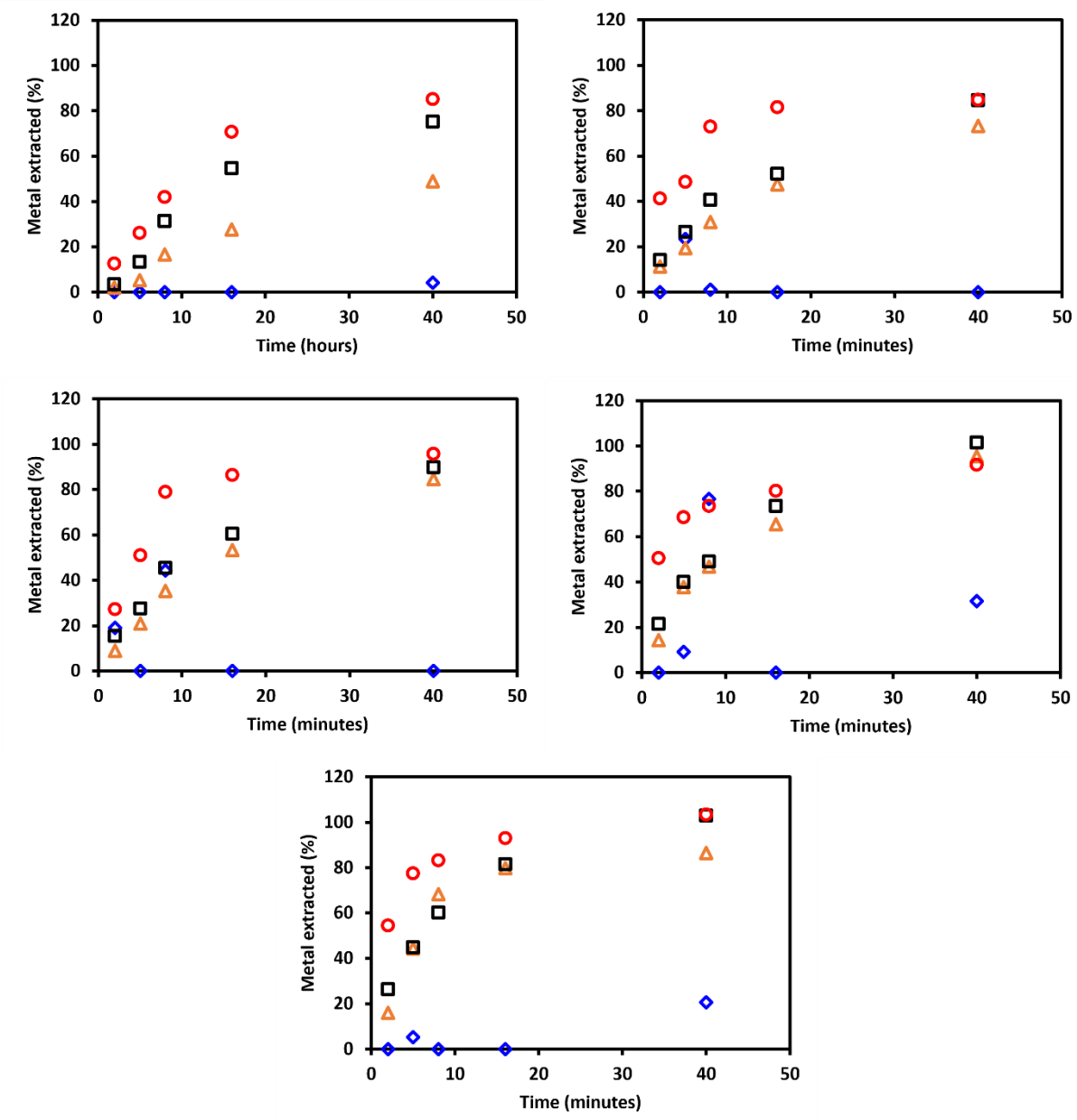

Figure 4-28 Amount (%) of Cu(□), Zn(○), Sn(◇), and Ni(△) extracted over time during the ferric leaching of 1-minute pulverised PCBs at 25 °C (**A**), 37 °C (**B**), 45 °C (**C**), 65 °C (**D**), and 75°C (**E**).

Leaching kinetic parameters, *n*, *k*, and E_a, were estimated from the Fe^{3+} reduction data presented in Figure 4-27 and are presented in Table 4-6. The PCB leaching was assumed to be dominated by Cu and the effect of other metals, such as Zn, Ni, and Sn was neglected due to their low concentration relative to Cu. Thus, Fe^{3+} leaching of Cu from PCBs was approximately

2nd order with respect to Fe^{3+} concentration and had no dependency on Fe^{2+} concentration. The proposed rate law 1 fitted the experimental Fe^{3+} reduction data well (R^2 >0.911) across the temperature range studied. The regression coefficients of > 0.974 were obtained from fitting the experimental Cu concentrations data to the modelled Cu concentrations (Figure 4-29), further validating the proposed rate law. Though best fittings are usually characterised by R^2 >0.95, the slight deviation here could be attributed to some Fe^{3+} reduction being due to oxidation of metals other than Cu. However, poor fittings were obtained for prediction of Zn, Sn, and Ni. Under assumptions made and within experimental errors, the rate law for the Fe^{3+} leaching of Cu from PCBs, as a function of Fe^{3+} concentration, can be expressed as:

$$\frac{d[Cu^0]}{dt} = -\frac{1}{2}k[Fe^{3+}]^2 \qquad \textit{Eq. 4-25}$$

Table 4-6 Estimated kinetic parameters for the Fe^{3+} leaching of 1-minute pulverised PCBs obtained by fitting Fe^{3+} reduction data (Figure 4-27) into the proposed rate law R1 and R2.

Rate law	Kinetic parameters	25 °C	37 °C	45 °C	65 °C	75 °C
R1	*n* (Ave)			1.89		
	k (min^{-1})	0.173	0.346	0.446	0.766	0.853
	R^2	0.948	0.948	0.941	0.911	0.911
R2	*n* (Ave)			1.89		
	m (Ave)			0.0		
	k (min^{-1})	0.161	0.322	0.408	0.774	0.902
	R^2	0.948	0.946	0.941	0.914	0.905

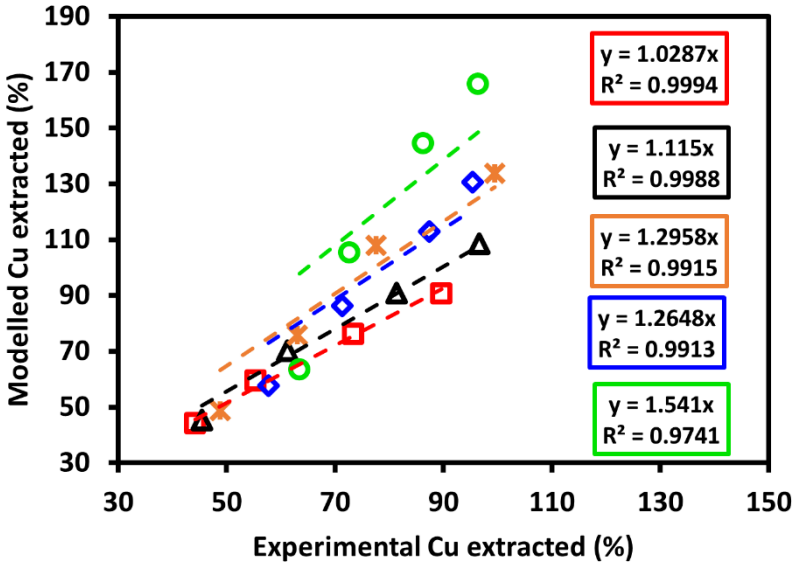

Figure 4-29 Parity plot for Cu for ferric leaching of 1-minute pulverised PCBs at 25 °C (□), 37 °C (△), 45 °C (✕), 65 °C (◇), and 75 °C (○).

The apparent activation energy, estimated from the Arrhenius plot (Figure 4-29), for the Fe^{3+} leaching of Cu from PCBs was 26.8 $kJ.mol^{-1}$. This suggested that the mechanism for Fe^{3+} leaching of Cu from PCB was mixed-controlled. Comparing the activation energy obtained here to literature values, with caution as discussed above, the activation energy obtained was comparable. Becci et al. (2019) obtained an activation energy of 18 to 25 $kJ.mol^{-1}$ for the Fe^{3+} leaching of Cu from PCBs at 30 to 70 °C. Yazici and Deveci (2014) obtained an activation energy of 18 $kJ.mol^{-1}$ for the Fe^{3+} leaching of Cu from PCBs at 20 to 80 °C.

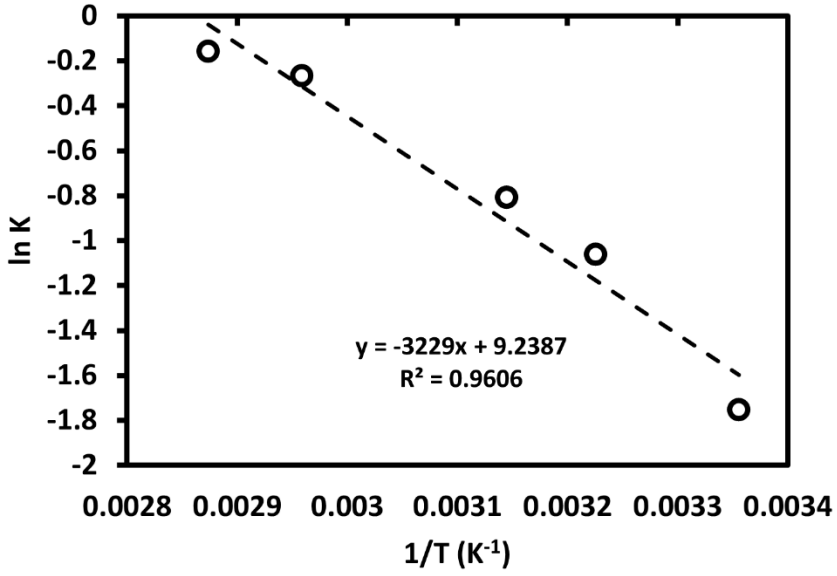

Figure 4-30 Arrhenius plot for the ferric leaching of 1-minute pulverised PCBs across the temperature range of 25 to 75 °C.

4.3.3.2 Acid leaching of PCBs

The 1-minute pulverised PCBs were also leached with the acid-only leaching using acidified water at initial pH 1.1, over the temperature range of 25 to 75 °C; these results are presented in Figure 4-31. The acid leaching of PCBs was slower compared to the ferric leaching. Based on the observed slope in the increase in pH and the inferred H^+ consumption rates, the acid leaching rate increased with increasing temperature. Within the initial 100 min, the pH remained below pH 1.3 at 25 °C, while it increased from pH 1.1 to above pH 1.5 at 75 °C. As the leaching progresses, the pH plateaued from approximately 400 min at 65 to 75 °C, while at 25 to 45 °C, it plateaued from approximately 700 min, indicating delayed complete leaching at lower temperatures. Similar to the observations in the acid leaching of elementary metals (section 4.3.1 and 4.3.2), higher final pH was observed at low temperatures, i.e. at approximately pH 2.8 at 25 °C, while pH remained below 2.0 at 65 and 75 °C. Such observed effect of temperature to the solution pH could be attributed to the oxygen solubility with respect to temperature as discussed Section 4.3.1.1. Noticeable was the higher final pH reached across all temperatures in the acid leaching of PCBs compared to leaching of elementary metals. This could be attributed to more metals available in the PCBs compared

to the limited added metals in the leaching of elementary metals, in addition to the natural alkalinity of PCBs (Arshadi et al. 2018).

At the addition of the PCBs, the redox potential sharply decreased from approximately 500 mV to below 300 mV across all temperatures. At 25 and 37 °C, the redox potential rapidly increased to approximately 400 mV over the initial 10 min and remained so for the next 60 min. Within the same leaching period, the redox potential decreased and remained at approximately 100 mV at 45 to 75 °C. This suggested that the onset leaching of PCBs was slightly delayed at lower temperatures, while at higher temperatures, instantaneous leaching was promoted by high temperatures. The redox potential gradually decreased to approximately 100 mV at 25 and 37 °C, indicating onset leaching of metals. The redox potential of approximately 100 mV during metal leaching was also observed at the leaching of mixed elementary metals. At the end of the leaching period, the redox increased to between 200 and 300 mV, which could be indication of complete metal leaching.

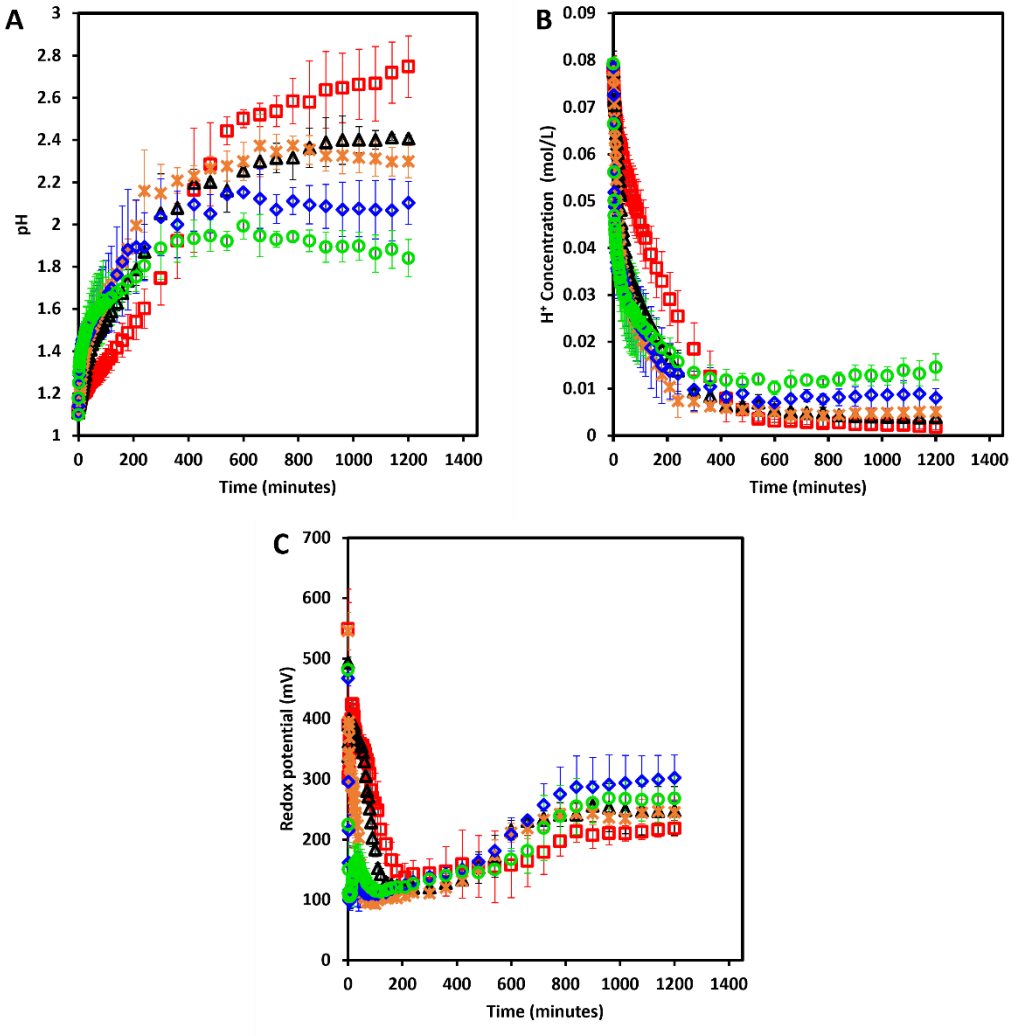

Figure 4-31 Change in pH (**A**), proton concentration (**B**), and redox potential (**C**) over time during the acid leaching of 1-minute pulverised PCBs at 25 °C (□), 37 °C (△), 45 °C (✕), 65 °C (◇), and 75°C (○). Error bars represent standard deviation, n = 3.

The progressive metal leaching (in %) for the acid leaching of PCBs is presented in Figure 4-32. The metal leaching rate and extent increased with an increased in temperature. At 25 °C, 1% Cu, 45% Zn, 12% Ni, and 0% Sn was solubilised within the initial 20 min, and over the 24 h leaching period, these yields increased to 72% Cu, 99% Zn, 73% Ni, and 10% Sn. With an increased in temperature to 75 °C, 16% Cu, 83% Zn, 45% Ni, and 19% Sn was mobilised within the initial 20 min and by the end of the leaching period, of 40 min, 96% Cu, 98% Zn, 94% Ni and 16% Sn had been leached. Across all temperatures, amount of Sn solubilised remained below 25% as Sn has low solubility in aqueous H_2SO_4 media (Castro and Martins 2009). Hong and Valix (2014) also reported improved leaching yields from <20% Al, Zn, and Cu to >80% over 24 h leaching with an increased in temperature from 30 °C to 90 °C during the sulfuric acid leaching (pH 1.0) of PCBs. Low yields at low temperatures of 25 °C, i.e. 39% Cu, 48% Al, 43% Zn, and 48% Ni over 48 h, are reported from acid leaching (H_2SO_4, pH 1.0) of PCBs (van Yken et al. 2020). This suggested that temperature is a crucial factor in the acid leaching of PCBs. In addition to the temperature, addition of stronger oxidants such as H_2O_2 have been shown to not only improve total metal yields but also the leaching rates (Ouchi et al. 2023). Jha et al. (2011) reported improved leaching of Cu from 60% to 97% over 120 min with an increase in the added concentration of H_2O_2 from 5 to 15% v/v during sulfuric acid leaching of PCBs.

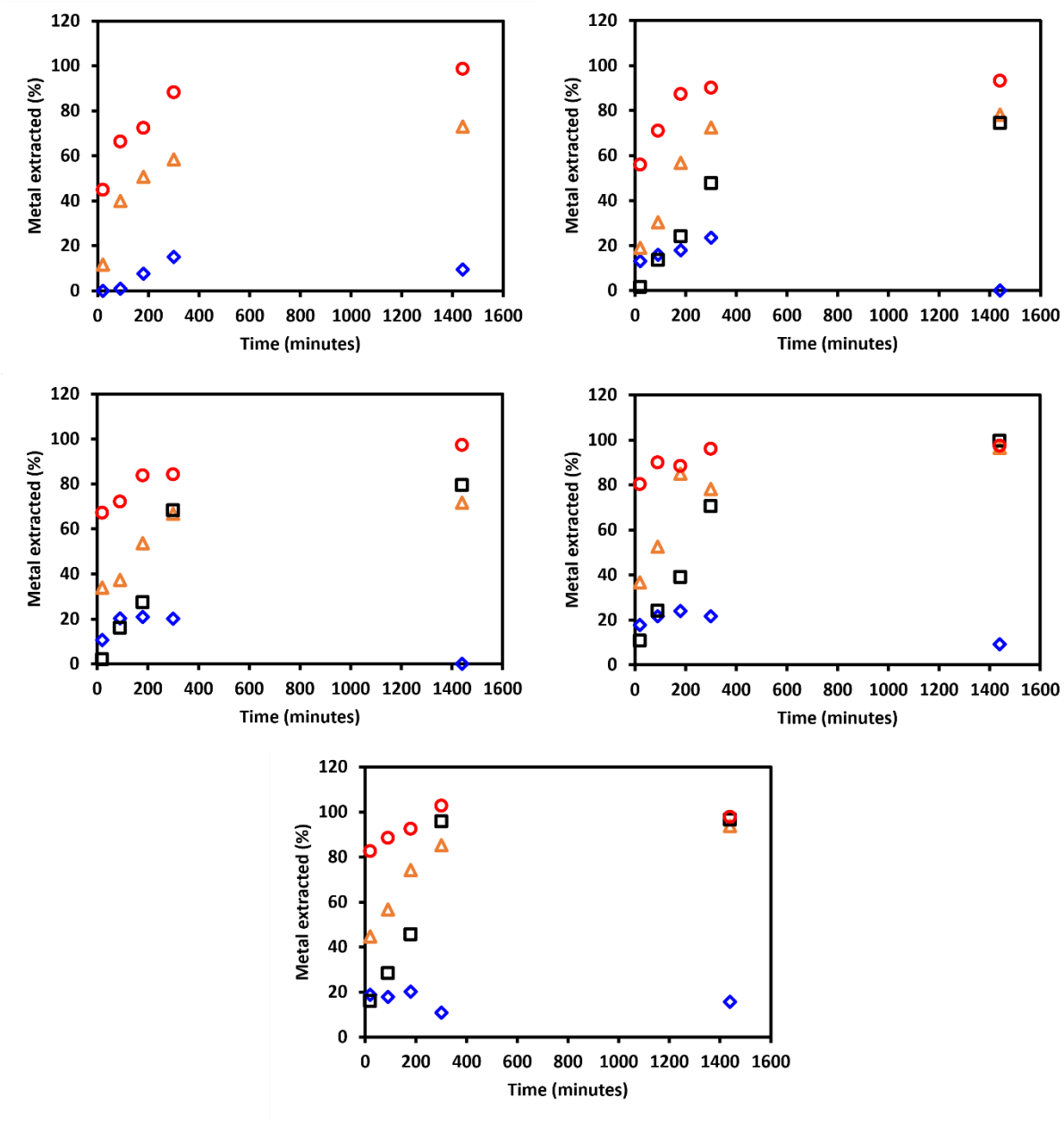

Figure 4-32 Amount (%) of Cu(□), Zn(○), Sn(◇), and Ni(△) extracted over time during the acid leaching of 1-minute pulverised PCBs at 25 °C (**A**), 37 °C (**B**), 45 °C (**C**), 65 °C (**D**), and 75°C (**E**).

With regards to relative metal leaching rates, as expected from electrochemistry (i.e. based on the standard reduction potential of the metal of interest to that of the oxidant), the instantaneous leaching rate of Zn was fastest, followed by Ni, then Cu with Sn solubilising the most slowly. This order of leaching rate was slightly different to that observed in the acid leaching of elementary metals, i.e. Zn>Cu>Ni>Sn for both individual and mixed metals. The total amount of metals solubilised here, especially at the low temperatures (25 to 45 °C), were relatively low compared to these observed in the acid leaching of elementary metals systems, which could be attributed to readily liberated metals in elementary metals. Over the 24 h leaching time, there were no precipitations observed based on the metal ions concentration

analysed. Cementation may require a longer reaction time. The absence of cementation was also observed in the acid leaching of mixed elementary metals. This could also be attributed to low pH in accordance with previous reports of a retard in cementation reactions at pH <3 (Sulka and Jaskuła 2003; Demirkıran et al. 2007; Hong and Valix 2014).

4.4 Conclusion

This study investigated the leaching behaviour of elementary metals, Cu, Zn, Ni, and Sn, as individual metals in their combinations, and from PCBs. Leaching was carried out using an acidic ferric lixiviant, and a lixiviant containing sulfuric acid only as oxidant, across the temperature range of 25 to 75 °C. The core objectives were to evaluate which of Fe^{3+} and H^{+} is the dominant oxidant, the relative metal leaching rates, and the associated leaching kinetics of these four metals, as elementary metals, individually and in mixed metal streams, and from complex PCBs. In all leaching systems studied, the acid leaching rates were slower than Fe^{3+} leaching under acidic conditions, suggesting that Fe^{3+} was a dominant oxidant. Fe^{3+} leaching of individual elementary metals was found to be rapid, with complete Fe^{3+} reduction and more than 90% Cu, 93% Zn, and 76% Ni (except at 37 and 45 °C) readily mobilised into solution within the initial 60 min across all temperatures. Complete Fe^{3+} reduction was also achieved within the same leaching time for Sn, indicating successful leaching of Sn, despite Sn precipitating out of solution as SnO. The final pH remained below 2 post the Fe^{3+} leaching in all elementary metal leaching systems, highlighting the importance of balancing out the required stoichiometric molar ratio of the added metal to the available Fe^{3+} oxidant to minimise Fe^{3+} precipitation at pH >2. Based on the Fe^{3+} reduction rate as a function of metal leaching, the relative Fe^{3+} leaching rates amongst leaching of individual and for mixed metals was Zn>Sn>Cu>Ni. For acid leaching of both individual and mixed metals, the relative leaching rate was Zn>Cu>Ni>Sn.

The Fe^{3+} leaching rates increased with increasing temperature. The average Fe^{3+} reduction rates as a function of metal leaching ranged at 6.87 – 8.01 g $Fe^{3+}.L^{-1}.h^{-1}$ for Zn, 3.75 – 4.59 g. $Fe^{3+}.L^{-1}.h^{-1}$ for Cu, and 4.03 – 5.27 g. $Fe^{3+}.L^{-1}.h^{-1}$ for Sn at 25 – 75 °C, respectively, while it was 0.60 -9.13 g. $Fe^{3+}.L^{-1}.h^{-1}$ for Ni at 37 – 75 °C. With high competition for Fe^{3+} oxidant in the multimetal system, the Fe^{3+} reduction rates ranged at 7.44 – 10.14 g. $Fe^{3+}.L^{-1}.h^{-1}$ for mixed metals at 25 – 75 °C, respectively.

The Fe^{3+} leaching kinetics were evaluated by fitting experimental data to rate law 1, which was formulated based on the Fe^{3+} reduction as a function of metal leaching:

$$\frac{d[Fe^{3+}]}{dt} = -k[Fe^{3+}]^{n} \qquad R1$$

For individual elementary metals, the leaching kinetics for Cu and Sn was 2nd order with respect to Fe^{3+} concentration, 4.6 (≈ 5th) order for Zn and 1st order for Ni. Dependency of the leaching rates on Fe^{3+} concentration and independence of Fe^{2+} concentration was demonstrated. The activation energies for Fe^{3+} leaching of Cu, Zn, Ni, and Sn as individual metals were estimated to be 32.7, 24.3, 84.5, and 18.6 $kJ.mol^{-1}$, respectively. This implied that

the leaching mechanism for Cu and Zn was mixed-controlled, Ni was chemical reaction-controlled, while Sn was diffusion-limited. For the Fe^{3+} leaching of mixed metals, leaching kinetics were assumed to be mainly dominated by the leaching of Cu, such that the kinetic parameters estimated were of Cu. To this effect, the Fe^{3+} leaching kinetics for Cu in the presence of other metals (Zn, Ni, and Sn) remained 2^{nd} order with respect to Fe^{3+} with no dependency on the Fe^{2+} concentration. The leaching mechanism was diffusion-controlled, as characterised by apparent activation energy of 16.3 $kJ.mol^{-1}$.

The Fe^{3+} leaching of PCBs was successfully achieved across all three particle sizes of PCBs studied. However, at a reduced leaching rates with an increase in particle size of the PCBs samples. The average volumetric Fe^{3+} reduction rates were 3.82, 2.94, and 1.77 g Fe^{3+} $L^{-1}.h^{-1}$ at 37 °C for 1-minute pulverised, 20-second pulverised, and 0.5 cm^2 PCBs, respectively This was attributed to the degree of metal liberation in PCBs with respect to particle size (surface area). Successful metal leaching even at the largest particle size of 0.5 cm^2 presented promising results in achieving some metal liberation with limited size reduction. Optimisation of metal leaching at such particle size is an important area for further study.

More than 75% Cu, 85% Zn, 49% Ni, and 4% Sn was readily solubilised from 1-minutes pulverised PCBs over 40 min leaching period across the temperature range studied, 25 to 75 °C. The final pH reached was higher than observed in elementary metals. This was attributed to the alkaline nature of PCBs and the availability of other metals other than the four metals of interest in our study. The relative order of ferric leaching rates from 1-minute pulverised PCBs was Zn>Cu>Ni>Sn, comparable to the relative leaching rates of elementary metals, except for Sn. The ferric leaching kinetics showed 2^{nd} order dependence on Fe^{3+} and was independent of Fe^{2+} concentration. Owing to the dominance of copper as base metal within the PCBs, this was consistent with the findings from elementary metals. The apparent activation energy was estimated to be 26.8 $kJ.mol^{-1}$, suggesting that the leaching mechanism of Cu from PCBs was governed by mixed reaction mechanism. Similar to leaching of elementary metals, the acid leaching of PCBs was slow compared to the Fe^{3+} leaching but enabled substantial leaching over extended time. Some 72% Cu, 99% Zn, 73% Ni, 9% Sn was solubilised over 1440 min across the temperature range; however, Sn was inconsistent as it precipitates out of solution. The relative metal leaching rates was in the following order: Zn>Ni>Cu>Sn.

With comparable leaching behaviour of elementary metals to the PCBs, this study demonstrated that leaching of individual metals prior to leaching of complex PCBs system can provide insight into the expected leaching behaviour and associated leaching kinetics. The fundamental leaching data provided here, which is limited to date in the literature, particularly that of elementary metals, is critical to the modelling of leaching of PCBs, both for hydrometallurgy and biohydrometallurgy approaches. Insight into relative metal leaching rates, for example, is vital in the design of process flowsheets for metal recovery, and in determining the number of tanks required and their residence time. Of particular interest in this study is the rate of ferric iron regeneration required through biological ferrous iron oxidation to optimise the recovery of base metals from PCBs prior to leaching of precious metals.

4.5 References

Abdel-Aal, E. A. (2000). Kinetics of sulfuric acid leaching of low-grade zinc silicate ore. Hydrometallurgy 55 (3), 247–254. DOI: 10.1016/s0304-386x(00)00059-1.

Adhapure, N. N.; Dhakephalkar, P. K.; Dhakephalkar, A. P.; Tembhurkar, V. R.; Rajgure, A. V.; Deshmukh, A. M. (2014). Use of large pieces of printed circuit boards for bioleaching to avoid 'precipitate contamination problem' and to simplify overall metal recovery. MethodsX 1, 181–186. DOI: 10.1016/j.mex.2014.08.011.

Akcil, A.; Erust, C.; Gahan, C. S.; Ozgun, M.; Sahin, M.; Tuncuk, A. (2015). Precious metal recovery from waste printed circuit boards using cyanide and non-cyanide lixiviants-A review. Waste management 45, 258–271. DOI: 10.1016/j.wasman.2015.01.017.

Alarifi, A.; Deraz, N. M.; Shaban, S. (2009). Structural, morphological and magnetic properties of $NiFe_2O_4$ nano-particles. Journal of Alloys and Compounds 486 (1-2), 501–506. DOI: 10.1016/j.jallcom.2009.06.192.

Arshadi, M.; Yaghmaei, S.; Mousavi, S. M. (2018). Content evaluation of different waste PCBs to enhance basic metals recycling. Resources, Conservation and Recycling 139, 298–306. DOI: 10.1016/j.resconrec.2018.08.013.

Arslan, F.; Bulut, G.; Kangal, M. O.; Perek, K. T.; Gul, A.; Gurmen, S. (2004). Studies on leaching of massive rich copper ore in acidic ferric sulfate solutions. Scandinavian Journal of metallurgy 33 (1), 6–14. DOI: 10.1111/j.1600-0692.2004.00662.x.

Barakat, M. A. (1998). Recovery of lead, tin and indium from alloy wire scrap. Hydrometallurgy 49 (1-2), 63–73. DOI: 10.1016/S0304-386X(98)00003-6.

Bas, A. D.; Yazici, E. Y.; Deveci, H. (2012). Recovery of silver from X-ray film processing effluents by hydrogen peroxide treatment. Hydrometallurgy 121-124 (1), 22–27. DOI: 10.1016/j.hydromet.2012.04.011.

Battino, R. (1981). Solubility data series. Oxygen and ozone 7, 412.

Becci, A.; Amato, A.; Rodríguez Maroto, J. M.; Beolchini, F. (2019). Prediction model for Cu chemical leaching from printed circuit boards. Industrial & Engineering Chemistry Research 58 (45), 20585–20591. DOI: 10.1021/acs.iecr.9b04187.

Bilczuk, D.; Olvera, O. G.; Asselin, E. (2016). Kinetic study of the dissolution of metallic nickel in sulphuric acid solutions in the presence of different oxidants. The Canadian Journal of Chemical Engineering 94 (10), 1872–1879. DOI: 10.1002/cjce.22576.

Boyanov, B. S.; Konareva, V. V.; Kolev, N. K. (2004). Purification of zinc sulfate solutions from cobalt and nickel through activated cementation. Hydrometallurgy 73 (1-2), 163–168. DOI: 10.1016/j.hydromet.2003.09.002.

Bryan, C. G.; Joulian, C.; Spolaore, P.; El Achbouni, H.; Challan-Belval, S.; Morin, D.; d'Hugues, P. (2011). The efficiency of indigenous and designed consortia in bioleaching stirred tank reactors. Minerals Engineering 24 (11), 1149–1156. DOI: 10.1016/j.mineng.2011.03.014.

Casas, j. M.; Crisóstomo, G.; Cifuentes, l. (2013). Dissolution of metallic copper in aqueous sulphuric acid - ferric sulphate solutions. Canadian Metallurgical Quarterly 45 (3), 243–248. DOI: 10.1179/cmq.2006.45.3.243.

Castro, L. A.; Martins, A. H. (2009). Recovery of tin and copper by recycling of printed circuit boards from obsolete computers. Brazilian Journal of Chemical Engineering 26 (4), 649–657. DOI: 10.1590/S0104-66322009000400003.

Chen, Y.; Liang, S.; Xiao, K.; Hu, J.; Hou, H.; Liu, B. et al. (2021). A cost-effective strategy for metal recovery from waste printed circuit boards via crushing pretreatment combined with pyrolysis. Effects of particle size and pyrolysis temperature. Journal of Cleaner Production 280, 124505. DOI: 10.1016/j.jclepro.2020.124505.

Corrans, I. J.; Scholtz, M. T. (1976). A kinetic study of the leaching of pentlandite in acidic ferric sulphate solutions. Journal of the South African Institute of Mining and Metallurgy 76 (10), 403–411.

Crundwell, F. K. (1987). Kinetics and mechanism of the oxidative dissolution of a zinc sulphide concentrate in ferric sulphate solutions. Hydrometallurgy 19 (2), 227–242. DOI: 10.1016/0304-386X(87)90007-7.

Delichere, P.; Hugot-Le Goff, A.; Yu, N. (1986). Identification by in situ Raman spectroscopy of the films grown during the polarization of nickel in sulfuric solutions. Journal of The Electrochemical Society 133 (10), 2106–2107. DOI: 10.1149/1.2108349.

Demirkıran, N.; Ekmekyapar, A.; Künkül, A.; Baysar, A. (2007). A kinetic study of copper cementation with zinc in aqueous solutions. International Journal of Mineral Processing 82 (2), 80–85. DOI: 10.1016/j.minpro.2006.10.005.

Domic, E. M. (2007). A Review of the development and current status of copper bioleaching operations in Chile. 25 Years of Successful Commercial Implementation. In Douglas E. Rawlings, D. Barrie Johnson (Eds.): Biomining. Berlin, Heidelberg: Springer Berlin Heidelberg, 81–95.

Du Plessis, C. A.; Batty, J. D.; Dew, D. W. (2007). Commercial applications of thermophile bioleaching. In Douglas E. Rawlings, D. Barrie Johnson (Eds.): Biomining. Berlin, Heidelberg: Springer Berlin Heidelberg, 57–80.

Gu, W.; Bai, J.; Lu, L.; Zhuang, X.; Zhao, J.; Yuan, W. et al. (2019). Improved bioleaching efficiency of metals from waste printed circuit boards by mechanical activation. Waste Management 98, 21–28. DOI: 10.1016/j.wasman.2019.08.013.

Habashi, F. (2017). Principles of Extractive metallurgy (1st Ed.). Routledge. DOI: 10.1201/9780203742112.

Hao, J.; Wang, X.; Wang, Y.; Guo, F.; Wu, Y. (2022). Optimization, kinetic studies of tin leaching from waste printed circuit boards and selective tin recovery from its pregnant solution. Metals 12 (6), 954. DOI: 10.3390/met12060954.

Havlik, T.; Orac, D.; Petranikova, M.; Miskufova, A. (2011). Hydrometallurgical treatment of used printed circuit boards after thermal treatment. Waste Management 31 (7), 1542–1546. DOI: 10.1016/j.wasman.2011.02.012.

Hong, Y.; Valix, M. (2014). Bioleaching of electronic waste using acidophilic sulfur oxidising bacteria. Journal of Cleaner Production 65, 465–472. DOI: 10.1016/j.jclepro.2013.08.043.

Jadhav, U.; Hocheng, H. (2015). Hydrometallurgical recovery of metals from large printed circuit board pieces. Scientific Reports 5, 14574. DOI: 10.1038/srep14574.

Jeon, S.; Park, I.; Yoo, K.; Ryu, H. (2015). The effects of temperature and agitation speed on the leaching behaviors of tin and bismuth from spent lead free solder in nitric acid leach solution. Geosystem Engineering 18 (4), 213–218. DOI: 10.1080/12269328.2015.1048836.

Jha, M. K.; Choubey, P. K.; Jha, A. K.; Kumari, A.; Lee, J.-C.; Kumar, V.; Jeong, J. (2012). Leaching studies for tin recovery from waste e-scrap. Waste Management 32 (10), 1919–1925. DOI: 10.1016/j.wasman.2012.05.006.

Jha, M. K.; Lee, J.-C.; Kumari, A.; Choubey, P. K.; Kumar, V.; Jeong, J. (2011). Pressure leaching of metals from waste printed circuit boards using sulfuric acid. JOM 63 (8), 29–32. DOI: 10.1007/s11837-011-0133-z.

Kaskiala, T. (2002). Determination of oxygen solubility in aqueous sulphuric acid media. Minerals Engineering 15 (11), 853–857. DOI: 10.1016/S0892-6875(02)00089-4.

Kaya, M. (2016). Recovery of metals and nonmetals from electronic waste by physical and chemical recycling processes. Waste Management 57, 64–90. DOI: 10.1016/j.wasman.2016.08.004.

Lambert, F.; Gaydardzhiev, S.; Léonard, G.; Lewis, G.; Bareel, P.-F.; Bastin, D. (2015). Copper leaching from waste electric cables by biohydrometallurgy. Minerals Engineering 76 (1), 38–46. DOI: 10.1016/j.mineng.2014.12.029.

Li, H.; Wu, H.-z.; Xiao, G.-x. (2010). Effects of synthetic conditions on particle size and magnetic properties of $NiFe_2O_4$. Powder Technology 198 (1), 157–166. DOI: 10.1016/j.powtec.2009.11.005.

Li, Y.; Liu, Z.; Li, Q.; Liu, Z.; Zeng, L. (2011). Recovery of indium from used indium–tin oxide (ITO) targets. Hydrometallurgy 105 (3-4), 207–212. DOI: 10.1016/j.hydromet.2010.09.006.

Luo, P.; Sun, B.-b.; Li, J.-x.; Lu, M.-t.; Wang, L.-z.; Jiang, J.-c. (2019). Effect of Antimony (III) on tin recovery by cementation on zinc powder under alkaline conditions. International Journal of Electrochemical Science 14 (3), 2621–2630. DOI: 10.20964/2019.03.70.

Luo, W.; Feng, Q.; Ou, L.; Zhang, G.; Chen, Y. (2010). Kinetics of saprolitic laterite leaching by sulphuric acid at atmospheric pressure. Minerals Engineering 23 (6), 458–462. DOI: 10.1016/j.mineng.2009.10.006.

Markus, H.; Fugleberg, S.; Valtakari, D.; Salmi, T.; Murzin, D. Y.; Lahtinen, M. (2004). Kinetic modelling of a solid–liquid reaction. Reduction of ferric iron to ferrous iron with zinc sulphide. Chemical Engineering Science 59 (4), 919–930. DOI: 10.1016/j.ces.2003.10.022.

Moosakazemi, F.; Ghassa, S.; Mohammadi, M. R. T. (2019). Environmentally friendly hydrometallurgical recovery of tin and lead from waste printed circuit boards. Thermodynamic and kinetics studies. Journal of Cleaner Production 228, 185–196. DOI: 10.1016/j.jclepro.2019.04.024.

Nicolle, M; Lampi, M; Valkama, K; Karonen, J. (2015). Leaching of copper sulphides. In Copper Cobalt Africa, incorporating the 8th Southern African Base Metals Conference.

Ouchi, T; Forsberg, K; Azimi, G; Alam, S; Neelameggham, N. R.; Kim, Hojong et al. (2023). Recovery of Copper Metal from Discarded Printed Circuit Boards (PCBs) by Hydrometallurgical and Electrometallurgical Processes. Rare Metal Technology 2023. The Minerals, Metals & Materials Series. DOI: 10.1007/978-3-031-22761-5_12.

Palazhchenko, O. (2012). Pourbaix Diagrams at Elevated Temperatures A Study of Zinc and Tin. M.S. ProQuest Dissertations and Theses (MR90892), 137.

Quinet, P.; Proost, J.; van Lierde, A. (2005). Recovery of precious metals from electronic scrap by hydrometallurgical processing routes. Mining, Metallurgy & Exploration 22 (1), 17–22. DOI: 10.1007/BF03403191.

Rossi, G. (2001). The design of bioreactors. Hydrometallurgy 59 (2-3), 217–231. DOI: 10.1016/s0304-386x(00)00161-4.

Samadifard, N.; Devine, C.; Edwards, E.; Mahadevan, K.; Papangelakis, V. (2015). Ferric sulfate leaching of pyrrhotite tailings between 30 to 55 °C. Minerals 5 (4), 801–814. DOI: 10.3390/min5040526.

Scott, K.; Chen, X.; Atkinson, J. W.; Todd, M.; Armstrong, R. D. (1997). Electrochemical recycling of tin, lead and copper from stripping solution in the manufacture of circuit boards. Resources, Conservation and Recycling 20 (1), 43–55. DOI: 10.1016/S0921-3449(97)01198-1.

Souza, A. D.; Pina, P. S.; Leão, V. A.; Silva, C. A.; Siqueira, P. F. (2007). The leaching kinetics of a zinc sulphide concentrate in acid ferric sulphate. Hydrometallurgy 89 (1-2), 72–81. DOI: 10.1016/j.hydromet.2007.05.008.

Speight, J.; Lange, N.; Dean, J. (2005). Lange's handbook of chemistry. 16th ed. New York, N.Y., London: McGraw-HillSpeight, J.; Lange, N.; Dean, J. (McGraw-Hill standard handbooks).

Sulka, G. D.; Jaskuła, M. (2003). Study of the kinetics of silver ions cementation onto copper from sulphuric acid solution. Hydrometallurgy 70 (1-3), 185–196. DOI: 10.1016/S0304-386X(03)00080-X.

Tromans, D. (1998). Temperature and pressure dependent solubility of oxygen in water. A thermodynamic analysis. Hydrometallurgy 48 (3), 327–342. DOI: 10.1016/S0304-386X(98)00007-3.

Tuncuk, A.; Stazi, V.; Akcil, A.; Yazici, E. Y.; Deveci, H. (2012). Aqueous metal recovery techniques from e-scrap. Hydrometallurgy in recycling. Minerals Engineering 25 (1), 28–37. DOI: 10.1016/j.mineng.2011.09.019.

Udayakumar, S.; Razak, M. I. B. A.; Ismail, S. (2022). Recovering valuable metals from waste printed circuit boards (WPCB). A short review. Materials Today: Proceedings 66 (5), 3062–3070. DOI: 10.1016/j.matpr.2022.07.364.

van Yken, J.; Cheng, K. Y.; Boxall, N. J.; Nikoloski, A. N.; Moheimani, N.; Valix, M. et al. (2020). Potential of metals leaching from printed circuit boards with biological and chemical lixiviants. Hydrometallurgy 196, 105433. DOI: 10.1016/j.hydromet.2020.105433.

Veit, H.M., Bernardes, A.M. (2015). Electronic Waste: Generation and Management. In Electronic Waste, Veit, H., Moura Bernardes, A. (eds): Topics in Mining, Metallurgy and Materials Engineering. Springer, Cham. DOi: 10.1007/978-3-319-15714-6_2

Verbaan, B.; Crundwell, F. K. (1986). An electrochemical model for the leaching of a sphalerite concentrate. Hydrometallurgy 16 (3), 345–359. DOI: 10.1016/0304-386X(86)90009-5.

Wu, Z.; Yuan, W.; Li, J.; Wang, X.; Liu, L.; Wang, J. (2017). A critical review on the recycling of copper and precious metals from waste printed circuit boards using hydrometallurgy. Frontiers of Environmental Science & Engineering 11 (5), 258. DOI: 10.1007/s11783-017-0995-6.

Xiang, Y.; Wu, P.; Zhu, N.; Zhang, T.; Liu, W.; Wu, J.; Li, P. (2010). Bioleaching of copper from waste printed circuit boards by bacterial consortium enriched from acid mine drainage. Journal of Hazardous Materials 184 (1-3), 812–818. DOI: 10.1016/j.jhazmat.2010.08.113.

Yang, C.; Li, J.; Tan, Q.; Liu, L.; Dong, Q. (2017). Green process of metal recycling. Coprocessing waste printed circuit boards and spent tin stripping solution. ACS Sustainable Chemistry & Engineering 5 (4), 3524–3534. DOI: 10.1021/acssuschemeng.7b00245.

Yang, T.; Xu, Z.; Wen, J.; Yang, L. (2009). Factors influencing bioleaching copper from waste printed circuit boards by *Acidithiobacillus ferrooxidans*. Hydrometallurgy 97 (1-2), 29–32. DOI: 10.1016/j.hydromet.2008.12.011.

Yazici, E. Y.; Deveci, H. (2014). Ferric sulphate leaching of metals from waste printed circuit boards. International Journal of Mineral Processing 133 (4), 39–45. DOI: 10.1016/j.minpro.2014.09.015.

Zhang, X.; Guan, J.; Guo, Y.; Yan, X.; Yuan, H.; Xu, J. et al. (2015). Selective desoldering separation of Tin–Lead alloy for dismantling of electronic components from printed circuit boards. ACS Sustainable Chemistry & Engineering 3 (8), 1696–1700. DOI: 10.1021/acssuschemeng.5b00136.

Zhu, N.; Xiang, Y.; Zhang, T.; Wu, P.; Dang, Z.; Li, P.; Wu, J. (2011). Bioleaching of metal concentrates of waste printed circuit boards by mixed culture of acidophilic bacteria. Journal of Hazardous Materials 192 (2), 614–619. DOI: 10.1016/j.jhazmat.2011.05.062.

CHAPTER 5

5 Exploring microbial adaptation of immobilised acidophilic cultures to improve microbial oxidation rates and copper tolerance in E-waste bioleaching

In the bioleaching of base metals from printed circuit boards (PCBs), microbial Fe^{2+} oxidation rate is the rate-determining step as it is the slower reaction relative to the Fe^{3+} reduction rate. This is exacerbated by inhibition of microbial culture by accumulated metal ions and dissolved non-metallic components of the PCBs within the bioleaching system, leading to a reduction in the specific ferrous iron oxidation rate and thereby the volumetric rate. This results in longer bioleaching durations, lower metal extraction, and ultimately, limited benefits of the microbial cultures in the system. To overcome these limitations, an improvement in the volumetric rate of microbial Fe^{2+} oxidation is key to improving bioleaching efficiency. This can be achieved by maintaining the specific Fe^{2+} oxidation rate through minimising inhibition of microbial culture as well as increasing the concentration of the active biomass as the volumetric Fe^{2+} oxidation rate is the product of the active cell concentration and the specific Fe^{2+} oxidation rate.

This study investigated the benefits of adaptation of the microbial culture to Cu^{2+} as Cu is a predominant metal in PCBs prior to bioleaching to minimise inhibition of microbial culture. Immobilisation of the microbial culture on polyurethane foam as biomass support particles (PUF-BSPs) is also explored in minimising inhibition and improving Fe^{2+} oxidation rates. It further investigated the potential compounded benefits of these two techniques in improving metal tolerance and Fe^{2+} oxidation. The outcome of this study was to provide an improved culture performance in the presence of increased concentration of Cu^{2+} as an inhibitory metal.

Authors' contributions

The primary supervisor Sue Harrison, and co-supervisors Athanasios Kotsiopoulos, and Elaine Govender-Opitz conceptualised the experimental approach with the primary author. The primary author Musa Maluleke performed the experiments, and data analysis, guided by Sue Harrison, Athanasios Kotsiopoulos, and Elaine Govender-Opitz, and wrote the manuscript. The draft manuscript was critically reviewed and edited by Elaine Govender-Opitz, Athanasios Kotsiopoulos, and Sue Harrison. The final draft was approved by the primary supervisor as a corresponding author.

Journal title: Exploring microbial adaptation of immobilised acidophilic cultures to improve microbial oxidation rates and copper tolerance in E-waste bioleaching

Musa D. Maluleke, Athanasios Kotsiopoulos, Elaine Govender-Opitz, and Susan T.L. Harrison

Centre for Bioprocess Engineering Research (CeBER), Department of Chemical Engineering, University of Cape Town, Rondebosch, Cape Town 7700, South Africa.

Minerals Engineering (https://doi.org/10.1016/j.mineng.2023.108560)

Abstract

The rate of ferric iron regeneration by microbial oxidation is the rate determining step in the bioleaching of printed circuit boards (PCBs). Therefore, improvement of the volumetric rate of ferric iron formation is key for the overall bioleaching efficiency. The volumetric rate is impacted by both the specific rate and the biomass concentration. Limiting the exposure of the bioleaching microorganisms to accumulated toxic metal ions in solution, as well as the presence of inhibiting material components in PCBs through biofilm formation and immobilisation, as well as their adaptation to these inhibitors, is proposed to mitigate against decrease in specific rate while biomass retention by immobilisation is expected to positively impact volumetric rate. In this study, a mixed mesophilic culture, consisting of *Leptospirillum (L.) ferriphilum*, *Acidithiobacillus (At.) caldus*, *Acidiplasma (Ap.) cupricumulans* as dominant species was immobilised on polyurethane foam (PUF) and adapted to 6.0 g/L Cu^{2+}. The rate of microbial ferrous iron oxidation by the immobilised culture was compared to that of planktonic cultures. Further, the performance of both the planktonic and immobilised Cu-adapted cultures (6.0 g/L of Cu^{2+}) were compared with non-adapted planktonic and immobilised cells in the presence of increasing Cu^{2+} concentrations (0 – 50 g/L Cu^{2+}).

Both the Cu-adapted planktonic cells and the non-adapted immobilised cells demonstrated improved tolerance to Cu^{2+} stress relative to non-adapted planktonic cells. The Cu-adapted planktonic cells showed higher volumetric ferrous iron oxidation rates (0.0359 ± 0.0023 g $Fe^{2+}.L^{-1}.h^{-1}$ at 22 g/L Cu^{2+}) than the non-adapted immobilised cells (0.0331 ± 0.0021 g $Fe^{2+}.L^{-1}.h^{-1}$) in the presence of Cu^{2+} concentrations exceeding 6 g/L. The Cu-adapted immobilised cells exhibited higher tolerance to Cu^{2+} stress and higher oxidation kinetics (0.0622 ± 0.0064 g $Fe^{2+}.L^{-1}.h^{-1}$) than the Cu-adapted planktonic and non-adapted immobilised cells. This study provides a novel approach for improving culture performance and minimising the inhibitory effect of Cu^{2+} ion on *L. ferriphilum* dominated cultures. High microbial activity and metal tolerance of Cu-adapted immobilised cells presents an opportunity for immobilised microbial systems to be used both in bioleaching of e-waste streams, such as PCBs, and in bioleaching of mineral concentrates, ores and wastes with Cu^{2+}-rich leachates.

5.1 Introduction

A biohydrometallurgical approach for the extraction of base metals of value from printed circuit boards (PCBs) is considered the least environmentally impactful technology as compared to the conventional pyrometallurgical and hydrometallurgical approaches (Tuncuk

et al. 2012a; Priya and Hait 2018). Metal dissolution is promoted by the oxidation of metals embedded on the PCBs using ferric iron (Fe^{3+}) as the primary oxidising agent in acidic environments. During this process, the Fe^{3+} oxidant is reduced to ferrous iron (Fe^{2+}) (Eq. 5-1). The acidophilic iron-oxidising microorganisms present accelerate the oxidation of Fe^{2+} back to Fe^{3+} (Eq. 5-2), thereby enhancing the extraction of base metals from PCBs. Continuous regeneration of the primary oxidant reduces reagent costs and results in considerably lower effluent volumes for disposal, thereby minimising the environmental burden. A key to the success of this approach is to achieve a sufficient rate of ferric iron regeneration, to balance the rapid rates of ferric leaching.

$$M^0(Cu^0) + 2Fe^{3+} \rightarrow M^{2+}(Cu^{2+}) + 2Fe^{2+} \qquad \textit{Eq. 5-1}$$

$$2Fe^{2+} + 0.5O_2 + 2H^+ \xrightarrow{microorganisms} 2Fe^{3+} + H_2O \qquad \textit{Eq. 5-2}$$

While bioleaching is a promising technology for PCB pre-treatment prior to recover of precious metals, one of the major challenges is the inhibition due to the accumulation of inhibitory levels of metal ions and other constituents of PCBs within the system. These decrease Fe^{2+} to Fe^{3+} turnover rates, affecting metal extraction rates adversely (Liang et al. 2010; Akcil et al. 2015a).

Inhibition of microbial growth at PCB concentrations greater than 10 g/L was observed in the study by (Brandl et al. 2001) where the authors investigated the bioleaching of PCBs using a mixed mesophilic culture dominated by *Acidithiobacillus (At.) thiooxidans* and *At. ferrooxidans*. As a result of these findings, Brandl et al. (2001) suggested two processing options that may reduce the impact of metal toxicity on microbial growth and activity: (i) microbial adaptation to high metal ion concentrations and, (ii) a two-step bioleaching process in which the metal leaching and ferric iron regeneration processes are separated. Microbial adaptation has been reported through acclimatisation of microbial culture to potential inhibitory metals prior to contact with the metal-rich solids. Microbial adaptation is by far the most commonly used method in mitigating microbial inhibition in PCB bioleaching (Ilyas et al. 2010; Arshadi and Mousavi 2014; Xia et al. 2017; Baniasadi et al. 2019; Tapia et al. 2022) owing to metal resistance being largely plasmid-borne in acidophilic biooxidation microorganisms. Adaptation is achieved by repeated sub-culturing of the microbial culture and gradual increase of the potential inhibitory metal ion or PCB solid loading (weight of solid PCB per volume of growth medium). Consequently, microorganisms attain tolerance to the inhibitory metal ions through their natural intra- and extracellular detoxification mechanisms (Bruins et al. 2000; Dopson et al. 2003; Xia et al. 2008; Valix 2017; Zhang et al. 2023). The benefits of microbial adaptation prior to bioleaching are recognised in the bioleaching of mineral sulfides (Dopson et al. 2003; Watling 2006; Xia et al. 2008; Kaksonen et al. 2018; Nkuna et al. 2022; Africa et al. 2013; Govender et al. 2015; Ngoma et al. 2018).

While adaptation has the potential to allow the specific ferric regeneration rates to be maintained at increased metal concentrations, the volumetric ferric regeneration rate has the

potential to be increased by increasing the microbial cell concentration by retaining cells in the reactor by immobilisation onto a solid phase. The advantages of using immobilised microbial systems over planktonic cultures for the bioleaching of mineral sulfides have been well documented (Nemati and Webb 1996; Rohwerder et al. 2003; Sand and Gehrke 2006; Kaksonen et al. 2018). These include the higher biomass accumulation and the ability to separate the solution from the microbial phase easily. Further, where a microbial biofilm forms, the chemical stratification from the solution phase to the cell membrane may occur (Groboillot et al. 1994; Sand and Gehrke 2006; González et al. 2013; Africa 2017), allowing the microbial biofilm to act as a diffusion barrier against toxic environments (Bruins et al. 2000; Dopson et al. 2003; Rohwerder et al. 2003; González et al. 2013). It is postulated that this improves microbial resistance to inhibitory metals. Microbial immobilisation techniques include encapsulation, covalent bonding, adsorption, gel entrapment, cross-linking, and adsorption/attachment (Guisan et al. 2020; Elakkiya et al. 2016). Depending on the technique adopted, a variety of support matrices may be used, including glass beads, ceramic saddles and rings, sand, wood chips, plastic supports and polyurethane foam (Guoqiang et al. 1992; Halfmeier 1993; Gómez et al. 2000; Guisan et al. 2020). On using polyurethane foam biomass support particles (BSP), there is a natural tendency of microbial cells to become entrapped within the foam matrix or to attach to solid surfaces, thereby colonising the BSPs (Zobell 1943b; Nemati and Webb 1996; Sand and Gehrke 2006; Suzana et al. 2013). This facilitates high biomass concentrations.

In this study, we bring together the advantages of microbial adaptation to copper and microbial immobilisation on polyurethane BSPs to maximise the rate of regeneration of the primary Fe^{3+} oxidant for bioleaching of PCBs using a mixed mesophilic microbial culture. Adaptation is limited to Cu^{2+} as predominant base metal in PCBs (Yang et al. 2014; Yang et al. 2009; Xiang et al. 2010; Tuncuk et al. 2012a; Tapia et al. 2022; Hubau et al. 2020; Bryan et al. 2015; Ilyas et al. 2010; Bizzo et al. 2014). While trace amounts of Cu^{2+} are essential for microbial growth, at elevated concentrations, Cu^{2+} can be inhibitory (Das et al. 1997; Xia et al. 2017; Bryan et al. 2015; Tapia et al. 2022). The impact of immobilisation and adaptation on performance in the presence of increasing Cu^{2+} concentrations are explored separately and in combination. With expected high Cu^{2+} concentrations in PCB bioleaching systems, overcoming its inhibitory effects on e-waste bioleaching is vital in process optimisation.

5.2 Experimental

5.2.1 Microbial culture and growth

A mixed mesophilic culture consisting of *Leptospirillum (L.) ferriphilum, Acidiplasma (Ap,) cupricumulans,* and *Acidithiobacillus* (At.) *caldus* as dominant species and grown on pyrite concentrate at 37 °C, served as the inoculum for experiments on both the immobilised and planktonic systems. Autotrophic basal salts (ABS) medium, composed of 7.5 g/L $(NH_4)_2SO_4$, 7.5 g/L Na_2SO_4, 2.5 g/L KCl, 25 g/L $MgSO_4.7H_2O$, 2.5 g/L KH_2PO_4, and 0.7 g/L $Ca(NO_3)_2.4H_2O$ and supplemented with 1.0 mL of trace element solution (Johnson et al. 2008), was used. The medium was prepared using acidified deionized water (pH 1.4, 96% H_2SO_4 and included 5.0 g/L Fe^{2+} ($FeSO_4.7H_2O$),) as the primary substrate. Concentration of cells was determined by

direct microscope cell counting using a Thoma counting chamber (depth of chamber: 0.02 mm and area: 0.0025 mm^2) using an Olympus BX40 phase contract microscope at 1000x magnification. Microbial speciation of the inoculum was determined using quantitative real time polymerase chain reaction (qPCR) through the procedures described in (Liu et al. 2006; Tupikina et al. 2013; Tupikina et al. 2014; Ngoma et al. 2015). Briefly, following the Genomic DNA (gDNA) extraction from the samples, the gDNA was analysed against 16S rRNA universal and species-specific primers (Tupikina et al. 2013; Ngoma et al. 2015). The qPCR results showed that the inoculum was characterised by 38% *L. ferriphilum*, 45% *At. caldus*, 15% *Ap. cupricumulans* with trace presence of *Ferroplasma*, *Thermoplasmatales* and *Cuniculiplasma* species observed.

5.2.2 Microbial immobilisation and adaptation

Autoclaved polyurethane foam (PUF), cut into 1.0 cm^3 cubes, was chosen as the biomass support particle for this study. Microbial immobilisation was carried out by placing 100 sterile, PUF cubes in a 1 L Erlenmeyer flask containing 400 mL ABS medium with 5.0 g/L Fe^{2+} and 5.0 g/L Fe^{3+}, at pH 1.4, and inoculating it with 10% v/v of the mixed mesophilic culture. Fe^{3+} was supplemented to elevate the initial redox potential to approximately 450 mV as microbial activity is encouraged at and above this initial redox potential. The culture was maintained at a constant temperature of 37 °C in a rotary shaking incubator at 120 rpm. Changes in solution pH, redox potential, Fe^{2+} and Fe^{3+} concentrations were monitored daily. Once the Fe^{2+} was depleted, 50% of the spent medium was replenished with fresh ABS medium containing 5.0 g/L Fe^{2+}. The culture was maintained over two months with periodic sub-culturing to replenish the substrate. Adaptation of immobilised cells to cupric ions (Cu^{2+}) was achieved by gradually increasing the concentration of Cu^{2+} ($CuSO_4.5H_2O$) over a two-month period, by 0.5 g/L Cu^{2+} at each subculturing, until a total concentration of 6.0 g/L Cu was obtained.

5.2.3 Scanning Electron Microscopy

Colonisation of the PUF support by the microbial culture was visually confirmed by scanning electron microscopy (SEM). Colonised biomass supports were fixed in 2.5% (v/v) glutaraldehyde for 8 to 24 h, at 4°C. The samples were then rinsed with sterile distilled water before being dehydrated through a series of alcohol washes using 30, 50, 90, 95, and 100% v/v (analytical grade ethanol), for 10 minutes at each step. Samples were dried further using hexamethyldisilazane (HDMS) and mounted onto an SEM stub covered with carbon glue. The stub was sputter-coated with carbon and visualised at various magnifications using the scanning electron microscope (FEI NOVA NANOSEM 230 with a field emission gun or Tescan MIRA3 with a Confocal Raman Imaging Extension).

5.2.4 Microbial activity tests at various inoculum sizes

Microbial activity tests were performed to assess the Fe^{2+} oxidation capacity of the microbial systems under investigation, namely, the non- and Cu-adapted planktonic cells as well as the non- and Cu-adapted immobilised cells. To determine the effect of inoculum size on the microbial Fe^{2+} oxidation rate in immobilised and planktonic systems, two sets of tests were prepared in 250 mL Erlenmeyer flasks, each containing 100 mL ABS medium (pH 1.4) with 5.0

g/L Fe^{2+} and 5.0 g/L Fe^{3+}. One set of tests was inoculated with microbially colonised PUF BSPs (3 – 9 cubes in each flask). The second set of tests was inoculated with the planktonic cells using an inoculum size between 0.2 - 20% v/v (10^6–10^8 cells/mL). The tests were maintained at 37 °C in a rotary shaking incubator at 120 rpm. Over the duration of the experiments, the variation in pH (867 Metrohm meter), redox potential (867 Metrohm meter, Ag/AgCl reference electrode), and Fe^{3+} and Fe^{2+} concentrations were monitored. Fe^{3+} and total iron (Fe^{tot}) concentrations were determined colorimetrically at 340 nm using the ferric chloride assay (Govender et al., 2012), selected owing to the limited effect of Cu^{2+} on the assay whereas Cu^{2+} interferes with other colorimetric Fe assays. The Fe^{2+} concentration was determined by the difference between Fe^{tot} and Fe^{3+} concentrations (Govender et al., 2012). All experiments were run in triplicate with the average measured parameters reported.

5.2.5 Microbial tolerance to Cu^{2+}

Microbial tolerance of the immobilised and planktonic cells to Cu^{2+} stress was investigated by comparing the Fe^{2+} oxidation rate of each microbial system, in the absence and presence of the inhibiting metal. Once the 250 mL Erlenmeyer flasks were set up, each containing 100 mL ABS medium (pH 1.4), 5.0 g/L Fe^{2+} and 5.0 Fe^{3+}, the Cu^{2+} concentrations ($CuSO_4.5H_2O$) in each flask were varied between 1.0 g/L and 50.0 g/L. Each test was performed in triplicate, with all flasks maintained at 37 °C in a rotary shaking incubator at 120 rpm. The microbial activity of both non- and Cu-adapted immobilised and planktonic cells was periodically monitored using the same procedures outlined in Section 5.2.4.

5.3 Results and discussion

5.3.1 Verification of biomass accumulation and immobilisation using Scanning Electron Microscopy (SEM)

The use of PUF as a biomass support particle is known to result in the high retention of cells in bioleaching systems (Nemati & Webb, 1996). Given the large specific area of the PUF-BSPs and the accumulation of microorganisms on these surfaces and within the interstitial spaces, high cell concentrations with their associated metabolic activity and high rates of microbial Fe^{2+} oxidation are commonly observed (Nemati & Webb, 1996). As microbial attachment is coupled with subsequent biofilm formation, a microbial immobilisation system presents an opportunity to develop diffusional barriers that potentially insulate microbial activity in metal-rich environments. Contributing to this protection, micro-conditions within the interstitial zones within the PUF-BSP are typically created.

After biomass growth and immobilisation onto the PUF-BSP over a two month period, microbial immobilisation and biofilm formation was confirmed by SEM using various magnifications (as demonstrated by the size bars: 20, 5, and 2 µm). Micrographs of the colonised PUF BSP (Figure 5-1D, E, & F) are compared to those of the control or non-colonised PUF (Figure 5-1A, B, & C).

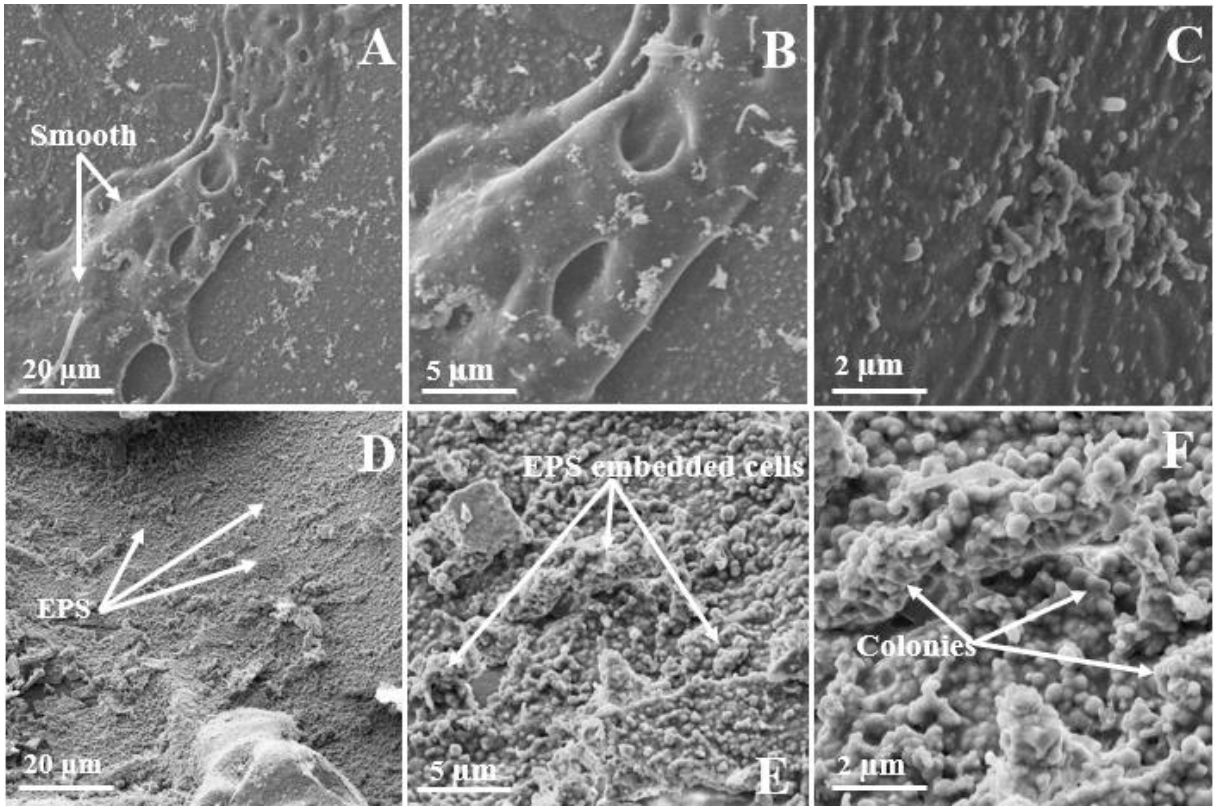

Figure 5-1 Scanning electron microscopy micrographs of non-colonised PUFs (**A**, **B**, & **C**) and colonised PUFs (**D**, **E**, & **F**) at various magnifications, i.e., demonstrated by the size bars 20, 5, and 2 µm.

Across multiple images of the control PUF support particles (with examples given in Figure 5-1A, B, & C), the surfaces showed less irregularities and were smoother than the colonised PUF-BSPs (Figure 5-1D, E & F), showing few cells on the surface, as expected. At the highest magnification (Figure 5-1C), some cell-like structures were observed on the surface of non-colonised PUF. This may have been due to residual microbial content of the BSPs prior to inoculation. A similar observed smooth surface of the PUF in the absence of microorganisms was also reported by (Hessler et al. 2017) when they visually analysed PUF surfaces using SEM prior to microbial colonisation of sulfate-reducing bacteria and after microbial detachment experiments. In Figure 5-1D-F, observing the inoculated BSPs, the colonised surface appeared fully covered with microorganisms embedded within extracellular polymeric substances (EPS). A clearly developed biofilm was observed on the colonised PUF-BSPs as the surface was increasingly magnified (Figure 5-1E & F). The SEM micrographs of non- and Cu-adapted colonised PUF were found to exhibit similar surface characteristics. A fully colonised surface of PUF-BSPs was also reported by (Nemati and Webb 1996) who immobilised *At. ferrooxidans* onto PUF-BSPs and studied the effect of the Fe^{2+} concentration on Fe^{2+} oxidation in a packed-bed column.

5.3.2 Microbial activity tests at various inoculum sizes

Microbial activity tests were performed to assess the correlation between microbial activity and the number of fully colonised biomass support particles used as inoculum i.e. 3, 6 or 9

microbial colonised PUF particles. Comparatively, parallel microbial Fe^{2+} oxidation experiments were performed with planktonic cultures, with inoculum sizes of 0.2, 2.0, 10, and 20% by volume (v/v), equivalent to 8.37×10^6 to 2.63×10^8 cells/mL. These results are compared in Figure 5-2.

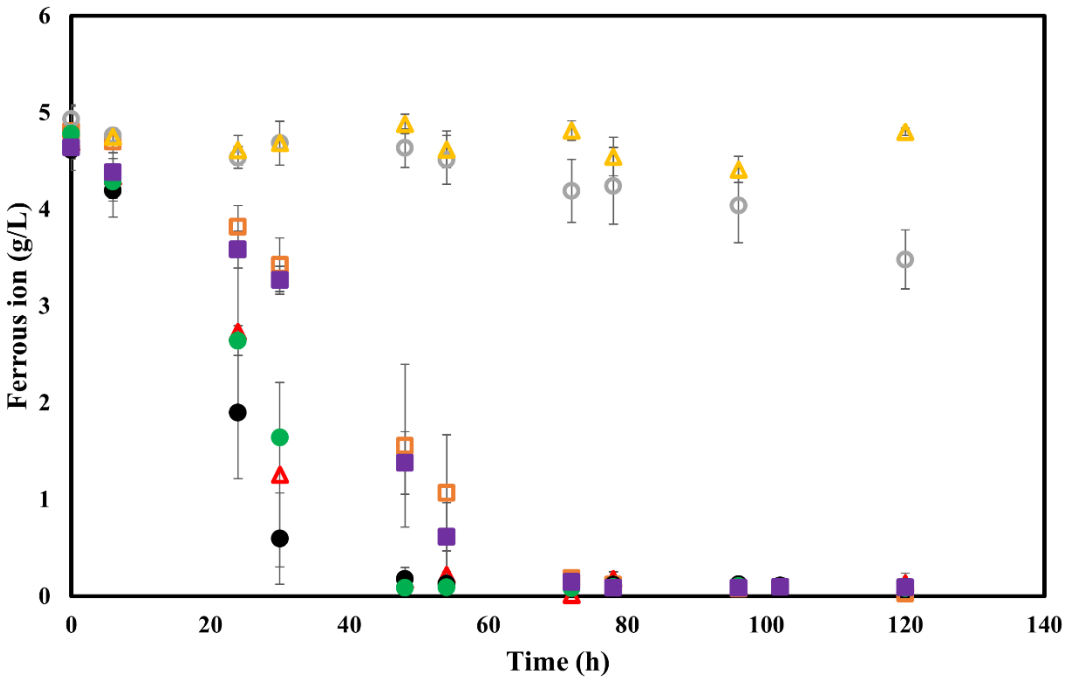

Figure 5-2 Ferrous iron utilisation at various inoculum sizes of planktonic cells (PC), i.e., 0.2 (△), 2 (○), 10 (□), and 20% v/v (△) and immobilised cells (IC), i.e., 3 (■), 6 (●), and 9 (●) PUF units of biomass support particles. Error bars represent standard deviation, n = 3.

From Figure 5-2, it was observed that the rates of microbial Fe^{2+} oxidation were dependent on the number of PUF support particles added. Complete microbial oxidation of ferrous iron was achieved within 48 h for the tests with 6 and 9 PUFs support particles, at a similar Fe^{2+} volumetric oxidation rates of 0.1178 ± 0.0366 (mean ± standard deviation, *n = 3*) and 0.1138 ± 0.0300 g $Fe^{2+}.L^{-1}.h^{-1}$, respectively. The test with 3 PUFs support particles only achieved complete ferrous iron oxidation after 78 h, at a lower volumetric rate of 0.0651 ± 0.0012 g $Fe^{2+}.L^{-1}.h^{-1}$ relative to the experiment with 6- and 9-PUFs.

For the planktonic tests with 10 and 20% v/v inoculum (3.16×10^7 and 2.63×10^8 cells per ml on inoculation), complete oxidation of ferrous iron was achieved within 78 and 48 h, at a volumetric rate of 0.0637 ± 0.0029 and 0.0814 ± 0.0166 g $Fe^{2+}.L^{-1}.h^{-1}$, respectively. The test with the 10% v/v inoculum size, 3.16×10^7 cells/mL, exhibited a similar volumetric Fe^{2+} oxidation rate to the tests with 3-PUFs (Figure 5-2). Their similarity was further confirmed statistically by performing a one-way ANOVA test. The null hypothesis stated that there is no difference in the volumetric Fe^{2+} oxidation rates between 3-PUFs and the 10% v/v planktonic

inoculum. The calculated F value of 0.448 was lower than F-critical of 7.71, while the p-value was 0.540. Hence the null hypothesis is upheld, indicating no significant difference in Fe^{2+} oxidation rate between these inocula. At 20% v/v, Fe^{2+} oxidation rate was increased by 27% relative to tests with a 10% v/v planktonic inoculum. In the immobilised system, the Fe^{2+}volumetric rate increased by 82% in the test with 3-PUFs to 6-PUFs. This was attributed to the higher cell densities since the volumetric ferrous iron oxidation rate is expected to be the product of the specific rate and cell concentration. However, the lack of proportional increase in rate with biomass concentration suggests that some further limitation may occur. (Chen and Cheng 2019) have demonstrated the increase in rate and extent of metal solubilisation during bioleaching of sewage sludge by a thermophilic culture dominated by *Sulfobacillus acidophilus*, again without proportional correlation to microbial cell concentration. Metal dissolution increased from 38 to 60% when inoculum size was increased from 5 to 20% v/v (Chen and Cheng 2019). Similar improvements in bioleaching efficiency with increased inoculum size are reported elsewhere (Yang et al. 2009; Bas et al. 2013). Tests with lower inoculum sizes (0.2 and 2.0% v/v) displayed reduced performance due to low cell numbers with limited substrate utilisation rates. Only about 30% of the initially added Fe^{2+} was oxidized with the 2% v/v inoculum size over a 120 h period (Figure 5-2).

Here, a comparison between immobilised cells and planktonic cells was based on microbial activity (calculated Fe^{2+} volumetric rates) rather than cell numbers, due to the difficulties encountered in quantifying immobilised cells. Despite successful detachment of the cells from the support particles (BSPs), cells remained embedded in clumps of EPS when visualised under the microscope, precluding their effective counting. Similar difficulties in quantifying immobilised cells following extended periods of colonisation have also been reported by Makaula (2019) who investigated microbial growth and activity over 30 days, during progressive colonisation of a mixed mesophilic culture consisting of *L. ferriphilum*, *At. caldus*, *Ferroplasma acidiphilum*, and *Acidiplasma cupricumulans*, on glass beads coated with pyrite waste rock. Microbial growth and activity progressed with time, with microbial activity significantly increased with the development of the EPS, from day 20. While total microscope counts were readily achieved in the early colonisation phase, following clumping of EPS-bound cells from day 20 total cell counts could not be quantified with accuracy (Makaula 2019).

5.3.3 Microbial activity test in the presence of Cu^{2+} stress

Copper is the dominant metal in PCBs and more than 90% Cu^{2+} can be readily leached by the lixiviant (Fe^{3+}), regenerated by microbial Fe^{2+} oxidation (Karwowska et al., 2014; Liang et al., 2016; Patel & Lakshmi, 2021; Wang et al., 2018). Owing to high Cu^{2+} concentrations in PCBs leachates, the inhibitory effect of Cu^{2+} on microbial Fe^{2+} oxidation by both non- and Cu-adapted microbial cultures was investigated. The Cu^{2+} concentrations were selected to represent the expected Cu^{2+} in leachates based on the solid loading of PCBs between 1 – 45% (w/v), with complete leaching, corresponding to approximately 1.0 – 50.0 g/L Cu^{2+}, as per our characterised PCBs samples. Given the similar microbial oxidation performance and comparable ferrous iron oxidation rates for Fe^{2+} oxidation tests inoculated with 10% v/v planktonic inoculum and with 3 colonised PUF-BSPs (Section 5.3.2), these were considered as

comparable inoculum size for microbial activity tests in the presence of increasing Cu^{2+} concentrations.

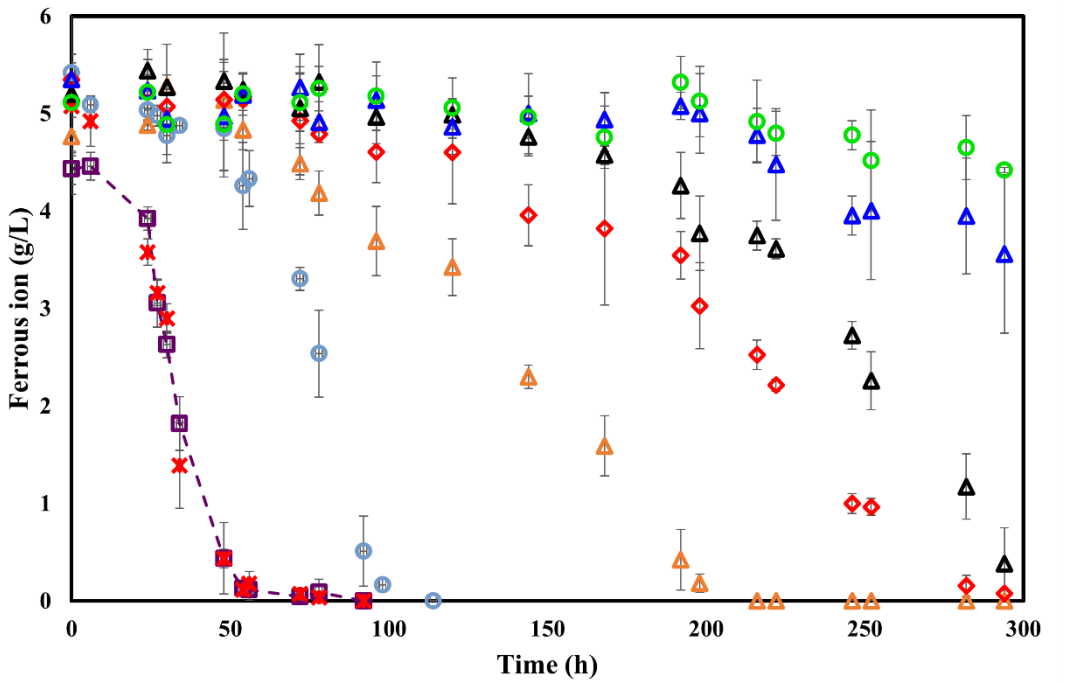

Figure 5-3 Ferrous iron oxidation over time by non-adapted planktonic cells (NA-PC) subjected to various Cu2+ concentrations, 0 (–■–), 1.0 (✖), 6.0 (○), 11.0 (△), 22.0 (◆), 33.0 (▲),44.0 (▲) and 50.0 g/L (●) for non-adapted planktonic cells. Error bars represent standard deviation, n = 3.

Microbial Fe^{2+} oxidation as a function of time by non-adapted planktonic cells in the presence of increasing Cu^{2+} stress is shown in Figure 5-3. This provides the baseline for comparison in assessing the role of pre-adaptation and immobilization in reducing Cu^{2+} inhibition, discussed below. No inhibition of microbial metabolic activity was observed at 1.0 g/L Cu. Cu^{2+} inhibition was observed from 6.0 g/L Cu^{2+}, indicated by 1.5-fold increase lag period preceding microbial oxidation relative to cells subjected to 0 and 1.0 g/L Cu^{2+} (Figure 5-3). The lag phase increased by 2.25-fold at 11.0 g/L Cu^{2+} and the volumetric Fe^{2+} oxidation rate was reduced to 0.0335 ± 0.0003 g $Fe^{2+}.L^{-1}.h^{-1}$, relative to 0.0768 ± 0.0096 g $Fe^{2+}.L^{-1}.h^{-1}$ in the absence of Cu^{2+} stress, resulting in 32% oxidation of the 5.0 g/L Fe^{2+} added within 120 h, compared to the complete ferrous iron oxidation within the same period at 6.0 g/L Cu^{2+} and below. Complete ferrous iron oxidation was achieved at 200 h by cells subjected to 11.0 g/L Cu^{2+}, while only 40% Fe^{2+} was oxidised in the presence of 22 g/L Cu^{2+} within 200 h. At 22 g/L Cu^{2+} stress, the volumetric Fe^{2+} oxidation rate was reduced by 69% (0.0237 ± 0.0016 g $Fe^{2+}.L^{-1}.h^{-1}$) relative to the control while only 50% Fe^{2+} was oxidised within 200 h. This was evident that non-adapted planktonic cells were susceptible to the Cu^{2+} inhibitory effect as their microbial activity was compromised by

Cu^{2+} with increasing severity as the Cu^{2+} concentrations increased (Figure 5-3). Although the culture performance was compromised, as evident by the prolonged lag phases, the microbial cultures appeared to adapt with time as evidenced by the positive, but reduced, volumetric rates with increased Cu^{2+} concentration. Complete microbial Fe^{2+} oxidation was achieved at approximately 300 h at 33.0 g/L Cu^{2+} whereas only 33 and 14% oxidation was achieved in the same period at 44 and 50 g/L Cu^{2+}, respectively. Following microbial adaptation, complete Fe^{2+} oxidation was achieved at 446 and 486 h (data not shown), with Fe^{2+} oxidation rates reduced by about 77-78%, i.e., 0.0180 ± 0.0013 and 0.0171 ± 0.0006 g $Fe^{2+}.L^{-1}.h^{-1}$, at 44.0 and 50.0 g/L Cu^{2+}, respectively. This severe inhibitory effect observed at high Cu^{2+} concentration is consistent with that reported by (Das et al. 1997; Bryan et al. 2015; Tapia et al. 2022; Kinnunen and Puhakka 2005).

Similar results were demonstrated by (Tapia et al. 2022) in their microbial activity tests in the presence of Cu^{2+} stress from 10.5 to 38.0 g/L Cu^{2+}. The authors reported that planktonic mixed mesophilic culture dominated by *Tissierella*, *Acidiphilium*, and *Leptospirillum* achieved maximum growth rate at 10.5 g/L Cu^{2+}, while at 18-28 g/L Cu^{2+}, the culture was adversely affected, demonstrated by a 168 h (7 days) lag phase, and complete microbial inhibition was observed above 33 g/L Cu^{2+} (Tapia et al. 2022). The natural ability of microorganisms to adapt to high metal ion stress can be attributed to the expression of genes conveying resistance to inhibitory metals through extra- and intracellular detoxification, and active transport of inhibitory metal ions by efflux pumps, amongst other adaptation mechanisms (Bruins et al. 2000; Dopson et al. 2003; Nkuna et al. 2022; Zhang et al. 2023).

To study a potential improvement in Cu^{2+} tolerance, planktonic cells were adapted to 6.0 g/L Cu^{2+} prior to microbial activity tests, corresponding to the Cu^{2+} present on leaching 6% w/v PCB solid loading. These Cu-adapted cells were subjected to the same Cu^{2+} stress as the non-adapted cells, with results presented in Figure 5-4. Adapting the cultures to Cu^{2+} improves their tolerance to high Cu^{2+} stress. Shorter lag phases were observed for Cu-adapted cultures (Figure 5-4) compared to non-adapted cultures (Figure 5-3) across all Cu^{2+} concentrations tested. Complete microbial Fe^{2+} oxidation was observed at approximately 140 h by Cu-adapted planktonic culture subjected to 11.0 g/L Cu^{2+} (Figure 5-4), compared to 54% Fe^{2+} oxidation within the same period for non-adapted culture (Figure 5-3). Volumetric Fe^{2+} oxidation rate of Cu-adapted planktonic cells decreased by 49% (0.0359 ± 0.0023 g $Fe^{2+}.L^{-1}.h^{-1}$) at 22 g/L Cu^{2+} stress, relative to the control (0.0703 ± 0.0029 g $Fe^{2+}.L^{-1}.h^{-1}$), compared to 69% reduction in oxidation rate at the same Cu^{2+} stress for non-adapted planktonic cells. Complete Fe^{2+} oxidation was observed within 300 h for the Cu-adapted culture at the highest Cu^{2+} concentration tested (50.0 g/L Cu^{2+}), compared to only about 14% Fe^{2+} utilised by the non-adapted culture at the same Cu^{2+} stress. This shows clear improvement in Cu^{2+} tolerance of the adapted cultures relative to the non-adapted culture. Improved tolerance to Cu^{2+} after pre-adapting an *At. ferrooxidans* culture was demonstrated by (Das et al. 1997). The authors adapted an *At. ferrooxidans* dominated culture to 25 g/L Cu^{2+} and compared microbial oxidation ability of the Cu-adapted cells to the non-adapted cells in the presence of Cu^{2+} stress (i.e., 5, 10, and 25 g/L Cu^{2+}). The non-adapted cells were reported to achieve complete Fe^{2+} oxidation at 44 and 78 h when subjected to 5 and 10 g/L Cu^{2+} and completely inhibited at 25 g/L Cu^{2+}; whereas the Cu-adapted cells achieved 100% Fe^{2+} oxidation even at 25 g/L Cu^{2+}

within 44 h (Das et al. 1997). Pre-adaptation of a bioleaching culture was also demonstrated by (Arshadi and Mousavi 2014; Xia et al. 2017). Although pre-adaptation can be time-consuming and may result in community shift (Xia et al. 2017; Nkuna et al. 2022), it presents a potential working approach to process improvement.

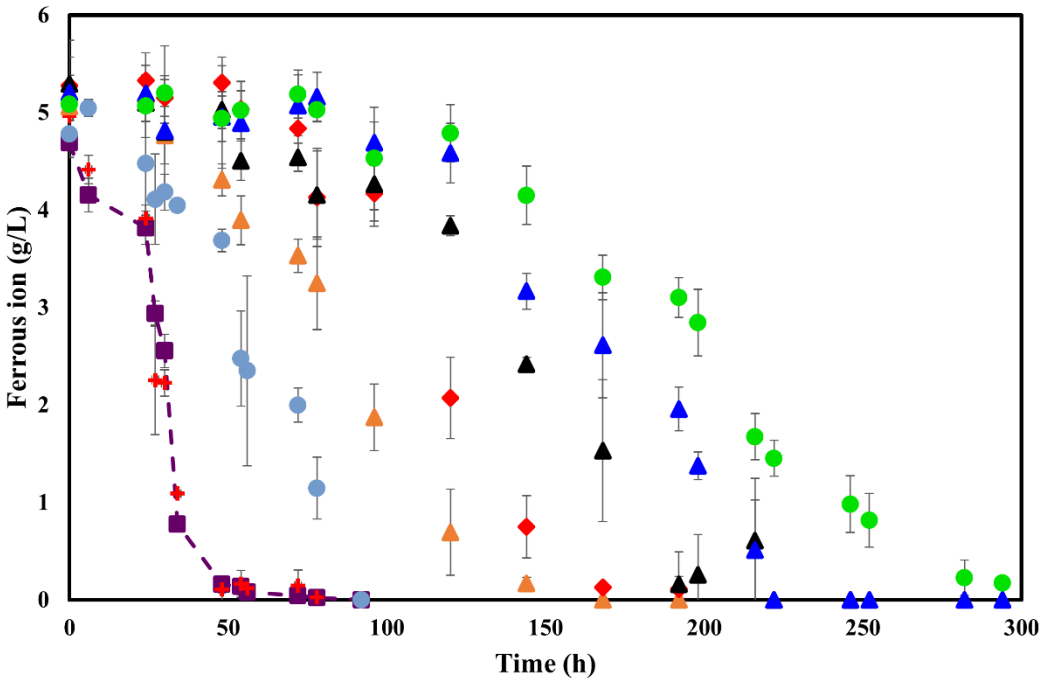

Figure 5-4 Microbial oxidation of ferrous iron by Cu-adapted planktonic cells (A-PC) at various Cu^{2+} concentrations, i.e., 0 (), 1.0 (), 6.0 (), 11.0 (), 22.0 (), 33.0 (), 44.0 (), and 50.0 g/L (). Error bars represent standard deviation, n = 3.

In light of the potential benefits of microbial immobilised systems over microbial planktonic systems (Armentia and Webb 1992; Elakkiya et al. 2016; Nemati et al. 1998; Nkuna et al. 2022; Sand and Gehrke 2006), microbial immobilisation was also considered as a potential method to improve microbial metabolic activity through increased biomass retention and to minimise microbial inhibition. The same microbial cultures used in the above free-suspended cell system were grown and maintained in the presence of PUF as a biomass support structure, to achieve a microbial colonised matrix and establish a biofilm (Figure 5-1). Figure 5-5 presents Fe^{2+} utilisation by non-adapted immobilised cells as a function of time. Although non-adapted immobilised cells were also susceptible to Cu^{2+}, they appeared to adapt to high Cu^{2+} concentrations faster than non-adapted planktonic cells. Reduced lag periods (by between 1.1 - 6.8-fold relative to the control) were observed for non-adapted immobilised cells across all Cu^{2+} concentrations tested (Figure 5-5), as compared to the long lag period (between 1.2 - 8.1-fold) observed in non-adapted planktonic cells (Figure 5-3).

Despite the volumetric rate being reduced by 57% (0.0331 ± 0.0021 g $Fe^{2+}.L^{-1}.h^{-1}$) in the presence of 22 g/L Cu^{2+} relative to the absence of Cu^{2+} stress (0.0778 ± 0.0042 g $Fe^{2+}.L^{-1}.h^{-1}$),

Fe^{2+} was completely oxidised within 220 h for non-adapted immobilised cultures, compared to about 50% Fe^{2+} oxidised at the same time and Cu^{2+} concentration for non-adapted planktonic cells. Comparably, the volumetric rate of Cu-adapted planktonic cells was reduced by 49% relative to control. At the highest Cu stress applied (50 g/L Cu^{2+}), the non-adapted immobilised cells were inhibited, with about 50% Fe^{2+} oxidised within 300 h, but to a lesser extent than the non-adapted planktonic cultures, where only about 24% Fe^{2+} was oxidised within the same period. These results suggested that prior adaptation of the microbial cultures to Cu^{2+} had more benefits than only microbial immobilisation. However, microbial immobilisation also improved metal tolerance relative to the typical non-adapted planktonic cultures in the bioleaching of PCBs. This suggested that the diffusional resistance presented by both mass transfer within the interstitial regions and into the biofilm served as a protection layer for immobilised cells against toxic Cu^{2+}. This observation corresponded with previous studies that indicated that the biofilm produced during cell attachment served as a diffusion barrier against toxic metal ions (Dopson et al., 2003; Vu et al., 2009). Thus, microbial immobilised systems may mitigate the microbial inhibition challenges faced in bioleaching systems with high Cu^{2+} concentrations. In addition, high cell density can be achieved in immobilised cell systems which, in turn, could improve the Fe^{2+} to Fe^{3+} volumetric rates and ultimately improve bioleaching efficiency.

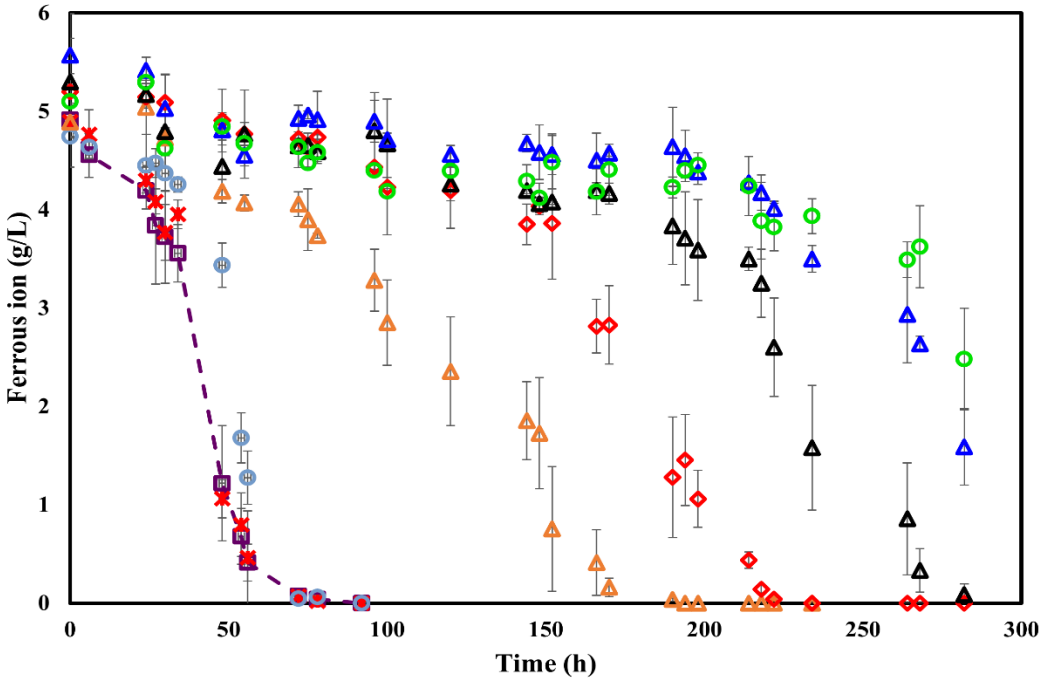

Figure 5-5 Ferrous iron oxidation by non-adapted immobilised cells (NA-IC) at various Cu^{2+} concentrations, i.e., 0 (–■–), 1.0 (✖), 6.0 (○), 11.0 (△), 22.0 (◇), 33.0 (▲), 44.0 (▲), and 50.0 g/L (○). Error bars represent standard deviation, n = 3.

Owing to the independent benefit of both Cu-adaptation and cell immobilisation, we explored their potential synergistic effect through the prior Cu-adaptation of immobilised cells to further improve their performance and metal ion tolerance. The culture was immobilised and

concurrently adapted to Cu^{2+} by increasing Cu^{2+} concentrations (by 0.5 g/L Cu^{2+}), up to 6 g/L Cu^{2+}, at every subculturing. Microbial Fe^{2+} oxidation by Cu-adapted immobilised cells over time is presented in Figure 5-6. Cu-adapted immobilised cultures exhibited the best tolerance to increasing Cu^{2+} stress. Further reduced lag periods (between 1.1 - 3.5-fold relative to control) preceding microbial Fe^{2+} oxidation were observed across all Cu^{2+} concentrations tested relative to non-adapted planktonic and immobilised cells, and Cu-adapted planktonic cells (Figure 5-7). Following the microbial lag phase, complete microbial oxidation was achieved across all Cu^{2+} concentrations tested but at volumetric rates reduced by between 14 – 62%, at 11.0 – 50.0 g/L Cu^{2+} stress for Cu-adapted immobilised cells. While in the same Cu^{2+} stress range, volumetric rate was reduced by 41 – 66%, 52 – 74%, and 56 – 78% for Cu-adapted planktonic cells, non-adapted immobilised and planktonic cells, respectively. The small difference in percentage reduced volumetric rate at the highest Cu^{2+} concentration across our four sets of inoculum could further suggest that once the lag period had been overcome, cultures could recover some of their performance during the exponential phase, subject to the level of stress they are exposed to. (Hubau et al. 2020) demonstrated similar finding when a planktonic mixed mesophilic culture dominated by *L. ferriphilum* and *Sulfobacillus benefaciens* was subject to stress by PCB leachate at a concentration range of 0 – 60% v/v of leachate added to medium with 10% v/v inoculum. The authors observed induced lag phase from 10% PCB leachates, with the lag phase increasing with the amount of PCB leachates added. However, following the lag period, the culture exhibited similar volumetric rates across PCB leachate stress (Hubau et al. 2020).

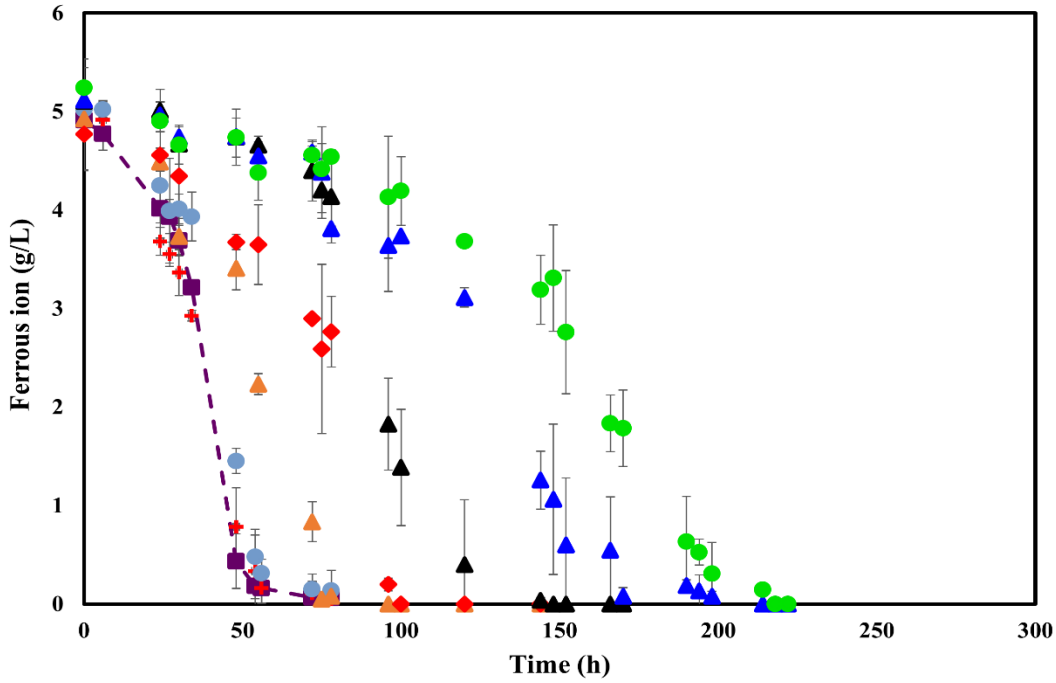

Figure 5-6 Microbial oxidation of ferrous iron by Cu-adapted immobilised cells (A-IC) subjected to various Cu^{2+} concentrations of 0 (■), 1.0 (✚), 6.0 (●), 11.0 (▲), 22.0 (◆), 33.0 (▲), 44.0 (▲), and 50.0 g/L (●). Error bars represent standard deviation, n = 3.

Notably, when the Cu-adapted immobilised cells were most stressed (at 50 g/L Cu^{2+}), all available Fe^{2+} was oxidised within 220 h (Figure 5-6). This is significant as one of the major drawbacks of bioleaching is that the process is slow as a result of slow microbial Fe^{2+} to Fe^{3+} turnover, among other factors. Fast regeneration of the required Fe^{3+} from Fe^{2+}, even in the presence of inhibitory metal ions, thus becomes a vital factor in improving the overall bioleaching process. Immobilisation and prior adaptation of the microbial cultures improved microbial tolerance to high Cu^{2+} concentration and the culture's performance over only adapting or immobilising the cultures. Across all Cu^{2+} concentrations tested, Cu-adapted immobilised microbial cultures presented better tolerance to high Cu^{2+} concentrations and improved culture performance (Figure 5-7). Figure 5-8 shows that at the highest Cu concentration tested (50.0 g/L), Cu-adapted immobilised cells achieved complete Fe^{2+} oxidation in a shorter period. Improved culture performance could be attributed to a resultant synergy of biofilm formation and prior adaptation of these immobilised cells to Cu^{2+}. This presents a greater opportunity to adopt Cu-adapted microbial immobilised systems not only in bioleaching of e-waste streams, such as PCBs, but also in Cu^{2+}-rich bioleaching systems. To the best of our knowledge, there are no reports in the literature on the adaptation of immobilised microbial cultures.

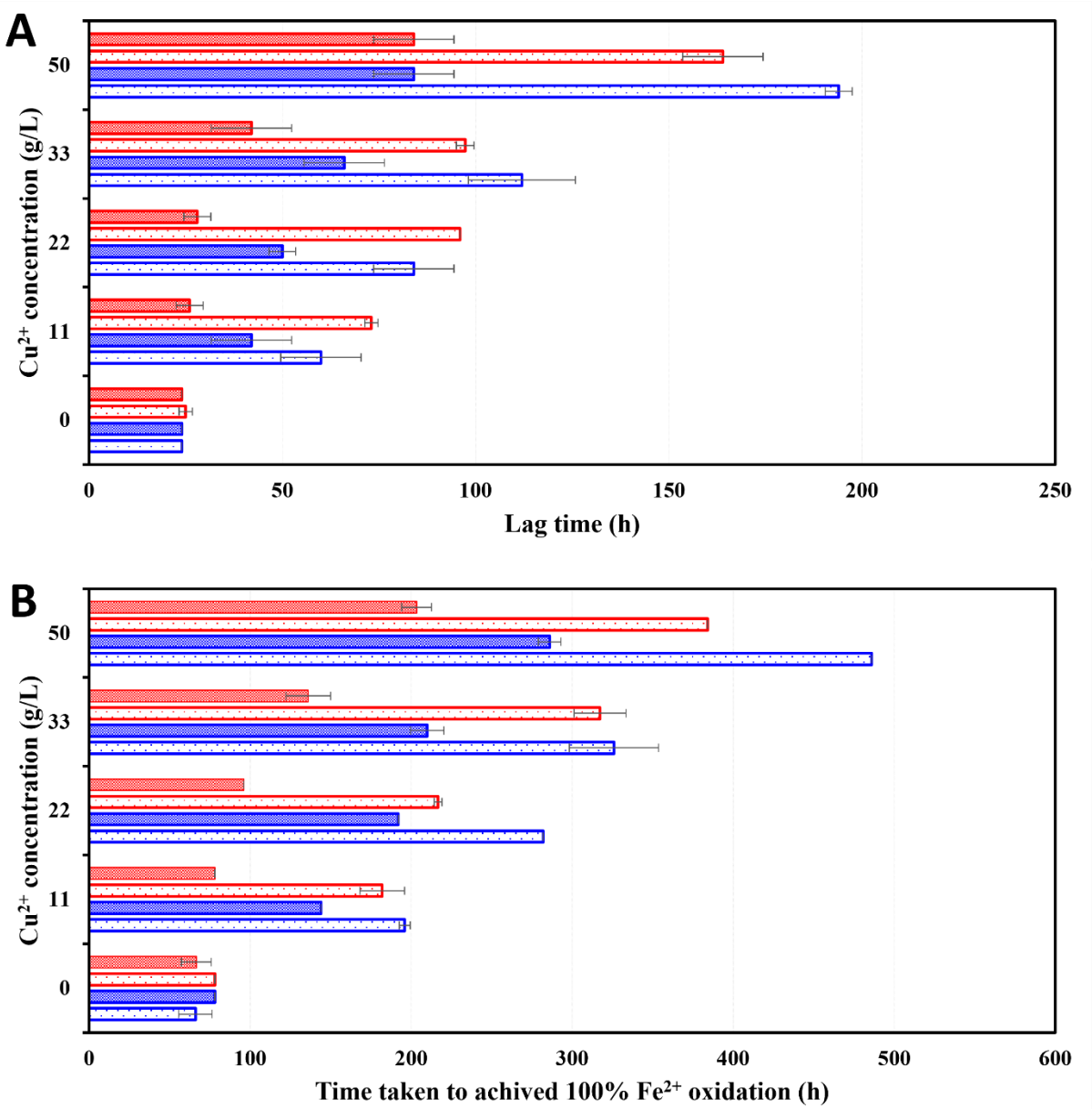

Figure 5-7 Comparison of (**A**) lag time required prior to onset microbial Fe^{2+} oxidisation, and (**B**) time taken to achieved 100% Fe^{2+} oxidation by NA-PC (), A-PC (), NA-IC (), and A-IC () subjected to increasing Cu^{2+} concentrations. Error bars represent standard deviation, n = 3

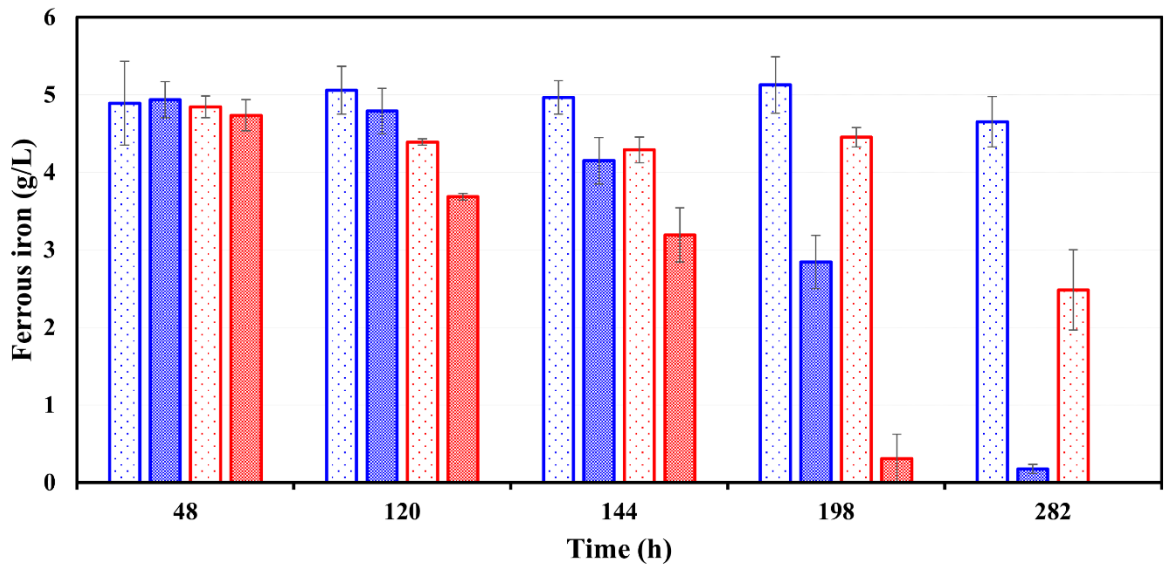

Figure 5-8 Comparison of ferrous iron oxidation over incubation period by NA-PC (), A-PC ( ), NA-IC (), and A-IC () subjected to 50.0 g/L Cu^{2+} concentrations. Error bars represent standard deviation, n = 3.

5.4 Conclusion

To exploit bioleaching as a technology of choice for treating low-grade PCBs to recover base metals prior to precious metal recovery, it is important to better understand the sub-processes involved. One such sub-process, microbial oxidation of ferrous iron, facilitates the regeneration of ferric iron, the primary oxidant in the bioleaching of PCBs, without ongoing chemical addition. The present study investigated the immobilisation of microbial cells on PUF and their adaptation to 6 g/L Cu^{2+}, the predominant inhibitory metal found in PCBs, as a method to improve the metabolic activity of microbial cells through minimising microbial inhibition by metal ions. This investigation demonstrated that prior adaptation of a mixed culture of planktonic cells, including *L. ferriphilum* as dominant iron oxidizing bacterium, to Cu^{2+} improves their tolerance to high Cu^{2+} concentration to a greater extent than only immobilising the microbial cultures; however, immobilised cultures also presented improved tolerance to Cu^{2+}. Above 33 g/L Cu^{2+}, more than 50% of the initially available Fe^{2+} was oxidised within 300 h for non-adapted immobilised cultures, compared to only about 25% oxidised within the same period and Cu^{2+} concentration for non-adapted planktonic cultures. High microbial metabolic activity and improved tolerance to Cu^{2+} ions for immobilised cells were attributed to the both the micro-environment within the PUF-BSP and the resultant biofilm associated with colonised microbial cells, which act as a diffusion barrier against inhibitory Cu^{2+}.

With the improved culture performance observed in non-adapted immobilised cells as well as in planktonic microbial cultures that have been adapted to copper, potential synergistic benefits of adaptation of immobilised cells to Cu^{2+} was investigated. Cu-adapted immobilised microbial cultures presented better tolerance to high concentrations of Cu^{2+} than non-

adapted planktonic and immobilised cells, and Cu-adapted planktonic cells. At the highest Cu^{2+} concentration tested of 50 g/L Cu^{2+}, all available Fe^{2+} was utilised within 220 h for Cu-adapted immobilised cells. This high Cu^{2+} tolerance and improved culture performance in Cu-adapted immobilised cells was attributed to the interactive benefits of diffusion limitations following retention in a micro-environment and biofilm formation and prior adaptation of the immobilised cells to Cu^{2+}. Furthermore, it gives added potential for higher cell concentrations to be used, as demonstrated in the study of inoculum size. Maintenance of improved culture performance at high Cu^{2+} concentrations present greater opportunities to adopt Cu-adapted immobilised cells systems in bioleaching of e-wastes streams and in bioleaching leaching systems that are typically rich in Cu. This study presents a novel approach to the mitigation of the inhibitory effect of Cu^{2+} in Cu rich bioleaching systems.

5.5 References

Africa, C.-J. (2017). Investigation of microbial metal-sulfide interfacial environments under mineral bioleach simulated conditions. PhD thesis, University of Cape Town.

Africa, C.-J.; van Hille, R. P.; Harrison, S. T. L. (2013). Attachment of *Acidithiobacillus ferrooxidans* and *Leptospirillum ferriphilum* cultured under varying conditions to pyrite, chalcopyrite, low-grade ore and quartz in a packed column reactor. Applied Microbiology and Biotechnology 97 (3), 1317–1324. DOI: 10.1007/s00253-012-3939-x.

Akcil, A.; Erust, C.; Gahan, C. S.; Ozgun, M.; Sahin, M.; Tuncuk, A. (2015). Precious metal recovery from waste printed circuit boards using cyanide and non-cyanide lixiviants - A review. Waste Management 45, 258–271. DOI: 10.1016/j.wasman.2015.01.017.

Armentia, H.; Webb, C. (1992). Ferrous sulphate oxidation using *Thiobacillus ferrooxidans* cells immobilised in polyurethane foam support particles. Applied Microbiology and Biotechnology 36 (5), 697–700. DOI: 10.1007/BF00183252.

Arshadi, M.; Mousavi, S. M. (2014). Simultaneous recovery of Ni and Cu from computer-printed circuit boards using bioleaching. Statistical evaluation and optimization. Bioresource technology 174, 233–242. DOI: 10.1016/j.biortech.2014.09.140.

Baniasadi, M.; Vakilchap, F.; Bahaloo-Horeh, N.; Mousavi, S. M.; Farnaud, S. (2019). Advances in bioleaching as a sustainable method for metal recovery from e-waste. A review. Journal of Industrial and Engineering Chemistry 76 (3–4), 75–90. DOI: 10.1016/j.jiec.2019.03.047.

Bizzo, W. A.; Figueiredo, R. A.; Andrade, V. F. D. (2014). Characterization of printed circuit boards for metal and energy recovery after milling and mechanical separation. Materials 4555–4566. DOI: 10.3390/ma7064555.

Brandl, H.; Bosshard, R.; Wegmann, M. (2001). Computer-munching microbes: metal leaching from electronic scrap by bacteria and fungi. Hydrometallurgy 59 (2), 319–326. DOI: 10.1016/S0304-386X(00)00188-2.

Bruins, M. R.; Kapil, S.; Oehme, F. W. (2000). Microbial resistance to metals in the environment. Ecotoxicology and Environmental Safety 45 (3), 198–207. DOI: 10.1006/eesa.1999.1860.

Bryan, C. G.; Watkin, E. L.; McCredden, T. J.; Wong, Z. R.; Harrison, S. T. L.; Kaksonen, A. H. (2015). The use of pyrite as a source of lixiviant in the bioleaching of electronic waste. Hydrometallurgy 152, 33–43. DOI: 10.1016/j.hydromet.2014.12.004.

Chen, S.-Y.; Cheng, Y.-K. (2019). Effects of sulfur dosage and inoculum size on pilot-scale thermophilic bioleaching of heavy metals from sewage sludge. Chemosphere 234, 346–355. DOI: 10.1016/j.chemosphere.2019.06.084.

Das, A.; Modak, J. M.; Natarajan, K. A. (1997). Studies on multi-metal ion tolerance of *Thiobacillus ferrooxidans*. Minerals Engineering 10 (7), 743–749. DOI: 10.1016/S0892-6875(97)00052-6.

Dopson, M.; Baker-Austin, C.; Koppineedi, P. R.; Bond, P. L. (2003). Growth in sulfidic mineral environments: Metal resistance mechanisms in acidophilic micro-organisms. Microbiology 149 (8), 1959–1970. DOI: 10.1099/mic.0.26296-0.

Elakkiya, M.; Prabhakaran, D.; Thirumarimurugan, M. (2016). Methods of cell immobilization and its applications. Internation Journal of Innovative Research in Science, Engineering and Technology 5 (4), 5429–5433. DOI: 10.15680/IJIRSET.2016.0504175.

Emmanuel Ngoma, I.; Ojumu, T. V.; Harrison, S. T.L. (2015). Investigating the effect of acid stress on selected mesophilic micro-organisms implicated in bioleaching. Minerals Engineering 75 (11), 6–13. DOI: 10.1016/j.mineng.2015.02.007.

Gómez, J. M.; Cantero, D.; Webb, C. (2000). Immobilisation of *Thiobacillus ferrooxidans* cells on nickel alloy fibre for ferrous sulfate oxidation. Applied Microbiology and Biotechnology 54 (3), 335–340. DOI: 10.1007/s002530000414.

González, A.; Bellenberg, S.; Mamani, S.; Ruiz, L.; Echeverría, A.; Soulère, L. et al. (2013). AHL signaling molecules with a large acyl chain enhance biofilm formation on sulfur and metal sulfides by the bioleaching bacterium *Acidithiobacillus ferrooxidans*. Applied Microbiology and Biotechnology 97 (8), 3729–3737. DOI: 10.1007/s00253-012-4229-3.

Govender, E.; Bryan, C. G.; Harrison, S. T.L. (2015). Effect of physico-chemical and operating conditions on the growth and activity of *Acidithiobacillus ferrooxidans* in a simulated heap bioleaching environment. Minerals Engineering 75, 14–25. DOI: 10.1016/j.mineng.2015.02.006.

Groboillot, A.; Boadi, D. K.; Poncelet, D.; Neufeld, R. J. (1994). Immobilization of cells for application in the food industry. Critical Reviews in Biotechnology 14 (2), 75–107. DOI: 10.3109/07388559409086963.

Guisan, J.; Bolivar, J.; López-Gallego, F.; Rocha-Martín, J. (2020). Immobilization of enzymes and cells. New York, NY: Springer USGuisan, J.; Bolivar, J.; López-Gallego, F.; Rocha-Martín, J. (2100).

Guoqiang, D.; Kaul, R.; Mattiasson, B. (1992). Immobilization of *Lactobacillus casei* cells to ceramic material pretreated with polyethylenimine. Applied Microbiology and Biotechnology 37 (3), 305–310. DOI: 10.1007/BF00210983.

Halfmeier, H. (1993). Potential of *Thiobacillus ferrooxidans* for waste gas purification. Part 2. Increase in continuous ferrous iron oxidation kinetics using immobilized cells. Applied Microbiology and Biotechnology 2, 582–587. http://scholar.google.com/scholar?hl=en&btnG=Search&q=intitle:Potential+of+Thiobacillus+ferrooxidans+for+waste+gas+purification+part+2#3%5Cnhttp://link.springer.com/article/10.1007/BF00175751.

Hessler, T.; Marais, T.; Huddy, R. J.; van Hille, R.; Harrison, S. T.L. (2017). Comparative analysis of the sulfate-reducing performance and microbial colonisation of three continuous reactor configurations with varying degrees of biomass retention. SSP 262, 638–642. DOI: 10.4028/www.scientific.net/SSP.262.638.

Hubau, A.; Minier, M.; Chagnes, A.; Joulian, C.; Silvente, C.; Guezennec, A.-G. (2020). Recovery of metals in a double-stage continuous bioreactor for acidic bioleaching of printed circuit boards (PCBs). Separation and Purification Technology 238 (3), 116481. DOI: 10.1016/j.seppur.2019.116481.

Ilyas, S.; Ruan, C.; Bhatti, H. N.; Ghauri, M. A.; Anwar, M. A. (2010). Column bioleaching of metals from electronic scrap. Hydrometallurgy 101 (3-4), 135–140. DOI: 10.1016/j.hydromet.2009.12.007.

Kaksonen, A. H.; Boxall, N. J.; Gumulya, Y.; Khaleque, H. N.; Morris, C.; Bohu, T. et al. (2018). Recent progress in biohydrometallurgy and microbial characterisation. Hydrometallurgy 180 (10), 7–25. DOI: 10.1016/j.hydromet.2018.06.018.

Kinnunen, P. H.-M.; Puhakka, J. A. (2005). High-rate iron oxidation at below pH 1 and at elevated iron and copper concentrations by a *Leptospirillum ferriphilum* dominated biofilm. Process Biochemistry 40 (11), 3536–3541. DOI: 10.1016/j.procbio.2005.03.050.

Liang, G.; Mo, Y.; Zhou, Q. (2010). Novel strategies of bioleaching metals from printed circuit boards (PCBs) in mixed cultivation of two acidophiles. Enzyme and Microbial Technology 47 (7), 322–326. DOI: 10.1016/j.enzmictec.2010.08.002.

Liu, C.-Q.; Plumb, J.; Hendry, P. (2006). Rapid specific detection and quantification of bacteria and archaea involved in mineral sulfide bioleaching using real-time PCR. Biotechnology and Bioengineering 94 (2), 330–336. DOI: 10.1002/bit.20845.

Makaula, D. (2019). Developing quantitative approaches to determine microbial colonisation and activity in mineral bioleaching and characterisation of acid rock drainage. PhD dissertation, University of Cape Town, Cape Town.

Nemati, M.; Harrison, S.T.L.; Hansford, G. S.; Webb, C. (1998). Biological oxidation of ferrous sulphate by *Thiobacillus ferrooxidans*. A review on the kinetic aspects. Biochemical Engineering Journal 1 (3), 171–190. DOI: 10.1016/S1369-703X(98)00006-0.

Nemati, M.; Webb, C. (1996). Effect of ferrous iron concentration on the catalytic activity of immobilized cells of *Thiobacillus ferrooxidans*. Applied Microbiology and Biotechnology 46 (3), 250–255. DOI: 10.1007/s002530050812.

Ngoma, E.; Borja, D.; Smart, M.; Shaik, K.; Kim, H.; Petersen, J.; Harrison, S. T.L. (2018). Bioleaching of arsenopyrite from Janggun mine tailings (South Korea) using an adapted mixed mesophilic culture. Hydrometallurgy 181 (1), 21–28. DOI: 10.1016/j.hydromet.2018.08.010.

Nkuna, R.; Ijoma, G. N.; Matambo, T. S.; Chimwani, N. (2022). Accessing Metals from Low-Grade Ores and the Environmental Impact Considerations. A Review of the Perspectives of Conventional versus Bioleaching Strategies. Minerals 12 (5), 506. DOI: 10.3390/min12050506.

Priya, A.; Hait, S. (2018). Extraction of metals from high grade waste printed circuit board by conventional and hybrid bioleaching using *Acidithiobacillus ferrooxidans*. Hydrometallurgy 177, 132–139. DOI: 10.1016/j.hydromet.2018.03.005.

Rohwerder, T.; Gehrke, T.; Kinzler, K.; Sand, W. (2003). Bioleaching review part A. Progress in bioleaching: fundamentals and mechanisms of bacterial metal sulfide oxidation. Applied Microbiology and Biotechnology 63 (3), 239–248. DOI: 10.1007/s00253-003-1448-7.

Sand, W.; Gehrke, T. (2006). Extracellular polymeric substances mediate bioleaching/biocorrosion via interfacial processes involving iron(III) ions and acidophilic bacteria. Research in Microbiology 157 (1), 49–56. DOI: 10.1016/j.resmic.2005.07.012.

Suzana, C. U. S. M.; Claudia, M.; A, M.; Larissa Guedes Fiuacute za, M. C. O.; Ra, T. D. S. (2013). Immobilization of microbial cells. A promising tool for treatment of toxic pollutants in industrial wastewater. African Journal of Biotechnology 12 (28), 4412–4418. DOI: 10.5897/AJB12.2677.

Tapia, J.; Dueñas, A.; Cheje, N.; Soclle, G.; Patiño, N.; Ancalla, W. et al. (2022). Bioleaching of heavy metals from printed circuit boards with an Acidophilic iron-oxidizing microbial consortium in stirred tank reactors. Bioengineering 9 (2), 79. DOI: 10.3390/bioengineering9020079.

Tuncuk, A.; Stazi, V.; Akcil, A.; Yazici, E. Y.; Deveci, H. (2012). Aqueous metal recovery techniques from e-scrap. Hydrometallurgy in recycling. Minerals Engineering 25 (1), 28–37. DOI: 10.1016/j.mineng.2011.09.019.

Tupikina, O. V.; Minnaar, S. H.; Rautenbach, G. F.; Dew, D. W.; Harrison, S. T.L. (2014). Effect of inoculum size on the rates of whole ore colonisation of mesophilic, moderate thermophilic and thermophilic acidophiles. Hydrometallurgy 149 (3), 244–251. DOI: 10.1016/j.hydromet.2013.10.010.

Tupikina, O. V.; Minnaar, S. H.; van Hille, R. P.; van Wyk, N.; Rautenbach, G. F.; Dew, D.; Harrison, S.T.L. (2013). Determining the effect of acid stress on the persistence and growth of thermophilic microbial species after mesophilic colonisation of low grade ore in a heap leach environment. Minerals Engineering 53 (4), 152–159. DOI: 10.1016/j.mineng.2013.07.015.

Valix, M. (2017). 18 - Bioleaching of electronic waste. milestones and challenges. In Jonathan W.-C Wong, Rajeshwar D. Tyagi, Ashok Pandey (Eds.): Current Developments in Biotechnology and Bioengineering: Elsevier, 407–442.

Watling, H. R. (2006). The bioleaching of sulphide minerals with emphasis on copper sulphides — A review. Hydrometallurgy 84, 81–108. DOI: 10.1016/j.hydromet.2006.05.001.

Xia, L.; Liu, X.; Zeng, J.; Yin, C.; Gao, J.; Liu, J.; Qiu, G. (2008). Mechanism of enhanced bioleaching efficiency of *Acidithiobacillus ferrooxidans* after adaptation with chalcopyrite. Hydrometallurgy 92 (3), 95–101. DOI: 10.1016/j.hydromet.2008.01.002.

Xia, M.-C.; Wang, Y.-P.; Peng, T.-J.; Shen, L.; Yu, R.-L.; Liu, Y.-D. et al. (2017). Recycling of metals from pretreated waste printed circuit boards effectively in stirred tank reactor by a moderately thermophilic culture. Journal of Bioscience and Bioengineering 123 (6), 714–721. DOI: 10.1016/j.jbiosc.2016.12.017.

Xiang, Y.; Wu, P.; Zhu, N.; Zhang, T.; Liu, W.; Wu, J.; Li, P. (2010). Bioleaching of copper from waste printed circuit boards by bacterial consortium enriched from acid mine drainage. Journal of Hazardous Materials 184 (1), 812–818. DOI: 10.1016/j.jhazmat.2010.08.113.

Yang, T.; Xu, Z.; Wen, J.; Yang, L. (2009). Factors influencing bioleaching copper from waste printed circuit boards by *Acidithiobacillus ferrooxidans*. Hydrometallurgy 97 (1-2), 29–32. DOI: 10.1016/j.hydromet.2008.12.011.

Yang, Y.; Chen, S.; Li, S.; Chen, M.; Chen, H.; Liu, B. (2014). Bioleaching waste printed circuit boards by *Acidithiobacillus ferrooxidans* and its kinetics aspect. Journal of Biotechnology 173, 24–30. DOI: 10.1016/j.jbiotec.2014.01.008.

Zhang, X.; Shi, H.; Tan, N.; Zhu, M.; Tan, W.; Daramola, D.; Gu, T. (2023). Advances in bioleaching of waste lithium batteries under metal ion stress. Bioresource and. Bioprocess. 10 (1), 2193. DOI: 10.1186/s40643-023-00636-5.

Zobell, C. E. (1943). The Effect of Solid Surfaces upon Bacterial Activity. Journal of Bacteriology 46 (1), 39–56. DOI: 10.1128/jb.46.1.39-56.1943.

CHAPTER 6

6 Microbial immobilisation and adaptation to Cu^{2+} enhances microbial Fe^{2+} oxidation for bioleaching of printed circuit boards in the presence of mixed metal ions

This study acknowledged that inhibition of microbial culture is not limited to predominant Cu^{2+} but also due to other individual metal ions such as Zn^{2+}, Ni^{2+}, or in their combinations, and/or other dissolved components of PCBs during bioleaching. With the promising results from Chapter 5 in terms of improved metal tolerance and ability to maintain high specific microbial oxidation rates in the presence of increased Cu^{2+} concentrations, this study further investigated the inhibitory effects of individual Zn^{2+}, Ni^{2+}, and Sn^{2+}. In addition, it investigated the inhibitory effect of mixed metals by combining these three metals with Cu^{2+} in compositions mimicking their expected concentrations in PCB leachates. It finally evaluated the effect of PCB leachates on Fe^{2+} oxidation, with the intention of understanding microbial inhibition beyond metal ions. The major results from this study are aimed at detailing potential inhibition by predominant base metal ions and PCB leachates to inform the selection of microbial cultures and reactor configurations at which microbial inhibition is minimised.

Authors' contributions

The experimental concept was put forward by Sue Harrison, Athanasios Kotsiopoulos, and Elaine Govender-Opitz. Experiment design, laboratory experiments, and were carried out by Musa Maluleke. Data analysis was performed by Musa Maluleke, guided and advised by both primary and co-supervisors, Sue Harrison, Athanasios Kotsiopoulos, and Elaine Govender-Opitz. The draft manuscript was written by Musa Maluleke for review and editing by Sue Harrison, Athanasios Kotsiopoulos, and Elaine Govender-Opitz. Sue Harrison approved the final draft manuscript as a corresponding author.

Journal title: Microbial immobilisation and adaptation to Cu^{2+} enhances microbial Fe^{2+} oxidation for bioleaching of printed circuit boards in the presence of mixed metal ions

Musa D. Maluleke, Athanasios Kotsiopoulos, Elaine Govender-Opitz, Susan T.L. Harrison

Centre for Bioprocess Engineering Research (CeBER), Department of Chemical Engineering, University of Cape Town, Rondebosch, Cape Town 7700, South Africa

Research in Microbiology (https://doi.org/10.1016/j.resmic.2023.104148)

Abstract

A circular economy requires effective re-use of finite resources, such as metals from waste electrical and electronic equipment (WEEE). Bioleaching for extraction and recovery of base metals from printed circuit boards (PCBs) before recovering precious metals has potential to increase metal circularity. However, inhibition by base metals released from the PCBs and accumulated in PCB leachates on microbial Fe^{2+} oxidation, a critical bioleaching sub-process for Fe^{3+} regeneration, can limit this approach. Here, we explore the potential of microbial immobilisation on polyurethane foam (PUF) and adaptation to cupric ions to minimise inhibition by mixed metals released from PCBs, particularly zinc, nickel, and tin, and enhancing Fe^{2+} oxidation rates in PCB bioleaching systems. A mixed mesophilic culture dominant in *Leptospirillum ferriphilum, Acidiplasma cupricumulans* and *Acidithiobacillus caldus* was immobilised on PUF and adapted to 6 g/L Cu^{2+}. Tolerance of Cu-adapted immobilised cells to the inhibitory metal ions Zn^{2+}, Ni^{2+}, and Sn^{2+}, as individual (0-10 g/L) and mixed metal ions at concentrations typically leached from PCBs at solids loadings of 0-20% (mass/volume) was compared to that of non-adapted immobilised cells. Further, the impact of solutes from PCB leachates were evaluated. Inhibition by individual metal ions decreased in the order Sn^{2+} > Ni^{2+} > Zn^{2+}. Inhibition of ferrous iron oxidation by mixed metal ions was synergistic with respect to individual metal ions. PCB leachates were more inhibitory than both mixed and individual metal ions even where metal concentration was low. Cu-adapted immobilised cells exhibited higher tolerance to increasing concentrations of inhibitory metal ions than non-adapted cells. These results are promising for the application of Cu-adapted cells in the bioleaching of PCBs and multi-metal concentrates.

6.1 Introduction

Recycling of metals from waste electrical and electronic equipment (WEEE) is key to both reducing metal pollution and driving towards an increasingly circular economy in which the demand for metals from virgin metals is minimised. In addressing this, the application of bioleaching in which acidic ferric leaching of metals is linked to microbial regeneration of ferric iron and acid by acidophiles to extract metals from printed circuit boards (PCBs) continues to receive attention owing to its potential for economic and environmental benefit over pyrometallurgy and hydrometallurgy (Moosakazemi et al. 2022; Tapia et al. 2022; Tuncuk et al. 2012a; Xia et al. 2017). This is postulated as biohydrometallurgical operating conditions are

typically less corrosive, the energy demands of extraction may be less as the working temperatures are generally low, and, most importantly, *in-situ* regeneration of the primary oxidant, ferric iron, is achieved in the presence of iron-oxidising acidophilic microorganisms such as *Leptospirillum (L.) ferrooxidans*, *Acidithiobacillus (At.) ferrooxidans* and *L. ferriphilum* as well as the archaea such as *Acidiplasma cupricumulans* and *Ferroplasma* sp., via Eq. 6-2(Baniasadi et al. 2019; Islam et al. 2020; Ji et al. 2022b; Tuncuk et al. 2012a; Wu et al. 2018).

$$2Fe^{3+} + M^{0} \rightarrow 2Fe^{2+} + M^{2+} \qquad \textit{Eq. 6-1}$$

$$2Fe^{2+} + 0.5O_2 + 2H^{+} \xrightarrow{Microorganisms} 2Fe^{3+} + H_2O \qquad \textit{Eq. 6-2}$$

Bioleaching technology has shown potential to be economically viable even for low-grade ores, suggesting this may hold true for PCBs. Further, it has potential to be developed across a range of operating scales with opportunity for distributed WEEE processing. These motivate interest in its further development. Research on PCB bioleaching has focused primarily on the factors affecting the rates and extent of both metal extraction and microbial leachate regeneration such as the concentration of ferric iron, solution pH, system temperature, pulp density, microbial strain(s) present, their inoculum sizes, and effect of metallic and non-metallic components of the PCBs on the microbial activity (Anaya-Garzon et al. 2021; Bas et al. 2013; Ilyas et al. 2010; Lambert et al. 2015; Yang et al. 2009; Zhu et al. 2011). A solution pH below 2 is required to avoid ferric iron precipitation as jarosite. Jarosite can deposit on PCBs, lowering metal surface area available and hence rate of metal extraction. Metals extracted such as cupric ions can complex with jarosite, adversely affecting downstream processes (Baniasadi et al. 2019; Priya and Hait 2018). To minimise continuous addition of acid during the bioleaching of metals from PCBs to keep the pH below 2, Bryan et al. (2015) investigated the addition of pyrite as its leaching and the associated sulfur oxidation results in *in-situ* generation of acid, while also supplementing Fe available in solution. Lambert et al. (2015) showed that the rate of copper extraction from electric cables is dependent on the concentration of the available Fe^{3+}, such that leaching kinetics are enhanced with increasing ferric iron concentration.

An adverse effect of accumulation of the mixed metals released on leaching has the potential to inhibit the growth and ferrous iron oxidation rates of acidophilic bacteria during bioleaching, and thereby regeneration of ferric iron and protons. This has been reported for the bioleaching of PCBs, WEEE and sulfide minerals (Brandl et al. 2001; Dopson et al. 2003; Edward et al. 2018; Khachatryan et al. 2021; Ojumu et al. 2008; Bryan et al. 2015). Inhibition in microbial ferrous iron oxidation can be caused by metals such as Fe^{2+} (substrate) (Nurmi et al. 2009; Ozkaya et al. 2007), Fe^{3+} (product) (Ozkaya et al. 2007; Khachatryan et al. 2021), as well as other base metal ions such as Zn^{2+}, Cu^{2+}, Al^{2+}, Ni^{2+} - as individual metal ions or in their combination (Das et al. 1997; Bryan et al. 2015; Li and Ke 2001; Nurmi et al. 2009; Lambert et al. 2015); as well as components liberated from PCBs (Anaya-Garzon et al. 2021; Bas et al. 2013; Brandl et al. 2001; Bryan et al. 2015; Hubau et al. 2020; Lambert et al. 2015) and other forms of e-waste such as plastic (Lambert et al. 2015) . Khachatryan et al. (2021) investigated

the effect of Fe^{2+} and Fe^{3+} ions on the growth and Fe^{2+} oxidation kinetics of *L. ferriphilum,* reporting that Fe^{2+} oxidation was competitively inhibited at concentrations between 4 g/L Fe^{3+} and 11.2 g/L Fe^{3+}. Similarly, Ozkaya et al. (2007) reported competitive inhibition of the *L. ferriphilum* by Fe^{3+} ions, from 5 g/L Fe^{3+} but complete Fe^{2+} oxidation was achieved even at 60 g/L Fe^{3+} after 55 h lag phase. Khachatryan et al. (2021) further studied the effect of Cu, Zn, Ni, and Co on the Fe^{2+} oxidation kinetics, showing decreasing toxicity of these metal ions as follows: $Co^{2+} > Zn^{2+} > Ni^{2+} > Cu^{2+}$. In an attempt to mitigate microbial inhibition, Lambert et al. (2015) adapted their culture to 16 g/L Cu^{2+} and 1 g/L Al^{3+} prior to bioleaching electric cables. Despite the prior adaptation, Fe^{2+} oxidation was adversely inhibited. They attributed the observed inhibition to the plastic components of the cables, amongst other factors, as a lag of 18 h was reported in the presence of the plastic coating relative to experiments without plastic (Lambert et al. 2015). Recently, Hubau et al. (2020) investigated the effect of varying (0 to 60% v/v) PCB leachate concentrations on microbial Fe^{2+} oxidation by a culture dominated by *L. ferriphilum* and *Sulfobacillus benefaciens*. They observed Fe^{2+} oxidation inhibition increased with increasing PCB leachate concentrations. However, even at their highest concentration of PCB leachates, complete Fe^{2+} oxidation was achieved within 600 h, suggesting that the culture slowly adapted to high concentration of PCB leachate.

Despite the research to date on factors affecting the bioleaching of PCB systems, microbial inhibition remains one of the major challenges limiting the commercialisation of the process. Approaches reported to process improvement include microbial adaptation to metal ions (Brandl et al. 2001; Dopson et al. 2003; Xia et al. 2008; Xia et al. 2017), and the separation of the sub-processes of chemical leaching of the PCBs and the microbial regeneration of the Fe^{3+} ions into two stages (Brandl et al. 2001; Hubau et al. 2020; Wu et al. 2018). Nemati et al. (1998) and Nemati and Webb (1996) reported the benefit of immobilised microbial cultures in enhancing ferric iron generation rates. Here, the microbial culture colonises a biomass support structure (Duku 2011; González et al. 2013; Horn et al. 2001; Nemati et al. 1998; Nemati and Webb 1996; Liu et al. 2019; Zhang et al. 2023). Despite the wide exploration and well-documented benefits of immobilised microbial systems in bioleaching of mineral sulfides at laboratory scale (Armentia and Webb 1992; Gómez et al. 2000; Nemati et al. 1998; Nemati and Webb 1996), there are limited studies on the adaptation of this strategy in the bioleaching of PCBs. Maluleke et al. (2024b) have demonstrated that microbial immobilisation using polyurethane foam (PUF)-based systems both enhances volumetric Fe^{2+} oxidation rates through increased biomass concentration and mitigates against the impact of Cu-induced inhibition of Fe^{2+} inhibition, augmenting the benefits of adaptation to the metal.

The present study explores the potential to exploit microbial immobilisation and microbial adaptation to Cu^{2+} as routes to minimise microbial inhibition by mixed metals released from PCBs and improve Fe^{2+} oxidation rates for application of bioleaching systems for metal recovery from PCBs. A mixed mesophilic culture of acidophiles was immobilised on polyurethane foam (PUF) as a biomass support structure and adapted to 6 g/L Cu^{2+} ions. The influence of Zn^{2+}, Sn^{2+}, and Ni^{2+} as (1) individual metal ions and (2) in combination in ratios modelled on a PCB leachate, as well as PCB leachates on microbial Fe^{2+} oxidation by the immobilised and adapted cultures was studied. Their response to increasing concentration of the inhibitory metal ions, both individually and as a metal mixture representative of PCB

leachate, was compared to that of non-adapted immobilised cultures. These findings are key to inform the design of the metal bioleaching process for recovery of base metals from PCBs prior to recovery of gold and platinum group metals (PGMs), thereby increasing circularity of the metals.

6.2 Materials and methods

6.2.1 Microbial culture growth and maintenance

The mixed mesophilic culture (dominated by *L. ferriphilum*, *At. caldus* and *Ap. cupricumulans* (>10% abundance)) used in this study was obtained from a stock culture maintained on 3% w/v pyrite concentrates in a 1 L batch stirred tank bioreactor at the CeBER laboratory (University of Cape Town). Microbial speciation of the inoculum was performed according to Tupikina et al. (2013) using quantitative real-time polymerase chain reaction (qPCR) with bespoke primers designed for the typical mesophilic acidophilic bioleaching microbes. The inoculum was made up of *L. ferriphilum* (38%), *At. caldus* (45%) and *Ap. cupricumulans* (15%), with additional species present at <1% abundance. Autotrophic basal salts (ABS) medium comprising of 7.5 g/L $(NH_4)_2SO_4$, 7.5 g/L Na_2SO_4, 2.5 g/L KCl, 25 g/L $MgSO_4.7H_2O$, 2.5 g/L KH_2PO_4, and 0.7 g/L $Ca(NO_3)_2.4H_2O$, with 1 mL trace elements, at pH 1.4 (adjusted with concentrated H_2SO_4) was used (Johnson et al. 2008b; Kolmert and Johnson 2001). The microbial activity of the stock culture was regularly monitored in terms of solution pH and redox potential, analysis of Fe^{3+}/Fe^{2+} ions concentrations, routine cell counts and microbial speciation. The concentration of planktonic microbial cells was determined by direct microscope cell count on Thoma counting chamber using phase contrast optics and an Olympus BX40 microscope at 1000x magnification.

6.2.2 Immobilisation on PUF and adaptation to Cu

Sterilised 1 cm^3 PUF cubes (open-pore PUF, SK:FI0884, supplied by Akwa Products, South Africa) were placed in a 400 mL sterilised ABS medium containing 5 g/L Fe^{2+} (added as $FeSO_4.7H_2O$) in a 1 L Erlenmeyer flask. The solution pH was adjusted to pH 1.4 using concentrated H_2SO_4 before inoculating with 10% v/v of the mixed culture and incubating at 37 °C with agitation at 120 rpm. The activity of the culture was monitored by regular measurements of redox potential, pH, and Fe^{3+}/Fe^{2+} concentrations. The culture was maintained by routine subculturing on substrate depletion at which point 50% v/v spent medium was replaced with fresh medium containing 5.0 g/L Fe^{2+} substrate. Microbial adaptation to Cu^{2+} ions was achieved by incrementally increasing Cu^{2+} concentrations (by 0.5 g/L Cu^{2+}) on each subculture, up to 6.0 g/L Cu (added as $CuSO_4.7H_2O$). The culture was maintained under these conditions for at least for 2 months before being used for Fe^{2+} oxidation study in the presence of inhibitory metal ions (Section 6.2.3).

6.2.3 Impact of metal ions on microbial oxidation of Fe^{2+} ions

The effect of inhibitory metal ion concentrations was investigated in triplicate in 250 mL Erlenmeyer flasks with a working volume of 100 mL using ABS medium containing 5.0 g/L Fe^{2+} at pH 1.4. Each flask was inoculated with 3 PUF units colonised with microbial culture adapted to 6.0 g/L Cu, then incubated with agitation at 120 rpm on an orbital shaker at 37 °C. Control

flasks were inoculated with three PUF units colonised with the mixed culture that had not undergone prior adaptation to Cu^{2+} and incubated at the same conditions. Although the present study focused on immobilised cells, planktonic cultures (non- and Cu-adapted cells) were run parallel to the immobilised cell systems. We demonstrated in Maluleke et al. (2024b) that three PUF units presented a similar Fe^{2+} oxidation rate to the planktonic culture inoculated at 10% v/v to achieve a starting cell concentration of 1.21 x 10^8 cell/mL in the absence of inhibitory metal ions, characterised by Fe^{2+} oxidation rates of 0.065±0.001 g $Fe^{2+}.L^{-1}.h^{-1}$ and 0.064±0.003 g $Fe^{2+}.L^{-1}.h^{-1}$, respectively (null hypothesis confirmed by the p-value of 0.540). As such, a 10% v/v inoculum of planktonic cells was used in this study. Inhibition by Zn^{2+}, Sn^{2+}, Ni^{2+}, as individual metal ions at 0, 1.0, 3.0, 6.0, 8.0, and 10.0 g/L, their combination, and PCB leachates was investigated. Both individual and mixed metal ions were prepared from their respective sulfate salts. The concentration of each metal in the mixed metal solutions was calculated based on its expected concentration at the specified PCB solid loading (%PCB w/v). The custom-made PCB sample was rich in Cu with <0.2% wt of other base metals, as shown in Table 6-1.

Table 6-1 Metal composition of PCBs (g metal/100 g PCB) reported across a range of PCB sources.

Metal composition (wt %)									Type of sample	Reference
Cu	Pb	Al	Sn	Zn	Fe	Ni	Ag	Au		
23.1	2.89	2.60	1.88	1.75	0.810	0.190	0.0200	1.40×10^{-3}	PCBs From E-waste scrap, Guangzhou, China	Xiang et al. (2010)
14.5	1.17	6.04	1.67	1.67	12.2	0.340	0.201	0.0440	PCBs from computer, toys, audio & video equipment, France	Hubau et al. (2020)
19.7	0	2.66	1.99	2.55	8.34	0.270	0.0500	0	PCBs from memory and motherboard of computers	Carvalho et al. (2018)
11.0	0	0	1.00×10^{-3}	0.0400	0.150	0.180	0	0	Custom made template, South Africa	Sample used in this study
27.5	2.91	1.32	3.43	2.86	1.60	0.400	3.00×10^{-3}	6.00×10^{-3}	Computer PCBs, Hunan, China	Guo et al. (2011)
8.90	3.15	0.750	1.00×10^{-3}	8.20	8.00	2.00	3.00×10^{-3}	1.00×10^{-3}	PCBs from E-waste scrap, Wuhan, China	Ilyas et al. (2010)
17.5	2.02	2.23	1.50	2.84	5.19	0.560	0.0130	1.00×10^{-3}	**Average**	

As such, to have a proportion of mixed metal which can be comparable (in terms of metal concentrations) to other characterised PCBs reported in the literature, five literature-reported PCB compositions were considered and their average metal content was calculated and used to inform mixed metal proportions (Table 6-1). The PCB solid loadings mimicked were 0, 5, 10, 15, and 20% w/v based on this average PCB metal composition with 100% extraction to solution assumed. The simulated PCB loadings included four metals of interest, Zn, Ni, Cu, and Sn and their prepared concentrations per solid loading are defined in Table 6-2.

Table 6-2 Metals added in the mixed metal composition and their respective concentration (g/L) per simulated PCB solid loading (%w/v).

Metal	Simulated % PCB solid loading (%w/v)				
	1%	5%	10%	15%	20%
Cu (g/L)	1.75	8.73	17.5	26.2	34.9
Zn (g/L)	0.285	1.42	2.84	4.27	5.69
Sn (g/L)	0.150	0.748	1.50	2.24	3.00
Ni (g/L)	0.0560	0.282	0.563	0.845	1.13

To study the effect of PCB leachates on Fe^{2+} oxidation, leachates from the PCB template were first prepared by Fe^{3+} leaching of 20% w/v PCBs in a 1 L stirred tank reactor (see Table 6-3). The concentration of the Fe^{3+} leaching agent was calculated based on the concentration of the base metal in the characterised PCB, and the known required leaching stoichiometry of 2 mol Fe^{3+}: 1 mol metal (Equation 1) (Tuncuk et al. 2012a; Yazici and Deveci 2014), resulting in 40.0 g/L Fe^{3+} being used to leach 20% w/v PCBs. Daily measurements of pH and redox potential, and analysis of Fe concentrations were performed to monitor metal leaching. At the end of the leaching, determined by the complete reduction of Fe^{3+} to $Fe^{2+,}$ the leachate was filtered through a 0.45 µm Whatman filter and analysed for the four metals of interest and Fe (Table 6-3). Varying amounts of 0, 10, 20, 30, 40, and 50% v/v by volume of PCB leachates were then added into the 250 mL Erlenmeyer test flasks to study Fe^{2+} oxidation in the presence of increasing PCB leachates concentrations while maintaining a total working volume of 100 mL.

Table 6-3 Metal concentrations (in g/L) in the leachate generated at a PCB solid loading of 20% and used to investigate the inhibitory effect of PCB leachates.

Metal	Concentration (g/L)
Cu	22.2
Fe	33.1
Ni	0.406
Zn	0.0930
Sn	0

6.2.4 Analytical techniques

6.2.4.1 Redox potential and pH

All redox potential measurements were conducted using a glass electrode (Metrohm, Model 6.0451.100) with 3 M KCl as electrolyte and an Ag/AgCl reference electrode, connected to the

pH/Eh 867 Metrohm meter. These are reported as redox potential relative to the Ag/AgCl reference. The pH measurements were carried out using an iConnect 854 pH electrode, connected to the Metrohm 867 meter.

6.2.4.2 Iron concentrations

Iron concentrations in the form of Fe^{3+} and Fe^{tot} were quantified spectrophotometrically using the colorimetric ferric chloride assay (Govender et al. 2012) with measurements at 340 nm wavelength using a Genesys 10S UV-Visible Thermo Scientific spectrophotometer. Reaction of HCl selectively with Fe^{3+} formed a ferric chloride complex quantified by absorbance at 340 nm to provide the concentration of Fe^{3+}. Further, reaction of the sample with potassium persulfate oxidised Fe^{2+} to Fe^{3+}. By measuring absorbance at 340 nm again, the total concentration of Fe (Fe^{tot}) was obtained. Fe^{2+} concentration was deduced from the difference.

6.3 Results and discussion

6.3.1 Effect of individual metals Zn, Ni, and Sn on microbial oxidation of Fe^{2+}

While Cu is the most abundant metal in typical PCBs, Zn, Ni, and Sn are among the next most abundant. Dissolution of these metals on PCB bioleaching may contribute to microbial inhibition (Khachatryan et al. 2021; Nurmi et al. 2009; Tapia et al. 2022; Tian et al. 2007; Xu et al. 2013; Zhang et al. 2023). Their impact on microbial Fe^{2+} oxidation was tested from 1.0 to 10.0 g metal/L. The oxidation of Fe^{2+} over time in the presence of increasing concentration of individual metal ions is presented in Figure 6-1, Figure 6-2, and Figure 6-4. Generally, microbial inhibition increased with an increase in the concentration of inhibitory metal ions in solution as observed by the increase in lag time and the increased time required to achieve the same extent of ferrous iron oxidation. On use of Cu-adapted immobilised cells, better tolerance was observed than for non-adapted immobilised cultures as shorter times were required to achieve complete Fe^{3+} regeneration as observed.

Across all Zn^{2+} concentrations investigated, no clear trend in Fe^{2+} oxidation as a function of Zn concentration was seen in the immobilised cultures (Figure 6-1C & D) and Cu-adapted cultures (Figure 6-1B & D). The 5 g/L Fe^{2+} was completely oxidised within 80 h in these cases for Zn^{2+} concentrations less than or equal to 10 g/L (Figure 6-1B-D), indicating the absence of Zn^{2+} inhibition in this range following adaptation to 6 g/L Cu^{2+}. For non-adapted immobilised cells, Zn inhibition was not observed below 8 g/L Zn^{2+}. In the non-adapted planktonic cultures, an extended oxidation period was observed with increasing Zn^{2+} concentration, largely due to an extended lag phase (Figure 6-1A). Complete Fe^{2+} oxidation was extended from 80 h at 0 and 1 g/L Zn^{2+} to 100 h at 8 and 10 g/L Zn^{2+}.

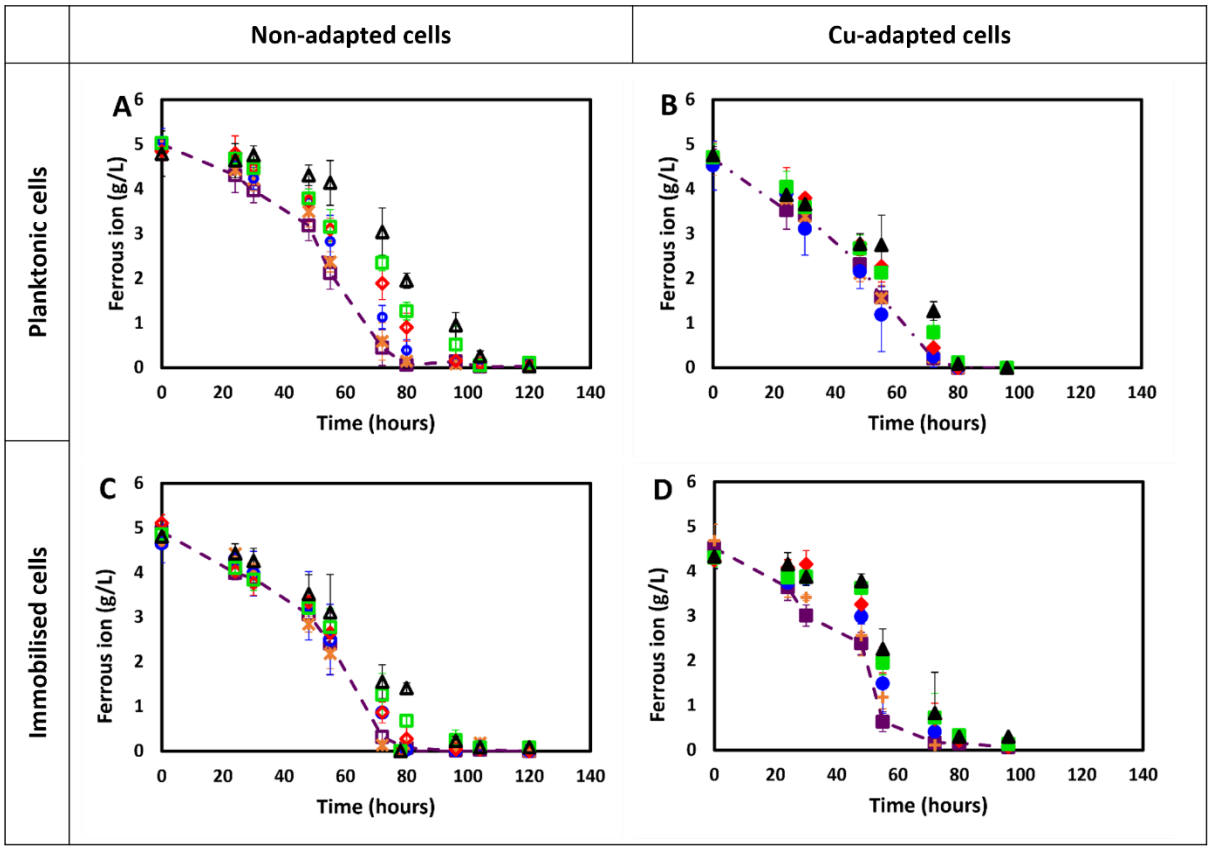

Figure 6-1 Progressive microbial Fe^{2+} oxidation by non-adapted planktonic (**A**) and immobilised cells (**C**), and Cu-adapted planktonic (**B**) and immobilised cells (**D**) in the presence of an increasing concentration of Zn^{2+} (0-10 g/L). Non-adapted cells **(A**, **C)**, 0 g/L (-□-), (✖)1 g/L, 3 g/L (○), 6 g/L (◇), 8 g/L (□), and 10 g/L (△). Cu-adapted cells (**B**, **D**), 0 g/L (-■-), 1 g/L (✚), 3 g/L (●), 6 g/L (◆), 8 g/L (■), and 10 g/L (▲). Error bars represent standard deviation, n = 3.

While complete Fe^{2+} oxidation has been reported by planktonic *L. ferriphilum* dominated cultures by Tapia et al. (2022), Bryan et al. (2015) , and Khachatryan et al. (2021), this was preceded by long lag phases (suggesting adaptation over time). Tapia et al. (2022) showed that a mixed culture of *Tissierella*, *Acidiphilium,* and *Leptospirillum* was able to tolerate up to 33 g/L Zn^{2+}. On investigating the effect of Zn^{2+} (10-150 mM, about 0.65-9.81 g/L) on Fe^{2+} oxidation by planktonic *L. ferriphilum*, Khachatryan et al. (2021) observed an increasing inhibitory effect of Zn^{2+} with increase in Zn^{2+} concentrations, with a minimal inhibitory concentration at 0.65 g/L Zn^{2+} and adverse microbial inhibition at 9.81 g/L (Khachatryan et al. 2021). While these authors show similar Zn inhibition of acidophilic cultures to those reported here, the positive impact of adaptation to Cu^{2+} and of immobilisation on enhancing tolerance to Zn has not been demonstrated previously.

Microbial Fe^{2+} oxidation in the presence of increasing concentration of Ni^{2+} ions is presented in Figure 6-2. Ni^{2+} inhibited Fe^{2+} oxidation from 3 g/L Ni^{2+} for both non-adapted planktonic and immobilised cells (Figure 6-2A and C). A prolonged lag phase was observed at elevated Ni^{2+} concentrations of 8 and 10 g/L, indicative of the inhibitory effects of Ni^{2+} increasing with an increase in Ni^{2+} concentration. These lag phases were exaggerated in the non-adapted

planktonic cultures over the non-adapted immobilised cultures. An elongated lag phase for non-adapted immobilised cells was observed at the highest Ni^{2+} tested (10 g/L), with about 10% (0.49 g/L) Fe^{2+} oxidised within 52 h relative to 48% (2.46 g/L) Fe^{2+} oxidised at 0 g/L Ni^{2+} within the same period (Figure 6-2C). In the non-adapted planktonic cultures, similar delayed oxidation at 52 h was found at 3, 6, 8 and 10 g/L Ni^{2+} and the time required for complete Fe^{2+} oxidation was extended to 104, 126, 126 and 212 h, respectively, at 3, 6, 8 and 10 g Ni^{2+}/L, compared with 85, 101, 104 and 122 h in the non-adapted immobilised cultures, and 80 h in the control. Bryan et al. (2015) also observed microbial inhibition of a planktonic *L. ferriphilum* culture at 3 g/L Ni^{2+}. Their culture was also observed to adapt to Ni^{2+} and recovered after about 300 h. Nonetheless, complete Fe^{2+} oxidation was not achieved, suggesting severe microbial inhibition by Ni^{2+} (Bryan et al. 2015). Following adaptation of the cultures in this study to 6 g Cu^{2+}/L, performance remained compromised at 3 g/L Ni^{2+} and above, but to a much lower level. An extended lag phase of 48 h was observed with an increase in Ni^{2+} concentration to 3 g/L and above for the Cu-adapted immobilised cells (Figure 6-2D). The Cu-adapted culture was observed to recover much more quickly compared to non-adapted culture across all Ni^{2+} tested, indicating the benefits of prior adaptation of the culture.

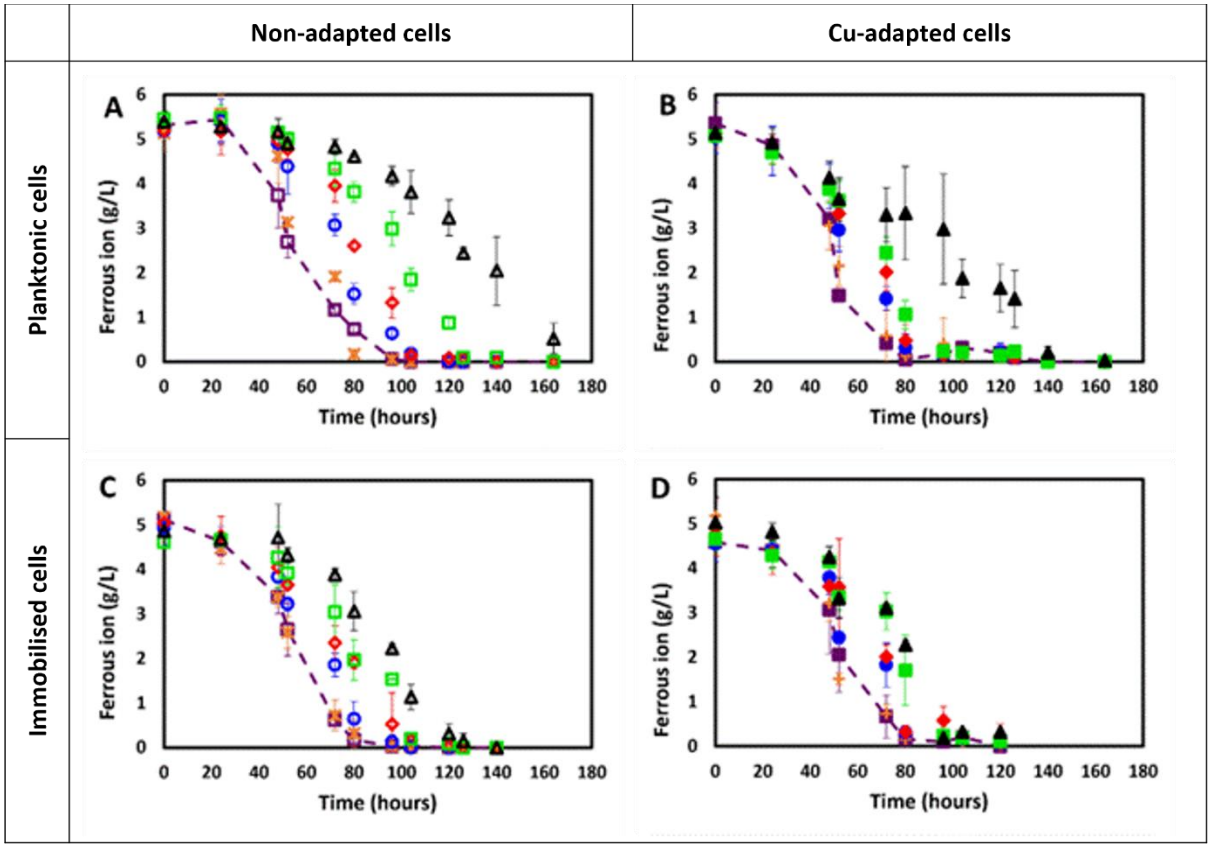

Figure 6-2 Progressive microbial Fe^{2+} oxidation by non-adapted planktonic (**A**) and immobilised cells (**C**), and Cu-adapted planktonic (**B**) and immobilised cells (**D**) in the presence of an increasing concentration of Ni^{2+} (0-10 g/L). Non-adapted cells **(A**, **C)**, 0 g/L (-□-), 1 g/L (✖), 3 g/L (○), 6 g/L (◇), 8 g/L (□), and 10 g/L (△). Cu-adapted cells (**B**, **D**), 0 g/L (-■-), 1 g/L (✚), 3 g/L (●), 6 g/L (◆), 8 g/L (■), and 10 g/L (▲). Error bars represent standard deviation, n = 3.

Tin solder is widely used to mount electronic components onto the surface of PCBs. As such, tin is one of the predominant metals across various PCBs. Tin can easily be leached from PCBs with HNO_3 and recovered by precipitation as SnO_2 (Yang et al. 2017b). On bioleaching PCBs, a low concentration of tin is detected in the leachate as it is also reported to precipitate out of the solution as SnO under these acidic conditions (Brandl et al. 2001; Ilyas et al. 2007). Although PCB leachates may contain a low amount of soluble Sn and some precipitated SnO, it is vital to understand their inhibitory effect on the microbial culture, particularly in the case of a one-stage reactor set-up. In the present microbial inhibitory studies, Sn was added as dissolved Sn^{2+}, however, a whitish/yellowish precipitate (SnO) was observed over time (Figure 6-3).

Figure 6-3 Observed precipitation in flasks containing tin, postulated to be SnO (Brandl et al. 2001; Bryan et al. 2015; Ilyas et al. 2007).

Reduction of available Fe^{3+} to Fe^{2+} (with increasing Fe^{2+} concentration) was observed (Figure 6-4A-D). Similar to observations in the presence of Zn^{2+} and Ni^{2+}, the culture exposed to 1.0 g/L Sn^{2+} remained unaffected for both non- and Cu-adapted immobilised cells and adapted planktonic cells with a small decrease in performance with non-adapted planktonic cells. A period of Fe^{3+} reduction and, possibly, a lag phase was observed with 3.0 g/L Sn^{2+} in both non- and Cu-adapted cultures (Figure 6-4A-D). While complete oxidation of Fe^{2+} was observed within 200 and 150 h, respectively for immobilised and planktonic cells, more rapid Fe^{2+} oxidation is clearly shown on adaptation (residual Fe^{2+} of 6 and 4.5 g/L at 96 and 120 h for non-adapted cultures vs 4.5 and 2.5 g/L, respectively, for Cu-adapted immobilised cultures). This delay in Fe^{2+} oxidation suggested an inhibitory effect of Sn^{2+} on both cultures.

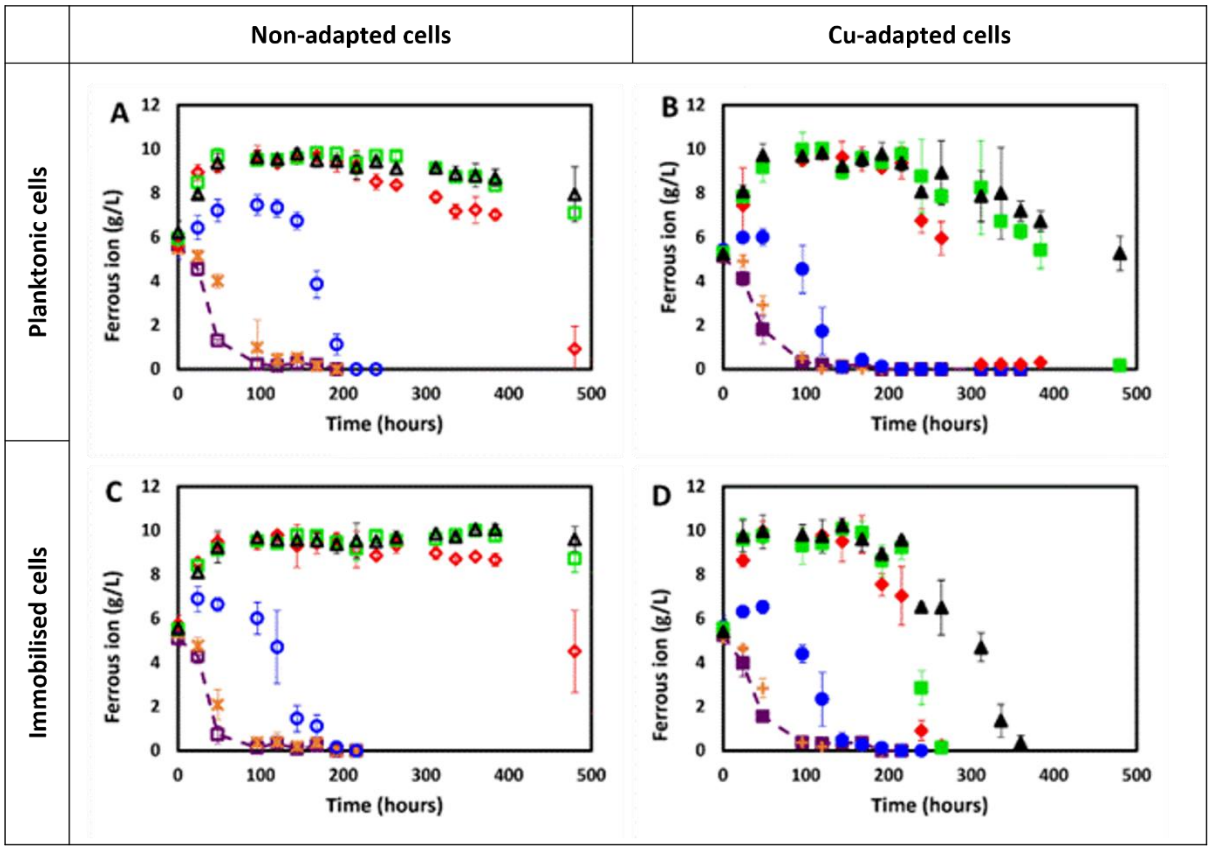

Figure 6-4 Progressive microbial Fe^{2+} oxidation by non-adapted planktonic (**A**) and immobilised cells (**C**), and Cu-adapted planktonic (**B**) and immobilised cells (**D**) in the presence of an increasing concentration of Sn^{2+} (0-10 g/L). Non-adapted cells **(A**, **C)**, 0 g/L (-□-), 1 g/L (✕), 3 g/L (○), 6 g/L (◇), 8 g/L (□), and 10 g/L (△). Cu-adapted cells (**B**, **D**), 0 g/L (-■-), 1 g/L (+), 3 g/L (●), 6 g/L (◆), 8 g/L (■), and 10 g/L (▲). Error bars represent standard deviation, n = 3.

A severe inhibitory effect, characterised by a longer lag phase (>470 and 220 h for non-adapted and Cu-adapted immobilised cultures, respectively, and 400 and 270 h for non-adapted and adapted planktonic cells, respectively), was observed at 8.0 g/L and 10.0 g/L Sn^{2+}. Despite the culture performance being severely compromised at 10.0 g/L Sn^{2+}, complete oxidation of 10 g/L Fe^{2+} was achieved at approximately 350 h for Cu-adapted immobilised cells. While within the same period, 8-10 g/L Sn^{2+} completely impeded the Fe^{2+} oxidation ability for both non-adapted planktonic and immobilised cells over a 500 h period (Figure 6-4C) while adapted planktonic cells achieved complete oxidation in the presence of 8 g /L Sn^{2+} and 40% oxidation at 10 g/L in 500 h. This difference showed that Cu-adapted cells had better tolerance to Sn^{2+} than non-adapted cells. Due to the complexity associated with precipitation of Sn, limited studies have reported on the effect of Sn on the bioleaching of PCBs (Brandl et al. 2001; Bryan et al. 2015; Ilyas et al. 2007). To the best of our knowledge, only. Bryan et al. (2015) investigated the inhibitory effect of Sn using a synthetic solution, and only up to 1.0 g/L Sn^{2+}. In addition to observed SnO precipitates, they reported microbial inhibition at 1.0 g/L Sn^{2+}, with their planktonic culture recovering only after about 500 h of

incubation (Bryan et al. 2015). The tolerance of the immobilised cells to elevated Sn^{2+} tested herein suggest the benefits of both immobilisation and prior adaptation to Cu.

Figure 6-5 shows a comparison of Fe^{2+} oxidation, in terms of % Fe^{2+} oxidised to Fe^{3+}, by both non- and Cu-adapted immobilised cells at increasing metal ions concentrations, within 80 h. Figure 6-6 shows comparison of the time taken to achieve complete microbial Fe^{2+} oxidation by all four set of inocula studied. Although the immobilised cells were adapted to Cu^{2+} only, they presented a better tolerance to increasing concentrations of all metals tested than non-adapted immobilised cells. This indicated that prior adaptation of the microbial culture to Cu^{2+} ions did not only improve their tolerance to Cu^{2+} but also to other inhibitory metal ions. (Li and Ke 2001) reported similar results with planktonic *At. ferrooxidans*-dominated culture, adapted to 25 g/L Cu^{2+}. Their Cu-adapted culture had higher tolerance to mixed metal ions (Cu^{2+}, Ni^{2+}, and Mg^{2+}) than Zn-adapted and non-adapted cultures. Moreover, their Cu-adapted culture exhibited higher bioleaching rates of nickel-bearing pyrrhotite (Li and Ke 2001). This ability of adapted cells to tolerate stress environments different to the adaptation conditions has also been reported by Xia et al. (2008). In their study, an *A. ferrooxidans* culture was adapted to 5% w/v chalcopyrite prior to assessing its ability to attach onto a mineral surface, and its tolerance to shear stress and Cu^{2+} in comparison to the non-adapted culture. The authors reported that in all these three extrinsic factors studied, the adapted culture performed better than non-adapted cells, and consequently, the adapted culture exhibited higher bioleaching rates (Xia et al. 2008).

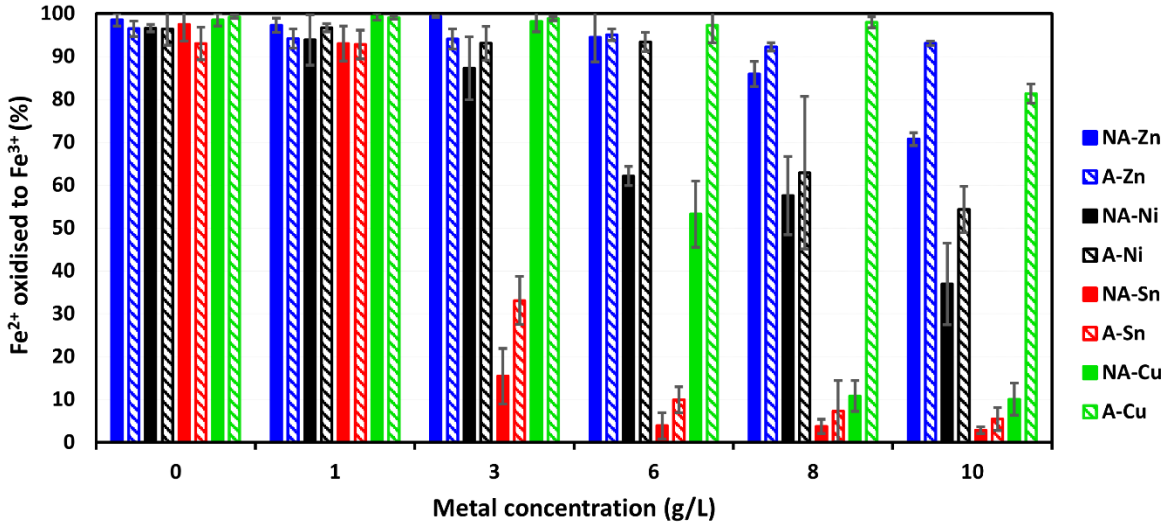

Figure 6-5 Fraction of Fe^{2+} oxidised (using a 5 g/L Fe^{2+} starting concentration) to Fe^{3+} by non-adapted immobilised cells (**NA-Zn**, **NA-Ni**, **NA-Cu**, and **NA-Sn**) and Cu-adapted immobilised cells (**A-Zn**, **A-Ni**, **A-Cu**, and **A-Sn**), at 80 h, when exposed to various concentrations (0-10 g/L) of individual metal ions (Zn^{2+}, Ni^{2+}, $Cu^{2+}$and Sn^{2+}). Error bars represent standard deviation, n= 3. Cu tolerance data presented here are presented in detail in (Maluleke et al. 2024b).

From Figure 6-5, it was evident that toxicity of the individual metal ions to both non- and Cu-adapted immobilised cells was as follows: $Sn^{2+} > Ni^{2+} > Zn^{2+}$. While the culture is more tolerant to Cu^{2+} than Ni^{2+} at concentrations of 3 g/L and below, the non-adapted culture is far more

inhibited by Cu^{2+} than Ni^{2+} in the concentration range of 6 – 10 g/L; however, following adaptation, the culture tolerates Cu^{2+} better than Ni^{2+} in the higher concentration range. This holds even when considering the additional Fe^{2+} oxidation required on exposure to Sn owing to its reduction of Fe^{3+}.

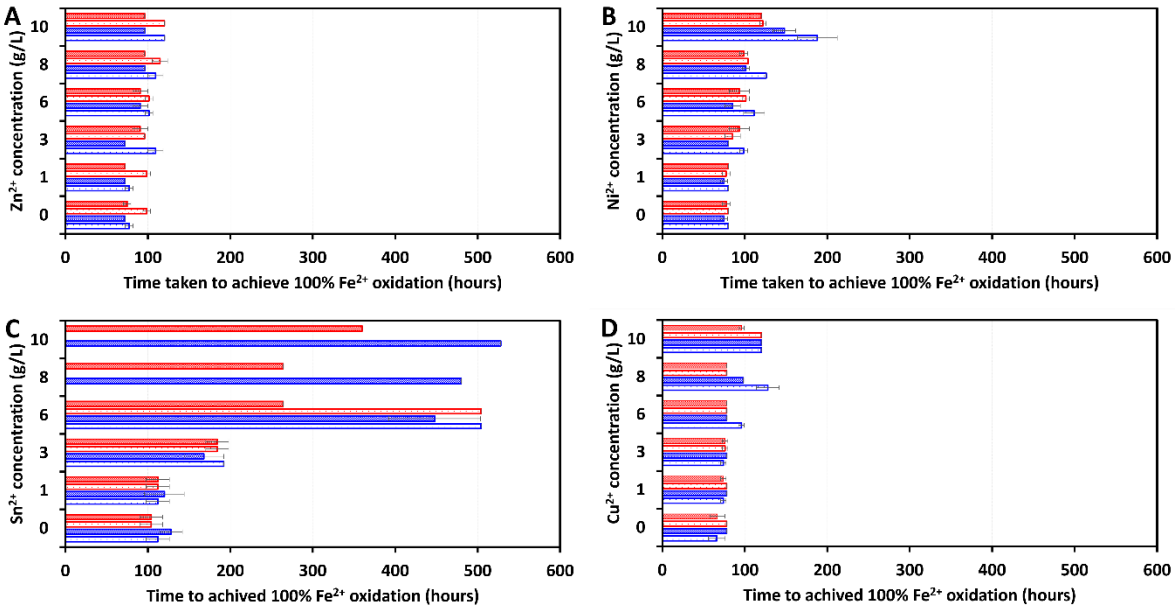

Figure 6-6 Time taken to achieve complete microbial Fe^{2+} oxidation by non-adapted planktonic cells (□), Cu-adapted planktonic cells (▩), non-adapted immobilised cells (▣), and Cu-adapted immobilised cells (▩); when exposed to increasing concentration of Zn^{2+} (**A**), Ni^{2+} (**B**), Sn^{2+} (**C**), and Cu^{2+} (**D**).

6.3.2 Effect of mixed metal ions on microbial Fe^{2+} ion oxidation

While trace amounts of metal ions such as Cu^{2+}, Zn^{2+}, are essential for microbial metabolism and growth, both individual and mixed metal ions inhibit the microbial culture at elevated concentrations (Nurmi et al. 2009; Ojumu et al. 2008; Tapia et al. 2022; Zhang et al. 2023). Inhibition by mixed metal ions may be exacerbated by the potential *in-situ* formation of complexes or by synergistic inhibition. In the bioleaching of PCBs, mixed base metals are leached and accumulate in solution simultaneously. Hence, understanding the tolerance of microbial cultures to mixed metal ions is vital in improving the bioleaching of PCBs. In Figure 6-7, Fe^{2+} utilisation by both non- and Cu-adapted planktonic and immobilised cells in the presence of mixed metal solutions, mimicking complete metal dissolution from PCB solid loadings of 0, 1, 5, 10, 15, and 20% w/v (Table 6-2) is presented.

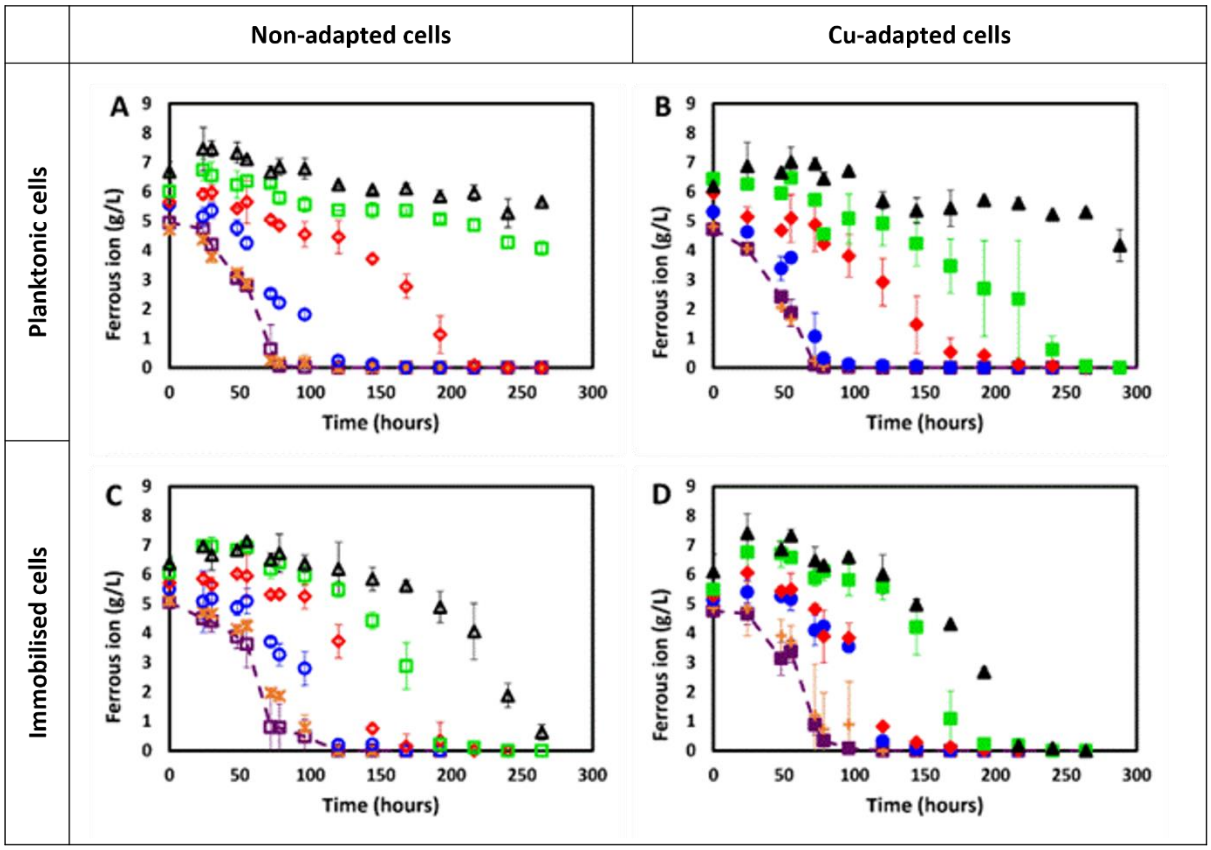

Figure 6-7 Microbial Fe^{2+} oxidation by non-adapted planktonic (**A**) and immobilised cells (**C**), and Cu-adapted planktonic (**B**) and immobilised cells (**D**) exposed to various concentrations of mixed metal ions (Cu^{2+}, Zn^{2+}, Sn^{2+}, and Ni^{2+}). Proportions of mixed metal ions were selected to mimic expected concentrations in solution at various PCB solid loading (0-20% w/v). Non-adapted cells **(A**, **C)**, 0% (-□-), 1% (✖), 5% (○), 10% (◇), 15% (□), and 20% (△)w/v. Cu-adapted cells (**B**, **D**), 0% (-■-), 1% (✚), 5% (●), 10% (◆), 15% (■), and 20% (▲)w/v. Error bars represent standard deviation, n = 3.

There was no effect on the Fe^{2+} oxidation using both non- and Cu-adapted cells at mixed metal concentrations simulating complete metal dissolution of 1% solids loading (Figure 6-7). The inhibitory effect of mixed metal ions was observed at the equivalent of 5% solids loading and above, evidenced by a lag phase, with the duration of the lag phase increasing with an increase in the amount of mixed metal ions added (Figure 6-7). Only about 25% and 38% Fe^{2+} was oxidised within 120 h for non-adapted planktonic and immobilised cells, respectively, subjected to mixed metal concentrations simulating a 10% solids loading (Figure 6-7A and C), compared to 43% and 68% Fe^{2+} oxidised by Cu-adapted planktonic and immobilised cells over the same period and at the same metal ion stress (Figure 6-7B and D). The two highest metal ion concentrations tested (15-20%) had a severe inhibitory effect to both non- and Cu-adapted cells, (Figure 6-7A-D). Figure 6-8 presents an increase in inhibition severity on microbial Fe^{2+} with an increase in simulated solid loading for both non- and Cu-adapted immobilised cells. Despite these delays, both microbial cultures adapted progressively to the metal ion stress, and complete Fe^{2+} oxidation was achieved within 264 h and 216 h for non- and Cu-adapted cells, respectively, in the presence of simulated 20% w/v. It is noteworthy that the tolerance

of immobilised cells to mixed metal ions surpassed that of planktonic cells. Non-adapted planktonic cells were completely inhibited at a simulated 20% solid loading (Figure 6-7A). However, adapting the culture to Cu^{2+} offered some improvement, with complete Fe^{2+} oxidisation achieved over 384 h.

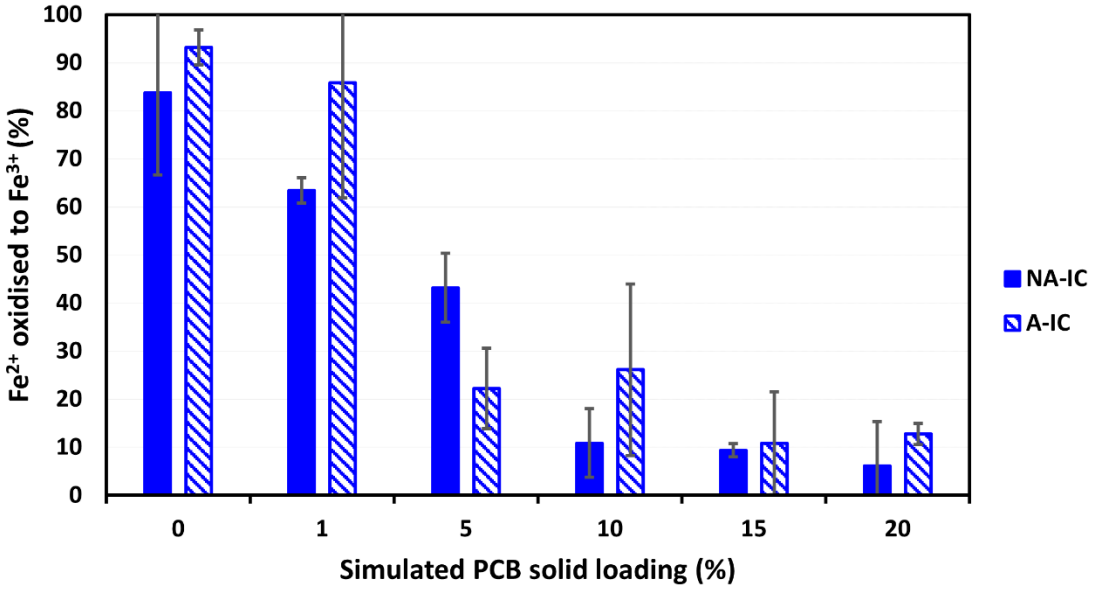

Figure 6-8 Fraction of Fe^{2+} oxidised (using a 5 g/L Fe^{2+} starting concentration) to Fe^{3+} by non-adapted immobilised cells (**NA-IC**) and Cu-adapted immobilised cells (**A-IC**), at 80 h, when exposed to various mixed metal composition representing simulated %PCB solid loading (0-20% w/v). Error bars represent standard deviation, n= 3.

Cu-adapted cells achieved complete microbial Fe^{2+} oxidation within 216 h when exposed to the mixed metal ion solution (34.91 g/L Cu^{2+}, 5.69 g/L Zn^{2+}, 1.13 g/L Ni^{2+}, and 2.99 g/L Sn^{2+}) from 20% solids loading, compared to complete Fe^{2+} oxidation achieved at 180 h, 100 h, and 150 h, for the Cu-adapted cells exposed to 39 g/L Cu^{2+} (Maluleke et al. 2024b), 6 g/L Zn^{2+} (Figure 6-1) and 1 g/L Ni^{2+} (Figure 6-2), and 3 g/L Sn^{2+} (Figure 6-4), respectively. This indicated that in comparison to individual metal ions, mixed metal ions had a stronger inhibitory effect, which could be attributed to a cumulative or synergistic effect with respect to individual metal ions. Similarly, this is found when comparing the residual Fe^{2+} concentration at 80 h across the single and mixed metal solutions at equivalent concentrations. In literature, most studies on the inhibition of metal ions on acidophilic cultures using synthetic solutions have focused on individual metal ions and planktonic cultures (Bryan et al. 2015; Edward et al. 2018; Khachatryan et al. 2021; Tapia et al. 2022; Xia et al. 2008). Das et al. (1997), Li and Ke (2001), and. Nurmi et al. (2009) investigated the potential inhibitory effect of typical metal ions in bioleaching leachates (Fe^{3+}, Fe^{2+}, Zn^{2+}, Cu^{2+}, Ni^{2+}, and Mg^{2+}) in their single, binary, and ternary combinations. In all these studies, the authors also reported synergistic inhibitory effects on cultures exposed to mixed metal ions, with ternary being more inhibitory than binary combinations (Das et al. 1997; Li and Ke 2001; Nurmi et al. 2009). To date, there is no study on the effect of mixed metal ions combined to mimic the metal proportions in PCBs. Although the concentrations of the metal ions Zn^{2+}, Ni^{2+}, Sn^{2+}, and others, may be low relative to that of Cu^{2+} in a typical PCB (Table 6-1), mimicking metal content of PCBs in this manner allows the

decoupling of potential inhibition by metallic and non-metallic components of the PCBs. The ability of the immobilised culture, particularly the Cu-adapted cells, to oxidise Fe^{2+} completely, even at the highest concentration of mixed metal tested is promising in terms of using the culture in the bioleaching of PCBs. Extending this study to metals, such as Al, Co, Cr, and Mg, also typically found in PCBs is recommended to further increase insight into understanding inhibition by a metallic component of the PCBs.

6.3.3 Effect of PCB leachates on microbial oxidation of Fe^{2+} ions

PCBs have the potential to exude non-metal compounds that are also inhibitory, hence the inhibitory effect of PCB leachates on the microbial activity of immobilised cells was also studied. The PCB leachates were prepared by abiotic Fe^{3+} leaching. Both non- and Cu-adapted immobilised cells were exposed to increasing concentrations of particulate-free PCB leachates ranging from the addition of 0, 10, 20, 30, 40, and 50% v/v leachate from 20% solids loading, which was approximately equivalent to 0-10% w/v solids loading of the PCB template. The immobilised cells were exposed to the PCB leachate solution to simulate the proposed two-staged reactor system in which the chemical leaching reactor is separated from but coupled to the microbial reactor; together these operate as a re-circulating continuous system. Hence, immobilised cells are only in contact with metal-rich leachates. The inhibitory effect of increasing the PCB leachate concentration on microbial Fe^{2+} oxidation is presented in Figure 6-9 below.

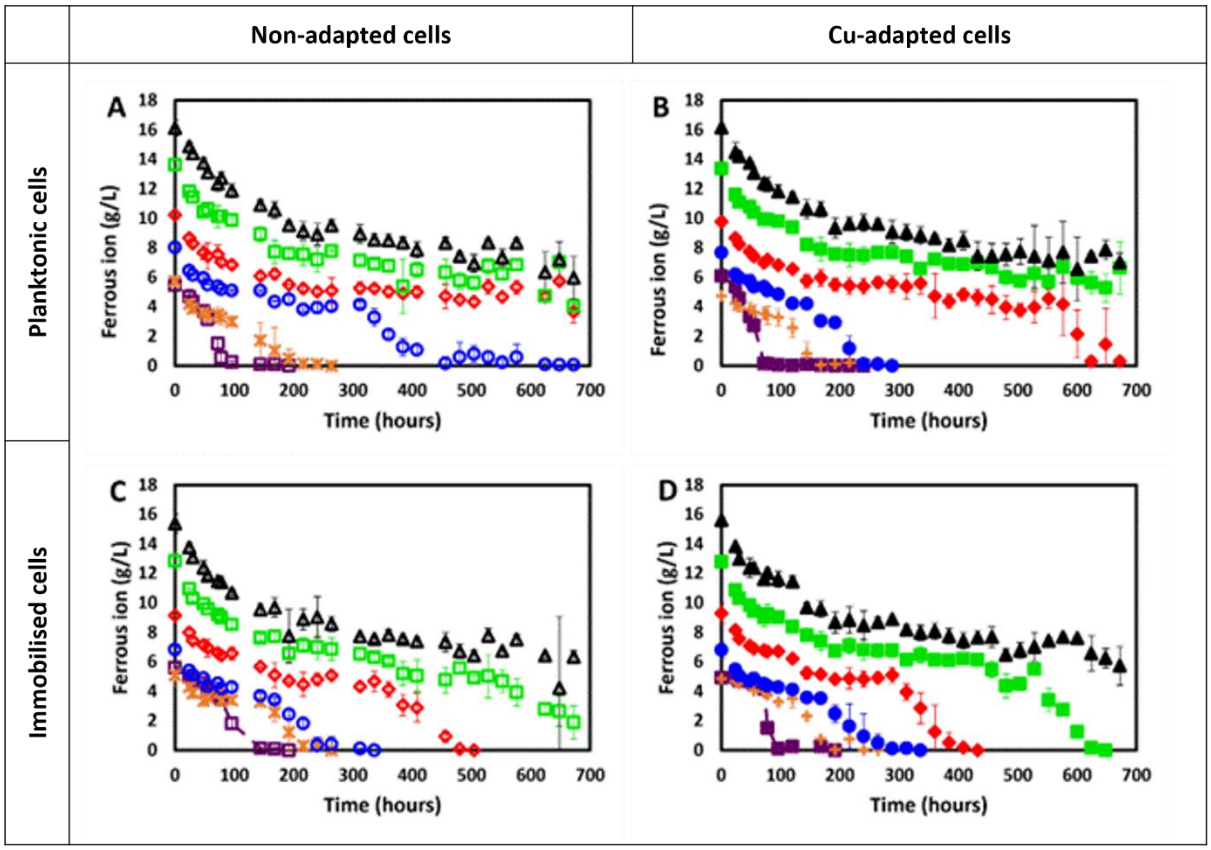

Figure 6-9 Microbial Fe^{2+} oxidation by non-adapted planktonic (**A**) and immobilised cells (**C**), and Cu-adapted planktonic (**B**) and immobilised cells (**D**) subjected to various concentration of PCB leachates (0-50% v/v). Non-adapted cells **(A**, **C)**, 0% ( ), 10% ( ), 20% ( ), 30% ( ), 40% ( ), and 50% ( )v/v. Cu-adapted cells (**B**, **D**) 0% ( ), 10% ( ), 20% ( ), 30% ( ), 40% ( ), and 50% v/v ( ). Error bars represent standard deviation, n = 3.

PCB leachates inhibited both non- and Cu-adapted cells from the lowest amount of leachate added of 10% v/v, with increasing severity with increasing concentration of PCB leachate (Figure 6-9A-D). With the addition of 10-20% leachate, by volume, from a 20% w/v PCB loading, Fe^{2+} oxidation was impeded, as evidenced by the lag phase of 168 h. However, both non- and Cu-adapted cultures recovered thereafter, and complete oxidation was achieved within a 300 h period, which suggests both cultures showed a similar level of inhibition. Microbial Fe^{2+} oxidisation was further impeded at 30% v/v. Nonetheless, Cu-adapted cells were able to completely oxidise all available Fe^{2+} ions at approximately 408 h (Figure 6-9D). While within the same period, non-adapted cells oxidised about 68% Fe^{2+} (Figure 6-9C). Increasing the PCB leachates to 40% v/v resulted in a lag phase of about 500 h, indicating a severe inhibitory effect on both cultures. Despite the cultures being compromised, Cu-adapted immobilised cells achieved complete Fe^{2+} oxidation at approximately 600 h, compared to 672 h for non-adapted immobilised cells. This suggested that Cu-adapted cells had better tolerance to increasing PCB concentration than non-adapted cells. At the highest concentration PCB leachates tested, 50% v/v, both cultures were completely inhibited over the 700 h experiment. Similar to observations in the presence of individual metals (Section 6.3.1) and mixed metals (Section 6.3.2), planktonic cells were more susceptible to increasing

concentrations of inhibitory metal ions than immobilised cells. Complete Fe^{2+} oxidation was achieved at 528 h for non-adapted planktonic cells subjected to 20% v/v PCB leachates and higher (Figure 6-9A). In contrast, for Cu-adapted planktonic cells subjected to 30% PCB leachates, 100% Fe^{2+} oxidation was achieved at 496 h and completely impeded at the higher concentrations tested (Figure 6-9B).

Limited studies have investigated the effect of PCB leachates on microbial Fe^{2+} oxidisation (Choi et al. 2004; Anaya-Garzon et al. 2021; Hubau et al. 2020), all using planktonic cultures typically with a 10% v/v inoculum (±10^7 cell/mL). To date, evaluation of inhibition of ferrous iron oxidation by immobilised cells in the presence of PCB leachates has not been reported. Using planktonic cells, authors reported that PCB leachates were inhibitory, with severity increasing with an increase in the concentration of leachate; however, these cultures generally showed progressive adaptation with time (Choi et al. 2004; Anaya-Garzon et al. 2021; Hubau et al. 2020). These planktonic results are consistent with the results in this present study. Anaya-Garzon et al. (2021) evaluated the inhibition of PCB leachates (0-80% v/v), prepared from Fe^{3+} leaching of 10% w/v PCB collected from various small appliances at the *Envie 2E Midi-Pyrenees* WEEE sorting centre (France), on a *L. ferriphilum* dominated culture, showing severe inhibition at 80% v/v. Caution should be practiced when comparing microbial tolerance to PCBs leachates (and solid PCBs) as PCBs are highly heterogenous, with different metallic and non-metallic contents.

When comparing the inhibitory effect of PCB leachates to that of individual and mixed metal ions, PCB leachates were more inhibitory under similar metal concentrations. At the highest concentration of PCB leachates tested, 50% v/v (11.1 g/L Cu, 0.0470 g/L Zn, 16.6 Fe g/L, 0.203 g/L Ni, and 0 g/L Sn), both the non- and Cu-adapted cells were severely impeded, while at the similar metal concentrations (individual and mixed metal ions), both cultures achieved complete oxidation. Complete microbial Fe^{2+} oxidation was achieved within 120 h by Cu-adapted immobilised cells subjected to individual Cu^{2+} (11 g/L), Zn^{2+} (1 g/L), Sn^{2+} (1 g/L), and Ni^{2+} (1 g/L). Within the same 120 h period, Cu-adapted cells oxidised 85% Fe^{2+} into Fe^{3+} when subjected to mixed metal composition simulating 10% PCB solid loading (Cu^{2+}: 17.5 g/L, Zn^{2+}: 2.8 g/L, Sn^{2+}: 1.50 g/L, and Ni^{2+}: 0.563 g/L). Although concentrations of these metal ions in individual and mixed metal compositions are higher than those in 50% v/v PCB leachates, only 27% Fe^{2+} was oxidised by Cu-adapted immobilised cells within 120 h. These PCB leachates are expected to contain both non-metallic components and other metal ions, which may contribute to the inhibitory effect.

6.4 Conclusion

This study investigated the inhibitory effect of Zn^{2+}, Sn^{2+}, and Ni^{2+}, as individual metal ions (0-10 g/L), in combination (simulating %PCB solid loading in the range of 0-20% w/v), and as PCB leachates (0-50% v/v) on the microbial Fe^{2+} oxidation by Cu-adapted immobilised cells. This performance was compared to both non-adapted immobilised cell cultures and to the performance of planktonic cultures, both in the presence and absence of copper adaptation. Cu-adapted immobilised cultures exhibited better tolerance across all inhibitory metal ions tested than non-adapted immobilised cells. This indicated that adapting the cultures not only improved their inhibitory tolerance to high Cu^{2+} concentrations, but also improved tolerance

toward Zn^{2+}, Sn^{2+}, Ni^{2+}, and even PCB leachates. Furthermore, in all cases using both adapted and non-adapted cultures, immobilised cultures performed better than planktonic cultures (of the same activity in the absence of the metal challenge) and showed more rapid adaptation to the metal or solute stress. These results show promise for the use of Cu-adapted immobilised microbial cultures in bioleaching of PCBs and other multi-metal concentrates. Microbial Fe^{2+} oxidation by immobilised cultures was impeded in the presence of 3-10 g/L of Ni^{2+} and Sn^{2+}, and the severity increased with an increase in the concentration of the metal ions. Despite these delays in Fe^{2+} oxidation, these cultures adapted progressively to high metal ion concentrations and complete Fe^{2+} oxidation was achieved even at the highest Zn^{2+}, Ni^{2+}, and Sn^{2+} concentrations tested. Inhibition of the individual metal ions on both non-adapted and Cu-adapted cultures was in the order of: $Sn^{2+} > Ni^{2+} > Sn^{2+}$. Cu^{2+} showed less inhibition than Ni^{2+} at low metal concentrations, but greater inhibition than Ni^{2+} at concentrations of 6 g/L and above. Mixed metal ions were more inhibitory to both cultures than individual metal ions suggesting a synergistic inhibitory effect with respect to individual metal ions. However, complete Fe^{2+} oxidation was achieved within 216 h by Cu-adapted cells, and at 264 h by non-adapted cells even at the highest concentration of metal ion tested (20% w/v). Finally, PCB leachates were more inhibitory than both individual and mixed metal ions. This was the case even where metal concentrations in PCB leachates were lower than in individual or mixed metal composition. Cu-adapted cells tolerated up to 40% v/v of a PCB leachate generated on complete chemical oxidation at a 20% solids loading, while non-adapted cells tolerated only up to 30% v/v; both cultures were completely inhibited at 50% v/v. High levels of inhibition by the PCB leachate could not be attributed to the dissolved metal ions, Cu^{2+}, Ni^{2+}, Sn^{2+}, and Zn^{2+} only, as the concentrations of these metals was lower than these tolerated in individual and mixed metals tested. It is postulated that the high levels of inhibition were due to synergistic action with the dissolved non-metallic component of the PCBs or the other dissolved metal ions (Cr, Co).

These findings support the development of a two-stage continuous progress for the bioleaching of base metals from WEEE in general, and specifically PCBs, in which an immobilised and adapted culture of Fe^{2+} oxidising microorganisms is used to maintain rapid generation of ferric iron for bioleaching of the PCBs.

6.5 References

Anaya-Garzon, J.; Hubau, A.; Joulian, C.; Guezennec, A.-G. (2021). Bioleaching of E-Waste: Influence of printed circuit boards on the activity of acidophilic iron-oxidizing bacteria. Frontiers in Microbiology 12, 669738. DOI: 10.3389/fmicb.2021.669738.

Armentia, H.; Webb, C. (1992). Ferrous sulphate oxidation using *Thiobacillus ferrooxidans* cells immobilised in polyurethane foam support particles. Applied Microbiology and Biotechnology 36 (5), 697–700. DOI: 10.1007/BF00183252.

Baniasadi, M.; Vakilchap, F.; Bahaloo-Horeh, N.; Mousavi, S. M.; Farnaud, S. (2019). Advances in bioleaching as a sustainable method for metal recovery from e-waste. A review. Journal of Industrial and Engineering Chemistry 76, 75–90. DOI: 10.1016/j.jiec.2019.03.047.

Bas, A. D.; Deveci, H.; Yazici, E. Y. (2013). Bioleaching of copper from low grade scrap TV circuit boards using mesophilic bacteria. Hydrometallurgy 138 (11), 65–70. DOI: 10.1016/j.hydromet.2013.06.015.

Brandl, H.; Bosshard, R.; Wegmann, M. (2001). Computer-munching microbes: Metal leaching from electronic scrap by bacteria and fungi. Hydrometallurgy 59 (2), 319–326. DOI: 10.1016/S0304-386X(00)00188-2.

Bryan, C. G.; Watkin, E. L.; McCredden, T. J.; Wong, Z. R.; Harrison, S.T.L.; Kaksonen, A. H. (2015). The use of pyrite as a source of lixiviant in the bioleaching of electronic waste. Hydrometallurgy 152 (2–3), 33–43. DOI: 10.1016/j.hydromet.2014.12.004.

Carvalho, M. de; Caldas, M.; Tenório, J.; Espinosa, D. (2018). Characterization of PCBs from obsolete computers aiming the recovery of precious metals. In Characterization of Minerals, Metals, and Materials 2018. TMS 2018. The Minerals, Metals & Materials Series. Springer, Cham. https://doi.org/10.1007/978-3-319-72484-3_16

Choi, M.-S.; Cho, K.-S.; Kim, D.-S.; Kim, D.-J. (2004). Microbial recovery of copper from printed circuit boards of waste computer by *Acidithiobacillus ferrooxidans*. Journal of Environmental Science and Health, Toxic/Hazardous Substances and Environmental Engineering 39 (11-12), 2973–2982. DOI: 10.1081/LESA-200034763.

Das, A.; Modak, J. M.; Natarajan, K. A. (1997). Studies on multi-metal ion tolerance of *Thiobacillus ferrooxidans*. Minerals Engineering 10 (7), 743–749. DOI: 10.1016/S0892-6875(97)00052-6.

Dopson, M.; Baker-Austin, C.; Koppineedi, P. R.; Bond, P. L. (2003). Growth in sulfidic mineral environments: Metal resistance mechanisms in acidophilic micro-organisms. Microbiology 149 (8), 1959–1970. DOI: 10.1099/mic.0.26296-0.

Duku, P. (2011). Biooxidation kinetics of *Leptospirillum ferriphilum* attached to a defined solid substrate. Master's thesis, University of Cape Town.

Edward, C. J.; Kotsiopoulos, A.; Harrison, S. T. L. (2018). Low-level thiocyanate concentrations impact on iron oxidation activity and growth of *Leptospirillum ferriphilum* through inhibition and adaptation. Research in Microbiology 169 (10), 576–581. DOI: 10.1016/j.resmic.2018.10.003.

Gómez, J. M.; Cantero, D.; Webb, C. (2000). Immobilisation of *Thiobacillus ferrooxidans* cells on nickel alloy fibre for ferrous sulfate oxidation. Applied Microbiology and Biotechnology 54 (3), 335–340. DOI: 10.1007/s002530000414.

González, A.; Bellenberg, S.; Mamani, S.; Ruiz, L.; Echeverría, A.; Soulère, L. et al. (2013). AHL signaling molecules with a large acyl chain enhance biofilm formation on sulfur and metal sulfides by the bioleaching bacterium *Acidithiobacillus ferrooxidans*. Applied Microbiology and Biotechnology 97 (8), 3729–3737. DOI: 10.1007/s00253-012-4229-3.

Govender, E.; Harrison, S.T.L.; Bryan, C. G. (2012). Modification of the ferric chloride assay for the spectrophotometric determination of ferric and total iron in acidic solutions containing

high concentrations of copper. Minerals Engineering 35, 46–48. DOI: 10.1016/j.mineng.2012.05.006.

Guo, C.; Wang, H.; Liang, W.; Fu, J.; Yi, X. (2011). Liberation characteristic and physical separation of printed circuit board (PCB). Waste Management 31 (9), 2161–2166. DOI: 10.1016/j.wasman.2011.05.011.

Horn, H.; Neu, T. R.; Wulkow, M. (2001). Modelling the structure and function of extracellular polymeric substances in biofilms with new numerical techniques. Water Science and Technology 43 (6), 121–127. DOI: 10.2166/wst.2001.0355.

Hubau, A.; Minier, M.; Chagnes, A.; Joulian, C.; Silvente, C.; Guezennec, A.-G. (2020). Recovery of metals in a double-stage continuous bioreactor for acidic bioleaching of printed circuit boards (PCBs). Separation and Purification Technology 238 (3), 116481. DOI: 10.1016/j.seppur.2019.116481.

Ilyas, S.; Anwar, M. A.; Niazi, S. B.; Afzal Ghauri, M. (2007). Bioleaching of metals from electronic scrap by moderately thermophilic acidophilic bacteria. Hydrometallurgy 88 (1-4), 180–188. DOI: 10.1016/j.hydromet.2007.04.007.

Ilyas, S.; Ruan, C.; Bhatti, H. N.; Ghauri, M. A.; Anwar, M. A. (2010). Column bioleaching of metals from electronic scrap. Hydrometallurgy 101 (3-4), 135–140. DOI: 10.1016/j.hydromet.2009.12.007.

Islam, A.; Ahmed, T.; Awual, M. R.; Rahman, A.; Sultana, M.; Aziz, A. A. et al. (2020). Advances in sustainable approaches to recover metals from e-waste-A review. Journal of Cleaner Production 244, 118815. DOI: 10.1016/j.jclepro.2019.118815.

Ji, X.; Yang, M.; Wan, A.; Yu, S.; Yao, Z. (2022). Bioleaching of typical electronic waste—Printed Circuit Boards (WPCBs). A Short Review. International Journal of Environmental Research and Public Health 19 (12), 7508. DOI: 10.3390/ijerph19127508.

Johnson, D. B.; Joulian, C.; d'Hugues, P.; Hallberg, K. B. (2008). *Sulfobacillus benefaciens* sp. nov., an acidophilic facultative anaerobic Firmicute isolated from mineral bioleaching operations. Extremophiles 12 (6), 789–798. DOI: 10.1007/s00792-008-0184-4.

Khachatryan, A.; Vardanyan, N.; Vardanyan, A.; Zhang, R.; Castro, L. (2021). The effect of metal ions on the growth and ferrous iron oxidation by *Leptospirillum ferriphilum CC* Isolated from Armenia Mine Sites. Metals 11 (3), 425. DOI: 10.3390/met11030425.

Kolmert, s.; Johnson, D. B. (2001). Remediation of acidic waste waters using immobilised, acidophilic sulfate-reducing bacteria. Journal of Chemical Technology and Biotechnology 76 (8), 836–843. DOI: 10.1002/jctb.453.

Lambert, F.; Gaydardzhiev, S.; Léonard, G.; Lewis, G.; Bareel, P.-F.; Bastin, D. (2015). Copper leaching from waste electric cables by biohydrometallurgy. Minerals Engineering 76 (1), 38–46. DOI: 10.1016/j.mineng.2014.12.029.

Li, H.-m.; Ke, J.-j. (2001). Influence of Ni^{2+} and Mg^{2+} on the growth and activity of Cu^{2+}-adapted *Thiobacillus ferrooxidans*. Hydrometallurgy 61 (3), 151–156. DOI: 10.1016/S0304-386X(01)00167-0.

Liu, X.; Liu, H.; Wu, W.; Zhang, X.; Gu, T.; Zhu, M.; Tan, W. (2019). Oxidative stress induced by metal ions in bioleaching of $LiCoO_2$ by an Acidophilic microbial consortium. Frontiers in Microbiology 10, 3058. DOI: 10.3389/fmicb.2019.03058.

Maluleke M D.; Kotsiopoulos, A.; Govender-Opitz E; Harrison, S.T.L. (2023). Exploring microbial adaptation of immobilised acidophilic cultures to improve microbial oxidation rates and copper tolerance in e-waste bioleaching. Minerals Engineering 207 (3), 108560. DOI: 10.1016/j.mineng.2023.108560.

Moosakazemi, F.; Ghassa, S.; Jafari, M.; Chelgani, S. C. (2022). Bioleaching for recovery of metals from spent batteries – A Review. Mineral Processing and Extractive Metallurgy Review 23 (2), 1–11. DOI: 10.1080/08827508.2022.2095376.

Nemati, M.; Harrison, S.T.L.; Hansford, G. S.; Webb, C. (1998). Biological oxidation of ferrous sulphate by *Thiobacillus ferrooxidans*. A review on the kinetic aspects. Biochemical Engineering Journal 1 (3), 171–190. DOI: 10.1016/S1369-703X(98)00006-0.

Nemati, M.; Webb, C. (1996). Effect of ferrous iron concentration on the catalytic activity of immobilized cells of *Thiobacillus ferrooxidans*. Applied Microbiology and Biotechnology 46 (3), 250–255. DOI: 10.1007/s002530050812.

Nurmi, P.; Özkaya, B.; Kaksonen, A. H.; Tuovinen, O. H.; Puhakka, J. A. (2009). Inhibition kinetics of iron oxidation by *Leptospirillum ferriphilum* in the presence of ferric, nickel and zinc ions. Hydrometallurgy 97 (3-4), 137–145. DOI: 10.1016/j.hydromet.2009.02.003.

Ojumu, T. V.; Petersen, J.; Hansford, G. S. (2008). The effect of dissolved cations on microbial ferrous-iron oxidation by *Leptospirillum ferriphilum* in continuous culture. Hydrometallurgy 94 (1-4), 69–76. DOI: 10.1016/j.hydromet.2008.05.047.

Ozkaya, B.; Sahinkaya, E.; Nurmi, P.; Kaksonen, A. H.; Puhakka, J. A. (2007). Kinetics of iron oxidation by *Leptospirillum ferriphilum* dominated culture at pH below one. Biotechnology and Bioengineering 97 (5), 1121–1127. DOI: 10.1002/bit.21313.

Priya, A.; Hait, S. (2018). Extraction of metals from high grade waste printed circuit board by conventional and hybrid bioleaching using *Acidithiobacillus ferrooxidans*. Hydrometallurgy 177, 132–139. DOI: 10.1016/j.hydromet.2018.03.005.

Tapia, J.; Dueñas, A.; Cheje, N.; Soclle, G.; Patiño, N.; Ancalla, W. et al. (2022). Bioleaching of heavy metals from printed circuit boards with an Acidophilic iron-oxidizing microbial consortium in stirred tank reactors. Bioengineering 9 (2), 79. DOI: 10.3390/bioengineering9020079.

Tian, J.; Wu, N.; Li, J.; Liu, Y.; Guo, J.; Yao, B.; Fan, Y. (2007). Nickel-resistant determinant from *Leptospirillum ferriphilum*. Applied and Environmental Microbiology 73 (7), 2364–2368. DOI: 10.1128/AEM.00207-07.

Tuncuk, A.; Stazi, V.; Akcil, A.; Yazici, E. Y.; Deveci, H. (2012). Aqueous metal recovery techniques from e-scrap. Hydrometallurgy in recycling. Minerals Engineering 25 (1), 28–37. DOI: 10.1016/j.mineng.2011.09.019.

Tupikina, O. V.; Minnaar, S. H.; van Hille, R. P.; van Wyk, N.; Rautenbach, G. F.; Dew, D.; Harrison, S.T.L. (2013). Determining the effect of acid stress on the persistence and growth of thermophilic microbial species after mesophilic colonisation of low grade ore in a heap leach environment. Minerals Engineering 53 (4), 152–159. DOI: 10.1016/j.mineng.2013.07.015.

Wu, W.; Liu, X.; Zhang, X.; Zhu, M.; Tan, W. (2018). Bioleaching of copper from waste printed circuit boards by bacteria-free cultural supernatant of iron–sulfur-oxidizing bacteria. Bioresources and Bioprocessing 5 (1), 233. DOI: 10.1186/s40643-018-0196-6.

Xia, L.; Liu, X.; Zeng, J.; Yin, C.; Gao, J.; Liu, J.; Qiu, G. (2008). Mechanism of enhanced bioleaching efficiency of *Acidithiobacillus ferrooxidans* after adaptation with chalcopyrite. Hydrometallurgy 92 (3), 95–101. DOI: 10.1016/j.hydromet.2008.01.002.

Xia, M.-C.; Wang, Y.-P.; Peng, T.-J.; Shen, L.; Yu, R.-L.; Liu, Y.-D. et al. (2017). Recycling of metals from pretreated waste printed circuit boards effectively in stirred tank reactor by a moderately thermophilic culture. Journal of Bioscience and Bioengineering 123 (6), 714–721. DOI: 10.1016/j.jbiosc.2016.12.017.

Xiang, Y.; Wu, P.; Zhu, N.; Zhang, T.; Liu, W.; Wu, J.; Li, P. (2010). Bioleaching of copper from waste printed circuit boards by bacterial consortium enriched from acid mine drainage. Journal of Hazardous Materials 184 (1), 812–818. DOI: 10.1016/j.jhazmat.2010.08.113.

Xu, Y.; Yin, H.; Jiang, H.; Liang, Y.; Guo, X.; Ma, L. et al. (2013). Comparative study of nickel resistance of pure culture and co-culture of *Acidithiobacillus thiooxidans* and *Leptospirillum ferriphilum*. Archives of Microbiology 195 (9), 637–646. DOI: 10.1007/s00203-013-0900-z.

Yang, C.; Tan, Q.; Liu, L.; Dong, Q.; Li, J. (2017). Recycling Tin from Electronic Waste. A problem that needs more attention. ACS Sustainable Chem. Eng. 5 (11), 9586–9598. DOI: 10.1021/acssuschemeng.7b02903.

Yang, T.; Xu, Z.; Wen, J.; Yang, L. (2009). Factors influencing bioleaching copper from waste printed circuit boards by *Acidithiobacillus ferrooxidans*. Hydrometallurgy 97 (1-2), 29–32. DOI: 10.1016/j.hydromet.2008.12.011.

Yazici, E. Y.; Deveci, H. (2014). Ferric sulphate leaching of metals from waste printed circuit boards. International Journal of Mineral Processing 133 (4), 39–45. DOI: 10.1016/j.minpro.2014.09.015.

Zhang, X.; Shi, H.; Tan, N.; Zhu, M.; Tan, W.; Daramola, D.; Gu, T. (2023). Advances in bioleaching of waste lithium batteries under metal ion stress. Bioresources and Bioprocessing. 10 (1), 2193. DOI: 10.1186/s40643-023-00636-5.

Zhu, N.; Xiang, Y.; Zhang, T.; Wu, P.; Dang, Z.; Li, P.; Wu, J. (2011). Bioleaching of metal concentrates of waste printed circuit boards by mixed culture of acidophilic bacteria. Journal of Hazardous Materials 192 (2), 614–619. DOI: 10.1016/j.jhazmat.2011.05.062.

CHAPTER 7

7 Bioleaching of printed circuit boards in a two-stage reactor system with enhanced ferric iron regeneration in a re-circulating packed-bed bioreactor

This chapter presents the bioleaching of printed circuit boards (PCBs) in a novel two-stage bioleaching reactor system. The chemical leaching kinetic knowledge (Fe^{3+} reduction rates) obtained through chemical leaching studies presented in Chapter 4 and the insight into mitigation of the inhibition of the microbial culture to maintain effective microbial Fe^{2+} oxidation rates presented in Chapters 5 and 6 were integrated to inform the configuration of the two-stage reactor system. Owing to the improved metal tolerance exhibited by Cu-adapted immobilised cells (A-IC), the integrated bioleaching system made use of A-IC immobilised on PUF-BSPs to leach pre-prepared PCBs in both one- and two-stage reactor systems. The highest volumetric Fe^{3+} reduction rate as a function of metal leaching across all Fe^{3+} leaching experiments at 37 °C was 8.15 g $Fe^{3+}.L^{-1}.h^{-1}$, observed for the Fe^{3+} leaching of mixed elementary metals. Conversely, a Fe^{2+} oxidation rate of 0.0802 g $Fe^{3+}.L^{-1}.h^{-1}$ by 3 units of PUF-BSPs with A-IC at the same temperature in the absence of inhibition was calculated. This meant that about 300 PUF-BSP units were required to match the Fe^{3+} reduction and microbial regeneration rates. Thus, 300 PUF-BSPs were packed into 6 columns (50 each column). The packed columns were connected in series and coupled to a stirred tank reactor for the chemical leaching of PCBs. On Fe^{3+} leaching of PCBs, the metal-rich stream was recirculated between the two reactors using a peristaltic pump at a flowrate of 0.5 L/h such that a residence time of 4 days across the columns was achieved. The 4 day residence time was informed by a 96 – 100 h period typically required to achieve complete Fe^{2+} oxidation in batch microbial activity studies (Part 2) in the absence of metal ions (no inhibitory metal added). As high initial concentrations of inhibitory metals added were observed to prolong the lag phase and adversely impeded Fe^{2+} oxidation, PCBs were added at an incremental rate of 3% w/v PCBs to minimise metal stress shock to the microbial culture. A one-stage reactor where both Fe^{3+} leaching and microbial Fe^{3+} regeneration occurred in one pot was considered.

In line with the overarching aims of this PhD project, the main result of this study was aimed at achieving matched volumetric rates of ferric leaching of base metals from PCBs with the microbial ferric regeneration rates.

Authors' contributions

Musa Maluleke, in collaboration with supervisors, Sue Harrison, Athanasios Kotsiopoulos, and Elaine Govender-Opitz conceptualised the experiment approach. Musa Maluleke designed

and performed the experiments. Data analysis was undertaken by Musa Maluleke under guidance of both primary and co-supervisors. The draft manuscript were prepared by Musa Maluleke and critically reviewed and edited by Sue Harrison, Athanasios Kotsiopoulos, and Elaine Govender-Opitz. The final draft was approved by the primary supervisor as a corresponding author.

Journal title: Bioleaching of printed circuit boards in a two-stage reactor system with enhanced ferric iron regeneration in a re-circulating packed-bed reactor from PCB leaching

Musa D. Maluleke, Athanasios Kotsiopoulos, Elaine Govender-Opitz, Susan T.L. Harrison

Centre for Bioprocess Engineering Research (CeBER), Department of Chemical Engineering, University of Cape Town, Rondebosch, Cape Town 7700, South Africa

Draft manuscript

Abstract

We report the bio-assisted leaching of PCBs in a continuous two-stage reactor system, comprised of a stirred tank reactor for chemical leaching of PCBs through the reduction of ferric iron, coupled to a packed-bed column bioreactor in which biological ferrous iron oxidation is optimised to regenerate the ferric leach agent. The bioreactor was packed with polyurethane foam biomass support particles colonised with the mesophilic mixed culture, dominated by *Leptospirillum ferriphilum*. On chemical leaching of the PCBs with acidic ferric iron in the stirred tank reactor, a ferrous-rich solution was generated and circulated through the packed bed bioreactor to re-oxidise the ferrous iron to ferric iron. A one-stage reactor system, where both PCB leaching and re-oxidation of the resultant ferrous iron occur in one pot, was run concurrently. PCB loading was varied from 3% to 18% (w/v) and the regeneration of the required ferric iron for leaching was studied. In both one- and two-stage systems, high bioleaching efficiency was achieved, with the two-stage system achieving 98% Al, 58% Ca, 93% Cr, 96% Cu, >100% Mg, 79% Ni, 80% Pb, >100% Sn, >100% Zn solubilisation from 18% PCB solid loading, whereas low release of 7% Co and 11% Sr was achieved. Despite the high PCB solid loading, microbial cultures maintained their oxidative activity post exposure to the leached metals, with more rapid Fe^{3+} regeneration occurring in the two-stage compared to the one-stage system. The two-stage reactor system exhibited an improvement of about 60% in the ratio of the Fe^{3+} reduction and regeneration rates relative to the one-stage reactor system. These findings present a promising approach to maximising metal recovery while maintaining and improving microbial activity in the bioleaching of PCBs. Such insight into the bioleaching of the elemental form of base metals from PCBs at the reactor level contributes to process design and optimisation, to enable upscaling and subsequent commercialisation of the process.

7.1 Introduction

Rapid advancement in renewable energy technologies, electric cars, low carbon technologies and electronic devices, amongst others, has led to a significant increase in demand for metals such as copper, cobalt, gallium, lithium, magnesium, neodymium, nickel. Consequently, there is an increasing deficit between the supply of these metals through the mining of virgin ores and their demand to support the growth in technology to support the move to a low carbon economy (Deetman et al. 2018; Oliveira et al. 2021; Watari et al. 2021; Zhang et al. 2017).

Moreover, the short life span of electronic devices has resulted in an environmental burden of electronic waste (e-waste) and the need to avoid its disposal in landfills. In addition, typical waste electrical and electronic equipment (WEEE) is far richer in metals than low-grade mineral ores. Together, these highlight the potential of mining of secondary resources and gaining traction toward a circular economy and sustainable practices that minimise the mining of virgin ores.

High concentrations of metals of value such as Cu, Zn, Ni, Co, Au, Al, and their high purity in e-waste has centered e-waste as one of the best secondary resources for these metals. Printed circuit boards (PCBs), one of the main and metal-rich components of e-waste, typically constitute 3-6% of the weight of e-waste and are increasingly targeted for recycling of metals of value. Extraction of base metals from PCBs through bioleaching prior to recovery of platinum group metals (PGMs) and other precious metals, including gold, continues to receive attention as a potential technology offering economic and environmental advantages, particularly for low-grade PCB treatment (Tuncuk et al. 2012a). In bioleaching, metal dissolution occurs through acidic ferric iron (Fe^{3+}) oxidation to solubilise and mobilise metals from PCBs into solution, with the concomitant reduction to ferrous iron (Fe^{2+}) (Eq. 7-1). Acidophilic microorganisms such as *Leptospirillum* (*L.*) *ferriphilum*, *L. ferrooxidans*, *Acidithiobacillus* (*At.*) *ferrooxidans*, *Acidiplasma* (*Ap.*) *cupricumulans*, *Ferroplasma* sp., use the resultant Fe^{2+} as an energy source through oxidising it to Fe^{3+} (Eq. 7-2). This regeneration of the Fe^{3+} leaching agent sustains and catalyses the bioleaching process (Adetunji et al. 2023).

$$2Fe^{3+} + M^0 \rightarrow 2Fe^{2+} + M^{2+} \qquad \textit{Eq. 7-1}$$

$$2Fe^{2+} + 0.5O_2 + 2H^+ \xrightarrow{Microorganisms} 2Fe^{3+} + H_2O \qquad \textit{Eq. 7-2}$$

One of the drivers towards bioleaching as an alternative to conventional pyrometallurgical approaches is the potential to recover metals selectively. An advantage over a conventional hydrometallurgical approach is this *in-situ* continuous regeneration of the Fe^{3+} leaching agent (Eq. 7-2), minimising ongoing addition of fresh leaching agent as well as resultant effluent. Despite advancement in bioleaching and its application at an industrial scale for extraction of metals such as Cu, Au, Ni, and Co from their respective virgin ores (Rawlings and Johnson 2007a; Morin 2008; Bryan et al. 2011; Harrison 2016b; Kaksonen et al. 2018), there is, to date, no commercial process for bioleaching of PCBs for base metal recovery. Extensive studies on bioleaching of PCBs using batch shake flask experiments are reported to explore operating factors such as appropriate solution pH of the system, choice of microbial consortia, particle size of the PCBs, effect of dissolved metal ions on microbial consortia. (Yang et al. 2009; Xia et al. 2017; Ji et al. 2022b; Adetunji et al. 2023; Anaya-Garzon et al. 2021). While these studies are useful for proof of concept and to determine operating windows, they have limited value for process optimisation. Of the limited studies that have investigated bioleaching of PCBs at reactor level, few have considered reactors above 1 L capacity (Rodrigues et al. 2015; Ilyas and Lee 2014; Xia et al. 2017; Hubau et al. 2020; Tapia et al. 2022). Ilyas et al. (2013) investigated bioleaching of PCBs by a planktonic *Sulfobacillus thermosulfidooxidans* and *Thermoplasma*

acidophilum dominated moderate thermophilic culture in a laboratory scale column (height: 58 cm and internal diameter: 13 cm, 2 L capacity), packed with 10 kg of pulverised PCBs, and coupled to a solution reservoir. The culture was recirculated between the column and the reservoir using a peristaltic pump. The culture was adapted to 20 g/L of mixed metal ions (Al^{3+}, Ni^{2+}, Fe^{3+}, Pb^{2+}, Sn^{2+}, Ag^{+}, and Zn^{2+}) over a two year period. The authors reported that about 78% Ni, 68% Al, 74% Zn, and 85% Cu were bioleached after 165 days (Ilyas et al. 2013). In a similar study, Chen et al. (2015) achieved 95% Cu extraction in a column bioreactor (height: 20 cm, internal diameter: 6.0 cm, and volume: 5 L, packed with 250 g pulverised PCB) when bioleaching the PCBs with planktonic *At. ferrooxidans* over 28 days. The reactor was operated in a manner similar to Ilyas et al. (2013). Their study further highlighted the influence of Fe^{3+} concentration on Cu extraction and they showed that Cu dissolution was impacted by diffusion of the leach agent to the reaction site which was impacted by jarosite precipitation on the surface of the PCBs (Chen et al. 2015), thus highlighting the importance of maintaining pH below 2. Recently, Tapia et al. (2022) investigated bioleaching of PCBs in a single stage stirred tank bioreactor (3L working volume) using a planktonic mixed mesophilic culture dominated by *Tissierella*, *Acidophilium* and *Leptospirillum* species, adapted to 5 g/L PCBs. The authors reported 69% Cu and 91% Zn extraction from 1% PCBs over 18 days.

Notwithstanding the proof of concept of bioleaching of PCBs and high metal extraction reported, there is, to date, no commercial PCB bioleaching process. One major challenge toward establishing this is the inhibition of the microbial culture by both the metals dissolved from PCBs, particularly as it is desirable to achieve high metal concentrations for efficient metal recovery, and the non-metallic component of the PCBs (Brandl et al. 2001; Bryan et al. 2015; Hubau et al. 2020; Lambert et al. 2015; Tapia et al. 2022), thus limiting the rate of microbial regeneration of Fe^{3+} (Eq. 2). Lambert et al. (2015) observed only a small improvement in leaching performance when bioleaching Cu from waste electric cables using *At. ferrooxidans* over chemical leaching in the absence of microorganisms and using the same starting ferric ion concentration, indicative of limited microbial Fe^{3+} regeneration. They attributed this limited benefit of the microorganisms in the system to their inhibition by the plastic components of the waste electric cables (Lambert et al. 2015). Tapia et al. (2022) studied microbial growth and ferrous iron oxidation of a mixed culture consisting of *Tissierella*, *Acidophilium*, and *Leptospirillum* in the presence of various concentrations of PCBs (0.5, 1.0, 1.5, and 2.0% PCBs). Although the culture was adapted to 0.5% PCB loading, the authors observed limited cell growth at 1.5 and 2.0 % PCBs, indicative of inhibition of the microbial culture.

Microbial adaptation to potential inhibitors (metal ions, pH, virgin ores, organics, and PCBs) in the system is widely used to minimise inhibition of microbial cultures (Ilyas et al. 2010; Arshadi and Mousavi 2014; Xia et al. 2017; Baniasadi et al. 2019; Ji et al. 2022b). Cu-adapted *At. ferrooxidans* outperformed a non-adapted culture when subject to high Cu^{2+} concentrations (50 g/L) and shear stress, thus the adapted culture exhibited higher bioleaching rates (Xia et al. 2008). We showed that the Cu-adapted culture established using an inoculum containing *L. ferriphilum*, *L. ferrooxidans* and *At. caldus* exhibited better tolerance to individual Cu^{2+} (50 g/L) (Maluleke et al. 2024b), to Zn^{2+} (10 g/L), Ni^{2+} (10 g/L), Sn^{2+} (10 g/L), mixed metals (Cu^{2+},

Zn^{2+}, Ni^{2+}, and Sn^{2+}), and to PCB leachates (40% v/v) when compared to non-adapted culture (Maluleke et al. 2024a).

Microbial immobilisation systems, in which microbial cells are colonised onto a biomass support structure has also been explored in mitigation of microbial inhibition in bioleaching systems. The biofilm associated with colonised cells has been reported to aid in minimising contact between cells and toxic metal ions, while the high cell retention facilitates faster Fe^{3+} regeneration (Bruins et al. 2000; Nemati et al. 1998; Nemati and Webb 1996; Dopson et al. 2003; Maluleke et al. 2024a, 2024a). Lately, there has been a growing interest in the use of a two-step bioleaching system for PCB bioleaching. In this approach, microbial growth and generation of the required Fe^{3+} oxidant is carried out in the absence of PCBs, whereafter, PCBs are contacted with the generated Fe^{3+} oxidant for metal leaching. Wu et al. (2018) reported 93% Cu extraction from 10% PCB solids loading (w/v) over 9 days through the two-stage process in which the production of the Fe^{3+} leaching agent (15 g/L) was carried out in batch in a 250 mL Erlenmeyer flask by planktonic *L. ferriphilum* and *Sulfobacillus thermosulfidooxidans* (Wu et al. 2018). Hubau et al. (2020) investigated a two-stage reactor system, where the production of Fe^{3+} from Fe^{2+} was achieved in a partially fluidized bubble column by *L. ferriphilum* and *Sulfobacillus benefaciens* immobilised on activated charcoal, before being fed into a stirred tank containing PCBs. Hubau et al. (2020) achieved 96% Cu, 73% Ni, 85% Zn, and 93% Co from 1% (w/v) PCBs at a 48 h hydraulic residence time, but reported microbial inhibition from 1.8% PCBs.

Limited studies have focused on microbial activity post exposure to solutions generated during PCB leaching i.e., in the presence of accumulated leached metal ions and extracts from the PCB resins. This study considers the use of a two-stage bioleaching reactor system, in which a packed-bed column bioreactor for continuous Fe^{3+} regeneration is coupled with a stirred tank reactor containing PCBs for chemical leaching. The column, packed with polyurethane foam biomass support particles (PUF-BSP) onto which the microbial culture is immobilised, is the site of production of the Fe^{3+} oxidant. The Fe^{3+}-rich stream exiting the column bioreactor was pumped into the stirred tank reactor for PCB leaching. The resultant Fe^{2+}-rich stream was recirculated back into the packed columns for Fe^{3+} regeneration. The ability of the bioreactor to regenerate Fe^{3+} at increasing PCB solid loading, and hence increasing solubilised metal concentrations was assessed. A comparative experiment was carried out in a one-stage reactor system in which Fe^{3+} regeneration and PCB leaching occur together in the stirred tank reactor. We hypothesised that the immobilised microbial system allows high cell concentrations to be achieved. Further, the diffusional resistance of metal transport to the enriched biomass accumulation sites within the interstitial regions and within the biofilm associated with colonised cells aids in minimising inhibition (González et al. 2013; Nemati and Webb 1996; Rohwerder et al. 2003; Sand and Gehrke 2006; Govender-Opitz et al. 2017); the latter has been demonstrated in Maluleke et al. (2024a and b). Successful immobilisation of the mixed mesophilic culture on PUF has already been confirmed by visual analysis of the microbial colonised PUF cubes by scanning microscope (SEM) (Maluleke et al. 2024b). Their improved activity over planktonic cells in the presence of potential inhibitory metals Cu^{2+}, Ni^{2+}, Sn^{2+}, and Zn^{2+} has been demonstrated in Maluleke et al. (2024a and b). Hence, in this study, we explore the potential for improved metal solubilisation from PCBs using the two-stage

bioreactor system with PUF-BSPs. In addition to the potential for improved performance, the two-stage configuration allows for inter-stage metal recovery to minimise metal ion accumulation and subsequent microbial inhibition in the bioreactor.

7.2 Materials and methods

7.2.1 Preparation of PCBs

Printed circuit boards used in this study were custom manufactured by Trax Interconnect (Pty) Ltd, one of the largest PCBs manufacturing companies in Cape Town, South Africa. Although the PCBs had no extraneous components (i.e., RAMs, PCI, and chip slots) soldered on, they represent the typical base design that the company's clients most frequently request. PCBs were first reduced by shredding the whole board using a bench Industrial Grab Shredder (length: 170 mm, width: 140 mm, and 14 circular blades) supplied by Filamaker Gmbh, Germany. Briefly, the whole board was shredded repetitively by passing the same board through the shredder six times (6x). The number of passes was informed by Prestele (2020a), who demonstrated that no further size reduction occurred above 6 passes. The shredded boards (PCB chips) were further reduced by pulverising for at least 20 seconds using a ring mill pulveriser supplied by The Ferguson Industrial Equipment group, Johannesburg, South Africa. Pulverising for 20 seconds further liberates metals by mechanical disruption of the outer layers of the PCBs and enabled further size reduction after shredding. The particle size distribution of the prepared PCB chips was determined by dry sieving the pulverised samples into five fractions (<1180 µm, 1180 µm, 1700 µm, 3350 µm, and 4750 µm) over 10 minutes using a sieve shaker (Filtra FTL0200). Results are shown in Figure 7-1. This material was representatively split for both analysis and test work.

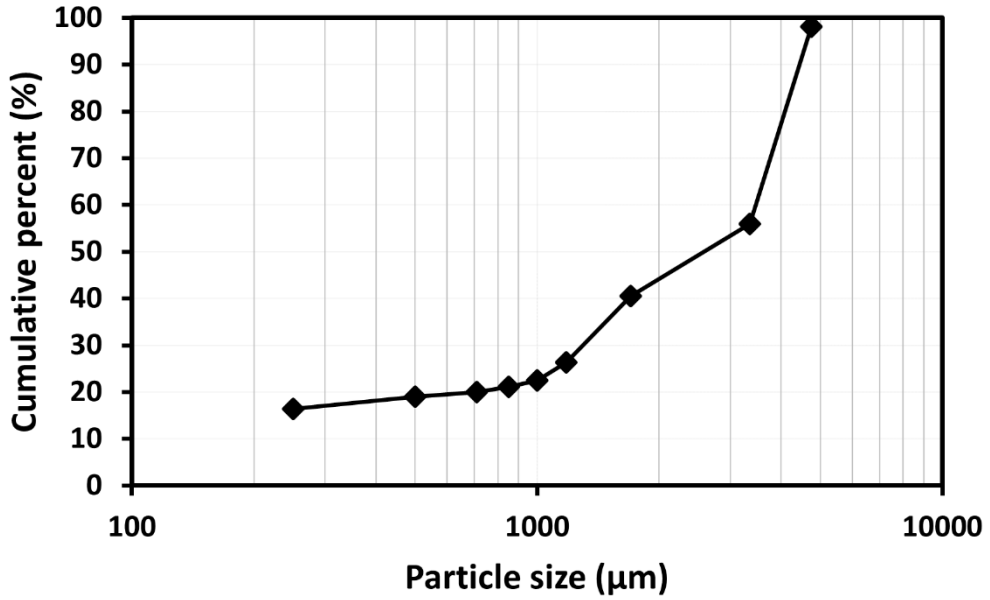

Figure 7-1 Particle size distribution of the crushed (6x) and pulverized (20 s) PCBs, shown as a cumulative percent.

To determine the metal content, PCBs were further pulverised for one minute. Representative samples (0.1 g) of the resultant powdered PCBs were digested by Aqua regia (i.e. 3 HNO_3: 1 HCl (v/v)), using a MARS microwave digester at 300 °C and 800 psi. The metal concentration of the filtrates was determined using Inductively Coupled Plasma Mass Spectroscopy (ICP-MS, Agilent 7900); results are shown in Table 7-1.

Table 7-1 Metal contents (g/100g) in the custom-made PCBs used in this study. The left-hand side provides the more abundant elements, and the right-hand side the less abundant elements.

Element	Content (%)	Element	Content (%) ($x10^{-3}$)
Cu	11.0	Sn	1.01
Fe	0.150	Cr	3.81
Zn	0.040	Pb	0.860
Ni	0.180	Mg	7.98
Al	0.090	V	2.71
Co	0.020	Mo	0.180
Ba	0.110	Zr	4.31
Sr	0.040	La	0.670
Ca	0.230	Ce	1.42
Si	0.280	*Au ($x10^{-5}$)	1.41

7.2.2 Microbial culture for ferric iron regeneration

A mixed microbial culture consisting of *Leptospirillum* (*L.*) *ferriphilum*, *Acidithiobacillus* (*At.*) *caldus* and *Acidiplasma* (*Ap.*) *cupricumulans* as dominant species and adapted to 6.0 g/L Cu^{2+}, as described in Maluleke et al. (2024b) was used. The culture was pre-immobilised onto polyurethane biomass support particles (PUF-BSPs) in a shake flask (Maluleke et al. 2024a; b).

7.2.3 One-stage reactor set-up

Bioleaching of PCBs in a one-stage reactor system was performed in a batch jacketed stirred tank glass bioreactor with a total working volume of 1 L, total height of 200 mm, solution height of 119 mm, and inner diameter of 106 mm (Figure 7-2) at a constant temperature of 37 °C. The bioreactor was fitted with four vertical baffles (height: 145 mm, outer diameter: 103 mm, baffle width: 12 mm, thickness: 5.1 mm, and distance between baffles: 61 mm), 90° apart. Mixing was achieved using a 4-bladed axial impeller with blades at a 45° pitch and an impeller diameter of 57 mm, powered by a Heidolph overhead stirrer operated at 400 rpm. Oxygen required for microbial oxidation of Fe^{2+} was supplied by aeration at a flowrate of 1% vvm through a L-shaped stainless-steel sparger positioned below the turbine. A coil reflux condenser with coolant circulated at 4 °C was used to minimize evaporation. To prevent

damage to the impeller by PCBs chips and minimise shear stress on the biomass support particles, two identical baskets (outer diameter: 78 mm, inner diameter: 45 mm, and height: 38 mm; made of a stainless-steel mesh with a mesh size of 0.18 x 0.18 mm) were designed and fitted into the bioreactor and secured in position on the shaft carrying the impeller – the lower basket housed the PCB chips and the upper basket housed 50 PUF biomass support particles colonised with a Cu-adapted mixed microbial culture. The baskets were fully submerged in the reactor medium. The bioreactor contained 1 L ABS medium, at pH 1.4, containing 5.0 g/L Fe^{3+} and 5.0 g/L Fe^{2+}. In the first cycle, no PCB was added to the bioreactor and it was operated until the available Fe^{2+} substrate was oxidised into Fe^{3+}. The 3% solid loading of PCBs was then introduced and increased through stepwise additions of 3% PCB chips to achieve 3%, 6%, and then up to 18 %w/v PCBs, across six operating cycles. In each cycle, complete microbial oxidation of the Fe^{2+} was achieved before increasing the PCB loading. Throughout the experiment, microbial activity was monitored by daily measurements of pH (Metrohm 867 meter), redox potential (Ag/AgCl reference, 3 M KCl, Metrohm 867 meter), and Fe^{2+}, Fe^{3+} and total Fe concentrations. Fe^{3+} and Fe^{tot} concentrations were determined colorimetrically at 340 nm using the ferric chloride assay with the Fe^{2+} concentration determined by difference (Govender et al. 2012). The release dissolved metal ions from PCBs was analysed using ICP-AES.

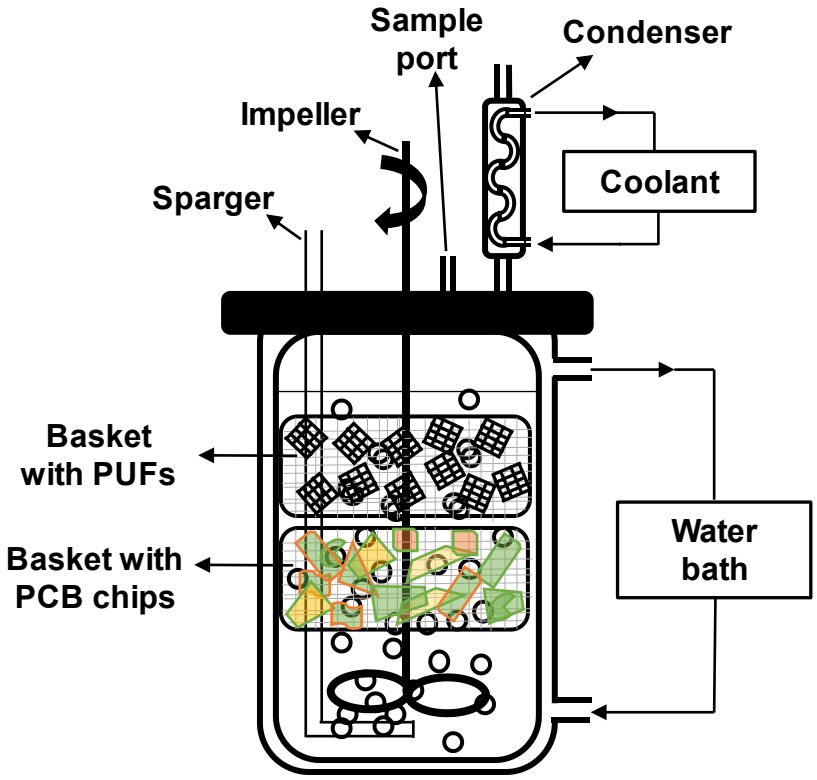

Figure 7-2 A schematic diagram of the one-stage reactor system used for bioleaching of PCBs with two stainless steel baskets, the lower basket housed PCBs and the upper housed 50 PUF biomass support particles colonised with Cu-adapted mixed microbial culture.

7.2.4 Two-stage reactor set-up

Figure 7-3 shows the two-stage reactor system comprised of a 1-litre stirred tank reactor (max. working volume) for chemical leaching of PCBs, coupled to a packed-bed bioreactor comprised of six columns connected in series, each with an 80 ml working volume, for microbial Fe^{2+}oxidation to the Fe^{3+} leach agent. The stirred tank reactor was set-up and operated under the same conditions as the one-stage bioreactor, with the exception of being fitted with only one basket (outer diameter: 78 mm, inner diameter: 45 mm, and height: 15 mm) for housing PCBs. No microbial culture was added to the STR as inoculum. Moreover, to maintain the same overall liquid working volume of 1 L in the two-stage as in the one-stage reactor system, the stirred tank reactor was operated at 520 mL while that of the packed bed system was 480 mL across the 6 columns. Each column bioreactor was packed with 50 PUF biomass support particles (PUF-BSPs) carrying the immobilised culture. The design of these column reactors and associated incubator was previously described by (Ghadiri et al. 2020). The glass column (diameter: 25 mm and height: 190 mm; Glasschem, Stellenbosch, South Africa) is closed at each end by a plastic screwcap, fitted with a glass inlet/outlet nipple and a neoprene seal to prevent leakage. The packed-bed column reactors were mounted vertically in the incubator and maintained at 37 °C. The ABS medium, enriched with solubilised metal ions, including Fe^{2+}, was pumped (MasterFlex peristaltic pump, model:77200-60) from the stirred tank reactor through the upflow packed beds at a flowrate of 0.05 L/h, yielding a residence time of 16 h per column, and 4 days across the 6 columns. The resulting Fe^{3+} rich medium was returned into the stirred tank reactor, such that the two-stage reactor system operated as a closed continuous flow loop (Figure 7-3). Similar to the single-stage system, the solid loading of PCBs in the STR was increased from 3 through 6 to 18 % (w/v) PCBs in 3% increments. Samples were taken daily, at the inlet of the first column (sample 1) as the solution exited the stirred tank reactor, at the inlet of each subsequent column (sample 2 – 6), and as the stream exited the last column (sample 7), to return to the stirred tank reactor. These were analysed for changes in solution pH, redox potential, Fe^{3+} and Fe^{tot} concentration, and base metal ions concentrations.

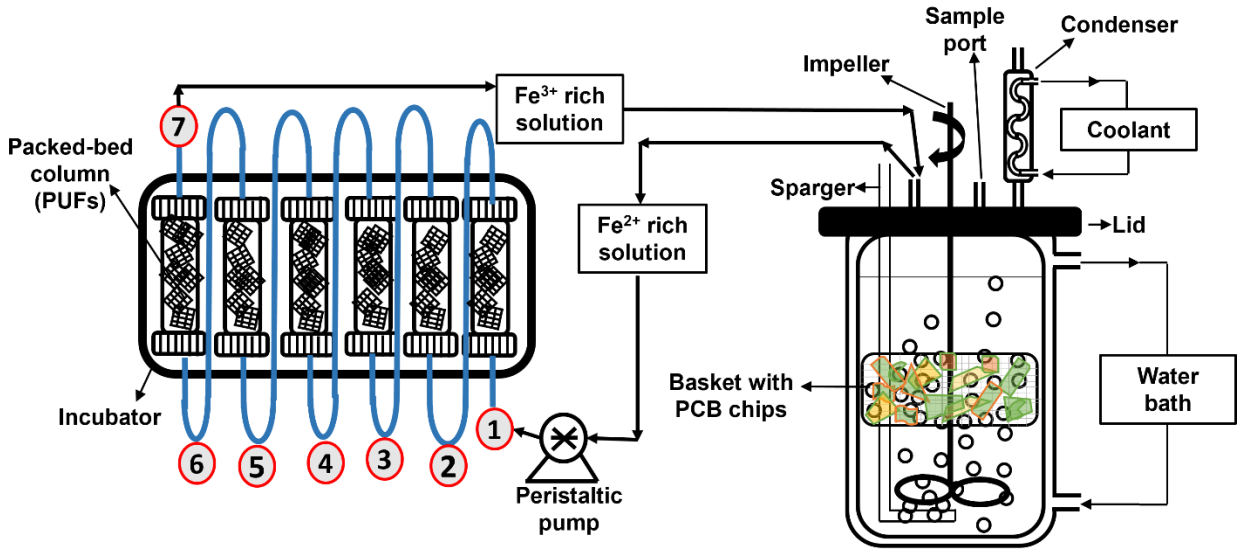

Figure 7-3 A schematic diagram of the two-stage reactor system used for bioleaching of PCBs with one stainless steel basket for housing PCB chips, coupled to a column bioreactor system packed with PUF biomass support particles (PUF-BSPs) carrying the immobilised culture and incubated at 37 °C.

7.3 Results and discussion

The rate of microbial regeneration of Fe^{3+} at an increasing PCB solid loading (0 – 18% weight PCB/volume, %w/v) was monitored in each system. In the first cycle (0% PCB), 5.0 g/L Fe^{3+} and 5.0 g/L Fe^{2+} were added and the system was run with daily monitoring of pH, redox potential, and Fe^{3+}, Fe^{2+}, and Fe^{tot}. Noteworthy, at 0% PCBs, the two-stage system was operated as an open continuous system without recirculation. Once the immobilised cells showed good activity, signified by complete microbial oxidation of Fe^{2+} into Fe^{3+} (Eq. 7-2) as the Fe-rich stream exits the last column (S7), the operation mode was changed to a closed continuous flow loop and 3% PCB (w/v) was added in the stirred tank reactor, while the Fe solution in the STR was changed to 10 g/L Fe^{3+}. Metals in the PCBs were mobilised into solution by the Fe^{3+} oxidant (Eq. 7-1) and the leachate recirculated across the PUF-BSPs. The system was monitored daily (pH, redox potential, and Fe^{3+}, Fe^{2+}, and Fe^{tot}, and dissolved metals concentrations), and PCB solid loading increased at the end of each cycle. The complete dataset for the one-stage system is presented in Figure 7-4 while the dataset for the two-stage system is presented in Figure 7-5. These present the ferrous iron oxidation performance and ferric iron leaching cycles, as well as changes in pH and redox potential over time. The PCB concentration in Figure 7-4 and Figure 7-5 is presented as the cumulative PCB solid loading within the system. The amount of Fe^{3+} reduced into Fe^{2+} on the addition of PCBs was dependent on the metal content of the added PCBs. Given the difference in the microbial loading between one- and two-stage reactor systems, it must be noted that the one-stage reactor system represents a microbially constrained system, providing a typical bioleaching base case system. The two-stage reactor system is designed to explore the feasibility and the opportunities offered in enhancing microbial Fe^{2+} oxidation rate and the potential to balance the volumetric rates of chemical leaching with microbial regeneration of lixiviant.

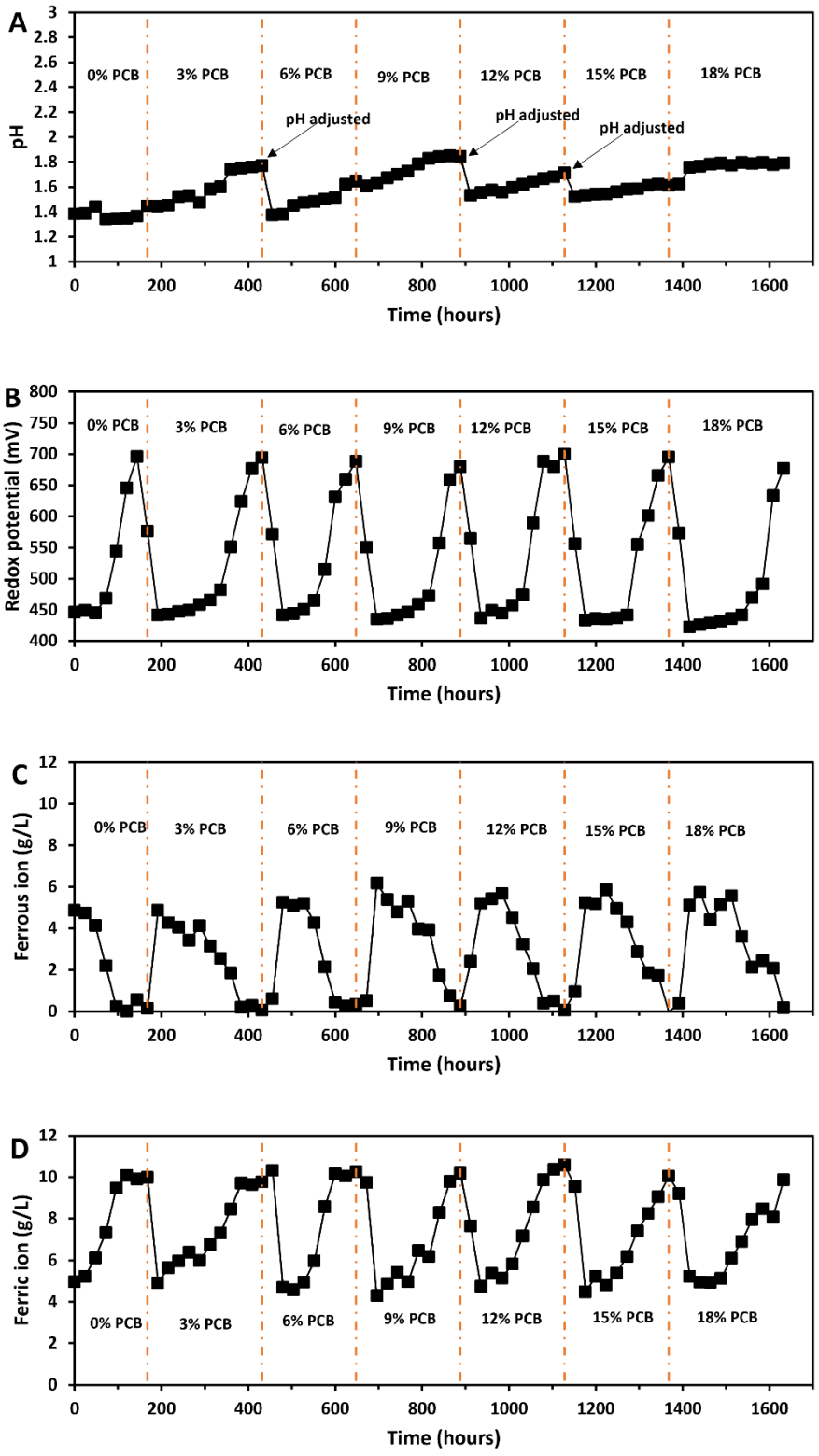

Figure 7-4 Monitoring pH (**A**), redox potential (**B**), ferrous (**C**) and ferric iron (**D**) concentrations in solution with time on the bioleaching of PCBs (increased amounts of crushed PCBs from 0 – 18% PCBs w/v) in a one-stage bioreactor. Vertical lines represent the time point at which each 3% PCB increment was added.

At 0% PCBs, the 5.0 g/L Fe^{2+} available was completely oxidised over 168 h in the packed-bed component of the two-stage reactor system (flow-through) and not oxidised in the STR (Figure 7-5). In comparison, complete Fe^{2+} oxidation was achieved at 120 h in the one-stage reactor system (Figure 7-4). As the two-stage reactor system was operated in as continuous open system, Fe^{2+} concentration in the STR (S1) remained at approximately 5 g/L, while it was oxidised to Fe^{3+} at contact with immobilised cells in the six column reactors (S2-S7). At 168 h, complete Fe^{2+} oxidation was observed at S6-S7, more than 90% Fe^{2+} oxidised at S3-S5 and 65% at S2. This was indicative of microbial oxidative activity across all columns.

With no inhibitory metal ions in the system (pre-PCB addition), the longer time required by the two-stage system to achieve 100% Fe^{2+} oxidisation may be attributed to the low residence time (about 16 h per column), which limits the time Fe^{2+} reactant spent in the reaction zone (microbial-Fe^{2+} contact time in the packed-bed), compared to the unlimited time in the reaction zone in the batch one-stage reactor system. At the addition of 3% PCBs, a net 5.07 and 4.93 g/L Fe^{3+} were consumed over 24 h in oxidising metals in PCBs in one- and two-stage reactor systems, respectively. This suggested similar high volumetric Fe^{3+} reduction rates of greater than 0.211 and 0.206 g $Fe^{3+}.L^{-1}.h^{-1}$ as a function of metals dissolution, respectively in one- and two-stage reactor system, while the amount of Fe^{3+} reduced was consistent with the 5.0 g/L Fe^{3+} calculated as required to leach the metal content of 3% w/v PCBs as per characterisation (Table 7-1). The resultant Fe^{2+} was completely oxidised over 288 h (from the time of PCB addition) in the one-stage system (Figure 7-4), at a volumetric Fe^{2+} oxidation rate of 0.0242 g $Fe^{2+}.L^{-1}.h^{-1}$. This highlights the high volumetric Fe^{3+} reduction rate of 8.72-fold faster than the Fe^{3+} microbial regeneration rate. Similar difference in rates is reported elsewhere in the literature rates (Lambert et al. 2015; Wu et al. 2018) and it is one of the drivers of designing a bioleaching system with enhanced microbial oxidation. The delay in complete Fe^{3+} regeneration in the one-stage system relative to the control (in the absence of PCBs, 0.0491 g $Fe^{2+}.L^{-1}.h^{-1}$) could be attributed to microbial culture being compromised by the addition of PCBs.

In the two-stage system, the resultant Fe^{2+} peaked at 5.79 g/L at 72 h from the time of PCB addition in S2, and residual Fe^{2+} concentration peaked only at 2.78 g/L in the effluent (S7). This suggested that about 52% of the resultant Fe^{2+} had been microbially oxidised back into Fe^{3+} through S2-S6 within 72 h. A complete Fe^{3+} regeneration was observed at 168 h at the effluent (S7), suggesting a volumetric microbial Fe^{2+} oxidation rate of 0.0594 g $Fe^{2+}.L^{-1}.h^{-1}$ across S2-S7, while it peaked at 216 h across the system. This delay in achieving the highest Fe^{3+} concentration across the system was attributed to a low flow rate (0.05 $L.h^{-1}$) and a longer time required to reach a complete closed-loop system. Here, a closed-loop system was defined as a state where the solution has made a full cycle, i.e., from the stirred tank reactor, through the packed bioreactor system and back to the stirred tank reactor. The net Fe^{3+} reduction rate was 3.47-fold faster than the net Fe^{3+} regeneration rate in the two-reactor system, suggesting an improvement of 60% in the Fe^{3+} delivery rate compared to the one-stage reactor system. This could be due to the high cell concentration in the two-stage system relative to the one-stage system, as only fifty colonised PUFs could be packed in the fitted basket in the one-stage system, compared to fifty PUFs per column (×6 columns) in the two-stage system. When accumulated solid loading was increased to 6% PCBs, a net amount of 5.64 g/L and 5.15 g/L

Fe^{3+} were reduced in oxidising metals in PCBs in one- and two-stage reactor systems over 24 h, respectively. The resultant Fe^{2+} was completely oxidised over 192 h in a one-stage (Figure 7-4) and 168 h in a two-stage system (Figure 7-5). Similarly, in a two-stage system, Fe^{3+} regeneration was faster than in a one-stage system.

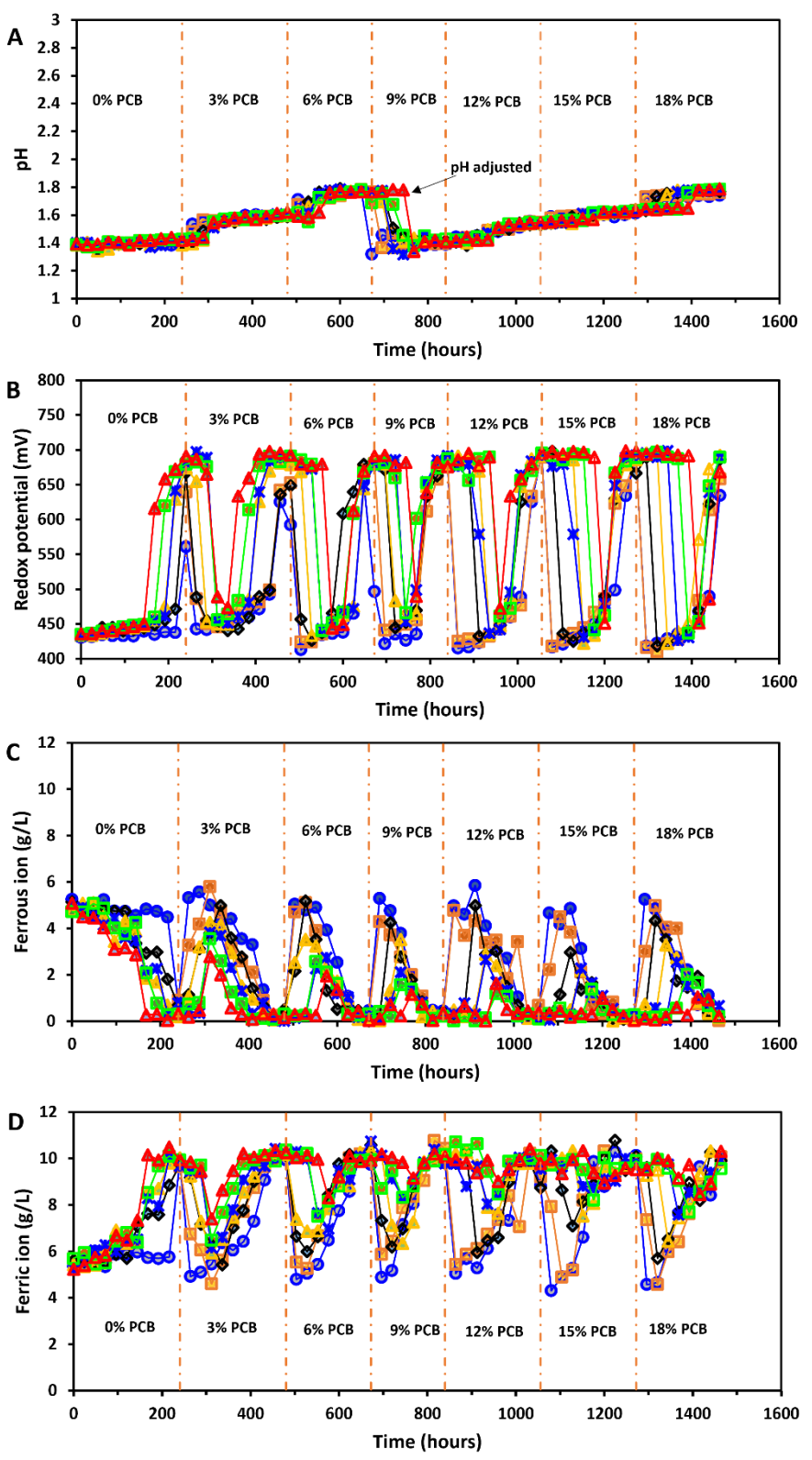

Figure 7-5 Microbial oxidation of Fe^{2+} by Cu-adapted cells immobilised on PUF-BSPs during bioleaching of PCB (increased from 0 – 18% PCB w/v) in a two-stage bioreactor. Vertical lines represent the time point at which each 3% PCB increment was added. Sample 1, S1 ( ), S2 ( ), S3 ( ), S4 ( ), S5 ( ), S6 ( ), and S7 ( ).

Ordinarily, the severity in inhibition of microbial culture by PCBs was expected to increase with an increase in % PCB loading. However, the Cu-adapted immobilised cells maintained their microbial activity such that complete Fe^{3+} regeneration was achieved in about 240 h at 9 to 18% PCB in the one-stage system. Similarly, complete oxidation of the resultant Fe^{2+} in a two-stage system subjected to 9 and 12% PCB was achieved in 144 and 168 h from the point of PCB addition. It must be noted that across all PCBs addition cycles, low ferrous iron concentrations were observed across columns 5 and 6 in the two-stage reactor systems (peak at 40% of the resultant Fe^{2+}), suggesting that sufficient Fe^{3+} regeneration occurs within column 1-4 under the PCB loading used. Hence column number may be reduced or loading increased.

Moreover, we postulate that the adopted approach of multiple dose addition of PCBs to subsequently achieve high cumulative %PCBs in solution, rather than a single dose addition of high %PCB, could have also contributed positively to microbial culture maintaining their high performance. Multiple dose addition of PCBs, which represents a move towards a continually fed system as desired for large-scale application, could have minimised metal ion shock stress on the microbial cultures, affording the culture the necessary time to rapidly adapt and recover even in the presence of increasing PCB stress. A similar positive response by microbial cultures as a result of multiple dose PCB addition has also reported by (Liang et al. 2010). The authors investigated the effect of single and multiple addition of PCBs on microbial growth and extent of metal extraction during bioleaching of PCBs by planktonic cells of *A. ferrooxidans* and *A. thiooxidans* in a batch shake flask. When 4, 6, 8, 10, and 12 g/L PCBs were added in separate bioleaching flasks at 48 h cultivation time, Cu extractions were 86, 83, 80, 75, and 71%, respectively, with adverse effect on microbial growth at 12 g/L PCBs noticed. Meanwhile, dose addition at an increment of 4 g/L at 48 h, 6 g/L at 96 h, and 8 g/L at 144 h, into the same flask (total of 18 g/L PCBs) resulted in a total of 78% Cu extracted with minimum effect to the microbial growth relative to single addition (Liang et al. 2010).

In this present study, microbial activity and rapid complete Fe^{3+} regeneration was achieved even at the highest PCB solid loading tested of 18% PCB in both one- and two-stage systems. As hypothesised, the higher tolerance of the Cu-adapted immobilised cells to increasing PCB solid loading could be attributed to the protection offered by cell retention in PUF-BSPs. Through this, both the biofilm associated with colonised cells (Tributsch 2001) and the hold-up of cells in interstitial micro-environments that are not consistent with the bulk fluid phase (Govender-Opitz et al. 2017) can be tailored to favor Fe^{2+} oxidation and assist in providing varying levels of the diffusion barrier. In these mechanisms, naturally excreted extracellular polysaccharides (EPS, a main component of biofilm) can bioabsorb (where EPS provides binding sites) metal ions and subsequently act as a barrier for toxins to interact with vital cellular components (Bruins et al. 2000; Luo et al. 2021; Zhang et al. 2023). Secondly, rapid Fe^{3+} regeneration by the Cu-adapted immobilised cells could be attributed to high cell concentrations achievable in immobilised microbial systems (Armentia and Webb 1992; Nemati and Webb 1996). Rapid Fe^{3+} regeneration is a function of both microbial population size and specific microbial oxidation rate of Fe^{2+} (Jones and Kelly 1983; Breed and Hansford 1999; Ojumu et al. 2006). Armentia and Webb (1992) reported a high microbial Fe^{2+} oxidation rate of 1.56 $g.L^{-1}.h^{-1}$ at a dilution rate of 0.31 h^{-1} by *At. ferrooxidans* immobilised on PUF. A high Fe^{2+} oxidation rate of 34.3 $g.L^{-1}.h^{-1}$, at a dilution rate of 6 h^{-1}, was achieved at initial Fe^{2+}

concentrations of 5 g/L by *At. ferrooxidans* immobilised on PUF-BSPs (Nemati and Webb 1996). In all these studies, high Fe^{2+} oxidation was attributed to high cell concentration achieved in the immobilised system. In the present study, attempting to quantify cell concentrations on the colonised PUF-BSPs was unsuccessful as the detached cells were observed to clump embedded in biofilm when viewed under a microscope, following standard detachment methods (Govender et al. 2013; Hessler et al. 2017). Attempts to free the cells from the EPS resulted in the breakup of the clumps into smaller ones with cells still embedded in biofilm, preventing accurate counting.

In a previous study (Maluleke et al. 2024a), a low Fe^{3+} regeneration rate was observed when three units of Cu-adapted immobilised PUF-BSPs were subjected to a 40% v/v PCB leachate (prepared by Fe^{3+} leaching of the same PCB sample as in this study), approximately equivalent to 9% w/v PCB. Complete Fe^{2+} oxidation was achieved at 600 h in the batch shake flask (Maluleke et al. 2024a) compared to at 240 and 144 h in the current study for one- and two-stage system, respectively. This difference in Fe^{2+} oxidation performance is attributed to cell concentration, through the higher number of PUFs added and potentially high cell density, leading to increase in volumetric Fe^{3+} regeneration rates.

Maintaining the Fe^{3+}/Fe^{2+} ratio at approximately 1 and above, such that redox potential remains above 400 mV (Figure 7-4B and Figure 7-5B) could have also promoted rapid Fe^{3+} oxidation rates. It has been demonstrated that acidophilic microorganisms, particularly *L. ferriphilum,* prefer a redox potential of above 400 mV owing to their poor ability to scavenge low ferrous iron concentrations (Bryan et al. 2012). It is therefore important to estimate concentrations of metal ions expected per PCB solid loading such that the Fe^{3+}/Fe^{2+} ratio is balanced during bioleaching to promote Fe^{2+} oxidation and microbial growth post PCB leaching.

With the continuous microbial regeneration of the Fe^{3+}, availing excess Fe^{3+} leach agent within the system, high bioleaching efficiency was achieved in both one- and two-stage systems. The final fraction of metals (%) solubilised in both systems at each PCB solid loading is presented in Figure 7-6. Briefly, there was a comparable final concentration of metals solubilised across solid loadings of PCBs in both systems. Average percent of metal solubilised across cumulative 3, 6, 9, 12, 15 and 18% PCB solid loading in the one-stage reactor system was 91% Al, 72% Ca, >100% Cr, 93% Cu, >100% Mg, 78% Ni, 82% Pb, >100% Sn, >100% Zn, 8% Co, and 12% Sr, while in the two-stage system, 98% Al, 58% Ca, 93% Cr, 96% Cu, >100% Mg, 79% Ni, 80% Pb, >100% Sn, >100% Zn, and low efficiency of 7% Co and 11% Sr were achieved. The values exceeding 100% are attributed to low concentration leading to some analytical uncertainty. Low concentrations of metals such as Sn are reported in PCB leachates as it precipitate out of solution as SnO_2 (Brandl et al. 2001; Bryan et al. 2015), while high bioleaching efficiency of metals such as Cu, Zn, Ni, is common in literature, high extraction of metals such as Sn may have been due to the low concentrations of such metals in the PCB sample used in this study (Table 7-1). The high extraction efficiency of metals reported highlights that PCB chips (prepared from 20 second pulverisation) can be used in PCB leaching processes, rather than powdered PCBs, while maintaining high metal extraction. This may allow a reduced

operational cost as milling of PCBs is energy intensive, with loss of metals in the process, and handling of finely milled PCB powders requires more energy intensive separation processes.

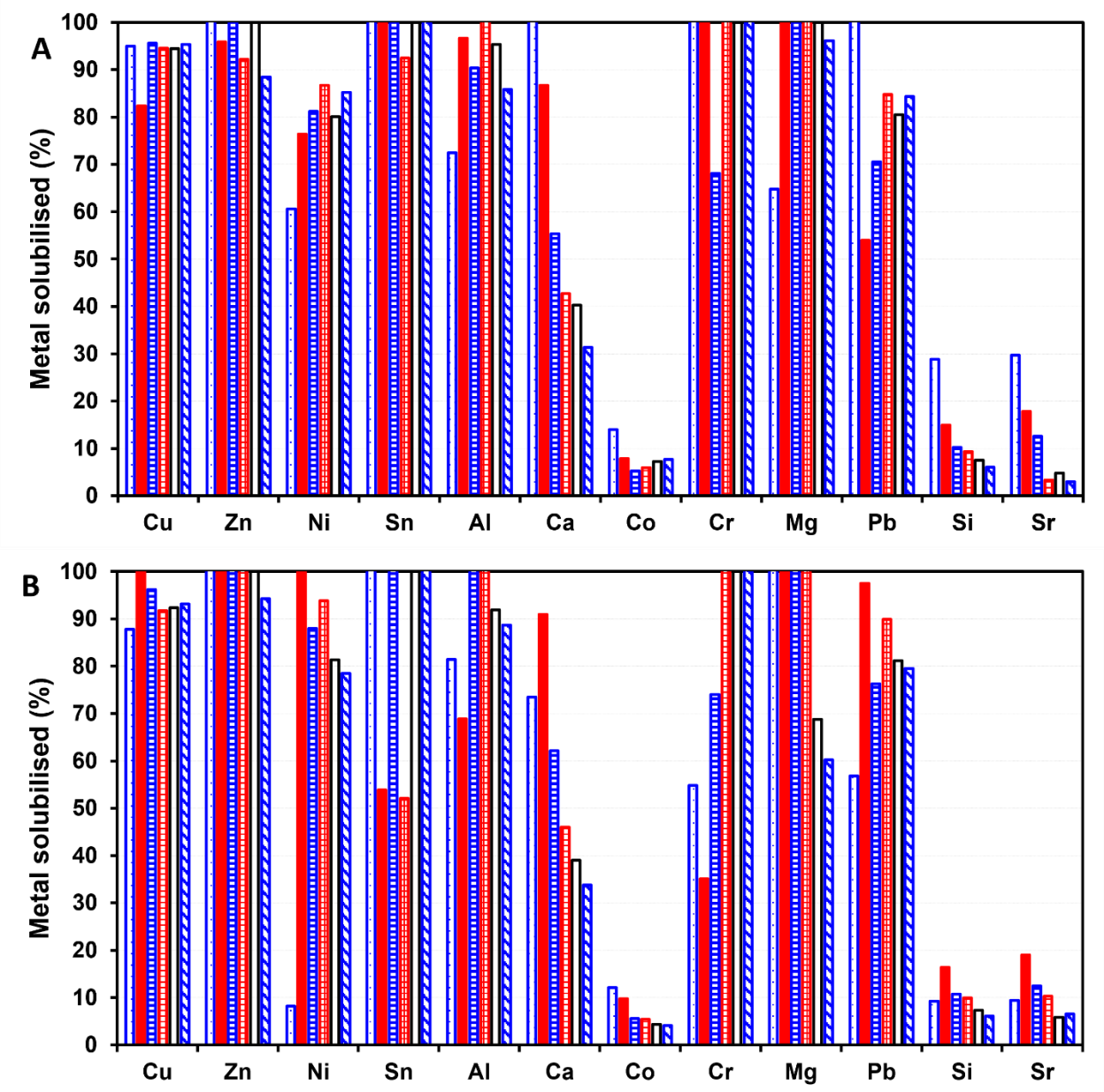

Figure 7-6 Final amount of metal (%) solubilised at cumulative 3 ( ), 6 ( ), 9 ( ), 12% PCB ( ), 15 ( ), and 18% PCB ( ) during bioleaching of PCB in the one-stage (**A**) and two-stage bioreactor (**B**).

Maintaining solution pH below 2 in bioleaching systems prevents Fe^{3+} oxidant precipitation out of solution as jarosite, thereby preventing removal of lixiviant. Moreover, jarosite can deposit on PCBs, limiting reaction surface area and thus the rate and extent of metal extraction. Subject to the amount of PCB added and its alkalinity content, the pH can increase above 2 in PCB bioleaching systems (Choi et al. 2004; Yang et al. 2009; Liang et al. 2010; Yang et al. 2014). In the present study, the solution pH was maintained below 2 with concentrated

H_2SO_4 whenever necessary. In the absence of PCBs, minimum change in pH was observed, i.e., from 1.38 to 1.40 and 1.39 to 1.44 in one- and two-stage systems (Figure 7-4A and Figure 7-5A) , respectively. On addition of 3% PCBs, the pH increase to a maximum of approximately 1.77 and 1.61 in one- and two-stage systems, respectively, attributed to the alkaline nature of the PCBs. Arshadi et al. (2018) demonstrated that while the alkalinity of PCBs could be due to their plastic content, metals such as Li, Na, K, Rb, Cs, Fr, Be, Mg, Ca, Sr, Ba and Ra, also add to the alkalinity of the PCBs. Moreover, while Fe^{3+} is the primary oxidant, some metal leaching is by proton (H^+) attack, which could contribute to the pH increase (Xiang et al. 2010; Bryan et al. 2015). The overall change in solution pH in the two-stage system was delayed relative to the one-stage system, owing to the plug flow nature of the column component. To prevent pH from increasing above 2, pH was adjusted to 1.37 in the one-stage system prior to the addition of PCBs. At 6% PCBs, pH increased to about 1.65 in the one-stage system, while in a two-stage system, it increased from about 1.60 to 1.78. Similar to the one-stage system, pH was adjusted to 1.32 prior to increasing to 9% PCB in the two-stage system. At the end of the 18% PCB cycle, the total amount of H_2SO_4 used in maintaining pH was 0.136 mol and 0.0815 mol in one- and two-stage systems. The low H^+ consumption was contrary to the expected high consumption of H^+ as per Eq. 7-2. Similar results are reported in other studies (Lewis et al. 2011; Lambert et al. 2015). The low changes in pH across the bioleaching cycles and the subsequent low total amount of acid used to maintain the pH in both one- and two-stage systems could be attributed to the low alkalinity content of the PCB sample and the excess amount of the Fe^{3+} leaching agent, minimising proton leaching.

The present study presents a promising approach to bioleaching of base metals from PCBs. The high solid loading of PCBs and concomitant high bioleaching efficiency achieved is central to the techno-economic feasibility of this bioleaching approach. Moreover, the continued microbial activity and rapid Fe^{3+} regeneration to move towards the balance in leaching rate and ferric iron regeneration rate in the reactor system with increasing PCB loading informs design of the bioleaching system.

7.4 Conclusion

The current study investigated the bioleaching of PCBs in a two-stage reactor system consisting of a stirred tank reactor for chemical leaching of PCBs, coupled to a packed-bed bioreactor system for microbial oxidation of Fe^{2+} for regeneration of the Fe^{3+} oxidant. The reactor set-up was operated as a closed continuous flow loop, such that the liquid stream from the stirred tank reactor, rich in Fe^{2+} and dissolved metals, was passed through the packed-bed bioreactor in which microbial ferrous iron oxidation took place and the resultant Fe^{3+}-rich stream was recirculated back into the stirred tank reactor. A one-stage reactor system, where both PCB leaching and Fe^{3+} regeneration occur in one pot, was investigated as a comparative base case. A cumulative 18% PCB solid loading was successfully leached with Cu-adapted immobilised cells maintaining their oxidative activity in both systems. The volumetric Fe^{3+} reduction rates as a function of metal dissolution from the added PCBs was 8.72-fold and 3.47-fold faster than the microbial Fe^{3+} regeneration rate, respectively, in the one- and two-stage reactor systems, suggesting an improvement of about 60% Fe^{3+} regeneration rate in the two-stage reactor system. High bioleaching efficiency of above 91% Al, 58% Ca, 93% Cr, 93% Cu,

100% Mg, 78% Ni, 80% Pb, 100% Sn, 100% Zn, and low efficiency of 7% Co and 11% Sr, was achieved in both systems. Complete microbial regeneration of Fe^{3+} was achieved more rapidly in the two-stage relative to the one-stage system. The two-stage setup enabled a high operating biomass concentration and associated increased microbial ferrous iron oxidation rate. The high 18% PCB solid loading and un-interrupted microbial Fe^{3+} regeneration rates, despite dissolved metals and PCB leachate accumulating, achieved in this study present a promising approach for the design of reactor systems for the bioleaching of base metals from PCBs, prior to recovery of PGM group metals. Their release through a biohydrometallurgical approach, with selective recovery, provides a promising approach to maximizing metal recovery for the circular economy.

7.5 References

Adetunji, A. I.; Oberholster, P. J.; Erasmus, M. (2023). Bioleaching of Metals from E-Waste using microorganisms. A Review. Minerals 13 (6), 828. DOI: 10.3390/min13060828.

Anaya-Garzon, J.; Hubau, A.; Joulian, C.; Guezennec, A.-G. (2021). Bioleaching of E-Waste. Influence of printed circuit boards on the activity of acidophilic iron-oxidizing bacteria. Frontiers in Microbiology 12, 669738. DOI: 10.3389/fmicb.2021.669738.

Armentia, H.; Webb, C. (1992). Ferrous sulphate oxidation using *Thiobacillus ferrooxidans* cells immobilised in polyurethane foam support particles. Applied Microbiology and Biotechnology 36 (5), 697–700. DOI: 10.1007/BF00183252.

Arshadi, M.; Mousavi, S. M. (2014). Simultaneous recovery of Ni and Cu from computer-printed circuit boards using bioleaching. Statistical evaluation and optimization. Bioresource Technology 174, 233–242. DOI: 10.1016/j.biortech.2014.09.140.

Arshadi, M.; Yaghmaei, S.; Mousavi, S. M. (2018). Content evaluation of different waste PCBs to enhance basic metals recycling. Resources, Conservation and Recycling 139, 298–306. DOI: 10.1016/j.resconrec.2018.08.013.

Baniasadi, M.; Vakilchap, F.; Bahaloo-Horeh, N.; Mousavi, S. M.; Farnaud, S. (2019). Advances in bioleaching as a sustainable method for metal recovery from e-waste. A review. Journal of Industrial and Engineering Chemistry 76, 75–90. DOI: 10.1016/j.jiec.2019.03.047.

Brandl, H.; Bosshard, R.; Wegmann, M. (2001). Computer-munching microbes: Metal leaching from electronic scrap by bacteria and fungi. Hydrometallurgy 59 (2), 319–326. DOI: 10.1016/S0304-386X(00)00188-2.

Breed, A.W.; Hansford, G.S. (1999). Effect of pH on ferrous-iron oxidation kinetics of *Leptospirillum ferrooxidans* in continuous culture. Biochemical Engineering Journal 3 (3), 193–201. DOI: 10.1016/S1369-703X(99)00018-2.

Bruins, M. R.; Kapil, S.; Oehme, F. W. (2000). Microbial resistance to metals in the environment. Ecotoxicology and Environmental Safety 45 (3), 198–207. DOI: 10.1006/eesa.1999.1860.

Bryan, C. G.; Davis-Belmar, C. S.; van Wyk, N.; Fraser, M. K.; Dew, D.; Rautenbach, G. F.; Harrison, S. T. L. (2012). The effect of CO_2 availability on the growth, iron oxidation and CO_2-fixation rates of pure cultures of *Leptospirillum ferriphilum* and *Acidithiobacillus ferrooxidans*. Biotechnology and Bioengineering 109 (7), 1693–1703. DOI: 10.1002/bit.24453.

Bryan, C. G.; Joulian, C.; Spolaore, P.; El Achbouni, H.; Challan-Belval, S.; Morin, D.; d'Hugues, P. (2011). The efficiency of indigenous and designed consortia in bioleaching stirred tank reactors. Minerals Engineering 24 (11), 1149–1156. DOI: 10.1016/j.mineng.2011.03.014.

Bryan, C. G.; Watkin, E. L.; McCredden, T. J.; Wong, Z. R.; Harrison, S.T.L.; Kaksonen, A. H. (2015). The use of pyrite as a source of lixiviant in the bioleaching of electronic waste. Hydrometallurgy 152 (2–3), 33–43. DOI: 10.1016/j.hydromet.2014.12.004.

Chen, S.; Yang, Y.; Liu, C.; Dong, F.; Liu, B. (2015). Column bioleaching copper and its kinetics of waste printed circuit boards (WPCBs) by *Acidithiobacillus ferrooxidans*. Chemosphere 141, 162–168. DOI: 10.1016/j.chemosphere.2015.06.082.

Choi, M.-S.; Cho, K.-S.; Kim, D.-S.; Kim, D.-J. (2004). Microbial Recovery of Copper from Printed Circuit Boards of Waste Computer by *Acidithiobacillus ferrooxidans*. Journal of Environmental Science and Health, Toxic/Hazardous Substances and Environmental Engineering 39 (11-12), 2973–2982. DOI: 10.1081/LESA-200034763.

Deetman, S.; Pauliuk, S.; van Vuuren, D. P.; van der Voet, E.; Tukker, A. (2018). Scenarios for demand growth of metals in electricity generation technologies, cars, and electronic appliances. Environmental Science & Technology 52 (8), 4950–4959. DOI: 10.1021/acs.est.7b05549.

Dopson, M.; Baker-Austin, C.; Koppineedi, P. R.; Bond, P. L. (2003). Growth in sulfidic mineral environments: Metal resistance mechanisms in acidophilic micro-organisms. Microbiology 149 (8), 1959–1970. DOI: 10.1099/mic.0.26296-0.

Ghadiri, M.; Harrison, S. T.L.; Fagan-Endres, M. A. (2020). Quantitative X-ray µCT measurement of the effect of ore characteristics on non-surface mineral grain Leaching. Minerals 10 (9), 746. DOI: 10.3390/min10090746.

González, A.; Bellenberg, S.; Mamani, S.; Ruiz, L.; Echeverría, A.; Soulère, L. et al. (2013). AHL signaling molecules with a large acyl chain enhance biofilm formation on sulfur and metal sulfides by the bioleaching bacterium *Acidithiobacillus ferrooxidans*. Applied Microbiology and Biotechnology 97 (8), 3729–3737. DOI: 10.1007/s00253-012-4229-3.

Govender, E.; Bryan, C. G.; Harrison, S. T.L. (2013). Quantification of growth and colonisation of low grade sulphidic ores by acidophilic chemoautotrophs using a novel experimental system. Minerals Engineering 48, 108–115. DOI: 10.1016/j.mineng.2012.09.010.

Govender, E.; Harrison, S.T.L.; Bryan, C. G. (2012). Modification of the ferric chloride assay for the spectrophotometric determination of ferric and total iron in acidic solutions containing high concentrations of copper. Minerals Engineering 35, 46–48. DOI: 10.1016/j.mineng.2012.05.006.

Govender-Opitz, E.; Kotsiopoulos, A.; Bryan, C. G.; Harrison, S. T.L. (2017). Modelling microbial transport in simulated low-grade heap bioleaching systems. The hydrodynamic dispersion model. Chemical Engineering Science 172, 545–558. DOI: 10.1016/j.ces.2017.07.008.

Harrison, S. T.L. (2016). Biotechnologies that Utilise Acidophiles. In Acidophiles: Life in Extremely Acidic Environments: Caister Academic Press, 265–284.

Hessler, T.; Marais, T.; Huddy, R. J.; van Hille, R.; Harrison, S. T.L. (2017). Comparative analysis of the sulfate-reducing performance and microbial colonisation of three continuous reactor configurations with varying degrees of biomass retention. Solid State Phenomena 262, 638–642. DOI: 10.4028/www.scientific.net/SSP.262.638.

Hubau, A.; Minier, M.; Chagnes, A.; Joulian, C.; Silvente, C.; Guezennec, A.-G. (2020). Recovery of metals in a double-stage continuous bioreactor for acidic bioleaching of printed circuit boards (PCBs). Separation and Purification Technology 238 (3), 116481. DOI: 10.1016/j.seppur.2019.116481.

Ilyas, S.; Lee, J.-c. (2014). Bioleaching of metals from electronic scrap in a stirred tank reactor. Hydrometallurgy 149 (2014), 50–62. DOI: 10.1016/j.hydromet.2014.07.004.

Ilyas, S.; Lee, J.-c.; Chi, R.-a. (2013). Bioleaching of metals from electronic scrap and its potential for commercial exploitation. Hydrometallurgy 131-132 (11–12), 138–143. DOI: 10.1016/j.hydromet.2012.11.010.

Ilyas, S.; Ruan, C.; Bhatti, H. N.; Ghauri, M. A.; Anwar, M. A. (2010). Column bioleaching of metals from electronic scrap. Hydrometallurgy 101 (3-4), 135–140. DOI: 10.1016/j.hydromet.2009.12.007.

Ji, X.; Yang, M.; Wan, A.; Yu, S.; Yao, Z. (2022). Bioleaching of typical electronic waste—Printed Circuit Boards (WPCBs). A Short Review. International Journal of Environmental Research and Public Health 19 (12), 7508. DOI: 10.3390/ijerph19127508.

Jones, C. A.; Kelly, D. P. (1983). Growth of *Thiobacillus ferrooxidans* on ferrous iron in chemostat culture. Influence of product and substrate inhibition. Journal of Chemical Technology and Biotechnology. Biotechnology 33 (4), 241–261. DOI: 10.1002/jctb.280330407.

Kaksonen, A. H.; Boxall, N. J.; Gumulya, Y.; Khaleque, H. N.; Morris, C.; Bohu, T. et al. (2018). Recent progress in biohydrometallurgy and microbial characterisation. Hydrometallurgy 180 (10), 7–25. DOI: 10.1016/j.hydromet.2018.06.018.

Lambert, F.; Gaydardzhiev, S.; Léonard, G.; Lewis, G.; Bareel, P.-F.; Bastin, D. (2015). Copper leaching from waste electric cables by biohydrometallurgy. Minerals Engineering 76 (1), 38–46. DOI: 10.1016/j.mineng.2014.12.029.

Lewis, G.; Gaydardzhiev, S.; Bastin, D.; Bareel, P.-F. (2011). Bio hydrometallurgical recovery of metals from Fine Shredder Residues. Minerals Engineering 24 (11), 1166–1171. DOI: 10.1016/j.mineng.2011.03.025.

Liang, G.; Mo, Y.; Zhou, Q. (2010). Novel strategies of bioleaching metals from printed circuit boards (PCBs) in mixed cultivation of two acidophiles. Enzyme and Microbial Technology 47 (7), 322–326. DOI: 10.1016/j.enzmictec.2010.08.002.

Luo, A.; Wang, F.; Sun, D.; Liu, X.; Xin, B. (2021). Formation, development, and cross-species interactions in biofilms. Frontiers in Microbiology 12, 757327. DOI: 10.3389/fmicb.2021.757327.

Maluleke, M. D.; Kotsiopoulos, A.; Govender-Opitz, E.; Harrison, S. T. L. (2024a). Microbial immobilisation and adaptation to Cu^{2+} enhances microbial Fe^{2+} oxidation for bioleaching of printed circuit boards in the presence of mixed metal ions. Research in Microbiology 175 (1-2), 104148. DOI: 10.1016/j.resmic.2023.104148.

Maluleke, M. D.; Kotsiopoulos, A.; Govender-Opitz, E.; Harrison, S. T.L. (2024b). Exploring microbial adaptation of immobilised acidophilic cultures to improve microbial oxidation rates and copper tolerance in e-waste bioleaching. Minerals Engineering 207 (3), 108560. DOI: 10.1016/j.mineng.2023.108560.

Morin, D. H.R. (2008). BioMinE. An integrated project for developing biohydrometallurgy in Europe—Executive summary of its activities and outputs after three years. Transactions of Nonferrous Metals Society of China 18 (6), 1328–1335. DOI: 10.1016/S1003-6326(09)60005-4.

Nemati, M.; Harrison, S.T.L.; Hansford, G. S.; Webb, C. (1998). Biological oxidation of ferrous sulphate by *Thiobacillus ferrooxidans*. A review on the kinetic aspects. Biochemical Engineering Journal 1 (3), 171–190. DOI: 10.1016/S1369-703X(98)00006-0.

Nemati, M.; Webb, C. (1996). Effect of ferrous iron concentration on the catalytic activity of immobilized cells of *Thiobacillus ferrooxidans*. Applied Microbiology and Biotechnology 46 (3), 250–255. DOI: 10.1007/s002530050812.

Ojumu, T. V.; Petersen, J.; Searby, G. E.; Hansford, G. S. (2006). A review of rate equations proposed for microbial ferrous-iron oxidation with a view to application to heap bioleaching. Hydrometallurgy 83 (1-4), 21–28. DOI: 10.1016/j.hydromet.2006.03.033.

Oliveira, R. P. de; Benvenuti, J.; Espinosa, D.C.R. (2021). A review of the current progress in recycling technologies for gallium and rare earth elements from light-emitting diodes. Renewable and Sustainable Energy Reviews 145, 111090. DOI: 10.1016/j.rser.2021.111090.

Prestele, M. P. (2020). Assessment of a Shredding Technology of Waste Printed Circuit Boards in preparation for Ammonia-based Copper leaching. Master's thesis, University of Cape Town

Rawlings, D.; Johnson, B. (2007). Biomining. Berlin: SpringerRawlings, D.; Johnson, B.

Rodrigues, M. L. M.; Leão, V. A.; Gomes, O.; Lambert, F.; Bastin, D.; Gaydardzhiev, S. (2015). Copper extraction from coarsely ground printed circuit boards using moderate thermophilic bacteria in a rotating-drum reactor. Waste Management 41, 148–158. DOI: 10.1016/j.wasman.2015.04.001.

Rohwerder, T.; Gehrke, T.; Kinzler, K.; Sand, W. (2003). Bioleaching review part A. Progress in bioleaching: fundamentals and mechanisms of bacterial metal sulfide oxidation. Applied Microbiology and Biotechnology 63 (3), 239–248. DOI: 10.1007/s00253-003-1448-7.

Sand, W.; Gehrke, T. (2006). Extracellular polymeric substances mediate bioleaching/biocorrosion via interfacial processes involving iron(III) ions and acidophilic bacteria. Research in Microbiology 157 (1), 49–56. DOI: 10.1016/j.resmic.2005.07.012.

Tapia, J.; Dueñas, A.; Cheje, N.; Soclle, G.; Patiño, N.; Ancalla, W. et al. (2022). Bioleaching of Heavy Metals from Printed Circuit Boards with an Acidophilic Iron-Oxidizing Microbial Consortium in Stirred Tank Reactors. Bioengineering 9 (2), 79. DOI: 10.3390/bioengineering9020079.

Tributsch, H. (2001). Direct versus indirect bioleaching. Hydrometallurgy 59 (2-3), 177–185. DOI: 10.1016/S0304-386X(00)00181-X.

Tuncuk, A.; Stazi, V.; Akcil, A.; Yazici, E. Y.; Deveci, H. (2012). Aqueous metal recovery techniques from e-scrap. Hydrometallurgy in recycling. Minerals Engineering 25 (1), 28–37. DOI: 10.1016/j.mineng.2011.09.019.

Watari, T.; Nansai, K.; Nakajima, K. (2021). Major metals demand, supply, and environmental impacts to 2100. A critical review. Resources, Conservation and Recycling 164, 105107. DOI: 10.1016/j.resconrec.2020.105107.

Wu, W.; Liu, X.; Zhang, X.; Zhu, M.; Tan, W. (2018). Bioleaching of copper from waste printed circuit boards by bacteria-free cultural supernatant of iron–sulfur-oxidizing bacteria. Bioresource. Bioprocess. 5 (1), 233. DOI: 10.1186/s40643-018-0196-6.

Xia, L.; Liu, X.; Zeng, J.; Yin, C.; Gao, J.; Liu, J.; Qiu, G. (2008). Mechanism of enhanced bioleaching efficiency of *Acidithiobacillus ferrooxidans* after adaptation with chalcopyrite. Hydrometallurgy 92 (3), 95–101. DOI: 10.1016/j.hydromet.2008.01.002.

Xia, M.-C.; Wang, Y.-P.; Peng, T.-J.; Shen, L.; Yu, R.-L.; Liu, Y.-D. et al. (2017). Recycling of metals from pretreated waste printed circuit boards effectively in stirred tank reactor by a moderately thermophilic culture. Journal of Bioscience and Bioengineering 123 (6), 714–721. DOI: 10.1016/j.jbiosc.2016.12.017.

Xiang, Y.; Wu, P.; Zhu, N.; Zhang, T.; Liu, W.; Wu, J.; Li, P. (2010). Bioleaching of copper from waste printed circuit boards by bacterial consortium enriched from acid mine drainage. Journal of Hazardous Materials 184 (1), 812–818. DOI: 10.1016/j.jhazmat.2010.08.113.

Yang, T.; Xu, Z.; Wen, J.; Yang, L. (2009). Factors influencing bioleaching copper from waste printed circuit boards by *Acidithiobacillus ferrooxidans*. Hydrometallurgy 97 (1-2), 29–32. DOI: 10.1016/j.hydromet.2008.12.011.

Yang, Y.; Chen, S.; Li, S.; Chen, M.; Chen, H.; Liu, B. (2014). Bioleaching waste printed circuit boards by *Acidithiobacillus ferrooxidans* and its kinetics aspect. Journal of Biotechnology 173, 24–30. DOI: 10.1016/j.jbiotec.2014.01.008.

Zhang, S.; Ding, Y.; Liu, B.; Chang, C.-c. (2017). Supply and demand of some critical metals and present status of their recycling in WEEE. Waste Management 65, 113–127. DOI: 10.1016/j.wasman.2017.04.003.

Zhang, X.; Shi, H.; Tan, N.; Zhu, M.; Tan, W.; Daramola, D.; Gu, T. (2023). Advances in bioleaching of waste lithium batteries under metal ion stress. Bioresource and Bioprocess. 10 (1), 2193. DOI: 10.1186/s40643-023-00636-5.

CHAPTER 8

8 Conclusions and recommendations

In this final chapter, an integrated discussion of the main components of the research and associated findings and contributions of this study is presented. This is followed by presentation of the overall conclusions and the significant contributions of this study. Recommendations for future work required towards further development and improvement of the bioleaching process for metal extraction from PCBs are also presented.

8.1 Integrated discussion

The substantial difference in rates of chemical leaching and regeneration of the ferric lixiviant, especially in the presence of inhibitory metal ions, has detracted from development of the bioleaching process for base metal recovery from printed circuit boards (PCBs). To exploit its potential, a closer matching of rates of ferric leaching of elemental metals and ferric iron regeneration by bio-oxidation is required. In investigating the bioleaching of base metals from PCBs in a novel two-stage reactor system, the reactor system design carefully considered matching of these two rates. The system was comprised of a chemical reactor within which Fe^{3+} leaching of PCBs occurs with the production of Fe^{2+}, coupled to a bioreactor for the microbial regeneration of the Fe^{3+} oxidant. As rigorous kinetic data on the leaching of elemental metals have not been reported in the literature to date, generation of these data was important, alongside the data on microbial Fe^{3+} regeneration rates in the presence of inhibitors, for the design of a process with matched rates on the leaching of key elemental metals. Thus, in this thesis, three key aspects of PCB treatment using bio-assisted leaching were addressed with the aim of further developing and improving the bioleaching process. These are (1) the evaluation and quantification of chemical leaching kinetics of key elemental metals present, (2) enhancement of the microbial Fe^{2+} oxidation kinetics for Fe^{3+} regeneration in the presence and absence of metal ions stress through adaptation to inhibitors and through cell retention by immobilisation, and (3) the integrated bioleaching approach in a two-stage reactor system (reactor studies).

In this thesis, the two subprocesses involved in bioleaching, that is, the production rate of the Fe^{3+} oxidant by microbial Fe^{2+} oxidation and the leaching of elemental metals by this Fe^{3+} lixiviant, have been investigated. This was achieved in the initial studies through the evaluation and quantification of the volumetric Fe^{3+} reduction rates as a function of metal leaching (Part 1) and the enhancement of microbial Fe^{2+} oxidation rates for regeneration of the primary Fe^{3+} oxidant in the presence of inhibitors associated with PCB leaching through adaptation of the microbial culture and cell-retention by immobilisation in biomass support particles (Part 2). Knowledge of the volumetric Fe^{3+} reduction and regeneration rates from Part 1 and 2 was brought together to inform the setup and operating conditions of an integrated two-stage bioleaching reactor system in Part 3.

In evaluating the volumetric Fe^{3+} reduction rates as a function of metal dissolution during the leaching of base metals from PCBs (Part 1), this study sought to evaluate the relative metal

leaching rates and associated leaching kinetics to understand both the regeneration rates of lixiviant required and the sequence in which metal ions accumulate in the leachates. These studies included: (i) determining the relative contribution of the Fe^{3+} and H^+ oxidants to leaching of the elemental metals, (ii) evaluating the relative metal leaching rates of the predominant metals in PCBs (i.e., Cu, Zn, Sn, Ni), and their relative leaching mechanisms, and lastly, (iii) developing a rate law expression to describe metal leaching. Each leaching study was carried out over five temperatures (25 – 75 °C). Evaluation of the effect of temperature on the leaching rate enabled the estimation of the relative activation energy through Arrhenius's analysis. The leaching mechanism was therefore inferred from the resultant activation energy.

Across all leaching experiments, Fe^{3+} leaching rates under acidic conditions were more rapid than H^+ leaching in the absence of Fe^{3+}, demonstrating that Fe^{3+} was the primary oxidant. This result was consistent with that reported in the literature on the leaching of PCBs (Section 2.3.1).

The Fe^{3+} reduction rate, as a dominant metal dissolution mechanism, increased with increasing temperature. At 37 °C, referenced as the optimum operating temperature for the microbial Fe^{3+} regeneration (Part 2 and 3), the relative volumetric Fe^{3+} reduction rate was 6.87, 4.17, 3.79, and 0.597 g $Fe^{3+}.L^{-1}.h^{-1}$ for Zn, Sn, Cu, and Ni, respectively. This suggested that in the Fe^{3+} leaching of individual elementary metals in acidic medium, the relative magnitude of the leaching rate was in the order of Zn>Sn>Cu>Ni, compared with Zn>Cu>Ni>Sn for the acid leaching systems. In both Fe^{3+} and H^+ leaching systems, Sn precipitated out as SnO_2 within the first hour of leaching.

In evaluating kinetic parameters, this study showed that the reaction order, *n*, for Fe^{3+} leaching of Cu, Zn, Sn, and Ni was estimated to be 2^{nd}, 5^{th},2^{nd}, and 1^{st}, respectively, with respect to the Fe^{3+} oxidant. The leaching mechanism for Cu and Zn was mixed-controlled, characterised by an apparent activation energy of 32.7 and 24.3 $kJ.mol^{-1}$, respectively. Ni leaching was found to be governed by a chemical reaction-controlled (84.5 $kJ.mol^{-1}$) mechanism, whereas Sn was diffusion-limited (18.6 $kJ.mol^{-1}$).

In evaluating the effect of a mixture of metals, created synthetically or present in PCBs, on the relative metal leaching rate and potential cementation reactions, the composition of the four metals added in the mixed metal study was comparable to the metal content in the PCBs used in this study. In addition, the required mole ratio of metal to oxidant was maintained. The PCBs were first shredded using an industrial bench shredder and pulverised into fine particles of <1180 µm using a ring mill pulveriser to increase the reaction surface area and liberate the metals. With high competition for the Fe^{3+} oxidant in the multi-metals system, the Fe^{3+} reduction rate was as fast as 8.15 g $Fe^{3+}.L^{-1}.h^{-1}$ for elementary mixed metals and 3.82 g $Fe^{3+}.L^{-1}.h^{-1}$ for PCBs at 37 °C. Though these rates were different due to limited metal liberation and surface area on PCBs relative to pure powder metals (<63 µm), the rate for PCBs was comparable to those of individual metals, particularly that of Cu. High extractions of the four base metals of interest were successfully achieved at comparable leaching rates to that of

elementary metals. However, the final pH reached in PCB leaching was higher due to the alkaline nature of the PCBs. A similar order in relative metal leaching rates for mixed and individual metals was observed, while that of PCBs was Zn>Cu>Ni>Sn and the slight change was attributed to Sn precipitation impacting the determination of the Sn leaching rate. The Fe balance at the end of the leaching and the comparable relative metal leaching rates suggested no synergistic effects and no cementation reactions occurred. This may be a result of the low amounts of Zn, Sn, and Ni relative to Cu. The Fe^{3+} leaching was 2nd order with respect to Fe^{3+} for both leaching systems. The overall apparent leaching mechanism for mixed metals was diffusion-limited as characterised by an apparent activation energy of 16.3 kJ.mol^{-1} and mixed-controlled with an apparent activation energy of 26.8 kJ.mol^{-1} for PCBs.

The comparable leaching behaviour between the leaching of elementary metals and PCBs shown in this study is noteworthy as it indicated that the leaching data for elementary metals could be used to model the leaching behaviour of complex PCBs. The relative kinetic data and associated kinetics provided here for metal leaching are critical in the development of a flowsheet for biohydrometallurgical metal extraction and recovery. Such data is scarce in literature and this study is the first to provide data describing the rate kinetics and mechanisms involved in the leaching of elementary finely divided Cu, Zn, Sn, and mixed metals. Cu leaching rates are previously reported for sheet copper.

The reduction of Fe^{3+} through metal dissolution and the microbial regeneration of Fe^{3+} from the resultant Fe^{2+} are interdependent subprocesses involved in bioleaching. Metals solubilised through chemical leaching (Part 1) are expected to accumulate within the leachates and could adversely inhibit microbial activity as emphasised in the literature review (Section 2.3.4). While continuous base metal recovery following leaching is desirable, effective recovery (not considered in this thesis but recommended for future study) requires accumulation of high metal concentrations. Thus, the second part of this thesis sought to evaluate the inhibitory effect of metal ions on microbial Fe^{2+} oxidation rates. The inhibitory effects of the four base metals, i.e., Cu, Zn, Ni, and Sn, in the form of metal ions, were evaluated separately and in combination. Inhibitory studies using individual metal ions provided a relative metal effect, whereas those involving mixed metal ions demonstrated potential compounded effects with respect to individual metal ions. In addition, PCB leachates were included to better evaluate the inhibitory effect of pure metal ions and non-metallic components of the PCBs.

With the rapid Fe^{3+} reduction rate observed in the chemical leaching studies (Part 1), microbial immobilisation on biomass support particles was investigated to potentially enhance the volumetric microbial Fe^{2+} oxidation rate through enhancing the volumetric biomass concentration and restricting the decrease in the specific ferrous iron oxidation rate through inhibition. Microbial adaptation to metal ions prior to bioleaching was considered to further mitigate metal inhibition of the ferrous iron oxidation rate. The mixed mesophilic culture used for adaptation consisted of *L. ferriphilum* (38%), *At. caldus* (45%) and *Ap. cupricumulans* (15%), with additional other species present at <1% abundance, at the start of the experiment. It was adapted to 6 g/L Cu^{2+} and immobilised on polyurethane foam as a biomass support structure (PUF-BSP). Its performance was investigated using four different inocula; namely, non-

adapted planktonic cells (NA-PC), non-adapted immobilised cells (NA-IC), Cu-adapted planktonic cells (A-PC), and Cu-adapted immobilised cells (A-IC).

Successful immobilisation of the microbial culture on the PUF-BSPs was confirmed by SEM. Following cell detachment from the PUF-BSPs, cells embedded in clumps of EPS on the PUF-BSPs were still visualised under the microscope. This was attributed to the fully developed nature of the biofilm. Incomplete detachment compromised direct biomass quantification throughout these experiments. A comparison between immobilised cells and planktonic cells with respective to the initial inoculum size was therefore based on microbial activity - evaluated on the basis of calculated volumetric rates of Fe^{2+}oxidation.

Inhibition studies were evaluated by comparison of the lag phase duration, the time taken to achieve complete Fe^{2+} oxidation, and the volumetric Fe^{2+} oxidation rate. In the absence of inhibitory metal ions, the volumetric microbial Fe^{2+} oxidation rates averaged at approximately 0.0795 g $Fe^{2+}.L^{-1}.h^{-1}$ across the four sets of inocula. On increasing concentration of inhibitory metal ions, these rates decreased to below 0.0131 g $Fe^{2+}.L^{-1}.h^{-1}$, alongside prolongation in the lag phase and time taken to achieve complete Fe^{2+} oxidation. The slow microbial Fe^{3+} regeneration rates here relative to faster Fe^{3+} reduction rates observed in the chemical leaching studies (Part 1) confirmed the mismatch in rates in bioleaching and the need to improve the Fe^{3+} regeneration rates. Furthermore, the decrease in Fe^{2+} oxidation rates with an increase in the severity of inhibition necessitated mitigation of microbial inhibition.

The time taken to achieve complete Fe^{2+} oxidation by the four inocula when exposed to the same concentration of 10 g/L of individual inhibitory metal ions is summarised in Table 8-1.

Table 8-1 The time taken to achieve complete microbial Fe^{2+} oxidation by four sets of inocula when exposed to 10 g/L individual metal ions

	Time taken (hours) to achieve complete Fe^{2+} oxidation at 0 and 10 g/L metal ion				
Inoculum	No metal	Cu	Zn	Sn	Ni
NA-PC	96	120	120	-	188
A-PC	94	120	96	528	148
NA-IC	98	120	120	-	122
A-IC	88	96	96	360	120

The data suggested that the inhibitory effect by individual metal ions was in the order of Sn^{2+} > Ni^{2+} > Cu^{2+} > Zn^{2+}. Moreover, the microbial tolerance to inhibitory effects amongst the four sets of inocula tested was in the order of A-IC > NA-IC > A-PC > NA-PC. The order of metal tolerance amongst the inocula remained the same in all inhibitory studies. Complete Fe^{2+} oxidation was achieved over 216 h by A-IC exposed to mixed metals solution (34.91 g/L Cu^{2+}, 5.69 g/L Zn^{2+}, 1.13 g/L Ni^{2+}, and 2.99 g/L Sn^{2+}) simulating 20% w/v PCBs, compared to 180 h at 39 g/L Cu^{2+}, 100 h at 6 g/L Zn^{2+}, 100 h at 1 g/L Ni^{2+}, and 184 h at 3 g/L Sn^{2+}. This suggested that mixed metals exhibited more severe inhibitory effects than individual metal ions even at low metal ion concentrations. The observed severe inhibition by mixed metals was postulated to be due to the synergistic inhibitory effect with respect to individual metal ions. At 40% v/v

PCB leachates (8.88 g/L Cu^{2+}, 13.24 g/L Fe, 0.162 g/L Ni^{2+}, 0.0372 g/L Zn^{2+}, and 0 g/L Sn^{2+}), equivalent to 9% w/v PCBs, A-IC achieved complete Fe^{2+} oxidation over 600 h, suggesting that the microbial activity in the presence of the PCBs leachate exhibited more severe inhibition than both individual and mixed metal ions. The severe inhibitory effect was attributed to the presence of other metals and non-metallic components present.

The observed improved metal tolerance by the adapted cultures suggested that adapting the culture to Cu^{2+} not only improved their tolerance to Cu^{2+} but also to other individual metal ions found in PCBs such as Zn^{2+}, Ni^{2+}, and Sn^{2+}, mixed metals, and PCB leachates. The improved metal tolerance exhibited by A-IC compared to the other inocula tested suggested compounded benefits of prior adaptation to Cu^{2+} and microbial immobilised system. These results were in accordance with the hypothesis that: (i) microbial Fe^{2+} oxidation could be improved by cell retention through immobilisation while metal inhibition is minimised by associated biofilm formation, and (ii) that the metal tolerance can further be improved by prior adaptation. This finding provides a novel understanding of microbial inhibition in immobilised culture and is a significant contribution to the field of biohydrometallurgy.

Owing to the improved metal tolerance exhibited by A-IC, the integrated two-staged bioleaching system was inoculated with A-IC. The overarching aim of this PhD project was to match the Fe^{3+} reduction rate as a function of metal dissolution to the microbial regeneration rate of Fe^{3+} from the resultant Fe^{2+}. Thus, the number of PUF-BSPs (with A-IC) required to match the two rates was projected from the previously established Fe^{3+} reduction rates in the presence of pure and mixed metals, together with the microbial Fe^{3+} regeneration rates quantified in the immobilisation studies. In the absence of inhibition, 3 units of PUF-BSPs (with A-IC) exhibited a Fe^{2+} oxidation rate of 0.0802 g $Fe^{2+}.L^{-1}.h^{-1}$ at 37 °C. Across all Fe^{3+} leaching experiments at the same temperature, the highest volumetric Fe^{3+} reduction rate of 8.15 g $Fe^{3+}.L^{-1}.h^{-1}$ was that of the Fe^{3+} leaching of mixed elementary metals. In aiding the matching of the Fe^{3+} reduction rates to microbial Fe^{3+} regeneration rates, 300 PUF-BSPs were thus packed into 6 columns (50 in each column) connected in series and maintained at 37 °C. As the packed columns were coupled to a stirred tank reactor for the chemical leaching of PCBs, the metal-rich stream was recirculated between the two reactors at a flowrate of 0.5 L/h such that a residence time of 4 days across the columns was achieved. The residence time was informed by a 96 – 100 h period typically required to achieve complete Fe^{2+} oxidation observed in batch microbial activity studies (Part 2) in the absence of metal ions. To minimise the prolonged lag phase observed at the addition of high metal concentrations (including PCB leachates) and subsequent adverse impediment of the Fe^{2+} oxidation in Part 2, PCBs were added at an incremental rate of 3% w/v PCBs to minimise metal stress shock to the microbial culture and to better mimic the anticipated semi-continuous process for application.

The one-stage reactor system was considered the base case study, where both Fe^{3+} leaching and microbial Fe^{3+} regeneration occurred in a single reactor containing 50 BSPs.

In both reactor systems, comparable high bioleaching efficiency was successfully achieved. In the two-stage reactor system, the average (across 3 – 18% w/v PCBs) metal solubilisation was 98% Al, 58% Ca, 93% Cr, 96% Cu, >100% Mg, 79% Ni, 80% Pb, >100% Sn, >100% Zn, 7% Co,

and 11% Sr. Although the volumetric Fe^{2+} oxidation rates decreased slightly with an increase in PCB loading, sufficient microbial activity was maintained even at the highest PCB loading.

In both reactor systems, Fe^{3+} reduction rates averaged at approximately 0.207 g $Fe^{3+}.L^{-1}.h^{-1}$ across all PCB loadings, which was faster than the microbial Fe^{3+} regeneration rates. The Fe^{3+} reduction rates were 8.72-fold faster than the microbial Fe^{3+} regeneration rates in the one-stage reactor but only 3.47-fold faster than that in the two-stage reactor system. This suggested an improvement of about 60% in the match between Fe^{3+} reduction and regeneration rates in the two-stage system relative to the one-stage reactor system. The difference in rates was attributed to limited biomass concentration and the exposure of microbial culture to PCBs in the one-stage reactor system relative to the two-stage system. Further improvement of the relative rates is expected to be achieved by further optimisation of relative retention times.

Although the Fe^{3+} reduction and microbial Fe^{3+} oxidation rates were not matched in this study, the conditions presented improved microbial activity even at high PCB loadings of 18% PCB relative to a typical threshold of 5% w/v PCB loading. These findings supported the central hypothesis that in improving bioleaching, microbial inhibition can be partially overcome by the separation of the process into its two sub-processes through a two-stage reactor system. Therefore, this study motivates for the selection of a two-stage reactor configuration with Cu-adapted immobilised cells for bioleaching of base metal from PCBs prior to the leaching of PGMs to maximise metal recovery and support the circular economy.

8.2 Concluding remarks

This study explored a novel two-stage reactor system for bioleaching of base metals from PCBs. In developing and improving the bioleaching process, this study provides a detailed understanding of the two sub-processes involved in the bioleaching of PCBs by evaluating the volumetric Fe^{3+} reduction rate as a function of metal dissolution and microbial Fe^{2+} oxidation rates in the presence of inhibitory metal ions.

On the chemical leaching of base metals from PCBs, this study provided the relative metal leaching behaviour and its associated leaching kinetics with respective to Fe^{3+} and H^+ oxidants. In comparing the Fe^{3+} and H^+ reduction rates as a function of metal dissolution, this study demonstrated that Fe^{3+} was the primary oxidant of the elemental metals. The relative metal leaching rates in the Fe^{3+} leaching system were in the order of Zn>Sn>Cu>Ni for both individual and mixed metals, compared to Zn>Cu>Ni>Sn in the acid leaching system. These relative metal leaching rates were comparable to those in Fe^{3+} leaching (Zn>Cu>Ni>Sn) of complex PCBs, except for Sn owing to it being prone to precipitation. These data on the Fe^{3+} reduction rates as a function of metal dissolution and the associated relative metal leaching rates are critical in understanding both the regeneration rates of lixiviant required in bioleaching and the sequence in which metal ions accumulate in the leachates. With observed comparable leaching behaviour between elementary metals and PCBs, this study suggests that the elementary metal leaching data can be used to model the leaching of complex PCBs process flowsheets.

On quantifying the microbial Fe^{3+} regeneration rates through Fe^{2+} oxidation, this study confirmed the low Fe^{3+} regeneration rates relative to faster Fe^{3+} reduction rates through metal dissolution, as emphasised in the literature. The low microbial Fe^{2+} oxidation rates were exacerbated by increasing concentrations of inhibitory metal ions, namely Cu^{2+}, Zn^{2+}, Ni^{2+}, and Sn^{2+}, as individual and in combination, and PCB leachates. Microbial immobilisation system was explored to improve volumetric Fe^{2+} oxidation rates by increasing cell concentration and minimising inhibition of microbial culture through biofilm formation to maintain specific Fe^{2+} oxidation rates. Microbial adaptation to Cu^{2+} was also explored to further enhance metal tolerance. In evaluating the relative metal inhibitory effect, this study observed that PCB leachates were more inhibitory, followed by mixed metals and individual metals being the least. Among individual metals, inhibition was in the order of Sn^{2+}>Ni^{2+}>Cu^{2+}>Zn^{2+}. Severe inhibition by mixed metals was attributed to synergistic inhibitory effect with respect to individual metal ions, while with PCB leachates, the severity could have been exacerbated by dissolved non-metallic components of PCBs and other dissolved metal ions. In comparing metal tolerance and volumetric Fe^{2+} oxidation rates between the four inocula in the presence of inhibitory metal ions, culture performance was in the order of A-IC > NA-IC > A-PC > NA-PC. Improved culture performance for immobilised cells was attributed to the micro-environment within the PUF-BSPs and the resultant biofilm associated with colonised microbial cells, which provided resistant diffusion against inhibitory metal ions. These findings supported the hypothesis that exploring microbial immobilisation and adaptation can result in compounded benefits in terms of improved Fe^{2+} oxidation rates and metal tolerance. This study is the first to explore such compounded benefits. The in-depth understanding of the relative metal inhibitory effect through exposure to individual metal ions and compounded metal inhibition when exposed to mixed metal ions and PCBs, as well as the explored range of inocula is of significant benefit in the mitigation of microbial inhibition in PCB bioleaching systems.

In the final part of this PhD study, the two sub-processes were further evaluated in an integrated two-stage bioleaching system for the leaching of base metals from PCBs. In aiding matched rates of Fe^{3+} reduction to the microbial Fe^{3+} regeneration rates, insight into the volumetric Fe^{3+} reduction rates relative to Fe^{3+} regeneration rates informed the operating parameters of the integrated system. The two sub-processes were successfully separated in the two-stage reactor system with high metal bioleaching efficiency achieved. Moreover, microbial activity was successfully maintained even at the highest PCB loading of 18% w/v post metal leaching compared to the threshold of 5% w/v PCBs commonly reported in literature. Although the Fe^{3+} reduction and the microbial Fe^{3+} oxidation rates were not fully matched, this study concluded that the promising reactor configurations adopted have the potential to maximise metal recovery while maintaining and improving microbial activity during the bioleaching of PCBs. The findings presented in this study are anticipated to contribute to improved process design and optimisation of the PCB bioleaching process, as well as to enable upscaling and subsequent commercialisation of the process.

8.3 Recommendations for future work

This study presents a novel two-staged bioleaching reactor system for the improvement of microbial Fe^{3+} regeneration rate during bioleaching of base metals from PCBs. In addition to

the successes in this study, it is recommended that improvements in the novel two-stage reactor system may be achieved by considering several further configurations of the two-reactor system:

1. A unit operation for the selective removal and recovery of metals leached may be included between the chemical leaching reactor and the ferrous iron oxidation reactor in the circuit.
2. While in this study, the reactor was operated as a closed system to assess the potential of the two-reactor system, an open continuous operated system, in which a fraction of the metal-rich stream is purged for subsequent metal recovery with concomitant fresh feed addition to the two-stage reactor system should be considered to overcome the observed decrease in volumetric Fe^{2+} oxidation with an increase in accumulated PCB loading.
3. The relative residence times in each component of the two -reactor system should be explored as should the number of columns comprising the ferrous iron oxidation component. Through varying flowrates for both the leachates through the packed-bed reactors and the purge, with minimal biomass wash-out ensured, improved space-time utilisation may follow.
4. To supplement Fe^{3+} and compensate the required H^+ to maintain acidic conditions as discussed in the literature review, the addition of pyrite should also be considered, particularly for the continuous operating mode.

For an in-depth understanding of the benefits offered by the microbial immobilised system, techniques such as isothermal microcalorimetry, CO_2 and O_2 off-gas analysis, and other techniques which can relate microbial growth and associated metabolic activity to estimate accumulated biomass quantity are recommended for future studies.

It is also recommended that analysis of EPS composition should be carried out to determine and quantify the polymeric substances present. This information may provide understanding of the potential metal-chelating agents as well as the potential for metal ion adsorption in the EPS. It is also expected to provide insight into the cell protection offered by the biofilm against inhibitory metal ions.

Other metals of importance in PCBs that are potentially inhibitory metals, such as Cr and Co which can be inhibitory even at low concentrations, should also be considered in expanding knowledge of inhibition.

In addition, to better understand the potential inhibitory effect of the non-metallic composition of PCBs, microbial culture should be subjected to epoxy resins (as a base of all PCBs) in the absence of metal ions.

APPENDICES

Appendix A: Supplementary materials for Chapter 3

A1: Determining Fe^{3+} and total iron concentration

The concentration of Fe^{3+}, Fe^{2+}, and total iron in samples was determined using a Fe^{3+} chloride colorimetric assay developed by (Govender et al., 2012). The reagents were prepared as follows:

- A 1000 mg/L Fe^{3+} solution ($Fe(NO_3)_3$ in HNO_3, Merck) was used as a standard solution.
- A 2 $mol.L^{-1}$ hydrochloric acid stock solution was prepared by adding 393.24 mL of 32% HCl into 1606.76 mL of deionised water.

A standard calibration curve relating Fe^{3+} concentration to absorbance was prepared in a concentration range of 0 – 150 mg/L Fe^{3+}.

- After necessary dilution using acidified deionised water, 2 mL of a sample was added into a test tube.
- 2 mL of 2 $mol.L^{-1}$ HCl was added into the same test tube to meet a sample to HCl reagent ratio of 1:1.
- The solution was vortexed for 1 minute.
- The well mixed solution was then carefully decanted into a 4 mL cuvette and its absorbance was recorded at 340 nm for Fe^{3+} concentration.
- The solution was then decanted from the cuvette back into the test tube and a scoop of potassium persulfate crystal (99.99%, Merck) was added.
- Thereafter, the test tube was vortexed for 1 minute and allowed to sit for 5 minutes for the excess potassium persulfate to settle at the bottom.
- The sample was carefully decanted back into the cuvette and absorbance was measured at the same wavelength as previously but for total Fe concentration.

The standard curve generated and used for all Fe concentrations is presented in Figure A1:

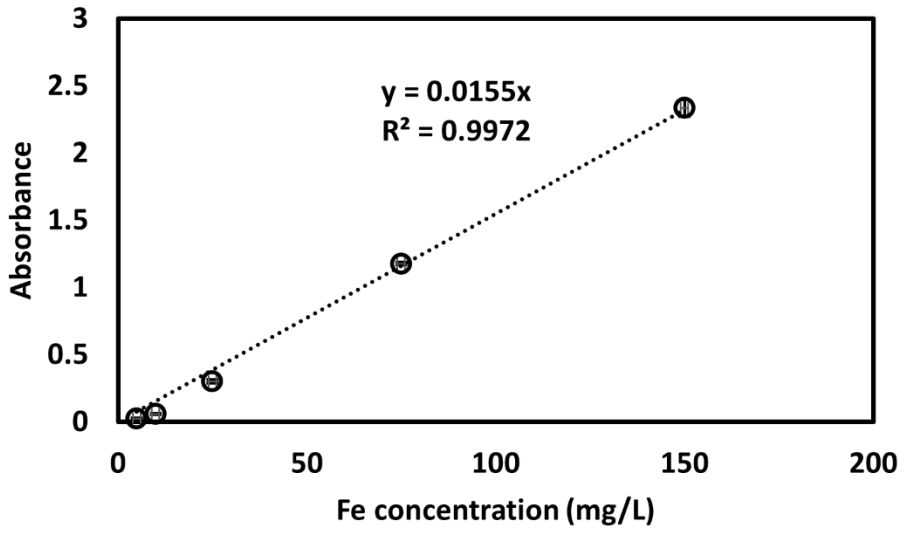

Figure A1. Standard calibration curve of Fe used to determine Fe^{3+} and Fetot. Error bars represent standard deviation, n = 3

Appendix B: Supplementary materials for Chapter 4

B1: Ferric leaching of Cu at different molar ratio

To validate the assumption that the H^+ leaching in the ferric leaching system is negligible, such that Fe^{3+} leaching is the dominant leaching mechanism Cu was leached at different moles to Fe^{3+}, i.e. 1:1 and 2:1 Fe^{3+} to metal mole ratio. The leaching was carried out at 37 °C, initial pH of 1.1 and Fe^{3+} concentration varied from 10 g/L (0.0470 mol) to 20 g/L (0.0903 mol), whereas Cu added was maintained at 2.50 g (0.0393 mol). At 10 g/L Fe^{3+}. These results are presented below.

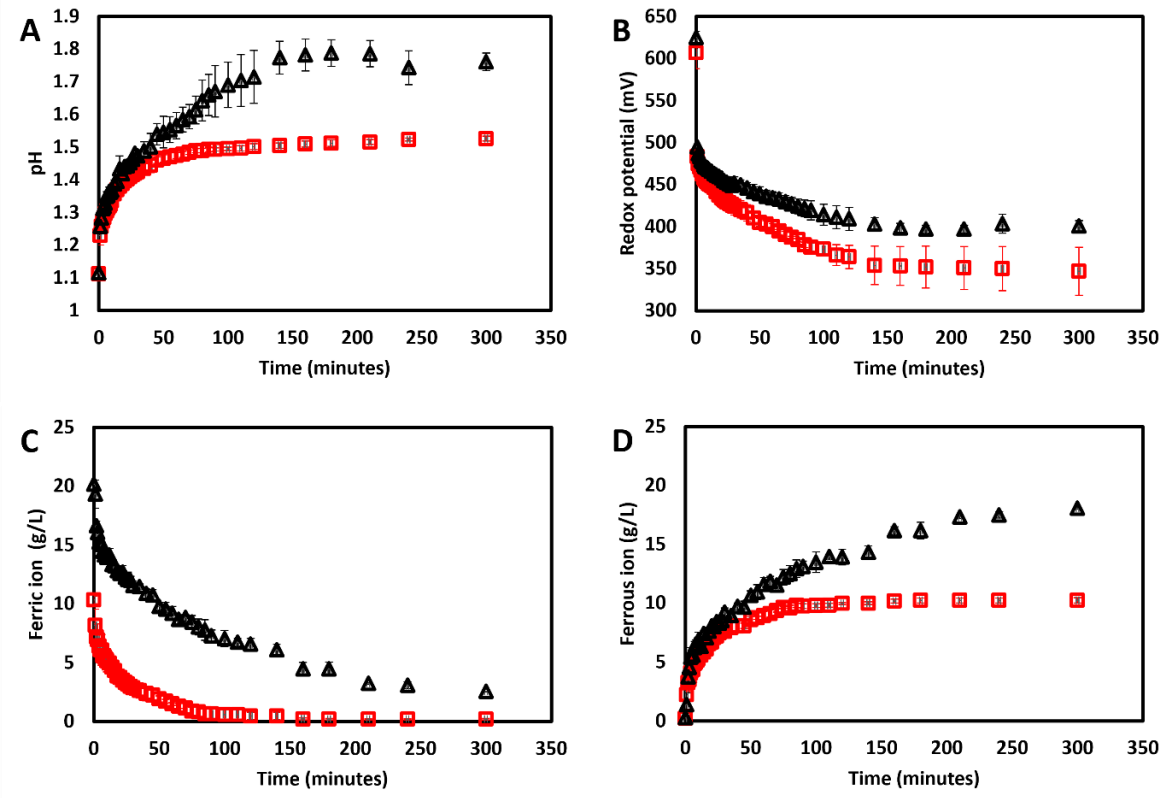

Figure B1. Change in pH (**A**), redox potential (**B**), Fe^{3+} (**C**) and Fe^{2+} (**D**) concentration over time during the ferric leaching of elementary Cu metal at 1:1 (□) and 2:1 (Δ) Fe^{3+}:Cu mole ratio. Error bars represent standard deviation, n = 3.

B2: The Nernst equation used to correct redox measurement

In the ferric leaching of Zinc elementary metal, the measured redox was affected and shifted from Fe^{3+}/Fe^{2+} coupling. The redox was then calculated from the dissolved ferric and ferrous iron ratio using the Nernst equation as follows:

$$E_h = E_0 + \frac{R.T}{z.F} \ln\left(\frac{C_{Fe^{3+}}}{C_{Fe^{2+}}}\right)$$

Where:

E_h – Redox potential (mV)

E_0 – Standard potential (mV)

R – Universal gas constant (8.31 $J.mol^{-1}.K^{-1}$

T – Temperature (K)

z – Number of moles of electrons

F – Faraday constant ($C.mol^{-1}$)

C_{Fe}^{3+} - Concentration of ferric iron ($mol.L^{-1}$)

C_{Fe}^{2+} - Concentration of ferric iron ($mol.L^{-1}$)

The calibration curve used is presented in Fig B2 below:

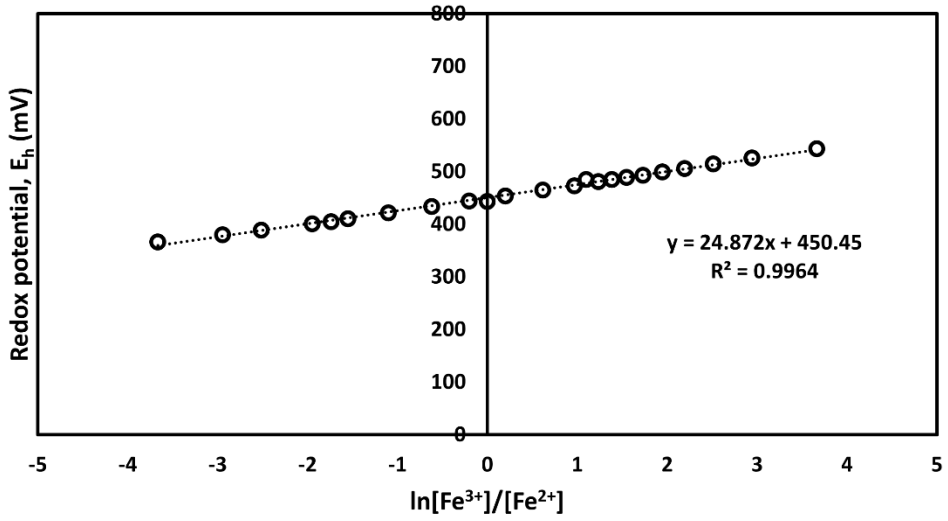

Figure B2. Standard calibration curve used to calculate redox potential from dissolved ferric iron to ferrous iron ratio.

B3: Ferric leaching of Ni powder at 25 °C

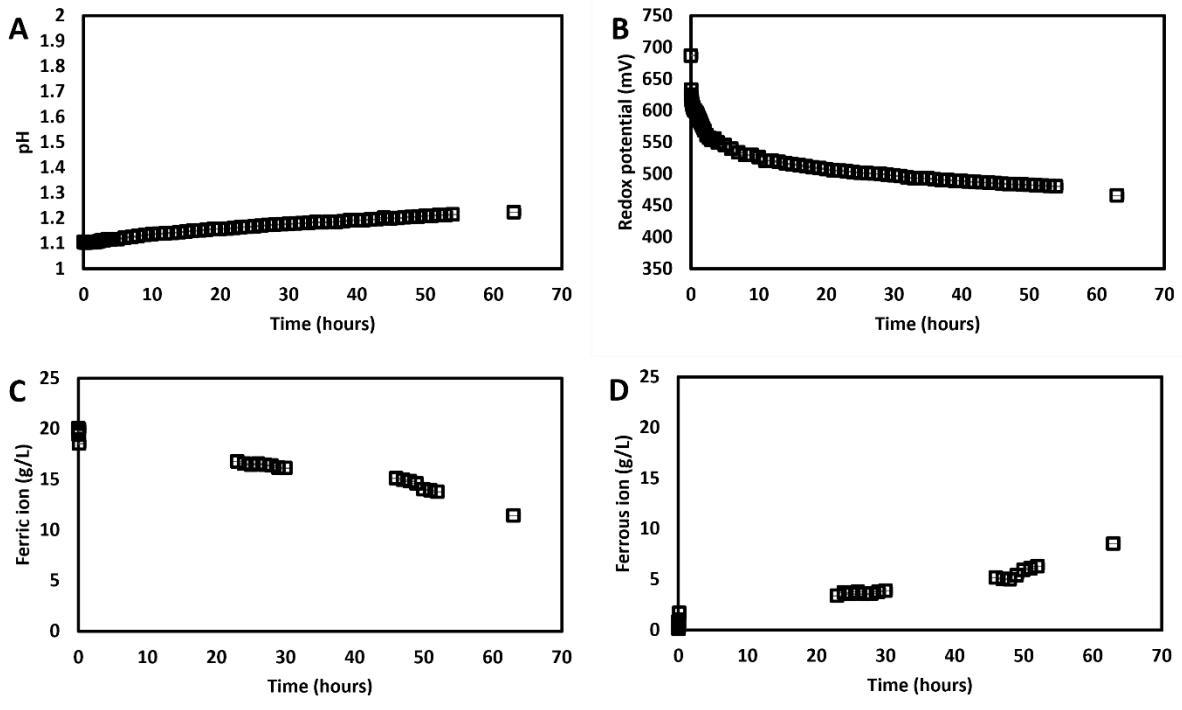

Figure B3. Change in pH (**A**), redox potential (**B**), Fe^{3+} (**C**) and Fe^{2+} (**D**) concentration during the ferric leaching of elementary Ni metal at 25 °C. Error bars represent standard deviation, n = 3.

Appendix C: Supplementary materials for Chapter 5

C1: One-way ANOVA

One-way ANOVA analysis for comparison of volumetric Fe^{2+} oxidation rates of planktonic cells to that of immobilised cells at various inoculum sizes.

Immobilised cells			Planktonic cells		
Inoculum	**Fe^{2+} rate (g/L/h)**	**STDEV, *n=3***	**Inoculum (% v/v)**	**Fe^{2+} rate (g/L/h)**	**STDEV, *n=3***
3-PUFs	0.0651	0.0012	0.2	0.0007	0.0005
6-PUFs	0.1178	0.0366	2	0.0097	0.0019
9-PUFs	0.1138	0.0300	10	0.0637	0.0029

Summary

Groups	**Count**	**Sum**	**Average**	**Variance**
Column 1	3	0.195	0.0649	1.77×10^{-6}
Column 2	3	0.191	0.0637	8.59×10^{-6}

ANOVA

Source of Variation	**SS**	**df**	**MS**	**F**	**P-value**	**F crit**
Between Groups	2.32×10^{-6}	1	2.32×10^{-6}	0.448	0.540	7.71
Within Groups	2.07×10^{-5}	4	5.17×10^{-6}			
Total	2.29×10^{-5}	5				

Appendix D: Supplementary materials for Chapter 7

D1: Design of incubator

The design of the incubator used to keep the packed-bed glass columns at 37 °C throughout the bioleaching of PCBs in a two-stage reactor system.

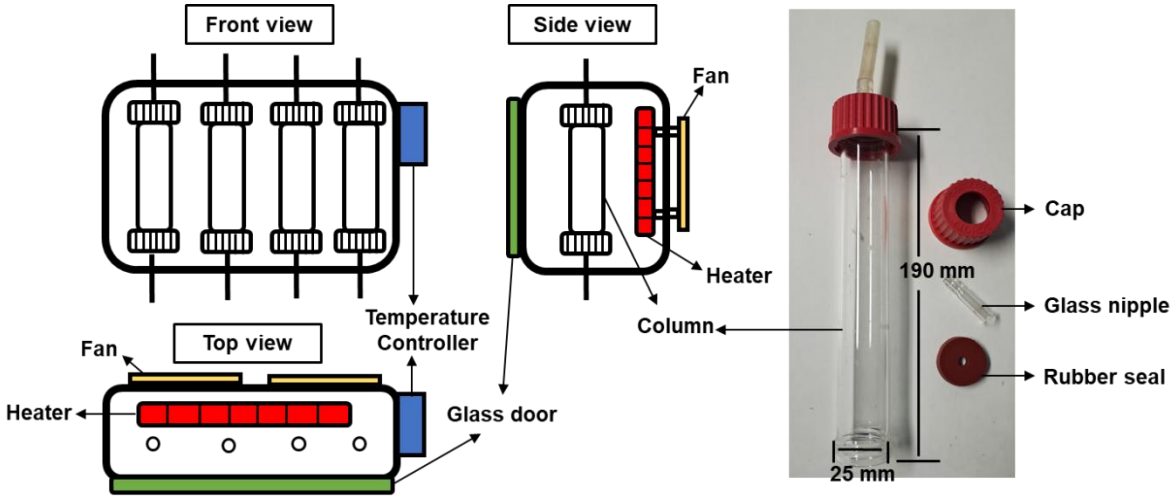

Figure D1. A schematic diagram of the design of the wooden incubator (from front, top and side view) used for incubation of the column packed-bed bioreactor used in the two-stage bioleaching of PCBs.